Utilization of industrial waste for value-added permanent sequestration of CO_2

Marco Dri

Submitted for the degree of Doctor of Philosophy

Heriot-Watt University

School of Engineering and Physical Sciences

September 2014

ABSTRACT

Mineral carbonation allows to permanently store CO_2 into materials rich in metal oxides. However, mineralization technologies still suffer of slow reaction rates and low carbonation efficiencies and, to improve them, there has been increasing interest in employing waste streams as feedstocks. In light of this, the aim of this thesis was to determine the potential use of wastes for permanent sequestration of CO_2. It was found that waste streams available for mineral carbonation in the UK have a capture potential of 1Mt/year, and in many cases, waste resources are located close to the CO_2 emitters. A novel closed-loop, multi-step mineralization process was developed. The process consists of extracting calcium from the feedstock followed by its precipitation as crystals of calcium sulphate, which are then converted into calcium carbonate. Carbonation efficiency of the process increased when temperature was raised and solid to liquid ratio and particle size reduced. A 74%, 67% and 59% of carbonation efficiency was achieved for steel slag, ground granulated blast furnace slag and phosphorus slag, respectively. Finally, a real case scenario, where the mineralization process would be retrofitted to a steel plant, was investigated. It was found that, because of the thermal and electrical energy required to run the process, the mineralization system would be carbon negative (i.e. storing more CO_2 than the amount emitted during the process) when the solid to liquid ratio would be 240g/l or higher.

ACKNOWLEDGEMENTS

Firstly, I would like to thank my supervisor Prof. Mercedes Maroto-Valer for her support throughout my PhD, from looking for funding the project to the last revision of the thesis. My gratitude goes also to Dr. Matthew Hall, Dr. Mark Gillot and Caterpillar UK Engines Company Limited for their help and support during several phases of the project.

I would like then to thank the Italian community at Department of Chemical Engineering at the University of Nottingham: Giorgio, Aimaro, Manuela, Riccardo e Laura. Tre anni intensi ma ricchi di battute, spensieratezza e simpatia. Grazie veramente!! Moreover, I must also mention the non-Italian community, all of those who I shared with my years at the University of Nottingham and I should especially thank Lee.

I am grateful to the Nottingham Wind Ensemble: John, Sandra, Dave, Colin, Margaret and all the others for welcoming and giving me the opportunity to practice my hobby in a nice and friendly environment, during my time in Nottingham.

A special thanks goes to all the friends who I left in Friuli, people who are always in my heart and I always enjoy meeting them when I visit my home place. The most important thanks goes to my family who, despite being far, supports me in my decisions and makes me feeling loved.

Finally, thanks Silvia just for being you.

ACADEMIC REGISTRY

Research Thesis Submission

Name*:*	Marco Dri		
School/PGI:	School of Engineering and Physical Sciences		
Version: *(i.e. First, Resubmission, Final)*	Final	Degree Sought (Award **and** Subject area)	Doctorate of Philosophy in Chemical Engineering

Declaration

In accordance with the appropriate regulations I hereby submit my thesis and I declare that:

1) the thesis embodies the results of my own work and has been composed by myself
2) where appropriate, I have made acknowledgement of the work of others and have made reference to work carried out in collaboration with other persons
3) the thesis is the correct version of the thesis for submission and is the same version as any electronic versions submitted*.
4) my thesis for the award referred to, deposited in the Heriot-Watt University Library, should be made available for loan or photocopying and be available via the Institutional Repository, subject to such conditions as the Librarian may require
5) I understand that as a student of the University I am required to abide by the Regulations of the University and to conform to its discipline.

* *Please note that it is the responsibility of the candidate to ensure that the correct version of the thesis is submitted.*

Signature of Candidate*:*		Date:	

Submission

Submitted By *(name in capitals):*	MARCO DRI
Signature of Individual Submitting:	
Date Submitted:	

For Completion in the Student Service Centre (SSC)

Received in the SSC by *(name in capitals):*			
1.1 Method of Submission *(Handed in to SSC; posted through internal/external mail):*			
1.2 E-thesis Submitted (**mandatory for final theses)**			
Signature:		Date:	

TABLE OF CONTENTS

LISTS OF FIGURES

LISTS OF TABLES

PUBLICATION LIST

Journal publications

Marco Dri, Aimaro Sanna, Mercedes Maroto-Valer. Mineral carbonation from metal wastes: Effect of solid to liquid ratio on the efficiency and characterization of carbonated products. Applied Energy, Volume 113, January 2014, Pages 512-523

Marco Dri, Aimaro Sanna, Mercedes Maroto-Valer. Dissolution of steel slag and recycled concrete aggregate in ammonium bisulphate for CO_2 mineral carbonation. Fuel Processing Technology, Volume 113, September 2013, pages 114-122

Aimaro Sanna, Marco Dri, Matthew R Hall, Mercedes Maroto-Valer (2012), Waste materials for carbon capture and storage by mineralisation (CCSM) – A UK perspective. Applied Energy, Volume 99, November 2012, Pages 545-554

Papers in conference proceedings

Marco Dri, Mercedes Maroto-Valer, Matthew Hall, Mark Gillott, Aimaro Sanna, Xialong Wang, Anton Zimmermann. Utilization of industrial waste materials for value-added permanent sequestration of CO_2. Proceedings of Fifth international conference on clean coal technologies 2011, 8-12 May, Zaragoza (Spain).

Marco Dri, Aimaro Sanna, Matthew Hall, Mercedes Maroto-Valer, Effect of solid to liquid ratio and scaling-up tests on mineral carbonation efficiency for thee different metal slags. Proceedings of the 9th European Conference on Coal Research and its Applications, The University of Nottingham, 10-12 September 2012, pp. 11.

Marco Dri, Aimaro Sanna, Mercedes Maroto-Valer, Mineral carbonation using metal wastes: effect of temperature on the efficiency of carbonation. Proceedings of ACEME13, Fourth International Conference on Accelerated Carbonation for Environmental and Materials Engineering. 10-12 April 2013 Leuven (Belgium)

CHAPTER 1 – INTRODUCTION

This chapter describes the challenges caused by climate change and possible solutions to the rising global carbon dioxide (CO_2) emissions in atmosphere. This vast release of CO_2 is producing unprecedented climatic consequences which humanity is called to face and tackle before irreversible damages are caused.

1.1 Climate change

In 2012, fossil fuels accounted for 82% of the total of world energy use [1.1]. However, the use of fossil fuels is facing significant challenges due to the vast amounts of CO_2 released into the atmosphere as a result of their combustion. Considering that CO_2 is a greenhouse gas, such large and increasing atmospheric CO_2 levels are causing climatic consequences [1.2]. In fact, recent observations (Figure 1.1) have conclusively shown the increase in global average air and ocean temperatures, melting of ice and snow and rising global sea levels.

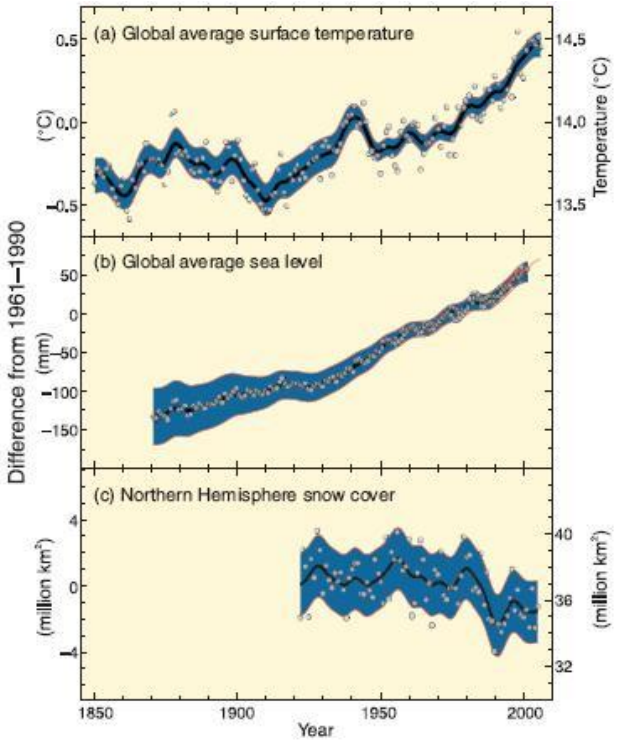

Figure 1.1: Trends of global average surface temperature, sea level and snow cover [1.3]

It is very unlikely that natural causes can explain the late 20th-century warming [1.3]. Data on average earth surface show that the second half of the 20th century was likely

the warmest 50-year period in the Northern Hemisphere in the last 1300 years. Climate models provide a suitable tool to study the various influences on the Earth's climate. The recorded global warming started during the second half of the 20th century is inconsistent with the scientific understanding of how the climate should respond to natural external factors such as variability in solar output and volcanic activity. This rapid warming, instead, is consistent with the scientific understanding of how the climate should respond to a rapid increase in greenhouse gases like that which has occurred over the past century [1.3]. When the effects of increasing levels of greenhouse gases are included in the earth system models, such as the European EC-EARTH or the American CCSM4, as well as natural external factors, the models produce good simulations of the warming that has occurred over the past century. The models fail to reproduce the observed warming when run using only natural factors. When human factors are included, the models also simulate a geographic pattern of temperature change around the globe similar to that which has occurred in recent decades [1.3].

Recently, an increasing number of severe climatic events have been recorded and climatologists believe that, continuing warming means that extreme weather, like floods, droughts and tropical storms, are likely to become more frequent and dangerous [1.3]. The emissions of CO_2 will continue to increase as the world economy grows, resulting in growth of the level of atmospheric CO_2, unless action is taken [1.2]. For this reason, in the last few years, scientific organizations and policy makers have been developing and implementing new low carbon energy technologies and policies. Legislation to cap CO_2 emissions has been introduced in some areas of the world in the form of carbon taxes (Sweden, Norway, Denmark, the Netherlands, Finland) [1.4] [1.5] or carbon-trade schemes (European Union and New Zealand) [1.6] [1.7]. To achieve a global reduction of CO_2 emissions both, renewable energies and carbon capture and storage are expected to play a key role in electricity production, as described in this chapter [1.8] [1.9].

1.2 World CO_2 emissions

Global CO_2 emissions were 32Gt in 2012 and CO_2 reached a concentration in atmosphere of 400ppm in June 2013 from 356ppm in 1992 and 280ppm in 1750s [1.10] [1.11]. Figure 1.2 reports the trends of atmospheric CO_2 concentration registered by the National Oceanic & Atmospheric Administration at Mauna Loa (Hawaii, USA). The red

line represents the CO_2 data measured as the mole fraction in dry air, while the black curve represents seasonally corrected data. It can be noticed the continuous increase in the CO_2 concentration, from less than 320ppm in 1960 to 400ppm in 2013.

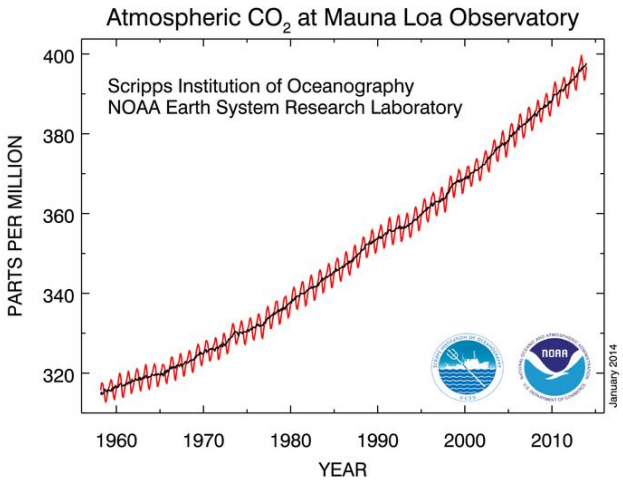

Figure 1.2: Average annual atmospheric CO_2 concentration at Mauna Loa observatory from 1960 to 2013 [1.11]

According to the Intergovernmental Panel for Climate Change (IPCC), by 2100 CO_2 atmospheric concentration could reach 540-970ppm [1.12], resulting in a global temperature increase due to the greenhouse effect of 1.8-4°C (Figure 1.3) [1.13]. It has been recently assessed that such temperature increase would have drastic impacts on human health, ecosystems, biodiversity, food availability, and coastlines [1.3].

Figure 1.3 shows temperature increase trends from year 2000 obtained from simulations under different scenarios [1.14]: A2 predicts a world with increasing global population during all the 21st century, strong economic development regionally oriented; A1B considers a future world of very rapid economic growth, population peak at mid-century and then it declines and the rapid introduction of new and more efficient technologies; energy sources in scenario A1B are balanced between fossil fuels and renewables. Scenario B1 is similar to A1B, but economic structure changes towards service and information technology, with reduction in material intensity and the introduction of clean and resource-efficient technologies. The scenario named constant composition commitment represents the case where concentration of greenhouse gases in atmosphere remain constant at the value of year 2000. For the scenarios A1B and B1 simulations were run beyond year 2100. The forecasted temperature trends range between the worst

case scenario A2, reaching a global warming of about 3.5°C by 2100 and the best case scenario given by the constant composition commitment reaching only about 0.5°C global temperature raise.

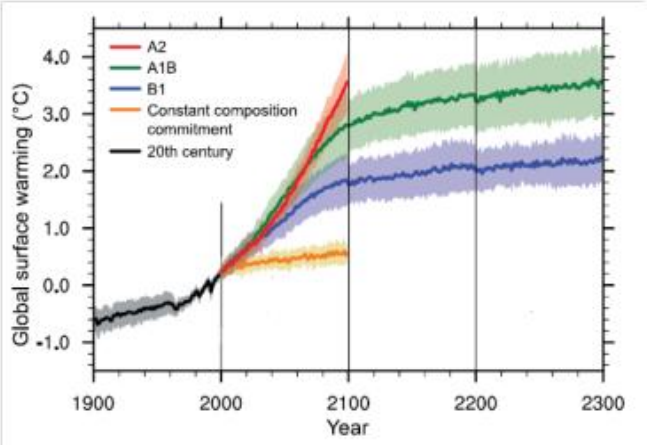

Figure 1.3: Prediction of global temperature increase according to different scenarios [1.13]

Figure 1.4 reports the share in CO_2 global emissions in 2012; the first five global emitters are China (27%), United States (16%), European Union (EU27) (11%) India (6%) and Russia (5%) [1.10] [1.15]. In year 2012 global CO_2 emissions increased by 1.4% compared to the previous year [1.10]. In 2009 emissions dropped 1%, while in years 2010 and 2011 they raised by 5 and 3%, respectively [1.15]. It should be noted that, increased emissions are due to developing countries i.e. in 2011 emissions in the EU27 decreased by 3% and in the United States by 2%, while China and India increased their emissions by 9% and 6%, respectively [1.15].

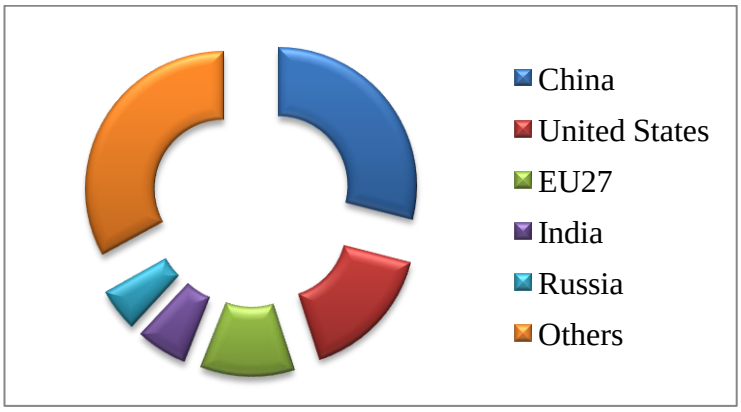

Figure 1.4: Share in global CO_2 emissions in year 2012 [1.10] [1.15]

Other interesting data are represented by the CO_2 emissions per capita, where China's CO_2 per capita emissions (7.2t/year) have reached developed European countries (7.5t/year), while the United States are still the largest emitters per capita (17.3t/year) [1.15].

1.3 Renewable energy sources

Zero emission energy technologies can produce electricity from natural resources which are renewable (naturally regenerated) like sunlight, wind, waves. Nowadays, renewable energy provides about 11% of the overall primary energy used worldwide while it plays an important role in electricity production; in 2012, in fact, renewable energy provided 21% of the overall electricity production [1.1].

In 2012, half of the electricity capacity added globally were renewable energy sources and the global renewable power capacity exceeds 1360GW which represents about 25% of the global power capacity (5360GW) [1.16]. Recent investigations [1.17] about renewable electricity costs in the UK from different renewable energy technologies are reported in Figure 1.5 for 2010 while Figure 1.6 predicts the situation for 2020. A general reduction of energy production cost from renewables is expected, thanks to the improvements in technology and increased efficiency for generating electricity [1.17]. It can be noticed that generation from combined cycle gas turbine (CCGT), the most efficient process for production of electricity from fossil fuels, is still more cost effective than all other renewable energy options. However, despite the shale gas development in the US, the latest projections say that renewable cost will drop further and they will surpass gas in the world energy mix by 2016 [1.18].

Among all the renewable energy options, onshore wind and small anaerobic digestion (AD) plants were the most economic in 2010, costing £75/127/MWh and £75-194/MWh, respectively. Moreover, they are expected to be the cheapest options also in 2020 with a cost of £71-122/MWh and £70-173/MWh, respectively. It should also be noted that solar photovoltaic (PV) is forecasted to be the technology achieving the highest drop in cost between 2010 and 2020, from £202-380/MWh to £136/250MWh.

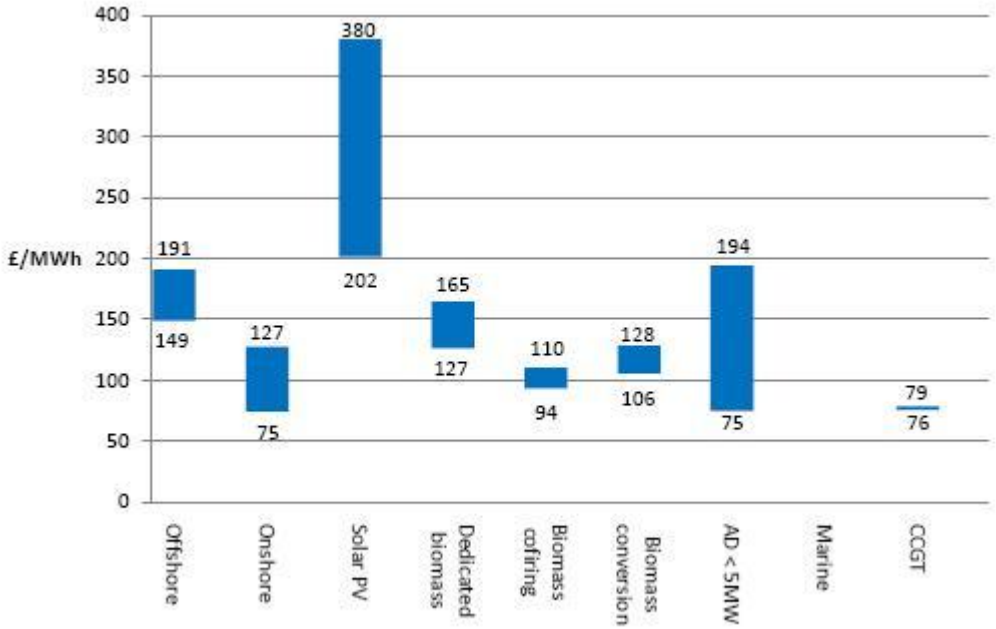

Figure 1.5: Cost ranges for renewable electricity technology for 2010 [1.17]

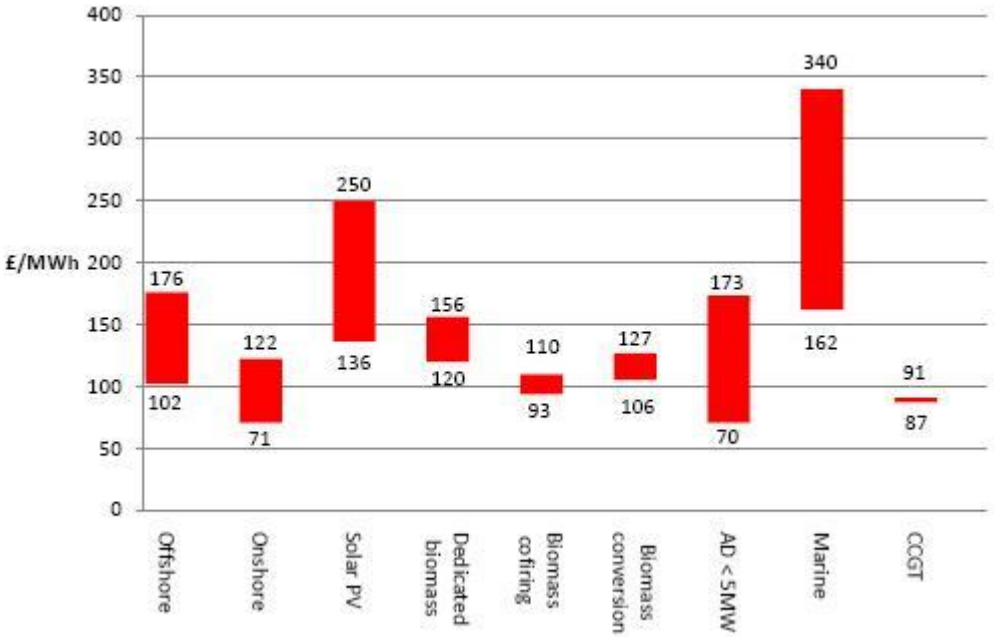

Figure 1.6: Estimated cost ranges for renewable electricity technology for 2020 [1.17]

In addition to reducing greenhouse gas emissions, renewable energies have a wide range of benefits: energy security, reduced import dependency, prevention of biodiversity loss, job creation, rural development and energy access [1.16]. These advantages are well known by policy makers who have been increasingly developing policies which

facilitate renewable energy development. In fact, in early 2012, at least 118 countries worldwide had renewable energy targets in place and these will be, together with energy efficiency, the foundations of a sustainable energy future [1.16].

1.4 CO_2 sequestration options

Renewable energy sources are expected to be the main source of energy in 2050, but fossil fuels will keep playing an important role in energy production due to their abundance and low cost [1.19]. Therefore, different options for reducing and sequester CO_2 emissions in atmosphere have been investigated, as outlined below.

Carbon dioxide capture and storage (CCS) technologies allow capturing CO_2 from flue gases of power plants, refineries and energy intensive industrial processes and, following compression, CO_2 is injected in suitable underground storage sites, away from the atmosphere.

Carbon capture utilization and storage (CCUS) includes the reuse of the captured CO_2 for a wide range of applications [1.9]. The most known technology included is enhanced oil recovery (EOR) where CO_2 is reused by injecting it in an oil or gas reservoir to increase the amount of hydrocarbons extracted. CO_2 is then stored in the reservoir and this technology can be considered also as a CCS option. Other CO_2 utilization routes are for products like beverage and fire extinguishers. Furthermore, there has been increasing interest in CO_2 application for the production of chemicals, hydrocarbons and fuels [1.9].

Recently, CCS has not seen significant progress and deployment as expected, in fact, only about 20Mt/year [1.20] are currently stored underground, compared to 32Gt/year CO_2 global emissions [1.10]. Therefore, an alternative technology, called mineral carbonation has attracted increasing attention [1.21]. The basic process consists of reacting CO_2 with a divalent metal oxide, such as calcium, magnesium or iron, to produce a metal carbonate and release heat.

$$MO(s) + CO_2(\mathrm{g}) \rightarrow MCO_3(\mathrm{s}) + Heat \qquad (1\text{-}1)$$

Despite the simple theoretical concept involved in mineral carbonation, this technology suffers from a wide range of challenges. Firstly, the reaction takes geological times to happen at ambient conditions [1.22]. Therefore, researchers have been focusing on developing different processes to speed-up the reaction, from increasing temperature and pressure to develop multi-step techniques able to facilitate the mineralization process using the addition of chemicals. Secondly, because in nature pure metal oxides are rarely available, it is necessary to identify the right feeding material, able to provide metal oxides in silicate form (natural rocks or waste streams). Thirdly, mineral carbonation is an exothermic reaction, however pre-treatment of the material (mining, crushing, grinding) requires considerable energy [1.22]. Therefore, research into reducing energy demand from feedstock preparation is required. Finally, by-products from mineral carbonation, because pure metal oxides are scarcely available (see Section 2.2.2), are generally a mixture of different phases (e.g. metal carbonates, silica, unreacted metal oxides etc.). Therefore, final separation steps are needed to obtain a range of products with a market value and further research is required [1.23].

1.5 Aim and objectives

The aim of this thesis was to determine the potential use of waste materials as feedstock for permanent sequestration of CO_2. A novel mineralization process was proposed and its feasibility, for several suitable feedstocks, was investigated.

Several objectives were carried out during the project and they are described below.

- To investigate state-of-the-art mineral carbonation in order to identify potential suitable waste materials to employ in the mineralization process proposed in the thesis.
- To assess the potential areas in the UK where mineral carbonation of waste materials can be applied, studying the availability and location of waste streams suitable for mineralization.
- To understand the physico-chemical characteristics of waste streams, assessing their suitability for mineralization using different analyses techniques (x-ray diffraction and x-ray fluorescence).
- To develop a novel multi-step mineralization process able to use waste streams as feedstocks.

- To investigate the process developed, understanding the mechanisms of dissolution and carbonation.
- To research into the best operational conditions, investigating the effect of the main parameters on the efficiency of carbonation.
- To assess the economic viability of the process when applied in a real case scenario, analyzing the energy and CO_2 balances of the process followed by the calculation of capital and variable costs.

According to the objectives identified, the thesis is structured as follows. Chapter 2 reviews the existing literature on mineral carbonation, then Chapter 3 presents the methodology used, analyses techniques and experimental set-up. Chapter 4 investigates the availability and potential CO_2 storage capacity of waste materials, while Chapter 5 discusses the mechanisms of dissolution during the first step of the proposed mineralization process. Chapter 6 presents the analyses on the effect of several parameters on the efficiency of carbonation for different waste streams, moreover, also the mechanisms of carbonation for these materials are presented in this chapter. Finally, Chapter 7 includes mass, energy, CO_2 balances of the overall process and also a cost evaluation in a real case scenario. Conclusions about the work presented in the thesis are then summarized in Chapter 8.

1.6 References

[1.1] IEA. International Energy Agency Monthly Energy Review: August 2013. http://www.eia.gov/totalenergy/data/monthly/pdf/mer.pdf. Date of consultation: September 2013.

[1.2] Goldberg P, Chen Z, O'Connor W, et al. CO_2 Mineral Sequestration Studies in US. National Energy Technology Laboratory, Department of Enegy, US. 1998.

[1.3] IPCC. Report: Climate change 2007. Contribution of Working Groups I, II and III to the Fourth Assessment Report of the Intergovernmental Panel on Climate Change. Cambridge, UK and New York, NY, USA: Intergovernmental Panel on Climate Change; 2007.

[1.4] Baranzini A, Goldemberg J, Speck S. A future for carbon taxes. Ecological Economics. 2000;32:395-412.

[1.5] Metcalf G, Weisbach D. The Design of a Carbon Tax. Harvard Environmental Law Review 2009;33.2:499-506.

[1.6] Skjærseth JB, Wettestad J. Making the EU Emissions Trading System: The European Commission as an entrepreneurial epistemic leader. Global Environmental Change. 2010;20:314-21.

[1.7] New Zealand Ministry for the Environment. The framework for a New Zealand emissions trading scheme: executive summary. Wellington, New Zealand: New Zealand Ministry for the Environment and The Treasury; 2007.

[1.8] Yamasaki A. An Overview of CO_2 Mitigation Options for Global Warming-Emphasizing CO2 Sequestration Options. Journal of Chemical Engineering of Japan. 2003;36:361-75.

[1.9] IPCC. IPCC special report on carbon capture and storage. Cambridge, UK and New York, NY, USA: IPCC Intergovernmental Panel on Climate Change; 2005.

[1.10] IEA. International Energy Agency Redrawing the energy-climate map report. Paris- France:IEA-International Energy Agency; 2013

[1.11] NOAA/ESRL. Average annual atmospheric CO_2 concentration at Mauna Loa observatory from 1960 to 2012. http://www.esrl.noaa.gov/gmd/ccgg/trends/2012.Date of consultation: October 2013.

[1.12] IPCC. Climate change 2001: the Scientific basis. Contribution of working group I to the third assessment report of the Intergovernmental Panel on Climate Change. Cambridge, UK and New York, NY, USA: Intergovernmental Panel on Climate Change; 2001.

[1.13] IPCC. Climate Change 2007: The Physical Science Basis. Contribution of Working Group I to the Fourth Assessment Report of the Intergovernmental Panel on Climate Change. Cambridge, UK and New York, NY, USA: Intergovernmental Panel on Climate Change; 2007.

[1.14] IPCC. A Special Report of Working Group III of the Intergovernmental Panel on Climate Change. Cambridge, UK and New York, NY, USA: Intergovernmental Panel on Climate Change; 2000.

[1.15] Olivier J, Janssens-Maenhout G, Peters J. Trends in global CO_2 emissions. The Hague - The Netherlands: PBL Netherlands Environmental Assessment Agency; 2012.

[1.16] Janet SL. Renewables 2012 Global Status Report. Paris: Renewable Energy Policy Network for the 21st Century; 2012.

[1.17] DECC. UK renewable enrgy roadmap. London: Department for Energy and Climate Change; 2011.

[1.18] IEA. Medium-Term Renewable Energy Market Report 2013. Paris- France: IEA-International Energy Agency; 2013.

[1.19] IEA. World Energy Outlook. Paris- France: IEA-International Energy Agency; 2012.

[1.20] Global CCS Institute. The global status of CCS 2012. Canberra, Australia: Global CCS Institute; 2012.

[1.21] Zevenhoven R, Wiklund A, Fagerlund J, Eloneva S, In't Veen B, Geerlings H, et al. Carbonation of calcium-containing mineral and industrial by-products. Frontiers of Chemical Engineering in China. 2010;4:110-9.

[1.22] Sanna A, Dri M, Hall MR, Maroto-Valer M. Waste materials for carbon capture and storage by mineralisation (CCSM) – A UK perspective. Applied Energy. 2012;99:545-54.

[1.23] Sanna A, Hall MR, Maroto-Valer M. Post-processing pathways in carbon capture and storage by mineral carbonation (CCSM) towards the introduction of carbon neutral materials. Energy & Environmental Science. 2012;5:7781-96.

CHAPTER 2 – CARBON DIOXIDE SEQUESTRATION BY MINERAL CARBONATION

This chapter introduces the basic concepts of CO_2 capture and underground (called also geological) storage followed by a literature review on mineral carbonation. This includes a description of potential feedstocks suitable for carbonation, their characteristics and availability. Then, the numerous processes available for mineral carbonation are classified and described, reporting also their costs. Finally, the use and potential market value of the carbonated products are described.

2.1 Carbon dioxide capture and storage (CCS)

Renewable energy sources will provide zero emission energy in the next decades, but, for the moment, fossil fuel technologies will continue to play a leading role in the energy production considering their availability and cost [2.1]. In 2020, for example, estimated price of electricity generated from combined cycle gas turbine will range between £87-91/MWh, while on-shore wind and off-shore wind will be at £71-122/MWh and £102-176/MWh, respectively [2.2].

Carbon dioxide Capture and Storage (CCS) is a portfolio of technologies which aims to capture the CO_2 produced from the combustion of fossil fuels for power generation and industrial processes. The CO_2 must, then, be transported to an underground storage site, where, it will be stored away from the atmosphere for a very long time [2.3].

2.1.1 Capture and storage options

Fossil fuel power plants are the primary candidates for applying CCS. Capture has the purpose to produce a concentrated stream of CO_2 (to reduce cost of transportation) which then will be compressed and sent to the storage site. There are three different technologies available for capturing CO_2 presented in Figure 2.1 [2.3].

- Post-combustion systems separate the CO_2 from the flue gases generated from the combustion of fossil fuels. Chemical sorbents (liquid or solids) or membranes are employed to capture the fraction of CO_2 (usually about 10-15%) from the flue gases rich in N_2.

- Pre-combustion systems produce carbon monoxide (CO) and hydrogen (H_2) from the fossil fuel (gasification) which then are separated and H_2 is burned and produces energy/heat without releasing CO_2 from the combustion. The CO stream, instead, is reacted with steam producing further H_2 for energy/heat production and CO_2 which is then compressed and transported to the storage site.
- Oxyfuel systems use pure oxygen for the combustion of the fossil fuels. An air separation unit, able to separate O_2 from air is required upstream. Flue gases generated consist of CO_2 and steam which is then condensed leaving mainly CO_2.

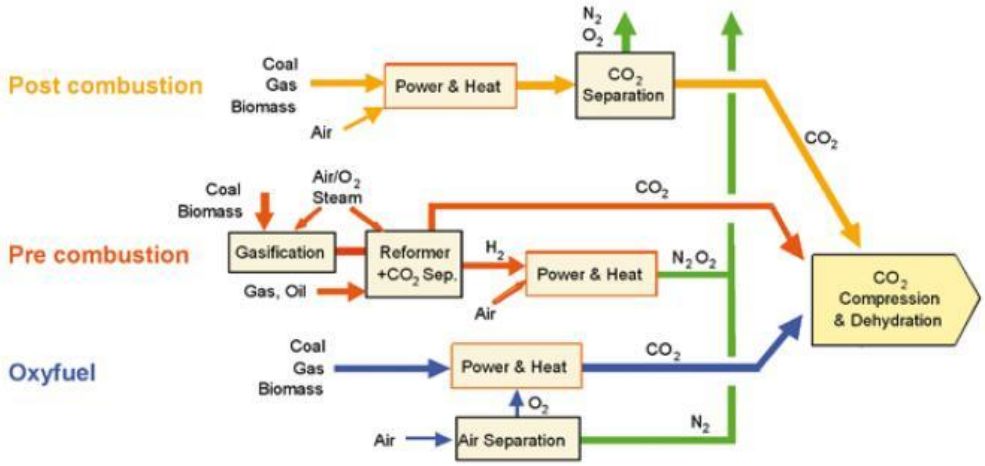

Figure 2.1: Overview of the CO_2 capture systems [2.3]

After capturing the CO_2 emitted from power plants, carbon dioxide is transported to an underground storage site. The different storage options are presented in Figure 2.2 and include depleted oil and gas reservoirs, saline aquifers, and oceans. Enhanced oil recovery (EOR) and enhanced coal bed methane recovery options benefit of both increasing oil and gas extracted and storing CO_2. EOR is a well established practice used to increase the oil production in mature fields by injecting CO_2 in the oil reservoir [2.4]. Therefore, lessons learnt from EOR may help developing CO_2 storage also in other potential sites such as saline aquifers and depleted gas and oil fields. In fact, EOR reduces overall CCS cost because of the increased oil production while storing CO_2. Storage in saline aquifers and depleted gas and oil fields, instead, does not have this economic benefit, however, it may be applied in many locations worldwide thanks to the large number of these sites.

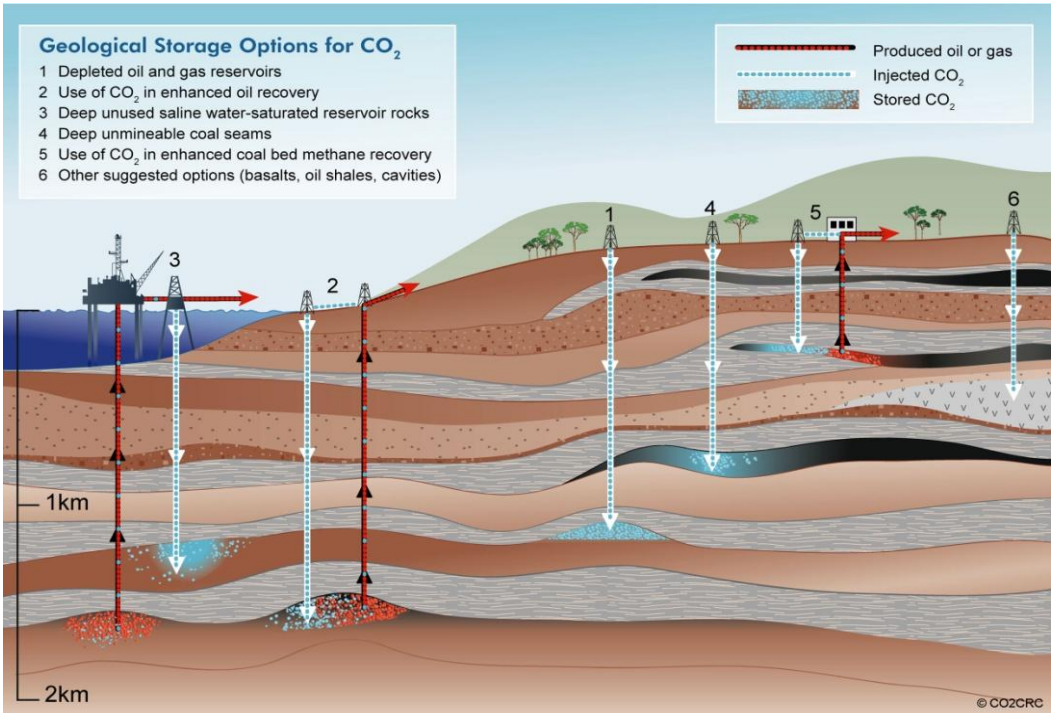

Figure 2.2: Geological storage options for CO_2 (image courtesy of CO2CRC [2.5])

2.1.2 CCS potential and cost

CCS is a bridge technology towards renewable energies which will be the zero-emission energy sources. CCS may reduce the cost of stabilizing CO_2 in atmosphere by 30% or more if it is included in a mitigation portfolio of technologies [2.3]. Thanks to strong policies, economic incentives and technology development, CCS has the potential of storing 230Gt by 2050, which corresponds to 33% reduction in global CO_2 emissions compared to today's levels. Therefore CCS alone cannot meet the target set by the Intergovernmental Panel for Climate Change (IPCC) of reducing carbon emission by 50% by 2050 [2.3] and renewable energies have also to play a key role [2.6].

CO_2 injection underground has been used in oil extraction (EOR) for about 40 years [2.7]. Nowadays, implementing CO_2 storage into depleted oil and gas fields and in saline aquifers has led to eight commercial CCS facilities in operation worldwide: Sleipner West (1Mt/year) and Snøhvit (0.7Mt/year) in Norway, Weyburn (3Mt/year) in Canada, Shute Creek gas processing (7Mt/year), Enid Fertilizer (0.68Mt/year), Val Verde Gas Plants (1.3Mt/year) and Century plant (5Mt/year) in USA, and In Salah (1Mt/year) in Algeria [2.4]. All of them, apart from Enid Fertilizer, are related to natural gas or syngas operations, and they store the CO_2 obtained from the gas cleaning operations into a deep saline aquifer or they use it for enhanced oil recovery. There are

also numerous demonstration plants in operation and others are planned [2.4] [2.8] [2.9]. However there is not yet a fully operating power plant integrated with CCS, and therefore, the global quantity of CO_2 stored underground is limited to only 20Mt/year [2.4]. It has been estimated that about 2000Gt of CO_2 can be stored underground worldwide [2.3], therefore, the annual global CO_2 emissions (about 32Gt [2.12]) represent only 1.6% of the amount of CO_2 which could be potentially stored by CCS. The main barriers to the development and deployments of CCS are the absence of financial and public support, high energy penalties, costs and potential impact due to possible CO_2 leakage [2.3].

Predictions of costs for CCS depend on its future development and deployment. Recent studies show that cost for CCS demonstration projects built in 2015 is 60-90€/$tCO_{2\ avoided}$ (£50-75/$tCO_{2\ avoided}$) [2.10]. This cost can be reduced to 30-45€/$tCO_{2\ avoided}$ (£25-38/$tCO_{2\ avoided}$) by 2030 thanks to the learning effects from the demonstration projects [2.10]. About 70% of the cost of CCS stands for the separation of CO_2 from the flue gasses [2.10] and this represent one of the challenges to further deployment of this technology [2.11].

2.2 Mineral carbonation

Due to a slow progress in the deployment of technologies which store CO_2 underground (about 20Mt/year [2.4], compared to 32Gt/year CO_2 global emissions [2.12]), and also because access to underground storage may not be feasible due to technical and/or economic restrictions [2.13], there has been an increasing interest in mineral carbonation [2.14]. Mineral carbonation (often referred in literature also as mineralization or mineral sequestration) was first suggested by Seifritz in 1990 [2.15]. Dunsmore then further investigated this option for CO_2 utilization and storage [2.16] followed by Lackner et al. in 1995 [2.17]. The process consists of reacting CO_2 with a divalent metal oxide (MO), such as calcium, magnesium or iron oxides, to produce a metal carbonate (MCO_3) and release heat.

$$MO(s) + CO_2(\mathrm{g}) \rightarrow MCO_3(\mathrm{s}) + Heat \qquad (2\text{-}1)$$

At ambient conditions, the gas-solid mineralization reaction takes place on geological time-scales and, therefore, research has focused on developing different processes to

speed up the reaction. Pure metal oxides, in nature, are scarcely available but they can be easily found in silicate form in rocks present on the earth surface, like serpentine ($Mg_3Si_2O_5(OH)_4$), olivine (Mg_2SiO_4) and wollastonite ($CaSiO_3$).

Mineralization can be divided into in-situ and ex-situ processes. In-situ mineralization is related to geological storage, i.e. injection of CO_2 underground but it differs in that it aims at accelerating the formation of carbonates with the alkaline-minerals present in the geological formation. Therefore, the mineralization mechanism in geological storage and in-situ mineral carbonation is the same [2.3] but the geological storage requires longer periods [2.18]. This is explained by the fact that when injecting CO_2 underground for in-situ mineralization, water at high pressure is added to increase the speed of the reaction, while for the CO_2 geological storage, pure streams of CO_2 are pumped underground. The first fully integrated in-situ mineralization project started in 2007 in Iceland [2.18] where CO_2 dissolved in water at high pressure (from a geothermal plant) is injected at 400-800m in a basalt formation underground [2.19]. The time-scale of in-situ mineral carbonation is shorter than CO_2 trapping in geological storage (hundreds of years instead of thousands for complete conversion into carbonates [2.19] [2.20]), but it still takes considerable time to permanently store CO_2 into carbonates. Ex-situ mineralization, instead, groups all the mineral carbonation processes which are not carried out in geological formation. An example of ex-situ mineralization plant employing minerals is shown in Figure 2.3, where the different stages of the process, from mining operations to transport of the final by-products, are presented. Mineralization of CO_2 produced from a coal power plant would involve solid minerals handling of a scale similar to a nowadays metal ore or mineral mining and processing activity [2.21] like the ones present in Australia, South Africa and Canada.

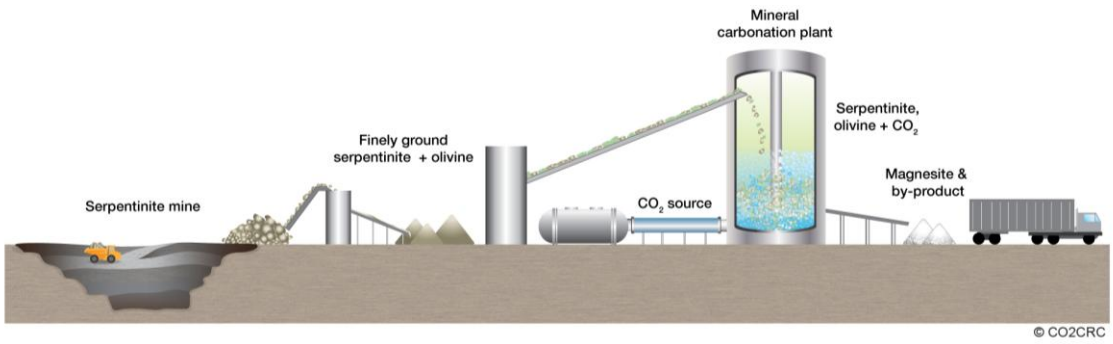

Figure 2.3: Mineralization plant employing natural minerals (image courtesy of CO2CRC [2.5])

2.2.1 History of mineral carbonation

This section presents the developments in mineral carbonation research in chronological order, more technical details on the processes mentioned are going to be reported in Section 2.3.

As mentioned in Section 2.2, mineral carbonation was firstly investigated in 1990 by Seifritz [2.15], then by Dunsmore in 1992 [2.16] followed by Lackner et al. in 1995 [2.17]. First mineralization technologies were based on processes using high temperature and high pressure reactors and research was focused into optimizing these systems. Lackner et al. in 1997 used pressurized CO_2 (340bar) at high temperature (300°C) to convert serpentine into carbonates by a solid-gas reaction [2.22]. Later, in 1998, Butt et al., were among the first to explore indirect gas-solid processes, where the mineralization carbonation reaction took place after leaching $Mg(OH)_2$, from silicate rocks using HCl [2.23]. The process was also able to regenerate and reuse the HCl employed. It was immediately noticed the improvement in the extraction and carbonation reaction rates (25% vs. 100% [2.23]) compared to previous studies using direct gas-solid reactions. Therefore, research started on the so called direct aqueous route.

One of the most known research groups developing the direct aqueous route was the Albany Research Centre (ARC) in the USA. They assessed a direct aqueous process optimizing the solution chemistry, heat treatment and grinding [2.24] as described in Section 2.3.2.2. This process was considered one of the most successful routes for mineral carbonation and a critical assessment of this method found that it would have an energy penalty of 20% in a coal power plant [2.21]. Furthermore, the Intergovernmental Panel for Climate Change (IPCC) in 2005 used the cost of the ARC process for their comparisons among different CCS options and interest for research in mineralization further increased. In fact, the number of papers published on peer-reviewed journals in the Science Direct database has seen a general increasing trend between years 2005 and 2012 (Figure 2.4).

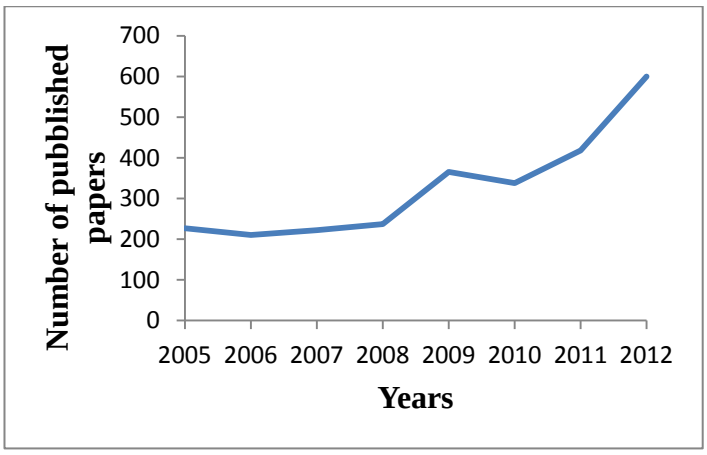

Figure 2.4: Number of published papers on peer-reviewed journals about mineral carbonation between years 2005 and 2012.

Over the last 10-15 years, Zevenhoven and his research group in Finland have developed firstly a high temperature direct gas-solid process able to reuse the heat released during the carbonation reaction [2.25] and then also an aqueous process [2.13]. However, due to the high energy requirements for maintaining high temperature and pressure during these processes, these direct carbonation routes do not seem feasible at industrial or even demonstration/pilot scale.

More recently, after exploring different options for direct mineral carbonation, researchers have also been investigating indirect carbonation routes, where metals are firstly extracted from the silicate minerals and then easily carbonated during a following step. There are numerous studies in this field employing different chemicals (HNO_3, HCl, H_2SO_4) for the extraction phase [2.26] [2.27] [2.28]. However, the main problem associated with this carbonation route is the fact that chemicals and acids cannot be recovered. This causes several environmental and economic issues, which can only be addressed if after extracting the metal ions from the feedstock the chemicals employed are regenerated and recycled. In light of this, latest research developments in mineral carbonation have focused on processes able to use indirect carbonation routes whilst reusing the chemicals utilised (e.g. [2.29] [2.30]). Otherwise, another route has been employing less hazardous substances for the environment, like organic or weak acids such as citrates, oxalates and ethylenediamine tetraacetic acid (EDTA) [2.31] [2.32] [2.33].

2.2.2 Elements and minerals for mineral carbonation

Potential elements which can carbonate are alkali (e.g. K, Na) and alkali earth (e.g. Ca, Mg) metals and other metals like Fe, Mn, Zn, Ni, Cu. However, most of the other metals listed are too valuable (Ni, Cu) or too rare (Mn, Zn) to be considered for mineralization. Alkali metals are unsuitable for CO_2 mineralization because they produce alkali bicarbonates, which are very soluble and therefore CO_2 may return to the atmosphere. Therefore, the most suitable elements for mineral carbonation are Ca and Mg. Fe is also suitable, but carbonation of this element means consuming a valuable ore which is usually employed in steel production [2.3].

Unfortunately, in nature, calcium and magnesium are scarcely available as pure oxides. They are mainly present as calcium and magnesium silicates contained in natural rocks available on the earth surface and the main candidates among the Mg-rich minerals are serpentine, dunite and peridotite. Serpentine ($Mg_3Si_2O_5(OH)_4$) can be found in different crystalline phases such as antigorite, lizardite and chrystolite. Dunite and peridotite are instead rocks formed mainly (more than 90%) by olivine mineral, $MgSiO_4$. Wollastonite ($CaSiO_3$) is instead a Ca-rich silicate rock [2.24].

Because of pure oxides are rarely available on the earth, the main carbonation reaction (2-1) becomes [2.3]:

$$(Mg,Ca)_xSi_yO_{x+2y+z}H_{2z}(s) + xCO_2(g) \rightarrow x(Mg,Ca)CO_3(s) + ySiO_2(s) + zH_2O(^{l}/_{g}) \quad (2\text{-}2)$$

Therefore, the mineralization reaction changes, releasing less heat. The reaction involving the pure metal oxide (MgO) releases 118kJ/mol as follows [2.3]:

$$MgO + CO_2 \rightarrow MgCO_3 + Heat(118\ kJ/mol) \quad (2\text{-}3)$$

When introducing olivine (Mg_2SiO_4) instead of the pure magnesium oxide, 95kJ/mol are released [2.3]:

$$^{1}/_{2}\, Mg_2SiO_4 + CO_2 \rightarrow MgCO_3 + {}^{1}/_{2}\, SiO_2 + Heat(95\ kJ/mol) \quad (2\text{-}4)$$

In the case of serpentine the reaction becomes [2.3]:

$$Mg_3Si_2O_5(OH)_4 + 3CO_2 \rightarrow 3MgCO_3 + 2SiO_2 + 2H_2O + Heat(64\ kJ/mol) \quad (2\text{-}5)$$

The trend of the equilibrium constant in function of the temperature for the reactions 2-3, 2-4 and 2-5 are shown in Figure 2.5. It can be seen that reactants are favored over products for temperatures below 300°C.

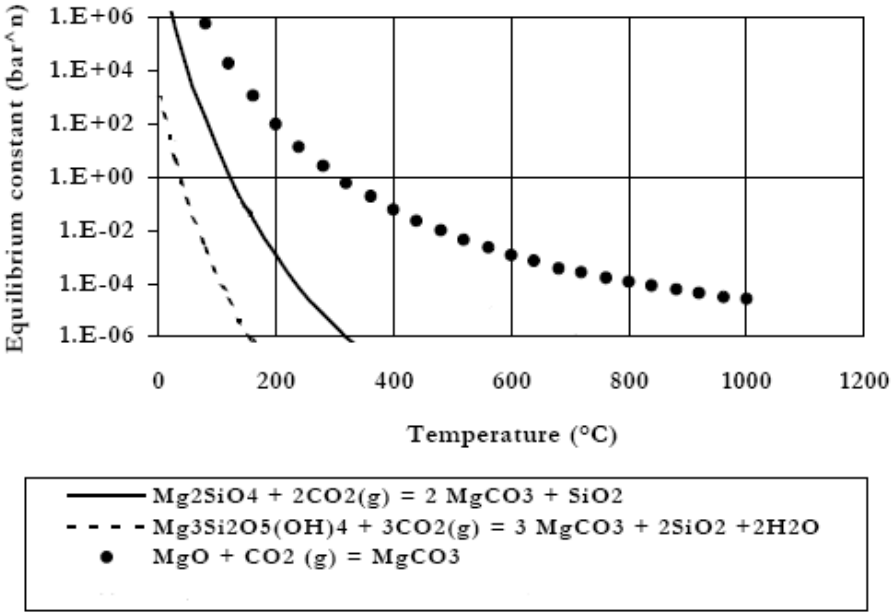

Figure 2.5: Equilibrium constant trend for carbonation of Mg oxide and Mg-rich minerals [2.25]

While, for Ca-rich minerals the mineralization reaction with pure metal oxide (CaO) is presented below [2.3]:

$$CaO + CO_2 \rightarrow CaCO_3 + Heat(179\ kJ/mol) \quad (2\text{-}6)$$

When using wollastonite ($CaSiO_3$) the reaction becomes [2.3]:

$$CaSiO_3 + CO_2 \rightarrow CaCO_3 + SiO_2 + Heat(90\ kJ/mol) \quad (2\text{-}7)$$

Since the equilibrium constants of reactions 2-6 and 2-7 are given by the partial pressure of CO_2, Figure 2.6 presents the predominance of reactants or products in function of the temperature.

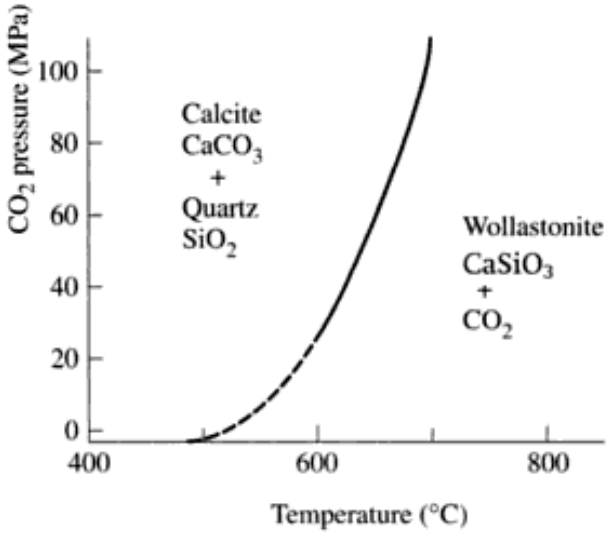

Figure 2.6: Pressure – temperature diagram for carbonation of Ca oxides or Ca-rich minerals [2.36]

2.2.2.1 Availability and capacity of natural minerals for mineral carbonation

Serpentine, olivine and wollastonite are the major minerals employed for research in mineral carbonation, because of their content in Mg/Ca silicates. In Figure 2.7 red dots represent locations where serpentine (Mg-rich mineral) is present, showing high abundance in North America and North Europe.

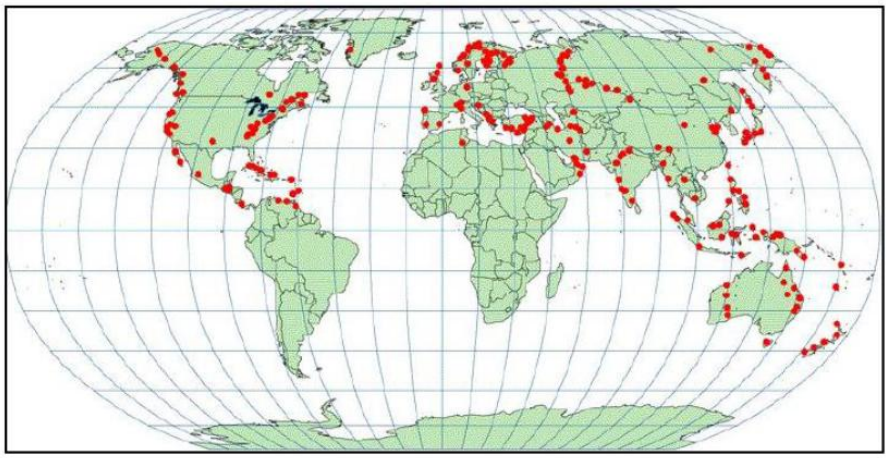

Figure 2.7: Worldwide distribution of serpentine [2.25]

It has been reported that in the USA there is enough mineral volume to store the total amount of USA CO_2 annual emissions (about 7Gt) for 500 years [2.31] and serpentine in eastern Finland could provide 2.5-3.5GtCO_2 storage capacity when Finnish annual emissions are only about 56MtCO_2 [2.34]. Apart from the just mentioned serpentine resources assessment, there has not been so far any other detailed geographical study on the location of olivine (Mg-rich mineral) and wollastonite (Ca-rich mineral) all over the world.

Different minerals have also distinct CO_2 uptake capacities, because of their nature and chemical composition. R_{CO2} is defined as the theoretical mass (Kg) of a given material necessary to convert a unit mass (Kg) of CO_2 into carbonates. Values of R_{CO2} are reported in Table 2.1, together with average metal oxides composition of mineral rocks and their potential CO_2 storage capacity [2.24] [2.35]. Olivine is the mineral able to store CO_2 more efficiently (i.e. requiring less material) and, together with serpentine, has the biggest storage capacity, while for wollastonite the capacity is smaller.

Material	**Formula**	**MgO [wt%]**	**CaO [wt%]**	**FeO [wt%]**	**R_{CO2} [kg/kg]**	**CO_2 Storage Capacity [1000Gt]**
Olivine	Mg_2SiO_4	45-50	0.1-0.5	6-10	1.8	100000
Serpentine	$Mg_2Si_2O_5(OH)_4$	38-45	0	5-8	2.3	100000
Wollastonite	$CaSiO_3$	-	35-48	-	3.6	Small

Table 2.1: Composition and storage capacity of mineral rocks [2.24] [2.35]

2.2.3 Waste materials for mineral carbonation

Alternatively to minerals, a wide range of waste materials have the chemical composition (i.e. rich in alkali earth metals) required for their utilization as feedstocks for mineral carbonation. They can be divided into different categories: metal waste streams (obtained from metal manufacturing industry), construction sector waste and ashes from combustion processes. The following sections present the production process and characteristics of each category, focusing on their suitability for mineral carbonation. Table 2.2 summarizes the origin and the main qualitative information about Ca content of the different waste streams. All the waste materials identified are mainly rich in calcium oxides, while minerals previously described (Section 2.2.2.1) are predominately formed by Mg silicates.

Waste stream	Waste origin	CaO [wt%]
Air Cooled Copper Slag and Water Cooled Copper Slag	Residues obtained during the smelting and refining of copper	0.6-10.9
Ground granulated blast furnace slag	Obtained from production of pig iron in blast furnaces	15-41
Steel slag	Obtained from the manufacturing process of steel from pig-iron	25-55
Recycled concrete aggregate	Obtained from demolition operations	17
Cement kiln dust	Obtained from portland cement and lime high-temperature rotary kiln production operations	31-44
Incinerator Sewage Sludge Ash	Derived from the processing of sewage from various sources	30
Pulverized fuel ashes	Produced in coal fired power plants from the burning of pulverized coal	1-40
Biomass and wood ash	Residues from combustion of biomass for power generation	24-46
Municipal waste incinerator bottom ashes	Residues from combustion of waste in incineration plants	32-53
Red mud	Waste slurry obtained from the production of alumina from bauxite	2-8
Oil shale ashes	Residue from combustion of oil shale	42-50
Air pollution control residues	Produced from cleaning gaseous emissions generated during combustion of wastes at incineration plants	50-60
Paper sludge incinerator ash	Obtained from incineration operation of the waste residue of the paper production process	45-69

Table 2.2: Origin and qualitative composition of suitable waste streams for mineral carbonation

2.2.3.1 Metal waste streams

Copper slag is the residue obtained during the smelting and refining of copper. The slag is cooled from approximately 1300°C to ambient temperature and this can happen in either air or in water baths, producing either Air Cooled Copper Slag (ACCS) or Water Cooled Copper Slag (WCCS), respectively. Each of these slags has slightly different characteristics. When the high temperature slag is cooled slowly in air, it forms a dense, hard crystalline product while pouring molten slag into water produces a granulated amorphous slag with slightly less calcium and magnesium oxides present [2.37]. CaO and MgO content in copper smelt slag have been reported in the range 0.6-10.9wt% and 0.75-3.7wt% [2.38] respectively. Phosphorus slag (PS) is the residue obtained from the

production of phosphorus smelting. PS tends to be black to dark gray, vitreous (glassy), and of irregular shape. CaO content in phosphorus slag is around 44wt% [2.39].

Ground granulated blast furnace slag (GGBS) is a by-product material obtained from production of pig iron in blast furnaces. The production process produces glassy aggregate granules rich in CaO (15-41wt% [2.40]). Steel slag (SS) is the by-product obtained from the manufacturing process of steel from pig-iron. There are mainly two types of SS: basic oxygen furnace slag (BOF) and electric arc furnace (EAF) slag, generated depending on the type of furnace employed for steel production. Typical SS composition includes CaO between 25-55wt% [2.39].

2.2.3.2 Construction sector waste streams

Recycled concrete aggregate (RCA) is the main waste stream of this category. Obtained from demolition operations, its quality depends on the separation process RCA undergoes. Typical CaO content of samples from UK is 17wt% [2.41].

Cement kiln dusts (CKD) are fine by-products of portland cement and lime high-temperature rotary kiln production operations. CKDs are captured in the air pollution control dust collection system. CaO content in this waste stream can vary between 31-44wt% [2.39].

2.2.3.3 Ashes from combustion processes

Incinerator Sewage Sludge Ash (ISSA) is the end line product derived from the processing of sewage from various sources. Sludge ash is a silty-sandy material which could have 30wt% CaO content and 3wt% MgO [2.42].

Pulverized fuel ashes (PFA, fly ashes) are produced in coal fired power plants from the burning of pulverized coal. Fly ashes consist of fine, powdery particles and are mostly glassy (amorphous). Composition of PFA varies depending on several factors like type and rank of the coal burned and type of burner. CaO content may vary from 1wt% in bituminous coals up to 40wt% in lignite coals [2.39].

Biomass and wood ash are residues from combustion and consist of fine powdery particles mostly amorphous. Chemical composition vary depending on the nature of biomass and wood burned with CaO content values between 24-46wt% [2.43].

Municipal waste (MW), before landfilling, is usually treated in incinerators plants where its volume is reduced. The final solid product obtained are municipal waste incinerator bottom ashes which have a highly variable composition depending on the nature of the waste material burned. Their CaO composition may vary between 32-53wt% [2.43] [2.44] [2.45].

2.2.3.4 Other materials

Other minor waste streams including red mud, oil shale, air pollution control residues and paper sludge have interesting chemical composition for mineral carbonation and have been previously investigated as outlined in this section. Red mud is a waste slurry obtained from the production of alumina from bauxite. Digestion of bauxite into a sodium and calcium hydroxide solution produces two different streams: alumina liquor for further processing and a highly alkaline slurry called red mud [2.46]. Red mud chemical composition may include Al_2O_3 (10-20wt%) and CaO (2-8wt%) [2.47]. Oil shale ash is the residue from combustion of oil shale, a low quality carbonaceous fossil fuel, for power production. The CaO content of oil shale ash can be between 42-50wt% [2.48] [2.49]. Air pollution control residues are produced from cleaning gaseous emissions generated during combustion of wastes at incineration plants. Typical CaO content ranges between 50-60wt% [2.50] [2.51]. Finally, paper sludge incinerator ash may be considered an interesting waste material for mineral carbonation. It is obtained from incineration operation of the waste residue of the paper production process and its CaO content may vary between 45-69wt% [2.43].

2.2.4 Advantages, challenges and cost of mineral carbonation

Mineral carbonation presents several advantages as described below. The mineralization reaction, which involves a pure metal oxide, requires no energy input, but also produces energy releasing heat (exothermic reaction, Section 2.2.2) [2.21]. Furthermore, the required feedstocks are abundant; minerals rich in magnesium and calcium can be easily found in rocks present on the earth surface, and therefore, mineral carbonation has got a vast potential for carbon sequestration (Section 2.2.2.1). Moreover, mineralization is the only form, together with agri-char, of permanent carbon sequestration. Geological

storage options may, potentially, leak over time and require accurate monitoring systems [2.21]. Finally, the carbonated end products could be a suitable revenue stream because they can be used as building materials, as partial substitutes of cement in concrete production [2.52] and in paper, chemical and textile industries and other industrial processes [2.53].

However, despite the advantages listed above, mineral carbonation suffers from a range of technical and economic barriers for further development and large-scale demonstration. Firstly, there is the high energy demand for pre-treatment of virgin minerals, including mining, crushing and grinding to prepare the material for the mineral carbonation reaction [2.3]. Secondly, the slow reaction rates, particularly for direct gas-solid reactions. In fact, gas-solid reactions are feasible only at high pressure and temperatures (as seen in Section 2.2.1) for rare pure calcium and magnesium oxides or hydroxides [2.54]. Finally, the management of by products; if the end products cannot be employed for any application, the most convenient place for their disposal would be mining sites. However, the average amount of materials to be disposed is about 50-100% by volume more of the raw material and therefore they must be stored in an environmentally suitable location [2.3].

Recently a few papers have reported costs of mineral carbonation and they are summarized here. O'Connor et al. estimated a cost of 54, 68, 74$/$tCO_{2\ avoided}$ (£33, 41, 45/$tCO_{2\ avoided}$) for olivine, serpentine or wollastonite, respectively [2.55]. These costs refer only to the mineralization process, therefore cost for capture and transport must be added (about £30-36/tCO_2 [2.21]) bringing the overall cost to £63-81/$tCO_{2\ avoided}$. Newall et al. estimated the cost of mineral sequestration process at 60-100$/$tCO_{2\ avoided}$ (£36-61/$tCO_{2\ avoided}$) [2.56] and this cost must be added to the cost for the capture and transport (about £30-36/tCO_2 [2.21]) bringing the technology to £66-97/$tCO_{2\ avoided}$. Huijgen et al. estimated a similar cost for mineral sequestration technology (using wollastonite) of 102€/$tCO_{2\ avoided}$ (62£/$tCO_{2\ avoided}$) [2.57]. In this case, the cost of capture and transport must also be added (£30-36/tCO_2), bringing the overall cost to £92-98/$tCO_{2\ avoided}$. Gerdemann et al. reported a cost of 112$/$tCO_{2\ avoided}$ (£68/$tCO_{2\ avoided}$) using wollastonite for their mineralization experiments [2.58].

All these cost evaluations agree that a tonne of CO_2 sequestered by mineralization (considering also cost of capture and eventual transport from the CO_2 production site to

the mineralization plant) ranges between £75-110/$tCO_{2\ avoided}$ and therefore costs are currently considered not competitive with those of CCS geological storage (£50-75/$tCO_{2\ avoided}$, Section 2.1.2) [2.59].

2.2.5 Environmental issues for mineral carbonation

Mineral carbonation processes, especially if carried out at large scale, may present several environmental issues. Firstly, the impact which can have large scale mining operations. If natural ores are employed as feeding material for large scale mineralization operations, significant mining operations are required. This would affect the natural environment/landscape and increased pollution due to transportation of feedstock/products. Secondly, the disposal/utilization of the carbonated materials must be considered. Carbonated products may be returned to the mineral ore mines but, because carbonated materials have a volume about 50-100% more than the raw material [2.3], if not re-used, a suitable location for their disposal must be found. Instead, if valuable products can be obtained from the process, no need of disposal will be required and a revenue stream can be generated. However, if mineralization was to be implemented on large scale, the production of large quantities of carbonated materials would over-saturate any potential market. Thirdly, the use of chemicals also needs to be assessed. Multi-step processes, presented in Section 2.3.3, in general employ chemicals for the extraction of metals from the feeding material. Some acids may be lost in the process (e.g. by products, effluent liquids) even if the process itself has been designed to recycle them completely. Furthermore, the need of replenishing the acids lost in the process involves extra energy and resources consumption due to their production process.

2.3 State-of-the-art in research on mineral carbonation

Several mineral carbonation technologies have been reported and they are presented in this section. The feeding material is usually pre-treated to increase its reactivity and there are different methods available, namely size reduction, heat activation and surface activation. Once the material is ready for mineralization reactions, there are different mineral carbonation technologies available and they can be divided (Figure 2.8) into direct carbonation (also called single-step processes) and indirect carbonation (known also as multi-step processes).

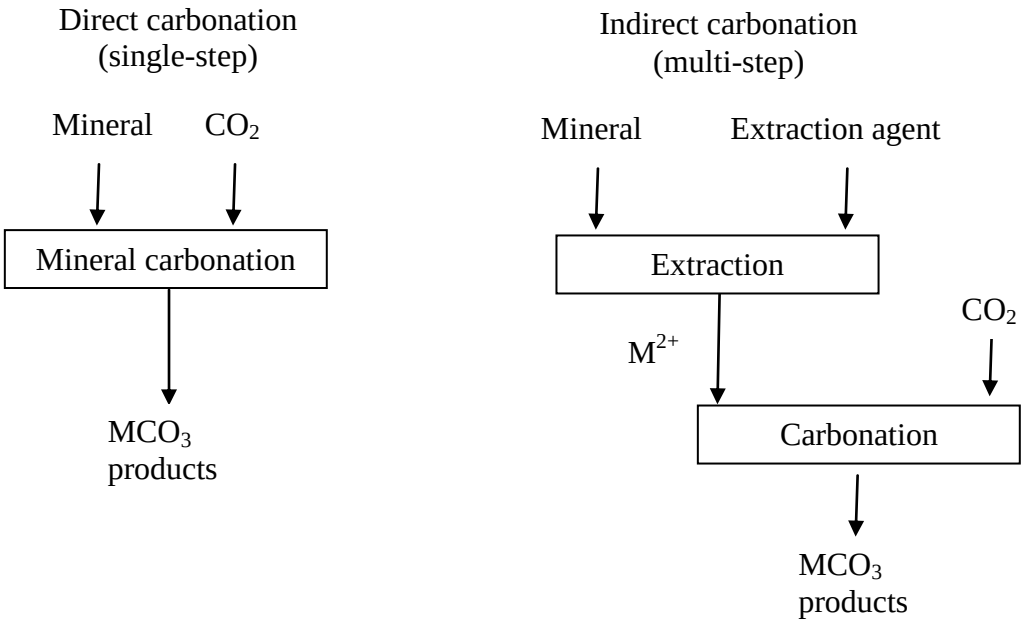

Figure 2.8: Direct (single-step) and indirect (multi-step) mineral carbonation processes

Single-step processes involve the reaction of feedstock material with CO_2, which is usually injected in a reactor maintained at a controlled temperature and pressure. During the process, carbonation takes place as aqueous or gas-solid reaction, depending whether water is introduced or not. In contrast, multi-step processes using chemicals, firstly extract the reactive fraction (e.g. pure metal oxide) from the feedstock, and secondly react it with CO_2 [2.60]. Table 2.3 lists different processes, which are described in the next Sections (2.3.2, 2.3.3), including also their main characteristics.

Several specific terms are employed to compare the different mineral carbonation processes. The most used are:

- extraction efficiency (%) represents how much of the initial metallic component (Mg, Ca, Fe) is extracted from the feedstock for the following carbonation step in multi-step processes.

- Carbonation efficiency (%) is used to quantify how much of the initial metallic component (Mg, Ca, Fe) is converted into metal carbonate.

- CO_2 conversion efficiency (%) indicates how much of the CO_2 employed for a mineral carbonation reaction is converted into metal carbonate.

Mineral carbonation process routes		
Single-step	Gas-solid	-Minerals react directly with gaseous CO_2 -Simplest mineralization method -Very slow for practical applications
	Aqueous	-Mineralization reaction happens in an aqueous solution -Pre-treatment of feedstock required to increase efficiency
Multi-step	HCl extraction	-Metal ion extracted by HCl and precipitated as hydroxide -Recovery of HCl -Energy intensive
	Molten salt	-Molten magnesium chloride salt used to extract metal ions -Metal ions precipitated as hydroxides -Energy intensive
	Other acids extraction	-Several acids used to extract metal ions from feedstock -High extraction efficiencies achieved (up to 100%) -Recovery of acids needed for the processes to be economically viable
	Bioleaching	-Bacteria combined with acid generating substances and silicate minerals extract metal ions -Low conversion rates -Passive and inexpensive carbonation route
	NaOH	-NaOH used to extract metal ions from feedstock -Energy intensive and long reaction time
	Ammonium salts	-Ammonium salts (e.g. NH_4HSO_4) used to extract metal ions from silicate rocks -Ammonium salts recovery -Low stoichiometric carbonation rate

Table 2.3: Summary of mineral carbonation process routes (modified [2.60])

Mineral carbonation becomes more economically viable if the final products are relatively pure and represent a potential revenue stream [2.13] (Section 2.4). Single-step processes, which react the feedstock directly with CO_2, have the disadvantage of producing slurries containing a mixture of different phases. The final product could be disposed with extra costs (e.g. management, transport, landfill) or needs further treatment (and energy consumption) to obtain pure final products. Multi-step processes,

instead, allow the production of different streams of high quality products. However, the multi-step processes require addition of chemicals and swing of operating conditions, which increase the energy consumption and cost related to the process.

The following sections describe pre-treatment techniques, i.e. size reduction, heat activation and surface activation (Section 2.3.1), while single and multi step-processes are presented in Sections 2.3.2 and 2.3.3, respectively.

2.3.1 Pre-treatment options

The most common pre-treatment technique is size reduction by grinding. The feedstock is grounded to a fine particle size before being used in the mineralization process in order to increase the surface area. Huijgen et al. investigated the effect of particle size on the efficiency of carbonation and found that when reducing the particle size from <7mm to <38μm, the efficiency increased from 12% to 60%, respectively [2.61]. O'Connor et al. also found that reduction of particle size, from 106-150μm to <37μm, increased conversion of CO_2 into carbonates, from 10% to 90% [2.62]. Despite the benefit on improving the efficiency of carbonation, grinding requires energy and causes extra CO_2 emissions. For example, grinding wollastonite from 0.1m to <38μm requires 56kWh/t, while for freshly produced steel slag (from 0.02m to <38μm) 31kWh/t are required [2.63]. The target for the UK Government is to achieve average emissions of 50gCO_2/KWh from electricity generation in 2030 while the level in 2008 was 500gCO_2/KWh [2.64]. Therefore, for the year 2014, producing 1kWh of electricity emits 380gCO_2, consequently, 21KgCO_2 and 12KgCO_2 would be emitted for every tonne of grinded wollastonite and steel slag, respectively.

In addition to size reduction, there are other pre-treatment options to increase the carbonation rate of a material. Heat activation can remove the hydroxyl (OH) groups. For example, when serpentine is heated at 600-650°C, OH groups evaporate:

$$Mg_3Si_2O_5(OH)_4 \rightarrow Mg_3Si_2O_5 + 4OH \quad (2\text{-}7)$$

Consequently, an open crystal structure is created [2.62] with enhanced reactivity (thanks to increased amount of reactive surface) for mineral carbonation, as observed experimentally [2.62]. As for mechanical treatment, also heat activation requires a

substantial amount of energy, in the range of 200-250kWh/t, 293kWh/t and 326kWh/t of material treated for serpentine, antigorite and lizardite serpentine, respectively [2.24] [2.26]. Surface activation, known also as chemical activation, instead increases the surface area of a material by reacting it with chemicals, steam or a combination of the two. For example, Maroto-Valer et al. increased the surface area of a serpentine sample from $8m^2/g$ to $330m^2/g$ activating it with sulfuric acid [2.26]; this process is similar to the first phase of the multi-step carbonation process presented in detail in section 2.3.3.1. However, chemical activation presents environmental issues unless the process is able to recover and reuse the large amounts of chemicals employed.

In conclusion, all pre-treatment options suffer from important drawbacks and so far size-reduction has been the process mostly employed.

2.3.2 Single-step processes

Single-step mineralization processes have the advantage of requiring a simple experimental set-up and do not need high quantity of reagents. Single-step processes can take place in either aqueous or gaseous phase and may involve feedstock pretreatment (e.g. size reduction), but not extraction of metal ions before carbonation.

2.3.2.1 Direct gas-solid reactions

The gas-solid reaction (2-1) is the most basic mineralization process and to increase its kinetics, high temperature and pressure are required (e.g. 300°C, 340bar [2.22]). However, increasing the temperature has a thermodynamic limit because the chemical equilibrium favors gaseous CO_2 over solid-bound CO_2 at high temperature [2.17]. This means that over a certain temperature, CO_2 is present as a gas and cannot be bound in any carbonated form. The maximum temperature at which mineralization can occur depends on CO_2 pressure and type of mineral (Table 2.4) [2.17]. Increasing the pressure, the maximum temperature also raises and it is interesting to notice that olivine and wollastonite present a lower maximum mineralization temperature (281°C and 241°C respectively) compared to serpentine (407°C).

The gas-solid approach was the first to be studied because of its design simplicity [2.17] and a 30% serpentine conversion efficiency was reported at 300°C, 340bar [2.22].

However, even under such high temperature and pressure, the processes are very slow (several days [2.22]).

Mineral	Tmax [°C]	p CO_2 [bar]
Calcium oxide	888	1
	1397	200
Magnesium oxide	407	1
	657	200
Calcium hydroxide	888	1
Magnesium hydroxide	407	1
Wollastonite	281	1
Olivine	242	1
Serpentine	407	1

Table 2.4: Maximum carbonation temperatures at corresponding pressure for several minerals [2.17]

Direct carbonation of pure metal oxides has instead been focusing on capture of CO_2 (instead of storage). This is because pure metal oxides are not widely available in nature and the impact of this process on the capacity for storing CO_2 would be rather small. The process, know as chemical-looping, allows capturing CO_2 from flue gases at relatively low temperature (200-300°C) forming Ca/Mg carbonates that decompose at 600-900°C and release a pure stream of CO_2 [2.60].

2.3.2.2 Direct aqueous carbonation

Direct aqueous mineral carbonation reacts CO_2 with silicate minerals in an aqueous suspension in a single step. The process is faster than the gas-solid reaction (few hours instead of few days [2.22] [2.55]) and it consist of three reactions which happen simultaneously. Firstly, carbon dioxide dissociates in water into H^+ and $HCO3^-$:

$$CO_2(g) + H_2O(l) \rightarrow H^+(g) + HCO_3^-(g) \quad (2\text{-}8)$$

The equilibrium constant of the reaction at 25°C is 1.7×10^{-3}, meaning that CO_2 has low solubility in water, remaining mainly as CO_2 molecules. As a consequence, the pH of the solution is only marginally affected by the reaction. Dissolution of CO_2 into water varies depending on temperature and pressure (Figure 2.9).

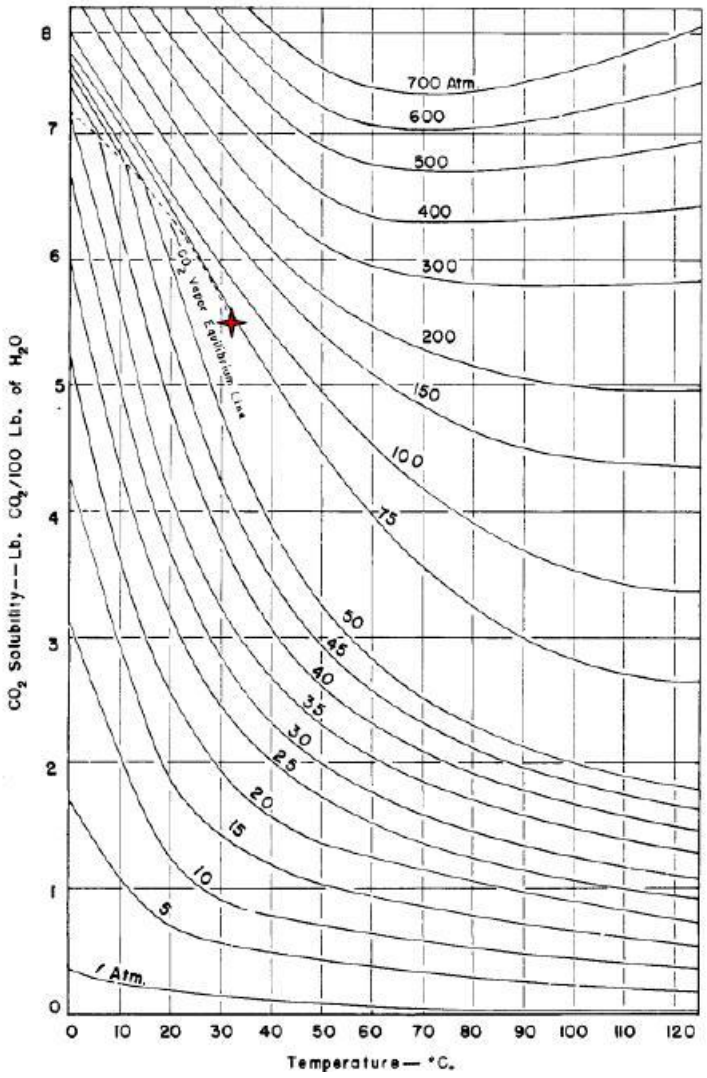

Figure 2.9: Solubility of CO_2 in water as function of temperature and pressure [2.65]

After dissolution of CO_2 in H_2O, Ca/Mg ions are extracted from the Ca/Mg silicates thanks to the protons H^+:

$$Ca/Mg\ silicates\ (s) + 2H^+(aq) \rightarrow (Ca/Mg)^{2+}(aq) + SiO_2(s) + H_2O(l) \qquad (2\text{-}9)$$

Finally, calcium or magnesium carbonates precipitate:

$$(\mathrm{Ca/Mg})^{2+}(\mathrm{aq}) + \mathrm{HCO_3^-} \rightarrow (\mathrm{Ca/Mg})\mathrm{CO_3}(\mathrm{s}) + \mathrm{H^+}(\mathrm{aq}) \qquad (2\text{-}10)$$

Usually, the rate limiting step of the direct aqueous mineralization processes is the leaching of Mg/Ca ions from the silicate minerals [2.66]. However, under certain process conditions (e.g., high temperature and/or low CO_2 pressure), the carbonation

may become limited by inhibition of growth or suppression of nucleation of the carbonate [2.66]. Park et al. have reported that the dissolution step of the alkaline earth metal no longer controlled the overall reaction rate, but the dissolution of CO_2 was the rate-limiting step [2.32]. Moreover, the formation of a layer of silica on the particle surface can reduce dissolution of Ca and Mg [2.29]. In fact, while Ca and Mg dissolve and go into solution, silica does not react and remains in a solid form, creating a layer which reduces further dissolution of metals present into the core of the particle.

One of the most known studies of this carbonation route was carried out at the Albany Research Centre, USA (Figure 2.10) [2.62]. Magnesium silicate rocks were firstly crushed, then grinded (<37μm), and the resultant fine particles were then carbonated using compressed CO_2 in a reactor employing distilled water or a 0.5M $NaHCO_3$ solution.

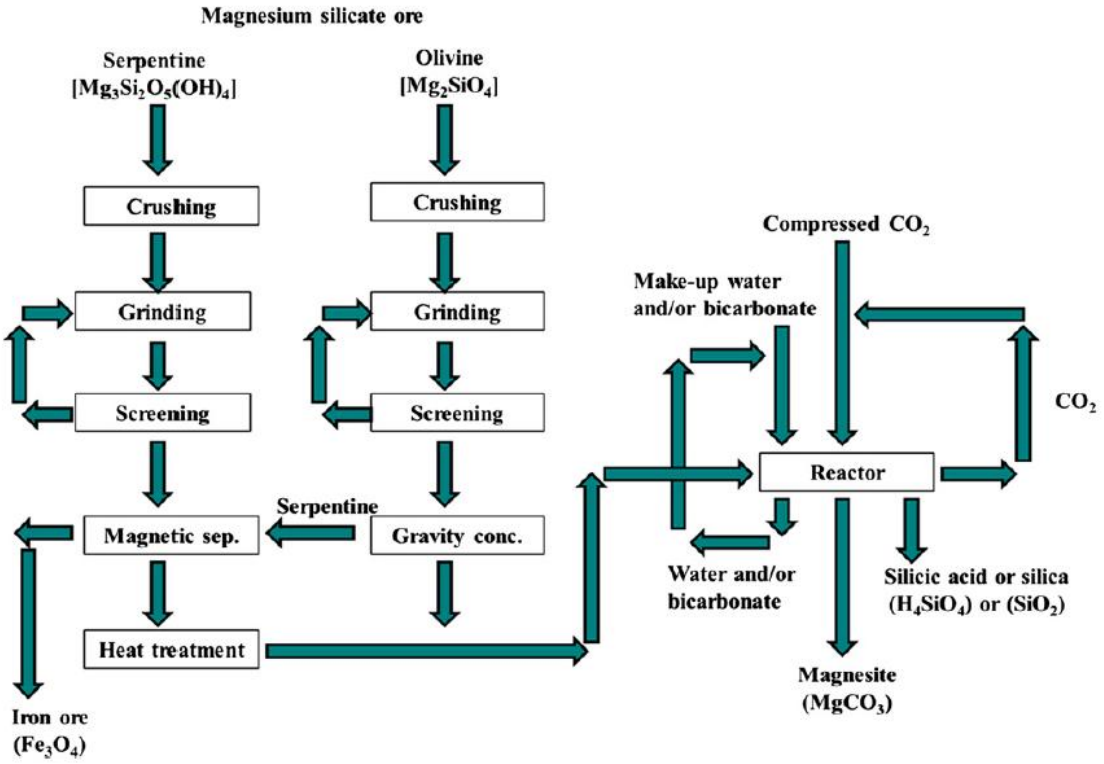

Figure 2.10: Flow diagram of the ARC direct aqueous mineral carbonation process [2.62]

Carbonation conversion of 90% was achieved for olivine in 24h using a distilled water solution at 185°C, 115bar. Maintaining the same experimental conditions, using instead a $NaHCO_3$ solution, a 84% conversion efficiency was achieved in 6 hours. Further

studies from the same research group showed that increasing the temperature raises the reaction rate but causes a reduction in solubility of CO_2 into water. Therefore, based on the experimental data obtained, optimum temperature for olivine was found to be 185°C (152bar) and 155°C (116bar) for heat-treated serpentine [2.55] [2.67]. Furthermore, wollastonite was found to require lower pressure, compared to Mg silicate minerals, to obtain a substantial conversion, usually in the range 10-40bar instead of 100-175bar [2.55].

Direct aqueous carbonation can be accelerated by using a wide range of chemicals like $NaHCO_3$, HCl, H_2SO_4, NaOH [2.26] [2.32] [2.62] [2.68] and also by using pre-treatment techniques, as already discussed [2.60]. Many efforts have been carried out by adding expensive chemicals to increase conversion efficiency for aqueous direct mineralization. However, unless these chemicals can be recycled, the process looks like uneconomic to be implemented at large scale [2.68].

2.3.3 Multi-step processes

Multi-step processes carry out mineralization in more than one stage. Usually, metal ions (e.g. Ca^{2+}, Mg^{2+}, Fe^{2+}) are extracted from the silicate minerals using acids. Afterwards, the extracted components are reacted with gaseous or aqueous CO_2 to produce metal carbonates. Research in multi-step processes has been focusing on different routes aimed at increasing the efficiency of each step, as described in the following sections.

2.3.3.1 HCl extraction

This process is based on the use of a strong acid (HCl) for extracting the metals from the silicate minerals at ambient pressure. Considering serpentine, the first reaction at 100°C is as follows:

$$Mg_3Si_2O_5(OH)_4(s) + 6HCl(l) + H_2O(l) \rightarrow 3MgCl_2 6H_2O(aq) + 2SiO_2(s) \quad (2\text{-}11)$$

Then, raising the temperature at 150°C, HCl is regenerated and MgCl(OH) is formed:

$$MgCl_2 6H_2O(aq) \rightarrow MgCl(OH)(aq) + HCl(aq) + 5H_2O(\text{g}) \quad (2\text{-}12)$$

Afterwards, when cooling down the system, magnesium hydroxide is produced:

$$MgCl(OH)(aq) \rightarrow Mg(OH)_2(s) + MgCl_2(aq/s) \quad (2\text{-}13)$$

Finally, magnesium hydroxide is carbonated with CO_2:

$$Mg(OH)_2(s) + CO_2(g) \rightarrow MgCO_3(s) + H_2O(l) \quad (2\text{-}14)$$

Lackner et al. [2.17] proposed this process but this carbonation route suffers from some important drawbacks mainly the energy requirement for water evaporation [2.69]. It was demonstrated that water evaporation requires about 4 times the energy generated by the power plant producing the CO_2 sequestered [2.70]. Moreover, iron can also be extracted and precipitated, becoming a contaminant during the carbonation process [2.71]. Furthermore, employing HCl raises several economic issues, e.g. cost of the acid, requirement of corrosive resistant materials and environmental issues about supply and disposal of the acid.

2.3.3.2 Molten salt extraction

This process was developed in an attempt to reduce the energy requirement for HCl extraction process. The process is in fact very similar to the one presented in the previous section, but instead of using HCl, $MgCl_2 \cdot 3.5H_2O$ is employed [2.69] [2.71]. The first extraction reaction takes place at 200°C, as follows:

$$Mg_3Si_2O_5(OH)_4(s) + 3MgCl_2 \cdot 3.5H_2O(aq) \rightarrow 6MgCl(OH)(aq) + 2SiO_2(s) + 9.5H_2O \quad (2\text{-}15)$$

Afterwards, because of water addition which dilutes the solution, magnesium hydroxide is precipitated at 150°C:

$$MgCl(OH)(aq) + nH_2O \rightarrow Mg(OH)_2(s) + MgCl_2 \cdot nH_2O(aq/s) \quad (2\text{-}16)$$

The $MgCl_2$ solution is partially dehydrated at 250°C to recover the solvent:

$$MgCl_2 \cdot nH_2O(aq) \rightarrow MgCl_2 \cdot 3.5H_2O(aq) + (n - 3.5)H_2O \quad (2\text{-}17)$$

Finally, magnesium hydroxide is separated and carbonated:

$$Mg(OH)_2(s) + CO_2(g) \rightarrow MgCO_3(s) + H_2O \quad (2\text{-}18)$$

$MgCl_2 \cdot 3.5H_2O$ is a very corrosive chemical and even if it is recovered in the process, due to losses or inefficiencies, the need of replenishing the amount of $MgCl_2 \cdot 3.5H_2O$ would be commercially unaffordable [2.71]. Furthermore, normal industrial processes for producing $MgCl_2 \cdot 3.5H_2O$ are based on HCl. Therefore, the requirement of non-corrosive materials and appropriate disposal of liquid/solid effluents, make also this process, as that for HCl (Section 2.3.3.1), economically unattractive [2.71].

2.3.3.3 Other acid extractions

Indirect mineral carbonation processes have employed different acids for leaching metals from the silicate minerals. Wang and Maroto-Valer employed ammonium sulfate ($(NH_4)_2SO_4$), ammonium chloride (NH_4Cl) and sulfuric acid (H_2SO_4) for extracting Mg from serpentine. H_2SO_4 resulted of being the most efficient, achieving 47% Mg extraction efficiency at 70°C in 3 hours [2.29]. Teir et al. used acetic acid (CH_3COOH), sulphuric acid (H_2SO_4), nitric acid (HNO_3) and formic acid (HCOOH), as well as HCl. Using HNO_3 and HCl solutions, 100% Mg from serpentine was extracted at 70°C in 2 hours [2.27]. Kakizawa et al. [2.33] also used acetic acid but employing Ca silicate minerals instead of serpentine. In this process, acetic acid extracts Ca and precipitates silica.

$$CaSiO_3(s) + 2CH_3COOH(l) \rightarrow Ca^{2+}(aq) + 2CH_3COO^-(aq) + H_2O(l) + SiO_2(s) \quad (2\text{-}19)$$

Afterwards, the solution reacts with CO_2 to carbonate the calcium and regenerate the acetic acid [2.33].

$$Ca^{2+}(aq) + 2CH_3COO^-(aq) + CO_2(g) + H_2O(l) \rightarrow CaCO_3(s) + 2CH_3COOH(l) \quad (2\text{-}20)$$

A conversion of 20% was reported after 1 hour at 60°C and 1bar employing wollastonite [2.33]. In addition, an estimation of cost (about £120/$tCO_{2\ sequestered}$) was reported, considering the energy costs and the investment costs.

Maroto-Valer et al. proposed instead the use of sulphuric acid for the dissolution of Ca/Mg from the serpentine matrix according to the reactions below [2.72].

$$Mg_3Si_2O_5(OH)_4 + 3H_2SO_4 \rightarrow 3MgSO_4 + 5H_2O + 2SiO_2 \quad (2\text{-}21)$$

$$MgSO_4 + H_2O + CO_2 \rightarrow MgCO_3 + H_2SO_4 \quad (2\text{-}22)$$

The acid can also be recovered and re-used within the process and it is recognized that only recovering and reusing the chemicals employed would make mineralization processes economically feasible [2.27].

Park et al. demonstrated that enhanced Mg leaching from serpentine can be obtained adding a mixture of 1vol% orthophosphoric acid, 0.9wt% oxalic acid and 0.1% EDTA in the solution [2.32].

All these routes use a stirred vessel/reactor at the conditions described above. Firstly, the extraction of the metals takes place, followed by the carbonation. However, it must be stressed that, employing acids reduces the pH of the solution and therefore the precipitation of carbonates [2.73]. It was reported that optimum precipitation of magnesium carbonates happens when pH ranges between 8 and 9 [2.73] [2.74].

2.3.3.4 Bioleaching

This mineralization route aims to extract metals from silicate minerals utilizing bacteria [2.75]. In nature, rock weathering is enhanced by naturally produced organic and inorganic acids [2.76]. The combination of silicate minerals, acid generating substances (AGS) and specific bacteria accelerates the mineralization processes. In fact, known

bacteria can convert the added generating substances (e.g. sulfides and elemental sulfur) into sulfuric acid as a by-product of their metabolism [2.75]. Consequently, the sulfuric acid leaches out metal ions from the silicate mineral rock and the metals ions can then be carbonated for the purpose of CO_2 sequestration. In summary, the acid generating substances provide nutrients to the bacteria and the bacteria produce sulfuric acid which leaches out metal ions from the silicate rock (Figure 2.11). Furthermore, bacteria use atmospheric CO_2 for their biological processes (e.g. synthesis of new cell material), and, therefore, CO_2 from atmosphere is fixed also thanks to these activities [2.75] [2.77].

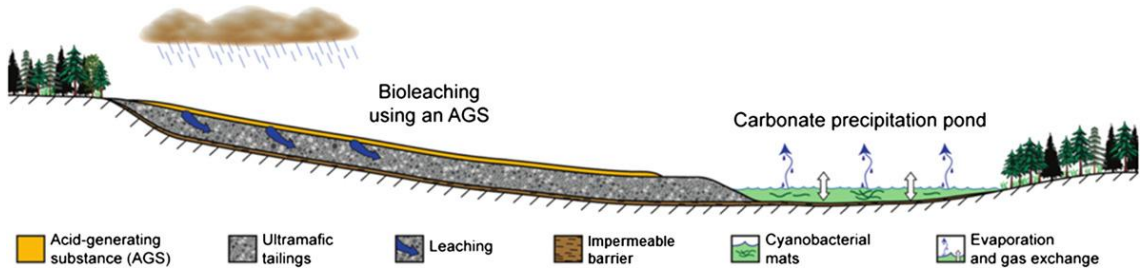

Figure 2.11: Bioleaching schematic picture for carbon sequestration in a geo-engineered tailing facility [2.77]

Bioleaching processes do not aim to achieve high leaching rates, because generation of acidic leachate in the environment must be avoided [2.77]. However, this carbonation route is favoured by some researchers because of its ability to use waste products (e.g. sulfur mine tailings) as acid source for accelerating mineral dissolution by bacteria for carbon sequestration [2.60].

2.3.3.5 NaOH extraction

Blencoe et al. developed this process which is based on using NaOH for the purpose of mineral carbonation employing Ca/Mg-rich feedstock [2.78]. The process is designed to take place at 200°C, p<15bar for 1-3days and the following reactions consider wollastonite as feeding material.

$$CaSiO_3(s) + NaOH(aq) \rightarrow NaCaSiO_3(OH)(s) \quad (2\text{-}23)$$

$$2NaOH(aq) + CO_2(aq) \rightarrow Na_2CO_3(aq) + H_2O(l) \quad (2\text{-}24)$$

$$Na_2CO_3(aq) + 3NaCaSiO_3(OH)(s) + H_2O(l) \rightarrow 4NaOH(aq) + CaCO_3(s) + NaCa_2Si_3O_8(OH)(s) \quad (2\text{-}25)$$

In a solution of NaOH, the silicate mineral reacts to form sodium calcium hydrosilicate (reaction 2-23), while NaOH also reacts with CO_2 to produce Na_2CO_3 (reaction 2-24). Finally, the two products of the reactions 2-23 and 2-24 together with H_2O produce NaOH to be re-used and $CaCO_3$ and $NaCa_2Si_3O_8(OH)$ to be disposed.

Major drawbacks for this process route are the reaction time (1-3 days) and the energy requirement for milling the feeding material (<10μm). In light of this, the process does not seem to be a promising technique for indirect mineral carbonation [2.60].

2.3.3.6 Ammonium salts extraction

Various ammonium salts have been investigated for multi-step mineralization processes. First to attempt this route, with the aim of production of silica from silicate minerals and not for storing CO_2, was Pundsack in 1967 [2.79]. Serpentine and ammonium hydrogen sulphate were employed to produce an intermediate product (magnesium sulfate) which then was reacted with ammonium bisulphate for the precipitation of magnesium carbonate. An analogue process was then developed by Park and Fan [2.28] and more recently by Wang and Maroto-Valer [2.29]. This last process aims at extracting magnesium from mineral rocks and producing different streams of useful by-products at ambient pressure. The overall process is a close loop, avoiding the use of new additives, recovering and reusing them at the end of the process (Figure 2.12 and Table 2.5).

In the first step, NH_3 is employed to capture CO_2 from flue gas to produce NH_4HCO_3. This step allows avoiding desorption and compression of CO_2, which is an energy intensive phase of amine-based capture technologies [2.80]. In the mineral dissolution step, 1.4M NH_4HSO_4 is used to extract Mg from serpentine ground to a particle size range 75-125μm. The Mg-rich solution is neutralized by NH_4OH addition, after which impurities in the leaching solution are removed by adding NH_4OH. In the carbonation step, Mg-rich solution reacts with the product from the capture step NH_4HCO_3 to precipitate carbonates. Since formation and stability of hydro-carbonates is temperature dependent, $MgCO_3 \cdot 3H_2O$ (nesquehonite) can convert to $4MgCO_3 \cdot Mg(OH)_2 \cdot 4H_2O$

(hydromagnesite) at temperatures above 70°C. Precipitation of hydromagnesite results in a solution that mainly contains $(NH_4)_2SO_4$. The final step is the regeneration of additives where $(NH_4)_2SO_4$ is heated up to 300°C to regenerate NH_3 for the capture process and NH_4HSO_4 to be reused in mineral dissolution.

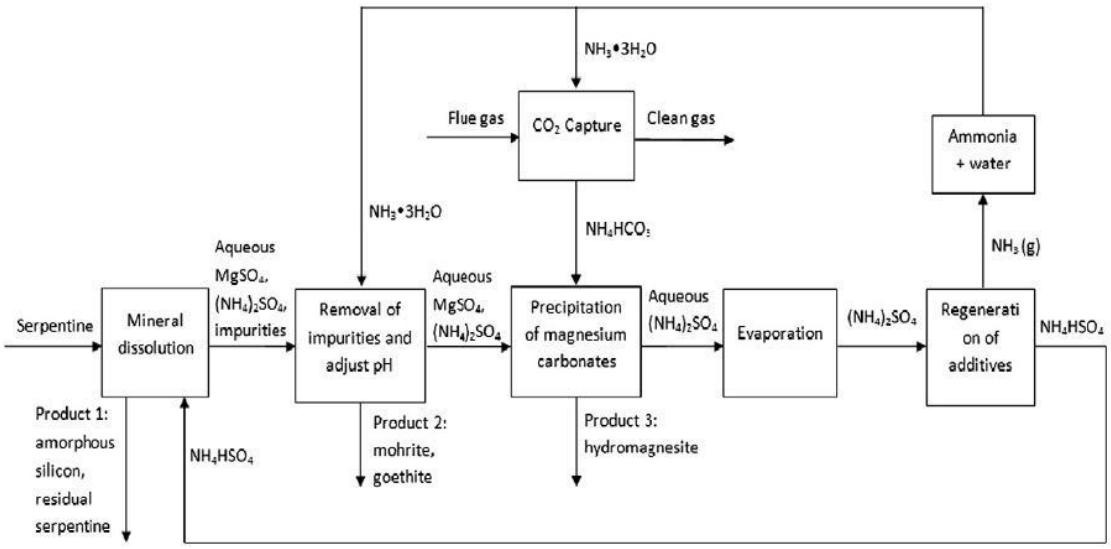

Figure 2.12: Flow diagram of the ammonium hydrogen sulfate mineralization process [2.29]

	Reaction equations	T (°C)	ΔH (kJ)	ΔG (kJ)
CO_2 capture	$NH_3 + CO_2 + H_2O \rightarrow NH_4HCO_3$	10	−127.0	−26.3
Mineral dissolution	$Mg_3Si_2O_5(OH)_4 + 6NH_4HSO_4 \rightarrow 3MgSO_4 + 2SiO_2 + 5H_2O + 3(NH_4)_2SO_4$	90	−141.1	−431.8
pH adjustment	$NH_4HSO_4 + NH_4OH \rightarrow (NH_4)_2SO_4 + H_2O$	25	−116.0	−134.4
Removal of impurities	$(Fe,Al,Cr)_2(SO_4)_3 + 6NH_4OH \rightarrow 2(Fe,Al,Cr)(OH)_3\downarrow + 3(NH_4)_2SO_4$	25	−673.0	−545.1
	$(Zn,Cu,Mn)SO_4 + 2NH_4OH \rightarrow (Zn,Cu,Mn)(OH)_2\downarrow + (NH_4)_2SO_4$	25	−191.4	−144.4
Carbonation	$MgSO_4 + 2NH_4HCO_3 \rightarrow Mg(HCO_3)_2 + (NH_4)_2\ SO_4$			
	$Mg(HCO_3)_2 + 2H_2O \rightarrow MgCO_3\ 3H_2O\downarrow + CO_2\uparrow$			
	Overall reaction			
	$MgSO_4 + 2NH_4HCO_3 + 2H_2O \rightarrow MgCO_3 \cdot 3H_2O\downarrow + (NH_4)_2SO_4 + CO_2\uparrow$	80	−6.6	−37.4
	Carbonate formation change			
	$5\ MgCO_3 \cdot 3H_2O \rightarrow 4MgCO_3 \cdot Mg(OH)_2 \cdot 4H_2O + CO_2\uparrow + 10H_2O$	80	69.5	−18.2
Regeneration of additives	$(NH_4)_2SO_4 \rightarrow NH_4HSO_4 + NH_3\uparrow$	300	111.6	90.4

Table 2.5: Chemical reactions and thermodynamic calculations for the ammonium hydrogen sulfate mineralization process [2.29]

Table 2.5 reports the ΔH (difference (Δ) in enthalpy (H)) between reactants and products, giving the heat required (endothermic reaction, $\Delta H>0$) for a reaction to happen or released (exothermic reaction, $\Delta H<0$). It can be noticed that all the reactions are exothermic with the exception of the regeneration of additives and the carbonate formation change. The Gibbs free energy (ΔG), also expressed in Joules, expresses if a

reaction happens spontaneously ($\Delta G<0$) or not ($\Delta G>0$) at a certain temperature and pressure. Therefore, the regeneration of additive reaction is the only non-spontaneous reaction in the process developed by Wang and Maroto-Valer (Table 2.5).

So far, optimization of the dissolution and carbonation steps for serpentine has been performed. Increasing the temperature of dissolution, extraction of magnesium from serpentine (and consequent formation of $MgSO_4$) raised up to 100% at 100°C in 3h [2.29]. Moreover, it was shown that adding NH_3 during the carbonation step improved the carbonation efficiency up to 95% conversion of Mg ions into hydromagnesite and the mass ratio $Mg/NH_4HCO_3/NH_3$ is the key factor controlling carbonation with an optimum ratio of 1:4:2 [2.14].

Sequestering CO_2 into serpentine using this process requires that the CO_2 emission source would be located near to the serpentine mining region and a NH_3 production site. Otherwise, transportation of NH_3 gas to the CO_2 emission source and NH_4HCO_3 to the CO_2 storage site would increase costs. Sequestering 1kmol of CO_2 in the capture step releases 0.5kmol of CO_2 in the overall carbonation reaction and 0.1kmol of CO_2 in the carbonate formation change (Table 2.5). Therefore, the CO_2 sequestration efficiency for single-pass stoichiometric conversion is lowered to 40% (1kmol of CO_2 sequestered, while 0.6kmol released), reducing considerably the theoretical storage capacity of the process.

An overall economic assessment of this process has not been carried out yet. Production of different streams of products would help in reducing costs as they may have market value. However, employing ammonia and ammonium salts, which are corrosive, involves using suitable material for the reactors and piping systems, increasing the cost of the technology. Moreover, impact of water employed on the economy of the process should also be considered. In fact, 4.9 and 16t/h of serpentine and water, respectively, are required to sequester 1t/h of CO_2 [2.81].

2.3.4 Mineral carbonation using waste materials

A large number of mineral carbonation studies has been carried out using minerals as their source of metal oxides. Lately, new investigations have indicated that industrial wastes require a lower degree of pre-treatment and less energy intensive carbonation

conditions, in comparison to raw minerals [2.82]. Many different industrial waste materials with suitable characteristics (i.e. rich in Ca, Mg oxides) have been investigated as feedstock for mineral carbonation, employing different processes. A summary is reported in Table 2.6 and they are discussed in the following sections.

Despite the large number of industrial waste streams investigated for mineral carbonation, only few studies have considered the economics of the processes. Mineral carbonation for steel slag costs have been reported to be 77€/$tCO_{2\ avoided}$ (£65/$tCO_{2\ avoided}$) [2.57], which is about 25% less than the cost estimated for mineralization of raw minerals (£75-110/$tCO_{2\ avoided}$, Section 2.2.4). This is mainly due to the fact that many industrial wastes are already available in appropriate particle size for mineral carbonation or require less grinding operations than mined ores [2.58] and they do not require any mining operation. It is also interesting to underline that the use of waste materials as feedstock for mineralization avoids the disposal requirements for such materials, transforming them into a potential revenue resource instead of a costly waste stream.

Waste category	Waste stream	Carbonation route and parameters	Experimental results	Reference
Municipal solid waste ashes	Air pollution control fly ashes	Single step-Aqueous carbonation-room temperature and pressure, 2-24h, L/S ratio 0.1-0.25-0.5l/Kg	At L/S 0.25l/Kg, 12% weight gain	[2.45]
	Air pollution control fly ashes	Single step-Aqueous carbonation-room temperature, 3bar, 3h, L/S 0.1-0.8l/Kg	At L/S 0.3l/Kg, 11% weight gain	[2.83]
	Air pollution control fly ashes	Single step-Aqueous carbonation-30-50°C, 1-10bar, 10min-48h, L/S ratio 0.02-0.6l/Kg	At L/S 0.2l/Kg, 30°C, 3bar, 1h, 25% weight gain	[2.84]
	Bottom ashes	Single step-Aqueous carbonation-30-50°C, 1-10bar, 30min-48h, L/S ratio 0-0.6l/Kg	At L/S 0.3l/Kg, 30°C, 10bar, 8h, 14% weight gain	[2.85]
Coal fly ashes	Coal fly ashes	Single step-Aqueous carbonation-155-185°C, 75atm (75bar), 1h, 100rpm	At both temperatures 50% weight gain	[2.86]

Waste category	Waste stream	Carbonation route and parameters	Experimental results	Reference
	Coal fly ashes	Single step-Aqueous carbonation-30-60°C, 10-40bar, 0-18h, L/S ratio 6.67-20l/Kg, 450rpm, 40µm	At 30°C, 18h, no pressure and temperature influence, 2.6% weight gain	[2.87]
Construction sector	Waste cement	Single step-Aqueous carbonation-room temperature, 0.9-3Mpa (9-30bar), 0-120min, S/L ratio 0.29-2.9wt% (2.9-29g/l), 900rpm, 100µm	At S/L 2.9wt% (29g/l), 3MPa (30bar), 120min, 30% Ca extraction	[2.88]
	Waste cement	Single step-Aqueous carbonation-room temperature, 5bar, 2h, L/S ratio 0.15l/Kg	14% weight gain	[2.89]
	Cement kiln dust	Single step-Aqueous carbonation-room temperature and pressure, 0-8days, L/S ratio 0-1.25l/Kg	At L/S 1.25l/Kg, 8 days, 80% carbonation efficiency	[2.90]
Metal wastes	Ground granulated blast furnace slag	Single step-Aqueous carbonation-room temperature, 5bar, 2h, L/S ratio 0.15l/Kg	7% weight gain	[2.89]
	Steel slag	Single step-Aqueous carbonation-25-225°C, 1-30bar, 2-30min, L/S ratio 2-20l/Kg, 100-2000rpm, 0-500µm	At 225°C, 30bar, 30min, 2000rpm, L/S 20l/Kg, <38µm, 74% carbonation efficiency	[2.91]
	Steel slag	Single step-Aqueous carbonation-28-150°C, 0.1-4MPa (1-40bar), 3-700h, L/S ratio 10l/Kg	At 150°C, 4MPa (40bar), 700h, 90% conversion efficiency	[2.13]
Other wastes	Oil shale ash	Single step-Aqueous carbonation-room temperature and pressure, 0-100min, 100rpm, 34-47µm	17-20% CO_2 bound	[2.48]
	Paper sludge ash	Single step-Aqueous carbonation-room temperature and pressure, 3-24h, L/S ratio 20l/Kg	30% conversion efficiency	[2.13]
	Red Mud	Single step-Aqueous carbonation-room temperature and pressure, 72h, <160µm	26% CO_2 bound	[2.47]

Table 2.6: Summary of mineral carbonation processes for waste materials

2.3.4.1 Mineral carbonation of municipal solid waste incinerator ashes

Production of municipal solid waste (MSW) is a global environmental problem and incineration is a common management option when recycling and re-using are not possible. When incinerated, mass reduction for waste ranges between 65-70% and ashes are produced from the combustion.

Wang et al. (2010) studied mineralization of MSW fly ashes and the effect of liquid to solid (L/S) ratio and reaction time [2.45]. Experiments were carried out at room temperature in a glass beaker, L/S ratio tested were 0.1, 0.25, 0.5 and reaction times were from 2 to 240h. Based on the weight gain of the sample, the best L/S ratio was 0.25 but most importantly it was found that mineral carbonation is a convenient pre-treatment method before ash landfilling. In fact, mineralization reduces leaching heavy metals from samples [2.45].

Li et al. in 2007 investigated the utilization of fly ashes from combustion of MSW in an accelerated carbonation step [2.83]. The efficiency of the reaction between ash and CO_2 was examined by measuring the weight increase between the initial dry powder and the dried final product. The authors used two different reactors. The first was a stainless steel chamber which could examine the influence of temperature on the reaction; a layer of ashes and water was placed in the reactor and then mixed CO_2 and N_2 were injected (3bar pressure). The measured pressure in the reactor allowed calculating the consumption of CO_2. The second reactor, which was employed to assess the optimum L/S ratio for carbonation, was a closed chamber containing 100%CO_2. Different values of L/S ratio were tested. Samples were carbonated for 3h at a pressure of 3bar. Results showed that the optimum carbonation reaction was achieved at ambient temperature and L/S ratio of 0.3l/Kg [2.83].

Baciocchi et al. (2009) investigated the carbonation of air pollution control residues fly ashes from a MSW incinerator. A 150ml stainless steel reactor was employed and different temperatures (30°C, 40ºC and 50ºC), CO_2 pressures (1, 3, 5, 7 and 10bar), L/S ratios (0.02, 0.1, 0.2, 0.4 and 0.6l/Kg) and reaction time (from 10min to 48h) were investigated. The ashes used in this study showed good reactivity with CO_2, due to the large content of calcium hydroxides. Under reaction conditions of L/S ratio 0.2-0.02l/Kg and temperature of 30-50°C, high CO_2 uptake capacities of over 250g/kg of residue were achieved in less than 1h using 100%CO_2 at 3bar [2.84]. Baciocchi et al.

in 2010 also investigated the effects of carbonation on the characteristics of bottom ash from refuse derived fuel (RDF). The carbonation tests performed assessed the influence of temperature, CO_2 pressure and L/S ratio. CO_2 pressure was observed to be the most important parameter. Keeping constant the particle size (0.425–0.150mm), the best result (14%CO_2 uptake capacity) was achieved with the highest pressure (10bar) at temperature of 30°C, L/S ratio of 0.3l/Kg, and 8h running time [2.85].

2.3.4.2 Mineral carbonation of coal fly ashes

Coal fly ashes are by-products from the combustion of coal during electrical production in power plants. Fauth et al. (2002) investigated fluidized bed ashes as feedstock for mineral carbonation. Their experiments were carried out in a continuous stirred tank reactor at two different temperatures (155°C and 185°C) and CO_2 pressure 75bar for 1 hour. Fly ashes were mixed in the reactor with water and an aqueous bicarbonate solution (0.5M Na_2CO_3/0.5$NaHCO_3$, 1MNaCl); For both temperatures, efficiency of carbonation achieved was 50% [2.86].

Montes-Hernandez et al. (2009) researched the use of coal fly ashes to sequester CO_2 by carbonation in a 2l reactor. In their experiments the effect of solid to liquid (S/L) ratio (6.67, 10, 20l/Kg), CO_2 pressure (10, 20, 30 and 40bar), reaction temperature (ambient, 30°C and 60°C) and reaction time (0-18h) were investigated. The carbonation efficiency was calculated considering the consumption of CO_2 in the reactor during the experiments. Results showed that pressure did not affect the carbonation efficiency and this seems to be contradictory with results from Baciocchi et al. and Huijgen et al. [2.84] [2.91]. This is probably because CO_2 pressure range investigated by Montes-Hernandez was higher (10-40bar) compared to the other two studies (1-10bar, 1-30bar) which instead observed the influence of pressure on carbonation at low values. Temperature and fly ash quantity slightly affected the carbonation of experiments carried out by Montes-Hernandez et al. and, finally, time of reaction was an important parameter. The carbonation efficiency achieved was 82% after 18h at 30°C. Therefore, this process can store a tonne of CO_2 in 38.2 tonnes of fly ashes [2.87].

2.3.4.3 Mineral carbonation of construction sector waste streams

Portland cement is the main compound used in the production of concrete. Waste cement is generated as a by-product of aggregate recycling process from demolition of

buildings, when concrete is pulverized and classified to separate aggregates from waste cement.

Iizuka et al. (2004) researched sequestration of CO_2 using waste cement. They proposed the utilization of a two step process, where the first one extracts calcium ions from the cement by pressurizing CO_2 and a second step to precipitate calcium carbonate when the pressure is reduced. For the experiments, a 500ml reactor was employed and the influence of pressure (9, 17 and 30bar), S/L ratio (2.9g/l, 15g/l and 29g/l) and time of reaction (0-120 min) were investigated. Results showed that extraction of calcium ions was more efficient at higher pressure, S/L ratio, and also increased with time of reaction. Furthermore, also the effect of particle size was investigated, showing that smaller particles (10-53µm) released calcium ions during the reaction quicker (about 25-30% in the first 20min) than bigger particles (10-200µm)[2.88].

Monkman and Shao (2006) analyzed the behavior of two different cements when reacting with CO_2. A closed reactor was employed, and, 2h reaction, 5bar CO_2 pressure and L/S ratio 0.15l/Kg were the main parameters used. The CO_2 uptake after carbonation was calculated based on the change in mass of the sample and achieved 12% and 14% for the two cements tested, with the formation of calcium carbonate as calcite [2.89].

Huntzinger et al. (2009) investigated mineral carbonation for cement kiln dust. Experiments were performed at ambient pressure and temperature in a 288l (60 by 60 by 80cm long) chamber, where CO_2 was continuously supplied to replenish the amount sequestered. The effect of reaction time (0-8 days) and L/S ratios (0-1.25l/Kg) were investigated, calculating the degree of carbonation based on the change in mass after the experiments. Results showed that mineral carbonation was more successful with higher L/S ratios and also with longer reaction times, reaching 80% after eight days and 1.25l/Kg L/S ratio [2.90].

2.3.4.4 Mineral carbonation of metal waste streams

Blast furnace slag is the residue from the production of iron from the raw mineral (e.g. magnetite, hematite). Monkman and Shao (2006) researched the behavior of GGBS during the reaction with CO_2. A closed reactor was employed, and, 2h reaction, 5bar

CO_2 pressure and L/S ratio 0.15l/kg were the main parameters of the carbonation reaction. The CO_2 uptake was calculated based on the change in mass of the sample and achieved 7% with the formation of calcium carbonate as aragonite [2.89].

Steel slag is the by-product of the production of steel. Huijgen et al. (2005) investigated the potential of steel slag for mineral carbonation. Experiments were performed in a 450ml reactor and the effects of several parameters were investigated including L/S ratio 2-20l/Kg, stirring rate 100-2000rpm, temperature 25-225°C, CO_2 pressure 1-30bar and reaction time 2-30min. Furthermore also the effect on the carbonation reaction of different particle size (<38µm, <106µm, <200µm, <500µm and <2000µm) was investigated. The carbonation efficiency was calculated based on the content of calcium in calcium carbonate compared to the initial total calcium. Results showed that carbonation efficiency increased when the temperature, pressure, time of reaction and stirring rate increased, whilst, carbonation efficiency decreased when particle size and L/S ratio increased. The maximum carbonation efficiency (74%) was achieved after the reaction at temperature 100°C, CO_2 pressure 19bar, particle size <38µm and stirring speed 500rpm [2.91].

Zevenhoven et al. (2010) researched the use of steel slag as feedstock for mineral carbonation. Experiments were carried out in a 25l reactor and the parameters employed for the reaction were CO_2 pressure (1bar, 10bar and 40bar), temperature (28-150°C), L/S ratio (about 10l/Kg) time (3-700h) and CO_2 vol% (1%, 10% and 40%). Tests showed that temperature, time and CO_2 vol% were important parameters for the reaction, increasing the efficiency at higher temperatures, for longer times of reaction and at higher concentration of CO_2 in the reactor (up to about 90% conversion efficiency). Pressure, instead, slightly affected the experiments, with small differences in results after tests at 10bar and 40bar [2.13].

2.3.4.5 Mineral carbonation of other waste streams

Oil shale ash is the residue from combustion of oil shale for power production. Uibu et al. (2010) designed an ash–water suspension carbonation process in a continuous mode laboratory-scale plant (consisting of a series of reactor columns) and investigated potential means of intensifying the water neutralization process. The pH levels in the reactors ranged from alkaline to almost neutral. This produced optimal conditions for

$Ca(OH)_2$ dissociation and $CaCO_3$ precipitation. The final products contained 0.6–2.0wt% of unreacted lime and 17–20wt% of bound CO_2 [2.48].

Paper bottom ash is obtained from waste paper incineration. Zevenhoven et al. (2010) analyzed the use of paper bottom ashes as feedstock for mineral carbonation. Experiments were carried out in a 25l reactor and the parameters employed for the reaction were CO_2 pressure (slightly above ambient), temperature (25°C), L/S ratio (10-50l/Kg) time (3-24h) and CO_2 vol% 100%. The most interesting finding in these experiments was the high purity of calcium carbonate produced by mineral carbonation, which varied between 90.5wt% and 98.5wt% [2.13].

Red mud is a waste slurry obtained from the process largely used to produce alumina from bauxite. Because of its high alkalinity (pH>13) its storage is a serious environmental issue and CO_2 can be used to neutralize it. Red mud carbonation reduces its toxicity (lowering the pH) and sequesters CO_2, although its sequestration capacity is limited [2.92]. Carbonated red mud can be employed in a wide range of applications, including land reclamation, fertilizer additive, plastic filler and cement production [2.93]. Mineral carbonation employing red mud was investigated following a direct aqueous process and the CO_2 which was possible to bound in the final product achieved 26% of the weight of the sample [2.47]. The main products of mineral carbonation were Na_2CO_3 and $NaHCO_3$ Because the main source of alkalinity is present in the liquid phase, usually as NaOH [2.47].

2.3.4.6 Summary of mineral carbonation of waste materials

Processes employed so far for mineral carbonation for industrial waste materials have been single-step via an aqueous route (Table 2.6). Other options like multi-step processes have not been investigated yet and this may allow, as seen in the previous sections, to reduce the energy requirement, making the process more economically viable.

The literature review conducted thus far allowed understanding that the parameters which affect the mineralization reaction are temperature, time, pressure, particle size and L/S ratio. Generally, CO_2 stored by mineral carbonation increases when the reaction happens at higher temperature and for longer time. Furthermore, mineralization results

improved when particle size decreases. The reported effect of pressure and L/S ratio on the efficiency of the process, instead, do not provide uniform results.

Interpretation of data available on the efficiency of the carbonation for the processes presented in Table 2.6 is problematic because of a lack of an uniform method for calculating the efficiency of carbonation. Some researchers (e.g. [2.45] [2.83] [2.84]) consider the weight gain of the sample, assuming that all weight increase is due to CO_2 stored and neglecting that other reactions may happen at the same time (i.e. hydration of silica, evaporation of volatile compounds during reactions at high temperature, etc.). A more suitable method to calculate the efficiency of carbonation is based on the amount of CO_2 consumed in the reactor during the experiments [2.87]. However, this method may be employed only in processes where CO_2 is directly injected into a reactor and cannot be accurately applied if CO_2 has been previously captured (e.g. NH_4HCO_3 obtained from the capture of CO_2 into NH_3) during a multi-step process [2.29]. In fact, the assessment of the amount of CO_2 previously captured, which has been effectively stored in the carbonated material, could be an issue (e.g. NH_4HCO_3 may not react completely during the carbonation step and it is difficult to assess the amount left at the end of the reaction). Efficiency of carbonation is, instead, accurately calculated when the exact amount of carbonates present in the initial and final samples can be assessed by analytical methods (i.e. thermo-gravimetric analysis) as reported by Huntziger et al. [2.90], Huijgen et al. [2.91] and Zevenhoven et al. [2.13]. Therefore, calculation of efficiency based on analytical methods is the most accurate method among the ones employed in the studies presented in Table 2.6.

2.4 Use of final products

Mineral carbonation can produce a range of products which can be divided into two groups:

- Mixture of carbonates (magnesium and calcium), silica sand, metal oxides (mainly iron) and residual silicate rock all in one final product. This group of products can be obtained from single-step technologies, for example the Albany Research Centre process [2.62].
- Different streams of final products (with variable purity level) like silica, carbonates and other metal oxides (mainly iron). These products can be obtained

from multi-step mineralization processes, where, after each phase, solid precipitated products can be collected. In this category, Teir et al. [2.34] and Wang and Maroto-Valer [2.29] processes are included.

Obviously, from a market value point of view, products with higher purity have bigger potential value than mixtures of different materials [2.94]. This is why, in an attempt to reduce the costs of mineral carbonation, recently, there has been an increasing interest in multi-step mineralization processes. In fact, they are able to produce different streams of final products [2.29] and, when the final products obtained from a process are already available for being sold on the market, this makes that technology more attractive.

The next sections present current applications and market value for the main product streams which can be obtained from mineral carbonation processes.

2.4.1 Silica applications and market value

Mineralization processes can produce, as by-product left from the extraction of metals from the feedstock, amorphous silica in a small size range (1-30µm). The main application for this material could be the construction sector, as filler or cement replacement [2.94]. Furthermore, high level of purity silica can be employed for electronic products, ceramics, refractory materials and iron and steel making. Table 2.7 presents the range of silica applications, properties required and the size of the current market for each application. It must be highlighted the high level of purity required for the different applications and the fact that it is difficult that by-products from mineral carbonation can reach such level of purity without further post-processing [2.94]. Therefore, silica from mineralization applications is likely to be mainly used as building material (cement additive).

In 2009 global production of silica was about 112Mt and average price of 1t was £189. Micro-silica (<2µm) has a higher market value (£390/t) but mineralization processes must be controllable to ensure the precipitation of such micro-sized material [2.94].

Silica type	Silica Applications	Properties	Market, Mt
Silica (overall)	building materials, refractories, fillers, semiconductors, circuit boards, cement additive	/	112
Silicon	deoxydiser in steel making, circuit boards, ceramix matrix composites, semiconductors	[#] SiO_2 > 98.5%; Fe_2O_3 < 0.1%, Al_2O_3 < 0.15%	[¥] 2.7
Ceramic sand	ceramics	SiO_2 > 97.5%; Fe_2O_3 < 0.2%, Al_2O_3 < 0.55%; particles < 75µm	/
Foundry sand	metal casting	SiO_2 > 98%; particles < 75µm	/
Refractory sand	refractory materials	SiO_2 > 95%	/
Flux sand	iron and steel making	SiO_2 > 90%	/

[#] Properties for feedstock for silicon production; [¥] precipitated silica, silica sol, silica gel, fumed silica

Table 2.7: Silica applications, properties requirement and market size [2.94]

2.4.2 Magnesium and calcium carbonate applications and market value

Currently, about 98% of magnesium carbonate (magnesite) is converted to magnesium oxide for applications such as refractory materials, mostly for iron and steel making. Global extraction of $MgCO_3$ is about 8.5Mt/year and about 8.0Mt/year are converted (calcinations process at 1450°C) into magnesium oxide. Therefore, magnesium carbonate, as such, can be employed only in a few applications (e.g. agriculture, construction sector). Therefore, due to the small size of these markets, $MgCO_3$ obtained would be employed mainly for low end applications like mining sites restoration [2.94].

Calcium carbonate is the main product from carbonation of waste materials (rich in calcium oxide) and wollastonite. Calcium carbonate can be employed in the construction sector as filler in cement. However, it is important to identify which mineral phases of calcium carbonate are produced by mineral carbonation and also the LOI (loss on ignition), chlorine and sulphate concentrations in order to assess their suitability as a potential cement additive [2.95]. Carbonated materials from mineralization were added into concrete cubes and they showed suitable properties according to BS EN 12390 [2.94].

In addition, calcite is employed in other industrial applications in the form of precipitated calcium carbonate (PCC) and ground calcium carbonate (GCC). However, for these applications, chemical and physical properties (e.g. average particle size and

distribution, morphology, specific surface area, chemical purity) have an important role [2.96]. Impurities, like iron and manganese in calcium carbonate produced from mineralization of steel slag, reduce the market value of calcite.

Global market for GCC was 72Mt in 2007 and 13Mt for PCC and its price can range between £350-550/t [2.94]. Therefore, if mineral carbonation was able to produce calcium carbonate of adequate quality to access these markets (e.g. with low impurities), it would become more economically viable. However, even if calcite from mineralization would not be able to meet those quality requirements, the products could be employed for low-end applications, such as mining site restoration.

2.4.3 Iron oxide applications and market value

Iron oxides are mainly employed as pigments for ceramics, porcelain and paints because of their tinting strength and resistance to acids [2.97]. In 2010 world production of iron oxides pigments was about 1.4Mt in 2006 and the average cost in the USA was about £142/t in 2008 [2.98]. Iron oxides are usually a combination of one or more ferrous or ferric oxides plus some impurities and their main application is as iron ore mineral. Therefore, mineral carbonation by-products can be employed in the iron and steel industries which have huge global demand. Iron ore had a market in 2010 of 2.4Gt and average price of £57/t [2.94].

2.5 Mineral carbonation pilot plants

As described earlier in Sections 2.1.2 and 2.2, mineral carbonation is a relatively new technology compared to underground storage of CO_2. Therefore, also the number of pilot plants available worldwide is lower. Nowadays mineral carbonation has been implemented in three pilot plants [2.99]:

- Calera process in the gas fired Moss Landing plant (CA, USA) has been running for about two years. The plant captures flue gas CO_2 (30kt/year) from a 10MW power generator at 90% efficiency. The Calera process at Moss Landing plant uses brines containing Ca or Mg ions to react with CO_2 in a reactor. There is no need of previous separation of the CO_2 from the flue gases and the final carbonate products are suitable for cement manufacture [2.100].

- Alcoa process at Kwinana (Western Australia) has been running since 2007. The process adds CO_2 to residues left after alumina is removed from bauxite. The Kwinana carbonation plant locks 70kt of CO_2 a year. The CO_2 is a by-product from the nearby ammonia plant which would otherwise be emitted. The second environmental benefit is that mixing CO_2 with residues from extraction of alumina reduces their pH level to values found naturally in many alkaline soils and the final products can be reused in road base, building materials or soil amendments [2.101].

- Skyonic group (USA) has developed a process able to remove CO_2 from flue gases and produce saleable carbonates and bicarbonates. The process can also remove SO_X, NO_2 and heavy metals from the flue gases. Furthermore, green chemicals, such as hydrochloric acid, bleach, chlorine, and hydrogen are also produced increasing the economics of the process. Skyonic is currently retrofitting Capitol's cement mill (San Antonio, USA) owned by Capitol Aggregates and by 2014 the plant should be fully operational and able to sequester 75kt/year of CO_2 [2.103].

Another process is at an advanced stage of development and a pilot plant will be soon operational. The University of Newcastle (Australia) in collaboration with GreenMag Group and Orica Ltd has recently unveiled plans for building a pilot mineral carbonation plant operational by 2017. However, details on the technology employed have not been disclosed. The process will sequester 100kt/year of CO_2 into serpentine minerals and the main aim is to reduce the cost of mineralization to about £25/tCO_2 [2.99] [2.102].

2.6 Conclusions

Carbon capture and storage could reduce CO_2 emissions. Underground storage has recently seen a slow deployment of the technology (about 20Mt/year stored compared to 32Gt/year global emissions) and, therefore, mineralization has gained increasing interest and needs further research. Mineralization is a relatively new option in the CCS portfolio compared to CO_2 underground injection which has been employed for EOR for about 40 years. Mineral carbonation, in fact, has been researched only since 1990. The numerous advantages of mineralization have been described in this chapter:

permanent sequestration of CO_2, exothermic reaction, abundant suitable feedstocks. However, there are also several drawbacks (e.g. slow reaction rates) which make costs of this storage option higher than CCS underground storage (£75-110/$tCO_{2\ avoided}$ for mineral carbonation while £50-75/$tCO_{2\ avoided}$ for CCS underground storage) .

Suitable feedstocks for mineral carbonation must be rich in calcium and/or magnesium and include natural silicate minerals (serpentine, olivine, wollastonite) as well as industrial waste streams (municipal solid waste ashes, coal fly ashes, construction sector wastes, metal wastes, etc.). There is a vast amount of published data about identification, characterization and mineral carbonation tests on suitable feedstocks for mineralization. Waste streams have variable composition due to the production processes but also caused by other factors (e.g. storage, weathering conditions, age of the sample etc.). Therefore, each waste stream should be deeply characterized before any mineralization experiments, to assess its characteristics and to understand its behaviour. In the future, new suitable materials for mineral carbonation may be produced from novel industrial processes or technologies and therefore new feedstocks may become available.

Mineral carbonation technologies can be divided mainly into two groups, namely single-step and multi-step processes. Every mineralization process has a specific kinetic of the reaction which is differently affected by the main parameters (temperature, pressure, time, S/L ratio, particle size). First mineralization studies were carried out investigating single-step processes, called also direct mineral carbonation. Afterwards, other routes were explored, from aqueous direct mineralization to aqueous indirect processes (multi-step). Furthermore, recently, techniques able also to regenerate and reuse the chemicals involved were studied. The main aim of all research efforts has been to reduce the costs involved with the technology. Multi-step processes, also able to regenerate and reuse the chemicals employed, seem to require less energy intensive and more economical conditions than single-step processes. However, so far, there is a lack of rigorous energy and mass balances reported for the processes proposed. When assessing a technology it is important to consider its technical feasibility but also its economic viability. Moreover, industrial waste streams have been employed only with single-step aqueous processes. There is, therefore, a need for studying multi-step processes applied to these waste materials. The effect of the parameters affecting

mineralization (i.e. temperature, time, pressure, particle size and L/S ratio) on the reactions in multi-step processes needs to be understood to identify the best conditions.

Another important aspect of mineral carbonation is the nature and potential value of the final products. In fact, mineral carbonation would look more attractive if the final products can be sold and become a revenue stream. Calcium and magnesium carbonate, silica and iron oxides are the main outcomes from mineralization processes and they have several applications, ranging from low-end (e.g. cement substitute, mining site restoration, land remediation) to high quality (e.g. specific industrial application). It is therefore necessary, when evaluating a mineralization process, to combine analyses of the efficiency of carbonation with characterization through appropriate techniques of the final products, allowing understanding any potential market value.

2.7 References

[2.1] O'Connor W, Dahlin D, Nilsen D, Walters R, and Turner P. Carbon dioxide sequestration by direct mineral carbonation with carbonic acid. Proceedings of the 25th International Technical Conf On Coal Utilization & Fuel Systems, Coal Technology Assoc, Clear Water, FL. 2000.

[2.2] DECC. UK Renewable Energy Roadmap. London: Department for Energy and Climate Change; 2011.

[2.3] IPCC. IPCC special report on carbon capture and storage. Cambridge, UK and New York, NY, USA: IPCC Intergovernmental Panel on Climate Change; 2005.

[2.4] Global CCS Institute. The global status of CCS 2012. Canberra, Australia: Global CCS Institute; 2012.

[2.5] CO2CRC. The Cooperative Research Centre for Green House Gas Technologies. http://www.co2crc.com.au/. Date of consultation: September 2013.

[2.6] Stangeland A. A model for the CO_2 capture potential. International Journal of Greenhouse Gas Control. 2007;1:418-29.

[2.7] Praetorius B, Schumacher K. Greenhouse gas mitigation in a carbon constrained world: The role of carbon capture and storage. Energy Policy. 2009;37:5081-93.

[2.8] van Alphen K, Noothout PM, Hekkert MP, Turkenburg WC. Evaluating the development of carbon capture and storage technologies in the United States. Renewable and Sustainable Energy Reviews. 2010;14:971-86.

[2.9] Hake J-F, Hovener H, Schenk O, Seiser O. CCS for Germany: Policy, R&D and demonstration activities. Energy Procedia. 2009;1:3917-25.

[2.10] McKinsey&Company. Carbon Capture and Storage: Assessing the economics. McKinsey & Company; 2008.

[2.11] Bachu S. CO_2 storage in geological media: Role, means, status and barriers to deployment. Progress in Energy and Combustion Science. 2008;34:254-73.

[2.12] IEA. International Energy Agency Redrawing the energy-climate map report. http://www.worldenergyoutlook.org/media/weowebsite/2013/energyclimatemap/RedrawingEnergyClimateMap.pdf. Date of consultation: September 2013.

[2.13] Zevenhoven R, Wiklund A, Fagerlund J, Eloneva S, In't Veen B, Geerlings H, et al. Carbonation of calcium-containing mineral and industrial by-products. Frontiers of Chemical Engineering in China. 2010;4:110-9.

[2.14] Wang X, Maroto-Valer MM. Integration of CO_2 Capture and Mineral Carbonation by Using Recyclable Ammonium Salts. ChemSusChem. 2011;4:1291-300.

[2.15] Seifritz W. CO_2 disposal by means of silicates. Nature. 1990;345:486.

[2.16] Dunsmore HE. A geological perspective on global warming and the possibility of carbon dioxide removal as calcium carbonate mineral. Energy Conversion and Management. 1992;33:565-72.

[2.17] Lackner KS, Wendt CH, Butt DP, Joyce EL, Sharp DH. Carbon dioxide disposal in carbonate minerals. Energy. 1995;20:1153-70.

[2.18] Matter JM, Broecker WS, Gislason SR, Gunnlaugsson E, Oelkers EH, Stute M, et al. The CarbFix Pilot Project–Storing carbon dioxide in basalt. Energy Procedia. 2011;4:5579-85.

[2.19] Matter JM, Broecker WS, Stute M, Gislason SR, Oelkers EH, Stefánsson A, et al. Permanent Carbon Dioxide Storage into Basalt: The CarbFix Pilot Project, Iceland. Energy Procedia. 2009;1:3641-6.

[2.20] Paukert AN, Matter JM, Kelemen PB, Shock EL, Havig JR. Reaction path modeling of enhanced in situ CO_2 mineralization for carbon sequestration in the peridotite of the Samail Ophiolite, Sultanate of Oman. Chemical Geology. 2012;330–331:86-100.

[2.21] Herzog H. Carbon sequestration via mineral carbonation: overview and assessment. MIT Laboratory for Energy and the Environment. 2002.

[2.22] Lackner KS, Butt DP, Wendt CH. Progress on binding CO_2 in mineral substrates. Energy Conversion and Management. 1997;38, Supplement:S259-S64.

[2.23] Butt DP, Lackner KS, Wendt CH, Vaidya R, Pile DL, Park Y, et al. The kinetics of binding carbon dioxide in magnesium carbonate. Conference: 23 international technical conference on coal utilization and fuel systems, Clearwater, FL (United States), 9-13 1998.

[2.24] O'Connor W, Dahlin D, Nilsen D, Gerdemann SJ, Rush GE, Walters R et al. Research status on the sequestration of carbon dioxide by direct aqueous mineral carbonation. 18th Annual International Pittsburgh Coal Conference. Newcastle, Australia 2001.

[2.25] Zevenhoven R., Kohlmann J. CO_2 sequestration by magnesium silicate mineral carbonation in Finland. *S*econd Nordic Minisymposium on Carbon Dioxide Capture and Storage. Goteborg, Sweden 2001.

[2.26] Maroto-Valer MM, Fauth DJ, Kuchta ME, Zhang Y, Andresen JM. Activation of magnesium rich minerals as carbonation feedstock materials for CO_2 sequestration. Fuel Processing Technology. 2005;86:1627-45.

[2.27] Teir S, Revitzer H, Eloneva S, Fogelholm C-J, Zevenhoven R. Dissolution of natural serpentinite in mineral and organic acids. International Journal of Mineral Processing. 2007;83:36-46.

[2.28] Park A-HA, Fan L-S. Mineral sequestration: physically activated dissolution of serpentine and pH swing process. Chemical Engineering Science. 2004;59:5241-7.

[2.29] Wang X, Maroto-Valer MM. Dissolution of serpentine using recyclable ammonium salts for CO_2 mineral carbonation. Fuel. 2011;90:1229-37.

[2.30] Kodama S, Nishimoto T, Yamamoto N, Yogo K, Yamada K. Development of a new pH-swing CO_2 mineralization process with a recyclable reaction solution. Energy. 2008;33:776-84.

[2.31] Krevor S, Graves C, Gosen BV, McCafferty A. Mapping the mineral resource base for mineral carbon-dioxide sequestration in the conterminous United States. US Geological Survey; 2009.

[2.32] Park AHA, Jadhav R, Fan LS. CO_2 mineral sequestration: Chemically enhanced aqueous carbonation of serpentine. Canadian Journal of Chemical Engineering. 2003;81.

[2.33] Kakizawa M, Yamasaki A, Yanagisawa Y. A new CO_2 disposal process via artificial weathering of calcium silicate accelerated by acetic acid. Energy. 2001;26:341-54.

[2.34] Teir S, Eloneva S, Fogelholm C-J, Zevenhoven R. Fixation of carbon dioxide by producing hydromagnesite from serpentinite. Applied Energy. 2009;86:214-8.

[2.35] Lackner KS. Carbonate chemistry for sequestering fossil carbon. Annual Review of Energy and the Environment. 2002;27:193-232.

[2.36] Wenk HF, Bulakh A. MInerals: their constitution and origin. Cambridge Univeristy Press. p. 297. 2004.

[2.37] Gorai B, Jana RK, Premchand. Characteristics and utilisation of copper slag—a review. Resources, Conservation and Recycling. 2003;39:299-313.

[2.38] Shi C, Meyer C, Behnood A. Utilization of copper slag in cement and concrete. Resources, Conservation and Recycling. 2008;52:1115-20.

[2.39] TFHRC. Turner Fairbank Highway Research Centre (TFHRC) manual on the use of waste and by-product materials in pavement construction. http://www.fhwa.dot.gov/publications/research/infrastructure/structures/97148/for.cfm2008. Date of consultation: October 2012.

[2.40] Al-Otaibi S. Durability of concrete incorporating GGBS activated by water-glass. Construction and Building Materials. 2008;22:2059-67.

[2.41] Limbachiya MC, Marrocchino E, Koulouris A. Chemical-mineralogical characterisation of coarse recycled concrete aggregate. Waste Management. 2007;27:201-8.

[2.42] Garcés P, Pérez Carrión M, García-Alcocel E, Payá J, Monzó J, Borrachero MV. Mechanical and physical properties of cement blended with sewage sludge ash. Waste Management. 2008;28:2495-502.

[2.43] Gunning PJ, Hills CD, Carey PJ. Accelerated carbonation treatment of industrial wastes. Waste Management. 2010;30:1081-90.

[2.44] Gunning PJ, Hills CD, Carey PJ. Production of lightweight aggregate from industrial waste and carbon dioxide. Waste Management. 2009;29:2722-8.

[2.45] Wang L, Jin Y, Nie Y. Investigation of accelerated and natural carbonation of MSWI fly ash with a high content of Ca. Journal of Hazardous Materials. 2010;174:334-43.

[2.46] Johnston M, Clark MW, McMahon P, Ward N. Alkalinity conversion of bauxite refinery residues by neutralization. Journal of Hazardous Materials. 2010;182:710-5.

[2.47] Sahu RC, Patel RK, Ray BC. Neutralization of red mud using CO_2 sequestration cycle. Journal of Hazardous Materials. 2010;179:28-34.

[2.48] Uibu M, Velts O, Kuusik R. Developments in CO_2 mineral carbonation of oil shale ash. Journal of Hazardous Materials. 2010;174:209-14.

[2.49] Uibu M, Kuusik R, Andreas L, Kirsimäe K. The CO_2 -binding by Ca-Mg-silicates in direct aqueous carbonation of oil shale ash and steel slag. Energy Procedia. 2011;4:925-32.

[2.50] Baciocchi R, Polettini A, Pomi R, Prigiobbe V, Von Zedwitz VN, Steinfeld A. CO_2 Sequestration by Direct Gas−Solid Carbonation of Air Pollution Control (APC) Residues. Energy & Fuels. 2006;20:1933-40.

[2.51] Amutha Rani D, Boccaccini AR, Deegan D, Cheeseman CR. Air pollution control residues from waste incineration: Current UK situation and assessment of alternative technologies. Waste Management. 2008;28:2279-92.

[2.52] Ingram KD, Daugherty KE. A review of limestone additions to Portland cement and concrete. Cement and Concrete Composites. 1991;13:165-70.

[2.53] Myers R. The 100 most important chemical compounds: a reference guide Greenwood Press; 2007.

[2.54] Zevenhoven R, Kavaliauskaite I. Mineral carbonation for long term CO2 storage: an exergy analysis. International Journal of Thermodynamics. 2004;7:23-31.

[2.55] O'Connor WK, Dahlin DC, Rush GE, Gerdemann SJ, Penner LR, Nilsen DN. Aqueous mineral carbonation: mineral availability, pretreatment, reaction parametrics and process studies. Albany, OR, USA.: Albany Research Center; 2005.

[2.56] Newall P, Clarke C, H. aH. CO_2 Storage as Carbonate Minerals. PH3/17: IEA Greenhouse Gas R&D Programme; 2000.

[2.57] Huijgen WJJ, Comans RNJ, Witkamp G-J. Cost evaluation of CO_2 sequestration by aqueous mineral carbonation. Energy Conversion and Management. 2007;48:1923-35.

[2.58] Gerdemann SJ, O'Connor WK, Dahlin DC, Penner LR, Rush H. Ex Situ Aqueous Mineral Carbonation. Environmental Science & Technology. 2007;41:2587-93.

[2.59] Styring P, Jansen D. Carbon Capture and Utilisation in the green economy: Using CO_2 to manufacture fuel, chemicals and material. University of Sheffield and Energy Research Centre of the Netherlands. 2011.

[2.60] Bobicki ER, Liu Q, Xu Z, Zeng H. Carbon capture and storage using alkaline industrial wastes. Progress in Energy and Combustion Science. 2012;38:302-20.

[2.61] Huijgen WJJ, Witkamp G-J, Comans RNJ. Mechanisms of aqueous wollastonite carbonation as a possible CO_2 sequestration process. Chemical Engineering Science. 2006;61:4242-51.

[2.62] O'Connor W, Dahlin D, Nilsen D, Walters R, Turner P. Carbon dioxide sequestration by direct mineral carbonation with carbonic acid. Proceedings of the 25th International Technical Conf On Coal Utilization & Fuel Systems, Coal Technology Assoc, Clear Water, FL. 2000.

[2.63] Huijgen WJJ, Ruijg GJ, Comans RNJ, Witkamp G-J. Energy Consumption and Net CO_2 Sequestration of Aqueous Mineral Carbonation. Industrial & Engineering Chemistry Research. 2006;45:9184-94.

[2.64] House of Parliament. Carbon footprint of electricity generation 2011. http://wwwparliamentuk/documents/post/postpn_383-carbon-footprint-electricity-generationpdf Date of consultation: January 2014.

[2.65] Dodds WS, Stutzman, LF, and Sollami BJ. Carbon Dioxide Solubility in Water, Industrial and Engineering Chemistry, 1956, Vol. 1, No. 1, 92-95

[2.66] Carey JW, Rosen EP, Bergfeld D, Chipera SJ, Counce DA, Snow MG, et al. Experimental studies of the serpentine carbonation reaction. In: Association CT, editor. 28th International Technical Conference on Coal Utilization & Fuel Systems. Clearwater, FL, USA 2003.

[2.67] Gerdemann SJ, Dahlin DC, O'Connor WK. Carbon dioxide sequestration by aqueous mineral carbonation of magnesium silicateminerals. 6th International Conference on Greenhouse Gas Control Technologies. Kyoto, Japan 2002.

[2.68] Sipilä J, Teir S, Zevenhoven R. Carbon dioxide sequestration by mineral carbonation: literature review update 2005-2007. Turku, Finland: Abo Akademi University, Faculty of Technology, Heat Engineering Laboratory; 2008.

[2.69] Wendt CH, Butt DP, Lackner KS, Ziock H-J. Thermodynamic considerations of using chlorides to accelerate the carbonate formation from magnesium silicates. Los Alamos, NM, USA: Los Alamos National Laboratory; 1998.

[2.70] IEA. CO_2 storage as carbonate minerals,Greenhouse Gas R&D Programme (IEA-GHG), prepared by CSMA Consultants Ltd, PH3/17. In: Agency IE, editor. Cheltenham - UK2000.

[2.71] Huijgen WJJ, Comans RNJ. Carbon dioxide sequestration by mineral carbonation. Petten, The Netherlands: Energy Research Centre of the Netherlands 2003.

[2.72] Maroto-Valer MM, Zhang Y, Kuchta ME, Andresen JM, Fauth DJ. Process for sequestering carbon dioxide and sulfur oxide. Patent number US7604787. 2004.

[2.73] Teir S, Kuusik R, Fogelholm C-J, Zevenhoven R. Production of magnesium carbonates from serpentinite for long-term storage of CO_2. International Journal of Mineral Processing. 2007;85:1-15.

[2.74] Wang X, Maroto-Valer M. Integration of CO_2 capture and storage based on pH-swing mineral carbonation using recyclable ammonium salts. Energy Procedia. 2011;4:4930-6.

[2.75] Bosecker K. Bioleaching: metal solubilization by microorganisms. FEMS Microbiology Reviews. 1997;20:591-604.

[2.76] Schwartzman DW, Volk T. Biotic enhancement of weathering and the habitability of earth. Nature. 1989;340.

[2.77] Power IM, Dipple GM, Southam G. Bioleaching of Ultramafic Tailings by Acidithiobacillus spp. for CO_2 Sequestration. Environmental Science & Technology. 2009;44:456-62.

[2.78] Blencoe JG, Palmer DA, Anovitz LM, Beard JS. Carbonation of metal silicates for long-term CO_2 sequestration. Patent Number WO200409043. 2004.

[2.79] Pundsack FL. Recovery of silica, iron oxide, and magnesium carbonate from the treatment of serpentine with ammonium bisulphate. Patent Number US3338667. 1967.

[2.80] Rhee CH, Kim JY, Han K, Ahn CK, Chun HD. Process analysis for ammonia-based CO_2 capture in ironmaking industry. Energy Procedia. 2011;4:1486-93.

[2.81] Wang X, Maroto-Valer MM. Optimization of carbon dioxide capture and storage with mineralisation using recyclable ammonium salts. Energy. 2013;51:431-8.

[2.82] Costa G, Baciocchi R, Polettini A, Pomi R. Current status and perspectives of accelerated carbonation processes on municipal waste combustion residues. Environmental monitoring and assessment. 2007;135:55-75.

[2.83] Li X, Bertos MF, Hills CD, Carey PJ, Simon S. Accelerated carbonation of municipal solid waste incineration fly ashes. Waste Management. 2007;27:1200-6.

[2.84] Baciocchi R, Costa G, Di Bartolomeo E, Polettini A, Pomi R. The effects of accelerated carbonation on CO_2 uptake and metal release from incineration APC residues. Waste Management. 2009;29:2994-3003.

[2.85] Baciocchi R, Costa G, Lategano E, Marini C, Polettini A, Pomi R et al. Accelerated carbonation of different size fractions of bottom ash from RDF incineration. Waste Management. 2010;30:1310-7.

[2.86] Fauth D, Soong Y, C. aW. Carbon sequestration utilizing industrial solid residues. Fuel Chemistry Division Preprints, US Department of Energy. 2002;47:37-8.

[2.87] Montes-Hernandez G, Pérez-López R, Renard F, Nieto JM, Charlet L. Mineral sequestration of CO_2 by aqueous carbonation of coal combustion fly-ash. Journal of Hazardous Materials. 2009;161:1347-54.

[2.88] Iizuka A, Fujii M, Yamasaki A, Yanagisawa Y. Development of a New CO_2 Sequestration Process Utilizing the Carbonation of Waste Cement. Industrial and Engineering chemistry research. 2004;43:7880-7.

[2.89] Monkman S, Shao Y. Assessing the Carbonation Behavior of cementitious Materials. Journal of Materials in Civil Engineering. 2006;18:768-76.

[2.90] Huntzinger DN, Gierke JS, Kawatra SK, Eisele TC, Sutter LL. Carbon Dioxide Sequestration in Cement Kiln Dust through Mineral Carbonation. Environmental Science & Technology. 2009;43:1986-92.

[2.91] Huijgen W, Witkamp G, Comans R. Mineral CO_2 sequestration by steel slag carbonation. Environmental Science & Technology. 2005;39:9676-82.

[2.92] Dilmore R, Lu P, Allen D, Soong Y, Hedges S, Fu JK, et al. Sequestration of CO_2 in mixtures of bauxite residue and saline wastewater. Energy & Fuels. 2008;22.

[2.93] Bonenfant D, Kharoune L, Sauve S, Hausler R, Niquette P, Mimeault M et al. CO_2 Sequestration by Aqueous Red Mud Carbonation at Ambient Pressure and Temperature. Industrial & Engineering Chemistry Research. 2008;47.

[2.94] Sanna A, Hall MR, Maroto-Valer M. Post-processing pathways in carbon capture and storage by mineral carbonation (CCSM) towards the introduction of carbon neutral materials. Energy & Environmental Science. 2012;5:7781-96.

[2.95] Mehta PK, Monteiro PJM. Concrete: Microstructure, Properties and Materials, 3rd edition: McGraw-Hill; 2006.

[2.96] Tai CY, Chen FB. Polymorphism of $CaCO_3$, precipitated in a constant-composition environment. AIChE Journal. 1998;44:1790-8.

[2.97] Cornell RM, Schwertmann U. Transformations. The Iron Oxides: Wiley-VCH Verlag GmbH & Co. KGaA; 2004. p. 365-407.

[2.98] Virta RL, Miller LD. Iron Oxide Pigments, USGS 2008 Minerals Yearbook. http://minerals.usgs.gov/minerals/pubs/commodity/iron_oxide/myb1-2008-fepig.pdf: U.S. Geological Survey; 2008.

[2.99] Global CCS Institute. Mineral carbonation sequestration. http://www.globalccsinstitute.com/publications/novel-co2-capture-taskforce-report/online/54351. Date of consultation: October 2013.

[2.100] Calera Corporation. Company website: http://www.calera.com/site/. Date of consultation: October 2013.

[2.101] Alcoa Inc. Company wesite: http://www.alcoa.com/australia/en/info_page/pots_rd.asp. Date of consultation: October 2013.

[2.102] Orica Ltd. Company website: www.orica.com. Date of consultation: October 2013.

[2.103] Skyonic Corporation. Company website: http://skyonic.com/. Date of consultation: October 2013.

CHAPTER 3 – METHODOLOGY

The methodology followed in the thesis is presented in this chapter. Procurement of suitable waste materials is the first step for developing a mineralization process. In Chapter 2 (Section 2.2.3) several waste streams were identified and described. In this work, nine waste streams rich in Ca content were selected from various providers, in the UK and Europe. The samples received were characterized by X-ray diffraction (XRD) and X-ray fluorescence (XRF) to assess the mineral phases present and the chemical composition, respectively (Section 5.2). Furthermore, in this chapter, details of the sample rig employed for the mineral carbonation experiments are also reported. Afterwards, the methodology used for characterising the solution samples, employing inductive coupled plasma mass spectrometry (ICP-MS), is described. Efficiency of carbonation is the most suitable parameter to report the degree of carbonation achieved during the mineralization process and it can be determined by thermo-gravimetric analyses (TGA). Moreover, morphology and chemical composition of the final carbonated products were investigated by scanning electron microscope (SEM). Finally, this chapter presents how the economics of the process was assessed after calculating the mass and energy balance.

3.1 Sample procurement

Identification of promising waste materials for mineral carbonation was described in the previous chapter (Section 2.2.3). Samples of nine different streams namely blast furnace slag, pulverised fuel ash, recycled concrete aggregate, steel slag, phosphorus slag, cement kiln dust, copper smelt slag, incinerator sewage sludge ash were procured from the UK and Europe. Full details of the Companies providing the samples and the location of the production sites cannot be disclosed because of confidentiality. However, some information on the origin of the different samples are reported in the following paragraph.

Blast furnace slag was obtained from a plant producing 1Mt of blast furnace slag per year. Pulverized fuel ashes were produced in a 2000MW coal power plant. Recycled concrete aggregate was received from the UK as a cube (15x15x15cm), which usually is employed for stress tests on concrete. Steel slag came from a plant producing 3.2Mt per year of steel in four electric furnaces. Phosphorus slag was received from a supplier of materials for road building and cement kiln dust from a cement plant producing about

50Mt per year of cement. Copper smelt slag came from a site extracting 35t per year of copper from raw minerals and the incinerator sewage sludge ash was received from a wastewater treatment plant serving an area with population of 450,000 inhabitants.

The samples were obtained from production plants where a representative amount of 2-3kg of each sample was collected from the residue of the manufacturing processes. Once received, the samples were stored in the same indoor location (at ambient temperature) prior to the experiments described below.

3.1.1 Sample preparation

The samples provided presented a wide range of different size. Pulverized fuel ashes, blast furnace slag, cement kiln dust and incineration sewage sludge ashes were obtained as already fine particles (<500μm). In contrast, steel slag and phosphorus slag consisted of agglomerates of 2-3cm size, but also of fine particles. Recycled concrete aggregate, instead, was received as a concrete block (15x15x15cm) normally utilized in the cement industry for testing its properties (e.g. compression). In this case, to reduce the particle size, a crusher was employed to obtain concrete pieces of 1-2cm. About 700g of each sample was grinded with a Tema mill, loading 50-70g of sample every run and grinding it for 2min. Afterwards, the grinded samples were homogenized using a riffle. This operation allowed to guarantee that the grinded material was representative of the sample. The material obtained was then employed for the following experiments and analyses.

The waste materials selected for mineralization experiments (steel slag, phosphorus slag, ground granulated blast furnace slag, Chapter 6) were sieved, using an automatic shaker, because particle size is one of the factors affecting mineral carbonation, as described in the literature review (Section 2.3.4.6). According to previous studies on mineral carbonation [3.1] [3.2] [3.3], two different size ranges were selected, 75-150μm and 150-300μm. Particle size distribution tests were performed on the different samples obtained after sieving. When studying the particle size distribution, d_{50} represents the value of the particle diameter at 50% in the cumulative distribution (i.e. 50% of the particles forming the sample have a diameter less than d_{50}). In the same way, d_{90} represents the value of the particle diameter at 90% in the cumulative distribution. Table 3.1 reports the values of d_{50} and d_{90} for the different samples employed for the mineral carbonation tests. It can be noticed that ground granulated blast furnace slag had the

lowest values of d_{50} and d_{90}, while the particle size 150-300µm could not be obtained since the sample tested did not contain particles in the size range 150-300µm (Section 6.3).

	75-150µm		150-300µm	
	d_{50} [µm]	d_{90} [µm]	d_{50} [µm]	d_{90} [µm]
Steel slag	101	125	215	259
Phosphorus slag	95	115	207	243
Ground granulated blast furnace slag	88	104	N/A	N/A

Table 3.1: Values of d_{50} and d_{90} for samples employed in mineral carbonation tests

Sieving operations, as well as milling and crushing, were performed handling materials with appropriate gloves and avoiding dust dispersion by using ventilating systems.

3.2 Sample characterization

Every waste stream has a high variability in composition and properties due to several factors including feedstocks used, process condition, storage, weathering conditions etc.. Therefore, samples collected required characterization to understand their composition and properties. The techniques selected in this study were X-ray fluorescence and X-ray diffraction. These techniques have been largely used for characterization of solid samples in mineral carbonation and have proved their reliability (e.g. [3.1] [3.2] [3.3]).

3.2.1 X-ray fluorescence

X-ray fluorescence (XRF) is used to obtain the chemical composition of a material. Some authors in literature choose Inductive Coupled Plasma Mass Spectrometry (ICP-MS) for analysing chemical composition of solid samples. However, it has been demonstrated that both techniques (XRF and ICP-MS) are reliable for detecting the chemical composition of a sample since, in some studies, the same author used either one or the other achieving the same accuracy of results ([3.1] [3.2]). XRF is a surface sensitive technique and while preparing the sample for analysis the homogeneity between the inner part and the surface of the specimen must be ensured. XRF is based on the emission of secondary electrons from a material after it has been excited by X-rays. Every material gives a different response to the X-rays and, therefore, the instrument can detect the chemical oxides contained in the sample analyzed. The X-ray

fluorescence principle is based on the fact that an X-ray beam excites and ejects an inner shell electron of an atom. Afterwards, another electron moves from a higher energy shell to fill the vacancy created. The energy difference between the two shells appears as X-ray emitted by the atom (called photon or fluorescent X-ray). The X-ray spectrum (peaks with different intensities), acquired during the XRF, reflects the energy emitted during the process and allows identifying the chemical oxides present in the sample and their concentrations [3.4]. The preparation process used for this analysis involved grinding 3g of sample (average grain size <50µm) and then a fusion bead was prepared (ensuring homogeneity of the sample between inner and external layer), heating the sample up to 1400°C (Figure 3.1). Afterwards, the bead was put into a PANalytical Axios Advanced XRF spectrometer with the X-ray tubes operating at 4kW output, 160mA. Results of the analyses are given in element (e.g. Ca, Mg, Si) in oxide form wt% with an instrumental accuracy of ±0.1wt%.

Figure 3.1: Fused bead preparation and prepared fused bead ready for XRF

3.2.2 X-ray diffraction

The most suitable technique to detect crystalline phases present in a material is X-ray diffraction (XRD). XRD is a bulk technique and it is based, as XRF, on X-rays and the way materials diffracted within and reflected from them. X-rays, of a known wavelength λ, are passed incident upon a sample at angle θ, in order to identify its crystal structure. The XRD is founded on the Bragg's law; it considers (a) two atomic planes of spacing d and (b) a monochromatic plane x-wave falling on them at an angle θ. (c) The path difference between the two reflections is 2d sin(θ) (Figure 3.2).

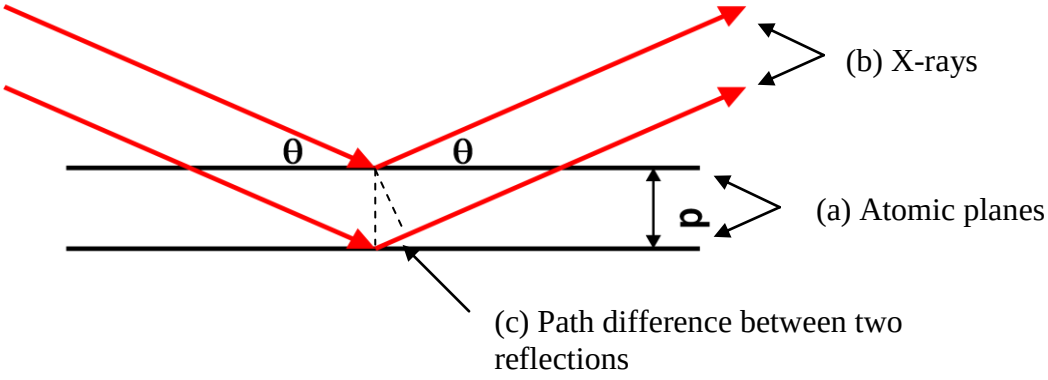

Figure 3.2: Bragg reflection on two atomic planes

If this path difference equals a whole number, n, of wavelength λ, then the phase difference between the two reflected beams is zero throughout the crystal. Therefore, according to the Bragg's law, maximum amplitude of the reflected wave is obtained for angles θ_n, where n is an entire number (i.e. 1,2,3 etc.):

$$2dsin(\theta_n) = n\lambda \qquad (3\text{-}1)$$

X-ray powder diffraction spectrometers consist, mainly, of an X-ray tube, a sample holder and a detector (Figure 3.3). The X-ray tube produces the X-rays, these are sent to the sample with a constant angular speed θ/min, and the detector also rotates at an angular speed of 2θ/min recording the intensity of the peaks.

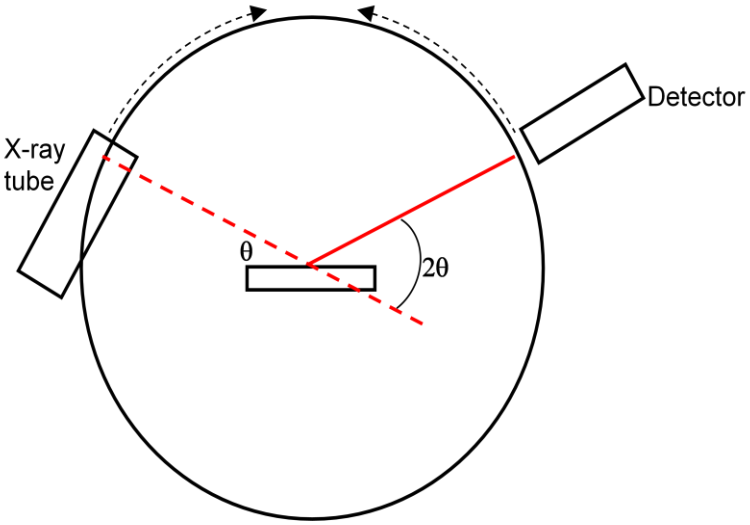

Figure 3.3: Basic layout of a X-ray powder diffraction spectrometers

When the spacing among different atomic planes is a multiple of the wavelength of the X-rays, according to the Bragg's law, the detector registers a peak of intensity due to the constructive interference. Instead, when the spacing among atomic planes is not a multiple of the wavelength, the detector records a flat pattern [3.5].

For this work, the preparation process involved grinding 10g of sample (average grain size <75μm), then placing the material in a sample holder for the analysis (Figure 3.4). The instrument employed was a HILTONBROOKS X-ray powder diffraction spectrometer and the standard XRD resolution parameters were: scan speed of 2 degrees 2θ per minute, step size 0.05θ in the range 0-90 2θ-degrees.

Figure 3.4: Prepared samples ready for XRD

Furthermore, XRD can be used to quantify the content of each crystalline phase in the sample and this technique is called quantitative XRD (QXRD). In this work two different QXRD computer software were used, to compare and corroborate the results obtained. For QXRD in the BRUCKER AXS EVA, the software used the relative intensity ratio (RIR) method. This involves a database which includes the RIRs (indicated as I/Ic) of all different phases, which were determined for any phase using a standard, usually Al_2O_3 (corundum) and SiO_2 (quartz) [3.6]. The software can calculate the percentage of each crystalline phase by comparing the database on the pattern analyzed. With higher number of phases present, the error in the results is bigger because of the approximation of every RIR used for the calculation [3.7].

In addition, the Rietveld refinement method was also used. This allows analysing the whole XRD pattern instead of a few indentified peaks, modelling it until the best fit is

achieved [3.6]. MAUD (Materials Analysis Using Diffraction) [3.8] software implements the Rietveld method and it was used to corroborate and compare QXRD results obtained from BRUCKER AXS EVA software. Results obtained from QXRD based on the Rietveld method are typically ±2.5% for concentrations >60wt%, ±5% for concentrations between 60 and 30wt%, ±10% for concentrations between 30 and 10wt%, ±20% for concentrations between 10 and 3wt% and ±40% for concentrations <3wt% [3.9].

3.3 Experimental rig for mineralization studies

The aim of this thesis is to investigate an innovative multi-step mineralization process for different waste streams (Section 1.5). Details of the process are reported in Chapter 5 (Section 5.1) while, in Figure 3.5, a simplified diagram presents the different phases of the process. The methodology employed for testing the mineral dissolution step (first block in Figure 3.5) is reported in Section 3.4, while, Section 3.5 reports the methodology employed for testing the sequence of mineral dissolution, pH adjustment and carbonation reaction.

The proposed process operates at ambient pressure, therefore, experiments testing mineral dissolution, pH adjustment and carbonation reaction were carried out in the experimental rig showed in Figure 3.6. A 500ml, 3-neck glass flask reactor (A) was employed. The system was heated by a temperature–controlled (letter B, RCT basic IKAMAG® safety control) silicone oil bath (C) incorporating a thermocouple (letter D, IKA ETS-D5) inserted into one of the necks of the reactor. The other neck of the glass flask was used for the pH meter probe (letter E, Orion 720A Plus). A stirrer was employed to continually mix the solution and the apparatus was connected to a water cooling system (F) via one of the necks to avoid evaporation losses. Samples were loaded into the glass reactor from the free neck (G) and, if required during the experiments or when experiments were concluded, the solution was collected and solid particles separated thanks to paper filters (pore size 0.22μm) and a vacuum pump (Fisher FB65540).

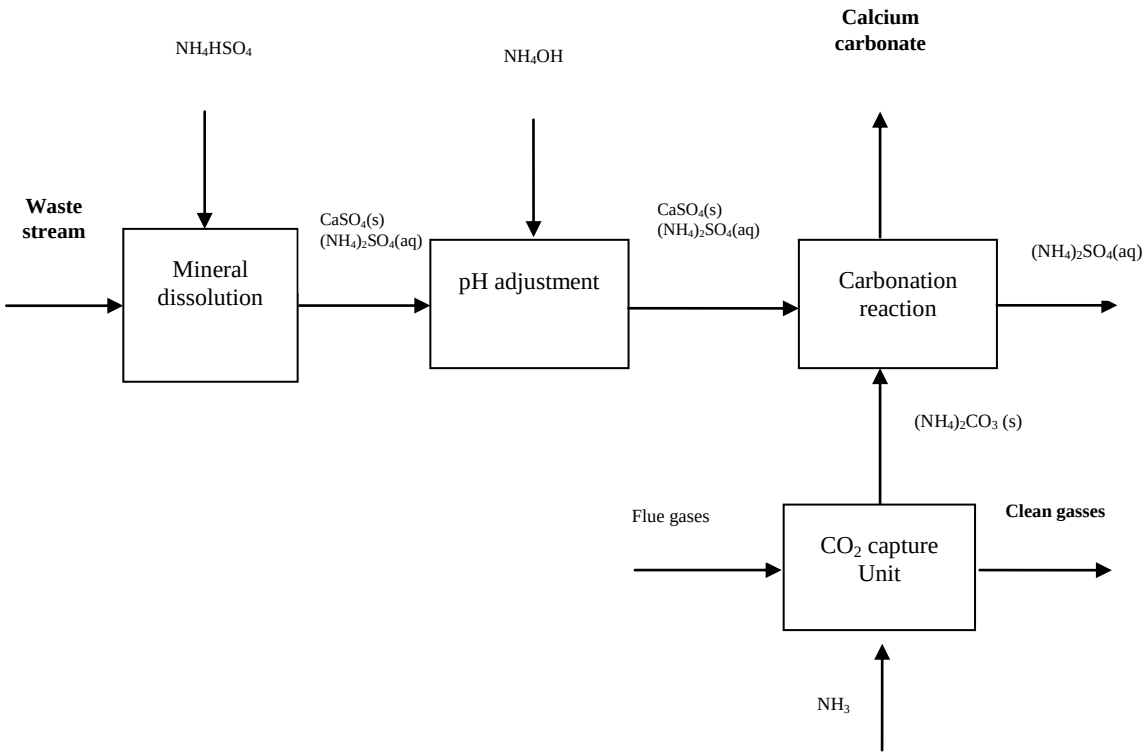

Figure 3.5: Simplified block diagram of the mineralization process investigated

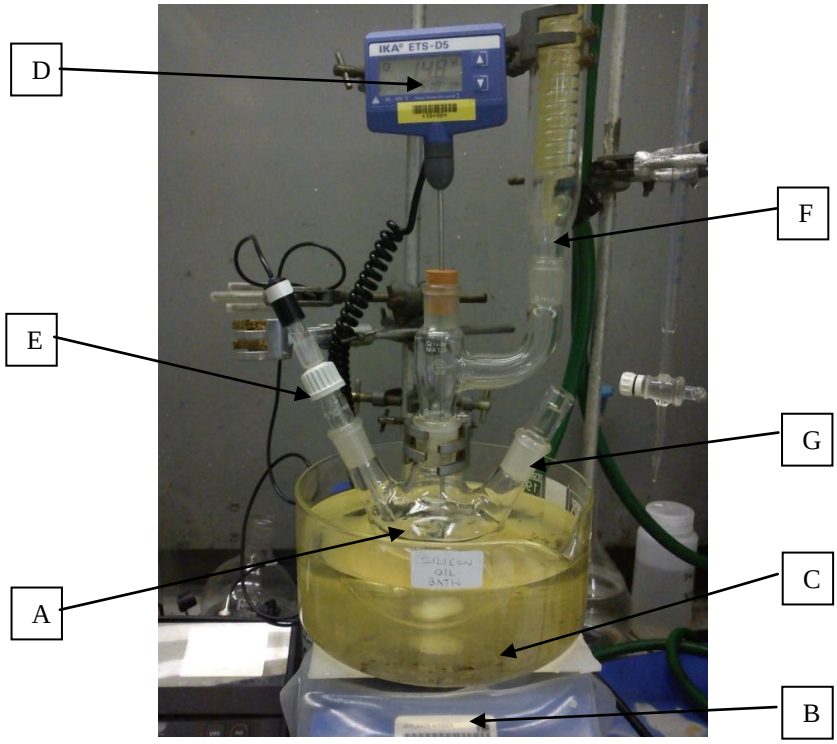

Figure 3.6: Mineralization experimental set-up: A) glass flask B) heater and temperature controller C) silicone oil bath D) thermocouple E) pH meter F) water cooling system G) sample loading neck

Mineral dissolution, pH adjustment and carbonation reaction steps (Figure 3.5) have been studied at lab-scale level. As described in the literature review (Section 2.3.4.6), the main parameters affecting mineral carbonation are temperature, S/L ratio and particle size. Accordingly, investigation on the effect of these parameters (Chapters 5 and 6) on the designed process are required to assess its feasibility. Table 3.2 reports the values of the parameters tested in this work.

Parameter	Values tested
Temperatures	25-40-50-65-90°C
S/L ratio	15-25-50g/l
Particle size	75-150μm, 150-300μm

Table 3.2: List and range of parameters investigated for the mineralization process

3.4 Chemical reagents

As seen in the Figure 3.5, in this thesis different chemical reagents were employed in the experiments. Crystalline ammonium sulfate (NH_4HSO_4) was obtained from Fisher Scientific in 500g container, 98% min. purity. Crystalline ammonium carbonate ($(NH_4)_2CO_3$) min. purity 96.4% in a 500g container was also obtained from Fisher Scientific. To avoid uptake of moisture they were stored sealed in a dessicator and the exposition of the reagents in the atmosphere at natural conditions was limited as much as possible. Batches of experiments were carried out during 5-10 consecutive days after which the reagents were bought new again. This has ensured that capture of moisture from $(NH_4)_2CO_3$ was negligible and the accuracy of mineral carbonation estimation was not affected.

3.5 Experimental conditions for testing the mineral dissolution step

Four waste streams (steel slag (SS), recycled concrete aggregate (RCA), phosphorus slag (PS) and ground granulated blast furnace slag (GGBS)) were selected (Section 5.2) for testing the dissolution step of the mineralization process (Figure 3.5 and Table 5.1). Employing the experimental set-up presented in Figure 3.6, 400ml solutions were used: 1.3M NH_4HSO_4 for tests on steel slag and ground granulated blast furnace slag, while 0.96M and 0.8M NH_4HSO_4 for phosphorus slag and recycled concrete aggregate, respectively (values of NH_4HSO_4 concentrations were slightly above stoichiometric). Samples employed were in the size fraction of 75-150μm to be consistent with a

previous study on serpentine [3.1]. The stirring rate (800rpm), S/L ratio (50g/l), time (3h), sampling procedure (employing a syringe to collect a small amount of solution at regular intervals) and initial temperature (50°C) were also identical to those employed by Wang and Maroto-Valer [3.1]. Furthermore, experiments were also carried out at 25°C and 90°C to understand the dissolution trends of the samples at different temperatures and determine the dissolution kinetics.

3.5.1 Characterization of solution samples

During the dissolution experiments, small amounts of solution (about 10ml) were sampled with a syringe at fixed intervals and solid particles were separated thanks to a syringe filter unit with 0.22 μm pore size. The solution obtained was then acidified with HNO_3 to ensure stability and comparability with calibration standards of the ICP-MS. Afterwards, these samples were analyzed by ICP-MS to measure the concentration of metals in ion form dissolved. The extraction (e.g. dissolution) efficiency of a specific metal (e.g. Fe, Mg, Ca) in a solution sample at time t (e.g. at 5, 10, 15 min) was calculated by:

$$\%X_{\text{dissolved}}(t) = \frac{m_{\text{metal extracted into solution}[g]}}{m_{\text{metal originally in the sample}[g]}} x100 \quad (3\text{-}2)$$

The mass of metal originally present in the sample was determined by XRF (Table 5.2), while the mass of metal extracted into solution was obtained from the ICP-MS analyses reporting the concentration of metal in the solution.

3.5.1.1 ICP-MS

ICP-MS allows analysing chemical composition of liquids, solids and gases. When loaded into the instrument the sample is introduced into an high-energy argon plasma where the material is split into individual atoms. The plasma consists of positively charged argon ions and electrons at about 7000K. When the individual atoms of the sample exit the high energy plasma, the mass spectrometer can detect the concentration of the atoms present in the sample based on their mass to charge ratio.

For this work the ICP-MS employed was a Thermo-Fisher Scientific X-Series 2 (Figure 3.7) which analyzed the concentrations of Mg, Si, Fe, Ca, Al, Ni, Mn, Cr, Cu, Al, Sr, Na and Ba.

Figure 3.7: Thermo-Fisher Scientific X-Series 2

3.6 Experimental conditions for testing the sequence of mineral dissolution and carbonation reaction steps

During the course of this study (Chapter 6) three waste streams (steel slag, recycled concrete aggregate, phosphorus slag and ground granulated blast furnace slag) were identified for testing the sequence of mineral dissolution, pH adjustment and carbonation reaction steps (Figure 3.5). Different S/L ratio, temperature and particle size were investigated (Table 3.2) employing the experimental set-up presented in Figure 3.6.

The 400ml solutions employed were prepared with slightly above stoichiometric NH_4HSO_4 (Table 3.3) based on i) the S/L ratio used in the experiments, ii) the concentration of metals (Ca in the raw materials, Chapter 5, Table 5.2) and iii) the theoretical dissolution reaction (Chapter 5, Table 5.1) between Ca silicates and NH_4HSO_4:

$$CaO \cdot SiO_2 + 2NH_4SO_4 \rightarrow CaSO_4 + SiO_2 + H_2O + (NH_4)_2SO_4 \quad (3\text{-}3)$$

		NH_4HSO_4 concentration [mol/l]	$(NH_4)_2CO_3$ concentration [mol/l]
SS	15g/l	0.39	0.20
	25g/l	0.65	0.32
	50g/l	1.3	0.65
PS	15g/l	0.29	0.16
	25g/l	0.48	0.24
	50g/l	0.96	0.48
GGBS	15g/l	0.39	0.20
	25g/l	0.65	0.32
	50g/l	1.3	0.65

Table 3.3: NH_4HSO_4 and $(NH_4)_2CO_3$ concentration used for the dissolution studies based on stoichiometric concentration required, S/L ratio and CaO content.

As an example, for experiments employing PS at 25g/l the concentration of NH_4HSO_4 was calculated as follows. CaO content in PS is 46.7% (Chapter 5, Section 5.2) which corresponds to 33.4% Ca content. Mineralization experiments used 400ml Millipore water, and therefore, for 25g/l concentration, 10g of PS were required. Hence, the Ca content into 400ml solution was 3.3g (0.084mol) and the Ca concentration was 0.21mol/l. From reaction 3-3, stoichiometric concentration of NH_4HSO_4 is twice as Ca concentration, i.e. 0.42mol/l. NH_4HSO_4 molar mass is 115g/mol, and consequently, the quantity of NH_4HSO_4 in 1l and 0.4l solution is 48g and 19.2g respectively. Assuming that the dissolution reaction will not deviate much from the stoichiometric conditions, NH_4HSO_4 employed for the experiment was 22g (0.48mol/l), 15% more than 19.2g, to ensure its full availability for the dissolution of Ca and precipitation of $CaSO_4$.

According to the analogue mineralization process developed for serpentine by Wang and Maroto-Valer [3.1] [3.2], the sequence of mineral dissolution, pH adjustment and carbonation reaction took place at different temperature and running time. Mineral dissolution was carried out at 50°C for 3 hours. The adjustment of pH and precipitation of impurities steps took place by adding ammonia water (NH_4OH) in the solution, and raising the pH at about 8.2-8.3. The carbonation reaction was then conducted for 1 hour at 65°C adding slightly above stoichiometric $(NH_4)_2CO_3$ (Table 3.3) to ensure its full availability for the carbonation reaction. The amount of $(NH_4)_2CO_3$ was calculated based on i) the waste stream and S/L ratio used in the experiments, ii) the amount of $CaSO_4$ produced during dissolution reaction (Chapter 5, Table 5.1) according to:

$$CaO \cdot SiO_2 + 2NH_4HSO_4 \rightarrow CaSO_4 + SiO_2 + H_2O + (NH_4)_2SO_4 \quad (3\text{-}4)$$

which then reacts with $(NH_4)_2CO_3$ as follows:

$$CaSO_4 + (NH_4)_2CO_3 \rightarrow CaCO_3 + (NH_4)_2SO_4 \quad (3\text{-}5)$$

As an example, for experiments employing PS at 25g/l the concentration of $(NH_4)_2CO_3$ was calculated as follows. From the dissolution step, the concentration of NH_4HSO_4 in solution was 0.48mol/l. From reaction 3-4, the concentration of $CaSO_4$ produced was 0.24mol/L (half of 0.48mol/l) which, according to reaction 3-5, is the same as the concentration of $(NH_4)_2CO_3$. Therefore, considering the molar mass of $(NH_4)_2CO_3$ of 96g/mol, the required amount of $(NH_4)_2CO_3$ per litre was 23g and for the 400ml solution 9.2g.

3.6.1 Characterization of mineralization products

The carbonated final solid residues obtained after filtering the final solution (Section 3.3) were dried overnight in an oven at 105°C. Characterization of the products obtained was performed by calculating the level of carbonation achieved (efficiency of carbonation) by XRF and XRD to analyse their chemical composition and crystalline phases present and by analyzing the morphology of the particles' surface employing the scanning electron microscope (SEM), as described below. Investigation on the nature and morphology of the particles performed with the SEM allows collecting further useful information for understanding the dissolution and carbonation steps if the process investigated in this thesis.

3.6.1.1 Efficiency of carbonation

Efficiency of carbonation achieved by employing a certain material as feedstock for mineralization experiments (i.e. including the sequence of mineral dissolution, pH adjustment and carbonation reaction) represents the degree of carbonation reached. The feeding materials used in this study were rich in Ca and the calculation of the degree of carbonation must be based on calcium carbonate produced. Consequently, carbonation efficiency for waste materials (i.e. Ca-rich) represents the wt% of Ca initially contained in CaO which is converted into $CaCO_3$ during the mineralization process, calculated as follows:

$$\xi_{Ca}\% = \frac{\text{Ca mass in } CaCO_3\text{(after carbonation)} - \text{Ca mass in } CaCO_3\text{(before carbonation)}}{\text{Ca total mass in feeding material}} \times 100 \quad (3\text{-}6)$$

The Ca mass in the feeding material can be calculated from XRF analyses on the parent sample, while $CaCO_3$ before and after experiments can be calculated from thermo-gravimetric analyses (TGA). TGA measures the weight change of a material as function of temperature in a controlled atmosphere. The analysis is performed by gradually raising at the desired heating rate the temperature in a furnace and the sample weight is measured on an analytical balance. The weight of the sample is plotted against temperature or time to illustrate the loss of moisture, water of hydration and decomposition of the material.

In the case of carbonated materials, calcium carbonate, when heated between 600-850°C releases CO_2 and leaves CaO [3.10] and consequently the mass of the sample decreases. It is therefore possible, thanks to the TGA, to link the mass loss due to the CO_2 evaporation between 600-850°C to the amount of Ca bounded in $CaCO_3$ in the initial solid sample, as follows:

$$\text{Ca mass in } CaCO_3 = \text{weight decrease}_{600-850°C}\% \times \frac{MW_{Ca}(\text{Kg/mol})}{MW_{CO_2}(\text{Kg/mol})} \times \text{mass of solid residue} \quad (3\text{-}7)$$

The instrument employed in this thesis for the TGA analyses was a TA Q500 (Figure 3.8).

Usually between 10-20mg of sample were loaded onto a pan and the analyses took place in nitrogen (N_2) atmosphere. The temperature heating ramp was 10°C/min, starting from ambient, with 10 minutes constant temperature at three different values: 105°C to allow residual moisture to evaporate; 500°C to stabilize the sample and prepare for the following temperature increase, during which the loss of weight was taken into account for the calculation of $CaCO_3$wt%; and finally 900°C to complete the degradation of the material.

Figure 3.8: TA Q500, instrument employed for TGA

3.6.1.2 Scanning electron microscope

A scanning electron microscope (SEM) allows specimens morphological characterization with resolution down to nanometer scale. A focused beam of high-energy electrons is used to generate a variety of signals on the sample surface. The path of the beam is correlated to a set of gray level pixels on a screen. The magnification on the monitor is simply computed by the ratio of the image width of the output medium divided by the field width of the scanned area. Information about the sample, including external morphology (texture), crystalline structures and orientation of materials making up the sample are revealed. In SEM analyses, the specimens are required to be electrically conductive or to be coated with a conductive layer (e.g. C, Pt, etc.).

When a sample is analyzed by SEM and therefore a beam of electrons is focused on the surface, incident electrons (IE) decelerate producing a wide range of different signals: secondary electrons (SE), backscattered electrons (BSE), diffracted backscattered electrons (EBSD, used to determine the crystal structure and orientation of minerals), X-rays and heat (Figure 3.9). SE and BSE are used for imaging samples: SE for showing the morphology and topography on samples, while BSE are valuable for illustrating contrast in composition in multiphase samples, as the different phases of different composition give different contrast in the image. SEM analysis is considered to be non-destructive because after the sample has been prepared on the holder and coated it can be analyzed several times at different intervals, providing the specimen is safely stored. Areas ranging from approximately 1 cm to 5 microns in width can be imaged in a scanning mode using conventional SEM techniques.

.

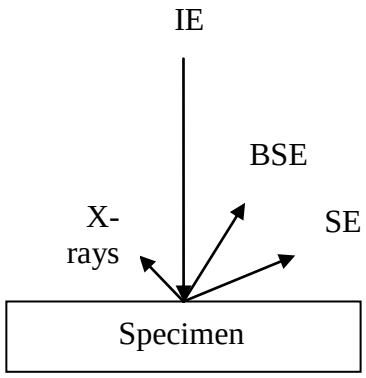

Figure 3.9: Signals generated from a sample analyzed with SEM

SEM can provide data on chemical composition of selected point locations on the sample. This approach is especially useful in qualitatively or semi-quantitatively determining chemical compositions, using energy dispersive X-ray spectroscopy, EDS. When incident electrons hit the surface, EDS detector can separate the characteristic X-rays produced by the sample. An energy spectrum is generated in order to determine the abundance of specific elements. EDS can be used to find the chemical composition of materials down to a spot size of a 2-3μm, and to create element composition maps over a much broader raster area. However, EDS can only detect the surface composition of a sample, not being a reliable technique if the particles investigated consist of different layers of materials

A SEM JEOL JSM-6400 (Figure 3.10) was employed in this work to study the morphology and composition of the particles. Secondary electron (SE) images were collected using 20kV beam voltage, 15mm working distance and the chemical microanalyses were performed with a Link ISIS 300 EDS microanalysis system fitted with a Si(Li) detector. SEM analyses required ~1g representative samples, obtained grinding and homogenizing the materials which were analyzed. Before the analysis the specimens were adhered to a carbon tab prior to sputter coating with platinum at 2.2kV for 90s.

Figure 3.10: SEM JEOL JSM-6400

3.7 Cost evaluation of the mineralization process studied

A cost evaluation of the mineralization process proposed (Figure 3.5) was carried out. For this purpose, a mass balance was firstly conducted considering the chemical reactions, reactants and products and their stoichiometric values. Among the different waste materials tested in the mineralization experiments, steel slag was the one chosen for the economic evaluation of mineral carbonation at industrial scale because of the impact of steel industry on the global CO_2 emissions. In fact, emission from steel plants account about 20% of the world CO_2 industrial emissions [3.11].

From the reaction list reported in Table 5.1 and data on the CO_2 emissions and steel slag production of a specific steel plant (where the technology may be applied), a mass balance for the mineralization process can be performed. These calculations allow assessing the quantity of chemicals required and products obtained and, consequently, investigate their economic impact on the mineralization process. Afterwards, an energy balance of the overall process can be performed. Heat released and required from each single step can be calculated using the thermodynamic calculations presented in Table 5.1 and the quantity of different inputs and outputs of each step of the process, obtained from the mass balance. The energy balance should also include an estimation of electrical consumption based on the design of the process and consequently the needs of electrical equipment (compressors, pumps, conveyors, agitators) to allow its operation. Once also the energy balance (heat and electricity) has been investigated, and therefore, the energy demand established, CO_2 emissions due to the process can be calculated. Afterwards, comparison between the CO_2 captured and CO_2 released, when the

mineralization process is implemented in a steel plant, allows evaluating the carbon balance. If it is negative, based on estimations of the capital investment, variable and other costs, the economic feasibility of the investigated multi-step process at industrial scale can be assessed.

3.8 References

[3.1] Wang X, Maroto-Valer MM. Dissolution of serpentine using recyclable ammonium salts for CO_2 mineral carbonation. Fuel. 2011;90:1229-37.

[3.2] Wang X, Maroto-Valer MM. Integration of CO_2 Capture and Mineral Carbonation by Using Recyclable Ammonium Salts. ChemSusChem. 2011;4:1291-300.

[3.3] Teir S, Revitzer H, Eloneva S, Fogelholm C-J, Zevenhoven R. Dissolution of natural serpentinite in mineral and organic acids. International Journal of Mineral Processing. 2007;83:36-46.

[3.4] Jenkins R. X-ray fluorescence spectrometry. Second edition ed: John Wiley & Sons inc.; 1999.

[3.5] Guinier A. X-ray diffraction in crystals, imperfect crystals and amorphous bodies. New York: Dover pubblications. pp 4-9; 1994.

[3.6] Connolly J. Introduction Quantitative X-ray Diffraction Methods. http://epswwwunmedu/xrd/xrdclass/09-Quant-intropdf2010. Date of consultation: November 2012.

[3.7] Johnson Q, R.S. Z. Checking and estimating RIR values. Advances in X-ray Analysis: JCPDS-International Centre for Diffraction Data; 2000.

[3.8] Lutterotti L. MAUD - Materials Analysis Using Diffraction. http://www.ing.unitn.it/~maud/index.html. Computer program. Date of consultation: November 2012

[3.9] Hillier S, Suzuki K, Cotter-Howells J. Quantitative determination of cerussite (lead carbonate) by X-ray powder diffraction and inferences for lead speciation and transport in stream sediments from a former lead mining area in Scotland. Applied Geochemistry. 2001;16:597-608.

[3.10] Huijgen W, Witkamp G, Comans R. Mineral CO_2 sequestration by steel slag carbonation. Environmental Science & Technology. 2005;39:9676-82.

[3.11] IEA. CO_2 emissions from fuel consumption: 2011 Highlights. Paris - France IEA-International Energy Agency; 2011.

CHAPTER 4 – WASTE MATERIALS FOR MINERAL CARBONATION - A UK PERSPECTIVE

This chapter aims at providing a picture of the potential use of waste streams for CO_2 storage in the UK. Firstly, from literature review, the chemical composition of a variety of suitable wastes for mineralization is reported. Afterwards, an assessment of the potential waste streams resources available in the UK together with their potential storage capacity are presented. It should be noted that availability of historical data on the production of some waste streams is limited. Information and data reported in this chapter are closely linked to the publication "Waste materials for carbon capture and storage by mineralisation (CCSM) – A UK perspective" listed in page XIV. The contribution of the author of this thesis to the development of such publication is mainly related to data collection and processing on waste streams availability and review of the drafts of the paper.

Detailed discussions on mineralization technologies available, effect of parameters, and efficiencies were reported in the literature review (Chapter 2), therefore, in this chapter, data from previous studies on mineralization experiments are presented only to understand the context in which they were performed.

4.1 Potential waste materials for mineral carbonation

Waste materials from a wide range of industrial processes are rich in calcium and magnesium oxides and hydroxides, which are desirable for mineral carbonation [4.1]. Both natural rocks and wastes, depending on their chemical composition, can be suitable for mineral carbonation. However, the potential utilization of waste can be more complex than natural rocks, as described here. Firstly, rocks are a resource in a specific location which could be the feedstock for mineral carbonation for hundreds of years. In contrast, a material previously considered as waste may find a use due to developments in technology. Secondly, technology changes can lead to the cessation of a particular waste production. Thirdly, changes in legislation such as increasing disposal costs for waste, could create markets for 'waste' as by-products. The availability of waste products can therefore be very uncertain. Moreover, difficulties in retrieving long-term data for past production and the unpredictable nature of future sources and availability of waste should also be considered.

As seen in the literature review (Section 2.2.3), waste streams are characterized by a high content of calcium oxides, and therefore, they can be used for mineral carbonation. Feedstock employed for mineralization include: Recycled concrete aggregate (RCA), steel slag (SS), ground granulated blast furnace slag (GGBS), pulverised fuel ash (PFA) including oil shale pulverised ash, incinerator bottom ash (IBA), air pollution control (APC) residue, cement kiln dust (CKD), incinerator sewage sludge ash (ISSA), paper sludge ash (PSA) and biomass ash (BA). Mineral carbonation using all the above materials has been demonstrated in several recent studies [4.2 - 4.8]. In this work the assessment of inorganic waste as a resource material for mineralization technology was carried out considering the volumes available in the UK, their chemical composition and their location. The future availability of these waste resources was also investigated and discussed in the following sections, along with the assessment of employing mineral carbonation technology as an intermediate process towards the re-use of mineral wastes. The parameters used to evaluate current and future potential of the mineral wastes as a resource for mineralization are:

- Amounts of waste streams available (including predicted future trends);
- Content of calcium, magnesium and other suitable metals for mineral carbonation (e.g. iron).

4.2 Chemical composition and CO_2 uptake of potential waste materials

Suitable waste materials for mineral carbonation, as seen in Chapter 2, must be rich in alkali metals (Ca/Mg). The literature review conducted allowed identifying several waste streams with these characteristics (Section 2.2.3) and a summary of their chemical composition is presented in Table 4.1. In the same table, the theoretical maximum CO_2 uptake ($TCO_{2\ uptake}$) expressed in wt% was calculated and reported for each potential UK mineralization waste from its chemical composition, using the modified Steinour formula [4.9] [4.10].

$$TCO_{2\ uptake} = 0.785 \times (\%CaO - 0.56 \times \%CaCO_3 - 0.7 \times \%SO_3) + 1.091 \times \%MgO + 0.71 \times \%Na_2O + 0.468 \times (\%K_2O - 0.632 \times \%KCl) \quad (4\text{-}1)$$

This method is based on the assumption that the total amount of Ca and Mg can be fully extracted from the waste, and subsequently, carbonated [4.11]. $TCO_{2\ uptake}$ and the

annual production of the waste in the UK were then used in Section 4.10 to calculate its theoretical annual maximum CO_2 storage potential ($TCO_{2\ capture}$ expressed in $MtCO_2/yr$) as follows:

$$TCO_{2\ capture} = \text{Waste available} \times TCO_{2\ uptake} \quad (4\text{-}2)$$

The experimental $CO_{2\ uptake}$ ($ECO_{2\ uptake}$, Table 4.1) in wt% expresses the experimental values of CO_2 uptake achieved thus far and reported in literature. $ECO_{2\ uptake}$ was calculated and reported in the next sections for each potential UK mineralization resource from experimental results found in literature. In addition, the experimental $CO_{2\ capture}$ ($ECO_{2\ capture}$ expressed in $MtCO_2/yr$) was calculated based on the waste availability, as explained in Formula 4-3, and it is reported in Section 4.10.

$$ECO_{2\ capture} = \text{Waste available} \times ECO_{2\ uptake} \quad (4\text{-}3)$$

Numerical values of $ECO_{2\ capture}$, expressing the amount of CO_2 which could be stored in waste materials, allow evaluating the potential of UK wastes as feedstock for mineral carbonation. All the waste streams investigated showed higher calcium content compared to magnesium.

Table 4.1 shows the high variability of the chemical composition of any given waste stream which directly depends on the starting material (e.g. coal, iron ore, municipal waste), production process and storage conditions. All SS, CKD, BA, oil shale ash, APC residue and PSA present high CaO content (40-70%) that is reflected in a high $TCO_{2\ uptake}$. MW incinerator bottom ash presents a large amount of SO_3 that lowers the MW ash $TCO_{2\ uptake}$. The state of the art of mineral carbonation using wastes indicates that the maximum $ECO_{2\ uptake}$ reached 20-25wt% for GGBS, SS, and APC residue, while largely available RCA and PFA present low $ECO_{2\ uptake}$, mainly because of their low Ca content.

The following sections describe in more detail, for each waste stream, their chemical composition, $TCO_{2\ uptake}$ and $ECO_{2\ uptake}$. Furthermore, data on their annual production in UK and historical trends (where available) are also reported with a final assessment of their potential for CO_2 storage.

	Chemical composition (wt%)							$TCO_{2\ uptake}$ (wt%)	$ECO_{2\ uptake}$ (wt%)
	CaO	MgO	Fe_2O_3	SiO_2	SO_3	Na_2O	K_2O		
Recycled concrete aggregate (RCA) a)	15-24	2-3		64.0		0.9	0.5	6[a]-22[4.21]	16-20[4.17]
Cement kiln dust (CKD) b)	34.5-46.2	1.5-2.1	2.9	16.4	22	0.5	4-5.8	0.5-30[4.51][4.4]	9-11[4.4][4.51]
Ground granulated blast furnace slag (GGBS) c)	15-41	8-11	0.5-0.9	34-36	1.4		0.6	20-44[4.21][4.37]	7-23[4.21][4.37]
Pulverized fuel ash (PFA) d)	1.3-10	1-2	13.8	56	4	0.5	0.1	6-9[4.30][4.27]	1.6-6.7[4.30][4.31]
Incinerator sewage sludge ash (ISSA) e)	9-37	3	5.6	40	0.3	0.7	2.3	15[4.4]	2[4.4]
Steel slag (SS) f)	25-55	1.5-15	1.6	1-27	8	0.3	0.1	24-52[4.11]	12-21[4.15][4.45]
Biomass and wood ash (BA) g)	24-46	8-9	1-1.3	5-17	0.63-3	0.5	14-21	50[4.4]	8[4.4]
Municipal waste incinerator bottom ash (IBA) h)	32-53	2.8	1-7.9	4-30	27.9	0.5	0.1	25[4.4]	3-14 [4.43][4.45][4.46]
Oil shale ash i)	42-50	5-6.5	4	2.1				15-45 [4.28][4.29]	9[4.29]
Air pollution control (APC) residue j)	50-60	8	0.5-1.5	10			2-6	50-58[4.48]	7-25 [4.19][4.46][4.48]
Paper sludge incinerator ash (PSA) k)	45-69	1.3-5.3	1-4.7	10-25	1-7	0-1	0-2	50[4.4]	17[4.4]

[a]: Assuming 75% of Ca in the RCA binds to CO_2

Table 4.1: Chemical composition of the carbonation resources a) [4.15] [4.21] [4.12] b) [4.4] [4.51] c) [4.13] [4.37] [4.59] d) [4.4] [4.30] [4.37] e) [4.14] f) [4.11] [4.59] g) [4.4] h) [4.4] [4.5] [4.60] i) [4.28] [4.29] j) [4.46] [4.57] k) [4.15] and their theoretical CO_2 uptake ($TCO_{2\ uptake}$) and the experimental uptake ($ECO_{2\ uptake}$)

4.3 Recycled concrete aggregate

Recycled concrete aggregate (RCA) results from the processing of inorganic material previously used in construction and principally including crushed concrete. The cement component of RCA consists of a series of calcium silicate hydrate and calcium aluminate hydrate compounds, as well as calcium hydroxide, which is highly alkaline. Therefore the most abundant mineral is SiO_2, 64wt%, followed by CaO whose content can vary between 15-24wt% (Table 4.1). Chloride ions from the application of de-icing salts to roadway surfaces or sulphates from contact with sulphate-rich soils can sometimes be present [4.14]. Due to the high variability in CaO content, RCA $TCO_{2\ uptake}$ is also very variable, 6–22wt% (Table 4.1) [4.15] [4.16]. Kashef-Haghighi and Ghoshal investigated the carbonation of a fresh concrete block using a flow-through reactor under a constant flow of CO_2 (20% in nitrogen balanced) at 20°C and 60min duration achieving an $ECO_{2\ uptake}$ ranging 16-20% [4.17]. An $ECO_{2\ uptake}$ value of 16.5% was achieved by direct carbonation at ambient temperature, 4bar pressure, 48min duration and a mean particle diameter of 80μm [4.20]. In this process, the cement powder was mixed with the desired amount of water (50wt%), moulded into bricks, cured with CO_2 and then dried overnight. Other investigations have attempted direct carbonation of RCA, but unfortunately they did not report the $ECO_{2\ uptake}$. For instance, Shtepenko et al. used a pressurized vessel purged with 2bar of pure CO_2 for 60min [4.18], while Iizuka et al. and Katsuyama et al. employed a two-step process for the extraction of Ca^{2+} from cement waste (30bar, 50°C) and sequent carbonation (1bar) in a stirring tank vessel [4.7] [4.16].

4.3.1 Assessment of UK resources

An annual average of about 52Mt of RCA is generated in the UK [4.23] [4.24], and the latest data available are presented in Figure 4.1. It can be noticed that between 2008 and 2009 there was a drop of about 10Mt in RCA production, from 58 to 48Mt, probably due to the crisis of the construction sector. The vast majority of RCA is currently re-used in construction applications as an aggregate, mainly for low-end applications, such as ‘hard core’ for building products and land reclamation. Thereby, the amount of RCA material sent to landfill and attracting taxes is small, reducing the need for virgin rock aggregate in the construction sector [4.22].

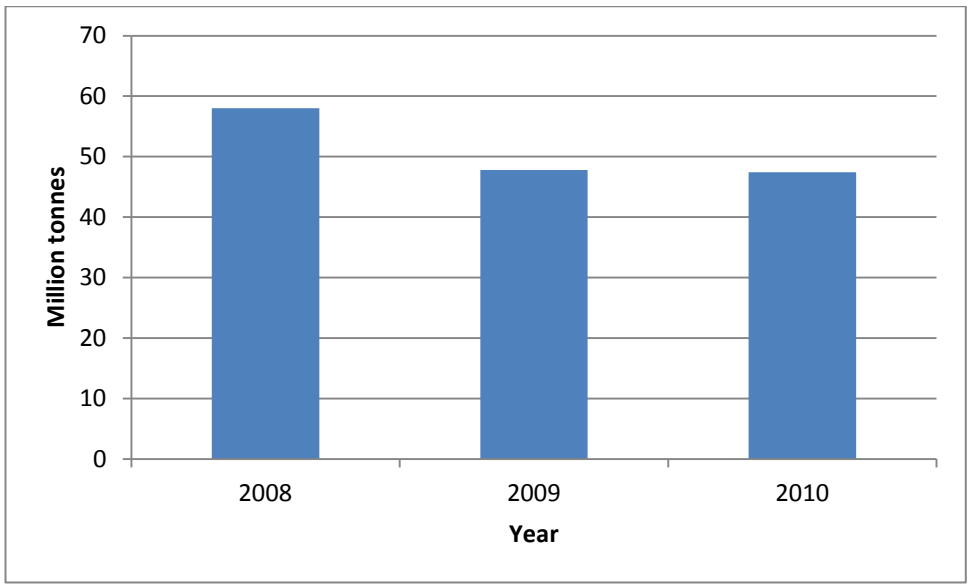

Figure 4.1: RCA production in the UK [4.23]

The UK construction sector is facing a number of fundamental changes over the next few years to develop a sustainable construction industry capable of delivering a low carbon future and to meet the current carbon, water and waste reduction targets [4.22]. Economic and legislative developments driven by increasing emphasis on reducing energy, water consumption and waste generation, and recycling and disposal issues, will influence future aggregate production trends, driving a radical change in the extraction and processing aggregates industry [4.22]. Therefore, it is expected that in the future there will be a further increase in the amount of RCA recycled [4.22].

4.4 Pulverized fuel ash from coal combustion

Pulverized-fuel ash (PFA), also known as coal fly ash (FA), is electrostatically precipitated from the flue gases of coal-burning power stations. PFA is a fine powder made up of individual fused ash particles with a diameter of about 10–15μm.

As seen in Table 4.1, the principal components of PFA are usually SiO_2, Fe_2O_3, MgO (1–2%) and CaO (1.3–10%). The properties of PFA are influenced by those of the coal burned, the burning techniques used and also by the type of flue gas system adopted [4.26].

Table 4.1 shows results from mineralization experiments at different conditions employing PFA. $TCO_{2\ uptake}$ of coal PFA is about 9wt%, and the $ECO_{2\ uptake}$ has been

reported to achieve about 7wt% maximum (Table 4.1) because of the relatively low content of CaO and MgO in the feedstock. Both direct aqueous carbonation of 40μm PFA particles at 30°C, 10bar, 18h [4.30] and aqueous carbonation under 2.7bar of pressure, 20% moisture and 120h [4.31] were investigated. Moreover, PFA carbonation at 30–90°C, 10 and 40bar, using a mean particle diameter of between 20 and 150μm and solid/liquid (S/L) ratios between 0.1 and 1l/kg, was carried out in a stainless steel autoclave reactor [4.27]. Other direct aqueous carbonation experiments were performed at 25-30-60°C, 10-20-30-40bar for 2h and results showed that 1t of coal PFA could sequester up to 26Kg of CO_2 [4.30].

Moreover, PFA from combustion of oil-shale has been investigated as feedstock material for mineral carbonation. This is relevant for countries such as Estonia, where the primary energy source is oil shale (low-grade carbonaceous fossil fuel) and pulverised fuel ash from oil-shale contains up 42-50% CaO (Table 4.1). When using ambient pressure and temperature in a continuous flow column reactor and stirring at 1000rpm, an $ECO_{2\ uptake}$ of 9wt% was reported for oil-shale PFA [4.29].

Whilst the quantities of coal PFA generated are large (Section 4.4.1), the low CaO and MgO contents limits the amount of CO_2 that can be converted to carbonates. Therefore, PFA cannot significantly reduce CO_2 emissions from coal fired power plants [4.1].

4.4.1 Assessment of UK resources

About 5.6Mt of PFA are produced every year in the UK [4.62], and this production has been constant in the last decades because of the stable employment of coal for power generation. In the coming years, for the same reason, the production of PFA is not expected to show substantial changes. In UK about 50% of PFA is used by a wide range of applications, including cement manufacturing (main use), asphalt, hydraulically bound mixtures, uses without any binding agent (e.g. fill material in embankments and as capping layers) or as grouts, where the material is hydraulically pumped or injected into the ground to fill void space. The remaining 50% of PFA is normally sent to landfill as conditioned ash in either a monofill or a lagoon and might be available for mineralization [4.22] [4.32].

4.5 Steel and iron slag

SS is the by-product of the manufacture of steel from pig iron (blast furnace) and metal scrap (electric arc furnace). As seen in Section 2.2.3, steel slag production can be subdivided into mainly basic oxygen furnace slag (BOF) (62%), electric arc furnace slag (EAF) (29%) and, moreover, secondary metallurgical slag such as ladle slag (9%) [4.33]. BOF slag generally has lower CaO content than EAF [4.33]. Secondary processes for further refinement of stainless steel through reduction of carbon content and pollutants, such as sulfur, also produce slags. To further refine the steel after coming out of the BOF or EAF, fluxes are added to the molten steel while in a ladle. The slag from this process is usually called ladle slag. The chemical composition of ladle slag is significantly different from that of steel furnace slag in that the former has a very low Fe content (only 2.4wt%) but higher Al content (13.4wt%) [4.33]. Also, a mixture of argon and oxygen, with the addition of cleaning agents to remove impurities, is added to the molten metal to decrease its carbon content. The oxygen combines with carbon in the unrefined steel to reduce the carbon level. The presence of argon enhances the affinity of carbon for oxygen, and thus, facilitates the removal of carbon forming argon oxygen decarburization slag (AOD) [4.36].

BOF and EAF steel furnace slags typically present CaO content between 25–55wt% (Table 4.1) making them suitable candidates for mineral carbonation. The maximum $TCO_{2\ uptake}$ (24 to 52wt%) reported in Table 4.1 would be enough to sequester about 40% and 10% of the CO_2 emissions from EAF and BOF processes, respectively [4.11] [4.34] [4.35].

Ground granulated blast furnace slag (GGBS) is a by-product from the production of iron, resulting from the fusion of fluxing stone (fluorspar) with coke, ash and the siliceous and aluminous residues remaining after the reduction and separation of iron from the ore [4.22]. The molten slag is equivalent to about 20wt% of iron production [4.14]. GGBS typically consists of silicates, alumino-silicates, and calcium-alumino-silicates and the most abundant compounds include dicalcium silicate, tricalcium silicate, dicalcium ferrite, merwinite (calcium magnesium disilicate), calcium aluminate, calcium-magnesium, iron oxide, and some free lime and free magnesia. GGBS usually contains CaO and MgO in the range of 15–41wt% and 8-11wt%, respectively (Table 4.1).

An $ECO_{2\ uptake}$ of 7–23wt% was reported for GGBS (Table 4.1). EAF, blast furnace slag and ladle slag showed an $ECO_{2\ uptake}$ on the order of 12wt%, 7wt% and 4.6wt%, respectively [4.15] [4.29]. The GGBS and EAF powders were subjected to 100% CO_2 at a constant pressure of 5bar for 2h [4.15]. Many other studies used these materials for mineralization experiments, for instance, GGBS indirect carbonation experiments were run in a batch reactor at 70°C, 40bar, 20% acetic acid solution (Ca extraction step) using particles between 125 and 250µm. This was followed by carbonate precipitation at 30°C and ambient pressure whilst being stirred at 600–700rpm for 2h in the presence of pure CO_2 and sodium hydroxide solution [4.35]. EAF accelerated carbonation tests were performed in stainless steel reactor at 50°C, 10bar pressure, a L/S ratio of 0.4l/kg and 100% CO_2 and at 75% relative humidity that was maintained using a saturated NaCl solution [4.38]. EAF carbonation under ambient pressure and temperature using 15% CO_2 balance in air for 65min and a S/L ration of 0.1l/kg [4.29] was also attempted. EAF and BOF slags were employed for leachability tests for extracting Ca^{2+} from <150µm powders, using a S/L ratio of 10kg/kg under continuous stirring and at 22°C in the presence of 0.5M NaOH, 0.5M H_2SO_4 or 0.5M HNO_3 [4.11]. AOD carbonation was performed at 30°C, 20% CO_2, at a S/L ratio of 0.5l/kg for 7 days [4.39]. $ECO_{2\ uptake}$ values from the numerous studies carried out on GGBS and SS range from 7–23wt% and 12-21wt% for GGBS and SS, respectively (Table 4.1).

4.5.1 Assessment of UK resources

Data available on SS production in UK are quite limited. A total of 1.25Mt of steel slag was produced in the UK in 2002 and a similar amount was generated in 2009. Also the production of steel in those two years was analogous, reaching about 12Mt [4.61]. Virtually all of the steel slag produced is employed as aggregate [4.40] [4.41] and therefore cannot be practically considered as mineralization resource in the near future.

The distribution of the SS is limited to only a few areas in the UK (Teesside, South Wales, Kent), and the majority of the works are close to port facilities that facilitate the transport of materials. The future availability of SS in UK might decline considering that the production of electric arc furnace (EAF) slag is expected to rise in the South East and can partially balance the decline of the BOF [4.61]. The latter is used for aggregate use and considering that the demand is expected to continue, there is little necessity to find alternative uses [4.40]. If mineralization technology can produce an

intermediate product with higher market value than the raw slags, then these waste materials might represent a resource for mineral carbonation.

About 3Mt of GGBS is generated in England and Wales every year and in recent years 75% of the total production of GGBS has been used as a cement replacement material by the concrete industry. The remaining fraction (25%) is air-cooled and used as an aggregate. Therefore, GGBS is not available for mineral carbonation and the choice between the two uses is dictated by production options, economics and demand [4.22] [4.23].

4.6 Bottom ash and air pollution control residue from incinerated municipal waste

Incinerator bottom ash aggregate (IBA) is processed from the material discharged into the burning grate of municipal solid waste (MSW) incinerators and comprises 80% to 90% of the total MSW ash production [4.22]. The most abundant elements in MSW ash are Si, Ca and Fe. IBA is a heterogeneous material, whose composition depends on the feed waste, combustion and quenching conditions used. IBA presents variable mineralogical structure, with amorphous and crystalline phases and (hydr)oxides, (alumino)silicates such as gehlenite ($Ca_2Al_2SiO_7$), hydrocalumite ($Ca_2Al(OH)_6[4.Cl_{1-x}O_x]\cdot 3H_2O$), calcium hydroxide $Ca(OH)_2$, calcite ($CaCO_3$) formed during quenching and storage, forsterite (Mg_2SiO_4), dicalcium silicate (Ca_2SiO_4) and hematite (Fe_2O_3) have been identified in bottom ashes [4.43]. Moreover, these ashes present heavy metals [4.4] [4.44]. Although ash composition can be expected to vary from facility to facility, chemical composition varies within relatively predictable ranges. Generally, IBA presents about 32–53% of CaO and about 3% of MgO (Table 4.1). The use of IBA in mineral carbonation may be an attractive option for this material, rather than being employed for the production of aggregates.

As presented in Table 4.1, municipal waste IBA has showed $ECO_{2\ uptake}$ values between 3–14wt%. IBA carbonation was carried out under different conditions: (1) using a pressurized reactor vessel (2bar) with pure CO_2 for 72h maintaining 75% relative humidity inside the reaction vessel, (2) using a stainless steel pressurized reactor at 10bar under 100% CO_2 atmosphere at 30°C for 24h at a S/L ratio of 0.3l/kg [4.43], and (3) direct gas–solid carbonation of incinerator bottom ash at ambient temperature and 3bar pressure for 2.5h in a stainless steel chamber [4.46].

Air pollution control (APC) residue from MSW incinerators consists of particulates that originate in the combustion zone area and are subsequently entrained in the combustion gas stream. Then, the particulates are carried into the boiler and air pollution control system together with reaction products and excess reagents resulting from flue gas treatment. The entrained particulates stick to the boiler tubes and walls or are collected in the APC equipment, which consists of scrubber, electrostatic precipitator and baghouse. Ash extracted from the combustion gas consists of very fine particles, with a significant fraction measuring less than 0.1mm in diameter [4.14].

APC residues mainly contain CaO (50-60wt%) and SiO_2 (10wt%) (Table 4.1). Other elements are also present in different percentages depending on the nature of the municipal waste: Cl, Al, Fe, Ca, Mg, K and Na. Abundance of Ca and Cl is due to their use in excess for acid gas abatement [4.19]. As regards to heavy metals, Zn, Pb, Cd, Cr, Cu, Hg, Ni are the most frequent. Also, trace quantities of very toxic organic compounds, such as polycyclic aromatic hydrocarbons (PAH) and chlorobenzenes (CB) may be present in these materials [4.47]. APC residue is a hazardous waste that may be reclassified to non-hazardous, following mineralization applications, by decreasing their metal ion leaching. Obviously, if materials containing chlorine would be employed for mineral carbonation, special health and safety precautions, with associated costs, would be required. However, the benefit of reclassification from 'hazardous' to 'non-hazardous' material would reduce the risk and cost associated with the disposal. The $ECO_{2\ uptake}$ of the APC residues was found ranging from 7 to 25wt% (Table 4.1). The carbonation experiments were performed using a modified muffle furnace, under a constant 100% CO_2 flow, with temperatures ranging from 200 to 500°C and with a residence time of 6h [4.48]. Also, direct gas–solid carbonation of APC residues was evaluated at ambient temperature and 3bar pressure for 2.5h in a stainless steel chamber [4.46].

4.6.1 Assessment of UK resources

The annual tonnage of IBA produced in the UK is about 1.2Mt where about 0.65Mt (55%) are currently used to produce aggregates [4.49]. Figure 4.2 presents the trends of production of IBA in UK in the last years and the fraction landfilled in 2011. The 2000 Waste Strategy predicted a rise of waste-to-energy of about 25% of municipal solid waste by 2020 [4.22]. This is likely to result in significant increases in the amount of

IBA available for mineralization which has already started in the recent years, as it can be noticed in Figure 4.2.

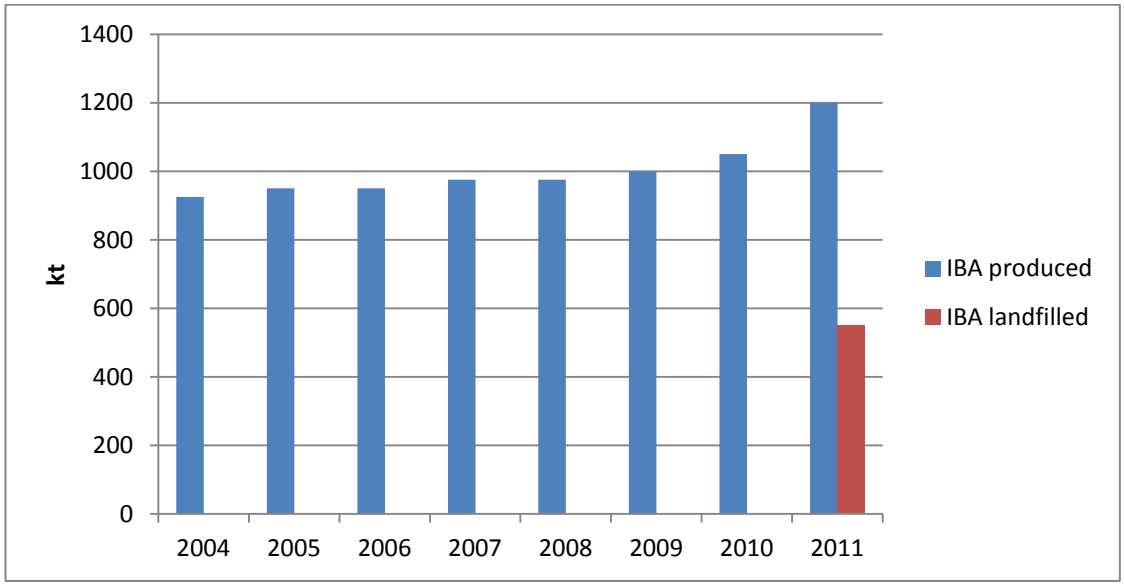

Figure 4.2: IBA from municipal waste produced in UK and fraction landfilled [4.49]

Previously, from 1996 to 2000, about 90% of the IBA produced in the UK was sent to landfill, but due to strict EU landfill directive, the space used for these hazardous wastes has significantly decreased and alternatives such as mineral carbonation are necessary [4.5]. However, the amount of IBA available for mineral carbonation will still be modest, i.e. below 1Mt [4.22].

There is limited information on historical data of APC residues produced. In 2010, about 162,000t were produced in the UK and 85%, about 138,000t, were sent to landfill as hazardous waste [4.50]. These residues are often transported over long distances for treatment and disposal, and alternative sustainable treatments would be beneficial [4.50]. APC residues are generated in the same locations as IBA and they might be used together as feedstock for mineral carbonation, increasing the amount of CO_2 sequestered in the incineration plant.

4.7 Cement kiln dust

Cement kiln dust (CKD) is a fine by-product of Portland cement and lime high-temperature rotary kiln production that is captured in the air pollution control dust collection system (e.g., cyclones, electrostatic precipitators). CKD is composed of fine

particulates of unburned and partially burned raw materials and it is collected from the combustion gases within pre-heater and kiln systems. Due to its caustic nature and potential as a skin, eye and respiratory irritant, CKD is a potentially hazardous waste. Typically, for every 100t of cement produced, 15–20t of CKD are generated [4.51] [4.52] [4.53]. The chemical and physical characteristics of CKD mainly depend on the method of dust collection employed at the facility.

The concentration of free lime in CKD is typically higher in the coarser particles captured closest to the kiln, while fine particles tend to exhibit higher concentrations of sulphates and alkalis. About 75% of the kiln dust particles are finer than 0.03mm. CKD from wet-process kilns tends to be lower in calcium content and richer in salts than the dust from dry-process kilns. CKD has a chemical composition similar to conventional Portland cement with the principal constituents being CaO, SiO_2 and Al_2O_3. As reported in Table 4.1, CaO and MgO content in CKD usually varies between 34% to 46% and 1.5% to 2.1%, respectively. The $ECO_{2\ uptake}$ was evaluated as being about 9-11wt% (i.e. every kg of CKD has potential to capture 0.09–0.11kg of CO_2) based on experiments using a direct carbonation route at ambient temperature and pressure over 3 days (38% relative humidity) in a column reactor [4.51] and ambient temperature and 2bar over 72h in a pressurized reaction vessel [4.4]. Results showed that despite the considerable differences in temperature, time and pressure employed, the experimental uptake of CO_2 reached almost the same values (9-11wt%, Table 4.1).

4.7.1 Assessment of UK resources

In 2008, the UK cement industry disposed about 46,000t of CKD in landfills [4.53]. The total annual tonnage of CKD being disposed of has fallen significantly since 1999, i.e. from 289,207t in 1999 to 46000t in 2008, because of new technology introduced in the cement production process. The production of CKD is expected to remain constant between 2010 and 2015, as shown in Figure 4.3, since the construction sector will not see a substantial expansion. The CKD produced in the UK per tonne of cement produced is very low (<1%) because the CKD is mainly recycled in the kiln during the production process.

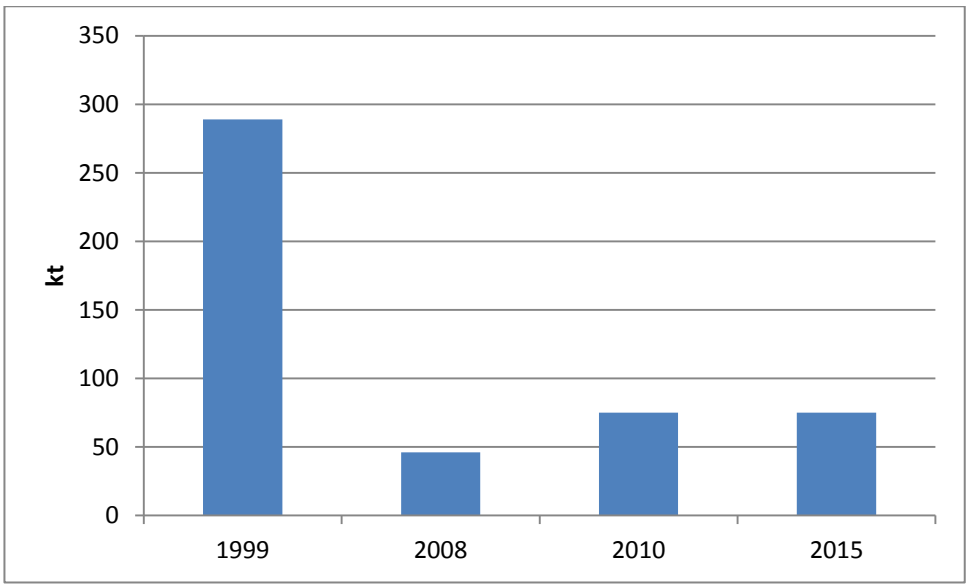

Figure 4.3: CKD produced and disposed in landfills in UK and forecasted production for year 2015 [4.46]

Before 2007, CKD together with sewage sludge could be used to improve soil fertility in land reclamation projects, but changes to legislation now precludes this use. Therefore, CKD sent to landfill raised to 75,000t in 2010 and it is expected to remain at this level at least untill 2015 [4.52].

However, the cement industry, which is a large CO_2 emitter, might decline in the UK due to the expected rise in the production costs because of EU regulations on CO_2 emissions. In fact, the EU Emission Trading Scheme, climate change agreements, carbon reduction commitments and a carbon levy can add a fee to pay because of the CO_2 emissions from the process. Therefore, the availability of CKD in the UK in the future years is not certain [4.54], but it is possible that it may decrease.

4.8 Other industrial waste resources for mineral carbonation

A number of other inorganic materials, such as incineration sewage sludge ash, paper and biomass sludge ash, can be considered as a small resource for carbonation in the UK. Although their production in UK is small it might be of primary importance in other countries based on their availability.

Incineration sewage sludge ash (ISSA) is the by-product produced during the combustion of dewatered sewage sludge in an incinerator. It contains between 9wt%

and 37wt% CaO (Table 4.1), and hence, is highly variable in terms of chemical composition. About 0.2Mt/year sewage sludge is produced in the UK [4.55] with approximated 0.08Mt/year of ISSA remaining after incineration (considering 40% of ash left after incineration) [4.14]. Currently, all ISSA produced is sent to landfill.

Paper sludge incineration ash (PSA) is the residue from incineration of the wastewater sludge from paper-making. It consists of residual fibres, fillers and chemicals and contains about 45–69% of CaO (Table 4.1). About 0.13Mt/year of PSA is produced in the UK. Currently 70% (or 0.091Mt) goes to end uses, such as brick and cement manufacturers, and the remaining 30% is landfilled [4.55].

Biomass ash (BA) is a by-product of the combustion of biomasses such as spent grains after beer and bio-ethanol production, rape-cake after oil extraction. Wood ash (WA) is generated from coal power station and combined electricity and heat generation plants using wood sources. BA and WA contain between 24% and 46% of CaO (Table 4.1). The production of biomass ash in UK is 0.062Mt/year. All sixteen major UK power plants are now co-firing a proportion of biomass, at an average level of 3% (energy basis) making use of a range of fuels including wood (virgin and recycled), olive cake, palm kernal expeller, sewage sludge and energy crops [4.56].

The $ECO_{2\ uptake}$ reported for BA, PSA and ISSA is about 8wt%, 17wt% and 2wt%, respectively (Table 4.1). All these materials were tested for CO_2 uptake using a reactor vessel in a 100% CO_2 atmosphere held at 2bar pressure and 75% relative humidity for 72h [4.4]. Detailed historical data on production of these waste streams in UK could not be found in any of the UK authorities databases accessible (e.g. Department of Environment, Food and Rural Affairs, Environment Agency). It is however reasonable to think that in the future they will not be available in such a quantity to store significant amounts of CO_2 by mineral carbonation.

4.9 Quarry waste as a potential resource

So far, wastes produced from industrial processes have been discussed for mineral carbonation. However, quarry waste can also be considered a potential feedstock for mineralization. Processing of crushed stone for use as construction aggregate consists of blasting, primary and secondary crushing, washing, screening, and stockpiling. These

operations produce significant amounts of waste, often referred to as quarry waste and fines. Usually sand and gravel workings do not produce permanent waste, while hard rock quarries produce variable amounts of quarry waste and fines. Quarry fines are the inherent fraction of an aggregate below 63μm, as defined by BS EN 1377:2. However quarry fines are more commonly defined as the sub-millimetre 'sand' fraction that is the undersize from screening coarse aggregate and the 63μm fraction, as the airborne dust, collected by extraction filters [4.57]. Only waste and fines from operations processing ultramafic rocks should be considered as potential resources but there are no such operations in the UK. However, the tailing remaining from the mining industry can represent an important resource for mineral carbonation in countries with large mining activities. For example, in South Africa, if quarry waste would be employed for mineral carbonation, the calculated CCS capacity only for the tailings obtained from the platinum industry would be 14Mt/year, which is about 4% of total annual South Africa CO_2 emissions [4.58].

4.10 Summary of UK waste streams as a resource for mineral carbonation

This chapter presented an up-to-date review of the potential applications of inorganic waste materials for mineral sequestration of CO_2. Waste production, availability, theoretical and experimental CO_2 uptake were discussed. A wide range of waste and industrial by-product resources are currently available in UK and could be used as feedstock for mineralization. However, many of them are already employed for other low-end applications. Table 4.2 summarizes this information and reports the quantity (Mt/year) of the waste materials that is produced in the UK, and the quantity (Mt/year) available for mineralization because not being currently reused/recycled. Furthermore, Table 4.2 also reports the potential and effective CO_2 that could be captured by mineral carbonation of waste materials. The theoretical CO_2 capture in Mt ($TCO_{2\ capture}$) was calculated by multiplying $TCO_{2\ uptake}$ (Table 4.1) by the waste availability (Formula 4-2), while the experimental CO_2 capture was calculated by multiplying the $ECO_{2\ uptake}$ (Table 4.1) by the waste availability (Formula 4-3).

Although RCA, SS, and GGBS are produced in UK, they do not currently present any tonnage available for mineral carbonation. In contrast PFA, APC, IBA, BA, ISSA, PSA and CKD are available for mineralization and their potential CO_2 capture capacity is about 1Mt/year or 0.2% of the total UK CO_2 emissions (about 490Mt). Currently, PFA represents the most abundant waste material to be used as mineral carbonation resource.

Table 4.2 also indicates that the experimental CO_2 capture capacity of the UK waste materials would be about 0.1Mt/year.

	Waste total production [Mt/yr]	**Waste availability [Mt/yr]**	**$TCO_{2\ capture}$ [Mt]**	**$ECO_{2\ capture}$ [Mt/yr]**
RCA	52[4.23][4.24]	0[4.23]	0	0
SS	1.25[4.59]	0[4.40][4.41]	0	0
GGBS	3[4.23]	0[4.22][4.23]	0	0
PFA from coal	5.6[4.62]	3.3[4.4][4.62]	0.752	0.05
APC from MW	0.13[4.19][4.50]	0.11[4.50]	0.064	0.016
IBA from MW	1.2[4.4][4.49]	0.55[4.49]	0.085	0.018
CKD	0.046[4.53]	0.046[4.53]	0.014	0.001
ISSA	0.08[4.14]	0.08[4.14]	0.012	0.0002
PSA	0.13[4.55]	0.039[4.55]	0.02	0.01
BA	0.062[4.56]	0.062[4.56]	0.03	0.005
Total	65	3.93	0.98	0.09

Table 4.2: Primary potential waste resources for carbonation in the UK, considering current materials reuse

It has to be stressed that the majority of the waste streams investigated are currently re-used for low-end applications to avoid landfill disposal costs and the aggregate levy in the case of primary aggregate production for the construction industry. For example, the use of the RCA into mineral carbonation could be technically viable integrating the mineralization plant after the crushing and sieving step of the construction and demolition waste, assuming that the properties of the carbonates produced could be compatible to commercial ones and also competitive in terms of cost. In such case, the $TCO_{2\ capture}$ for RCA would be 11.4Mt/yr which represents about 2.3% of UK annual CO_2 emissions.

Furthermore, SS and GGBS, that have high $ECO_{2\ uptake}$ (~20wt%), are generally located close to the CO_2 emitter and could also be attractive candidates for mineral carbonation. Figure 4.4 shows the distribution of all the waste resources and the main CO_2 emitters in the UK, including potential future resources, such as steel and blast furnace slags. The location of the mineral waste is widely distributed across the UK, and in many of

the cases, the waste resource is located very close to CO_2 emitters. In particular, the South East, South Wales, the East Midlands and the North East are regions with higher potential for mineral carbonation, considering the wastes available. Indeed, steel and cement works and incinerators represent ideal locations for the application of this technology considering that CCS by geological storage mainly targets large power emitters. Consequently, the use of waste resources for mineral carbonation, if proved of being a technically feasible and economically viable option, could be considered as a niche market that could employ relatively small amounts of feed materials for mineralization.

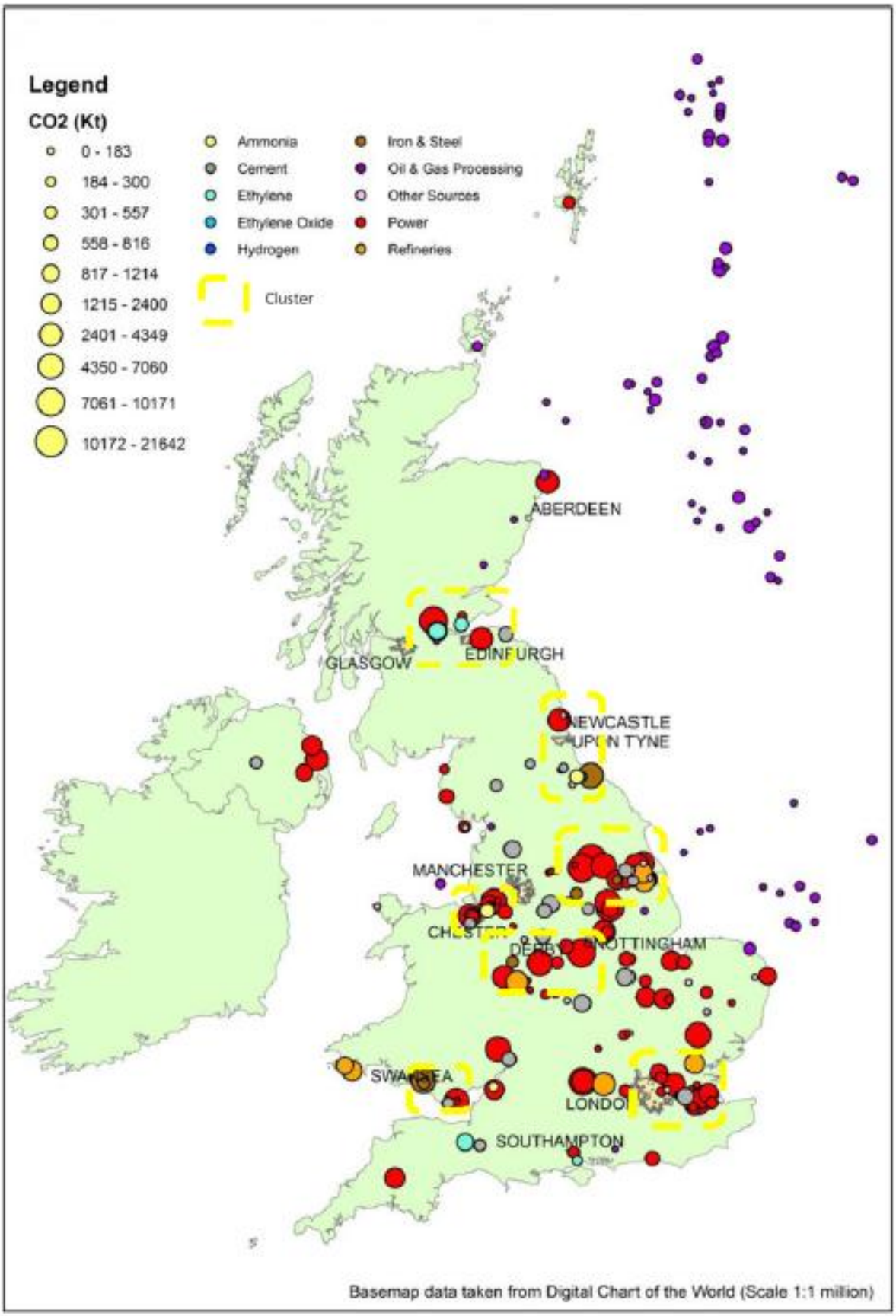

Figure 4.4: Waste resources for mineral carbonation and CO_2 emitter locations [4.63]

4.11 References

[4.1] Bobicki ER, Liu Q, Xu Z, Zeng H. Carbon capture and storage using alkaline industrial wastes. Progress Energy Combustion 2012;38:302–20.

[4.2] Huijgen WJJ, Comans RNJ, Witkamp GJ. Cost evaluation of CO_2 sequestration by aqueous mineral carbonation. Energy Conversion Management 2007;48:1923–35.

[4.3] Gunning PJ, Hills CD, Carey PJ. Production of lightweight aggregate from industrial waste and carbon dioxide. Waste Manage 2009;29(10):2722–8.

[4.4] Gunning PJ, Hills CD, Carey PJ. Accelerated carbonation treatment of industrial wastes. Waste Manage 2010;30(6):1081–90.

[4.5] Li X, Fernández Bestos M, Hills CD, Carey PJ, Simon S. Accelerated carbonation of municipal solid waste incineration fly ashes. Waste Management 2007;27(9): 1200-6.

[4.6] Teir S, Eloneva S, Fogelholm CJ, Zevenhoven R. Carbonation of minerals and industrial by-products for CO_2 sequestration. In: Proceedings of the 3rd international green energy conference, June 17–21, Västerås, Sweden; 2007. ISBN: 978-91-85485-53-6.

[4.7] Iizuka A, Fujii M, Yamasaki A, Yanagisawa Y. Development of a new CO_2 sequestration process utilizing the carbonation of waste cement. Industrial and Engineering Chemistry Research 2004;43:7880–7.

[4.8] Uibu M, Kuusik R. Mineral trapping of CO_2 via oil shale ash aqueous carbonation: controlling mechanism of process rate and development of continuous-flow reactor system. Oil Shale 2009;26(1):40.

[4.9] Steinour HH. Some effects of carbon dioxide on mortars and concrete-discussion. Journal of the Americal Concrete Institute 1959;30:905.

[4.10] Huntzinger DN, Gierke JS, Kawatra SK, Eisele TC, Sutter LL. Carbon dioxide sequestration in cement kiln dust through mineral carbonation. Environmental Science Technology 2009;43(6):1986–92.

[4.11] Doucet FJ. Effective CO_2-specific sequestration capacity of steel slags and variability in their leaching behaviour in view of industrial mineral carbonation. Mineral Engineering 2010;23(3):262–9.

[4.12] Limbachiya MC, Marrocchino E, Koulouris A. Chemical-mineralogical characterisation of coarse recycled concrete aggregate. Waste Management. 2007;27:201-8.

[4.13] Al-Otaibi S. Durability of concrete incorporating GGBS activated by water-glass. Construction and Building Materials. 2008;22:2059-67.

[4.14] TFHRC. Turner Fairbank Highway Research Centre (TFHRC) manual on the use of waste and by-product materials in pavement construction. www.fhwa.dot.gov/publications/research/infrastructure/structures/97148/for.cfm2008. Date of consultation: September 2011.

[4.15] Monkman S, Shao Y. Assessing the carbonation behavior of cementitious materials. Journal Materials in Civil Engineering 2006;18(6):768–77.

[4.16] Katsuyama Y, Yamasaki A, Iizuka A, Fuhii M, Kumagai K, Yanagisawa Y. Development of a process for producing high-purity calcium carbonate ($CaCO_3$) from waste cement using pressurized CO_2. Environmental Progress 2005;24:162–70.

[4.17] Kashef-Haghighi S, Ghoshal S. CO_2 sequestration in concrete through accelerated carbonation curing in a flow-through reactor. Industrial and Engineering Chemistry Research 2010;49:1143–9.

[4.18] Shtepenko O, Hills C, Brough A, Thomas M. The effect of carbon dioxide on-dicalcium silicate and Portland cement. Chemical Engineering Journal 2006;118:107–18.

[4.19] Baciocchi R, Costa G, Polettini A, Pomi R, Prigiobbe V. Comparison of different reaction routes for carbonation of APC residues. Energy Procedia 2009;1(1):4851–8.

[4.20] Teramura S, Isu N, Inagaki K. New building material from waste concrete by carbonation. Journal Materials Civil Engineering 2000;12:288–93.

[4.21] Stolaroff JK, Lowry GV, Keith DW. Using CaO- and MgO-rich industrial waste streams for carbon sequestration. Energy Conversion Management 2005;46:687–99.

[4.22] WRAP. Management of non-aggregate waste; 2010. www.wrap.org.uk/ downloads/Management-of-non-aggregate-waste-report.2ef2d355.10267.pdf.

[4.23] Defra. DCLG: Survey of arisings and use of construction, demolition and excavation waste as aggregate in England in 2008; 2010. www.defra.gov.uk/statistics/environment/waste/wrfg09-condem/. Date of consultation: September 2011.

[4.24] Lawson N, Douglas I, Garvin S, McGrath C, Manning D, Vetterlein J. Recycling construction and demolition wastes – a UK perspective. Environmental Management Health 2001;12(2):146–57.

[4.25] Brown P, Jones T, BéruBé K. The internal microstructure and fibrous mineralogy of fly ash from coal-burning power stations. Environmental Pollution 2011;159(12):3324–33.

[4.26] Vassilev SV, Vassileva CG. A new approach for the classification of coal fly ashes based on their origin, composition, properties, and behaviour. Fuel 2007;86(10–11):1490–512.

[4.27] Muriithi GN, Gitari MW, Petrik LF, Ndungu PG. Carbonation of brine impacted fractionated coal fly ash: Implications for CO_2 sequestration. Journal Environmental Management 2011;92:655–64.

[4.28] Uibu M, Velts O, Kuusik R. Developments in CO_2 mineral carbonation of oil shale ash. Journal of Hazardous Materials 2010;174:209–14.

[4.29] Uibu M, Kuusik R, Andreas L, Kirsimäe K. The CO_2-binding by Ca–Mg–silicates in direct aqueous carbonation of oil shale ash and steel slag. Energy Procedia 2011;4:925–32.

[4.30] Montes-Hernandez G, Perez-Lopez R, Renard F, Nieto JM, Charlet L. Mineral sequestration of CO_2 by aqueous carbonation of coal combustion fly-ash. Journal of Hazardous Materials 2009;161:1347–54.

[4.31] Reddy KJ, Gloss SP, Wang L. Reaction of CO_2 with alkaline solid wastes to reduce contaminant mobility. Water Resources 1994;28(6):1377–82.

[4.32] WRAP and EA. Pulverised fuel ash and furnace bottom ash: a Technical report on the manufacture of products from pulverised fuel ash (PFA) and Furnace bottom ash; 2009.
www.environmentagency.gov.uk/static/documents/Business/Technical_report_for_the_manufacture_of_products_from_pulverised_fuel_ash_and_furnace_bottom_ash_.pdf.
Date of consultation: September 2011.

[4.33] Gahan CS, Cunha ML, Sandström Å. Comparative study on different steel slags as neutralising agent in bioleaching. Hydrometallurgy 2009;95(3–4):190–7.

[4.34] Miklos P. The utilization of electric arc furnace slags in Denmark. Proceedings of 2nd European slag conference. Düsseldorf; 2000.

[4.35] Lekakh SN, Rawlins CH, Robertson DGC, Richards VL, Peaslee KD. Kinetics of aqueous leaching and carbonization of steelmaking slag. Metallurgical and Materials Transactions B 2008;39B:125–34.

[4.36] Shi C. Characteristics and cementitious properties of ladle slag fines from steel production. Cement Concrete Research 2002;32:459–62.

[4.37] Eloneva S, Teir S, Salminen J, Fogelholm CJ, Zevenhoven R. Fixation of CO_2 by carbonating calcium derived from blast furnace slag. Energy 2008;33: 1461–7.

[4.38] Baciocchi R, Costa G, Di Bartolomeo E, Polettini A, Pomi R. Wet versus slurry carbonation of EAF steel slag. Greenhouse Gas Science Technology 2011;1(4):312–9.

[4.39] Santos R, François D, Vandevelde E, Mertens G, Elsen J, Van Gerven T. Process intensification routes for mineral carbonation. Greenhouse Gas Science Technology 2011;1(4):287–93.

[4.40] DCLG. Survey of arisings and use of alternatives to primary aggregates in England, 2005 – Other materials, DLCG, London; 2007. www.communities.gov.uk/publications/planningandbuilding/surveyother2005. Date of consultation: September 2011.

[4.41] Defra. Estimated total annual waste arising by sector in United Kingdom: 1997–2003, e-Digest of environmental statistics; 2006. www.defra.gov.uk/environment/statistics/index.htm. Date of consultation: September 2011.

[4.42] MEPS. Global iron and steel production to 2014, steel industry and market analysts, MEPS(Int.) Ltd., 263 Glossop Road, Sheffield, S10 2GZ, England; 2010. www.meps.co.uk/publications/PDF/sub-form3.PDF. Date of consultation: September 2011.

[4.43] Baciocchi R, Costa G, Lategano E, Marini C, Polettini A, Pomi R, et al. Accelerated carbonation of different size fractions of bottom ash from RDF incineration. Waste Management 2010;30(7):1310–7.

[4.44] Ecke H. Sequestration of metals in carbonated municipal solid waste incineration (MSWI) fly ash. Waste Management 2003;23:631–40.

[4.45] Johnson DC. Accelerated carbonation of waste calcium silicate materials. SCI Lecture Paper Series 2000;108:1–10.

[4.46] Fernandez Bertos M, Li X, Simons SJR, Hills CD, Carey PJ. Investigation of accelerated carbonation for the stabilisation of MSW incinerator ashes and the sequestration of CO_2. Green Chemistry 2004;6:428–36.

[4.47] Quina MJ, Bordado JC, Quinta-Ferreira RM. Treatment and use of air pollution control residues from MSW incineration: an overview. Waste Management 2008;28:2097–121.

[4.48] Baciocchi R, Polettini A, Pomi R, Prigiobbe V, Von Zedwitz NV, Steinfeld A. CO_2 Sequestration by direct gas-solid carbonation of air pollution control (APC) residues. Energy Fuel 2006;20:1933–40.

[4.49] Defra. municipal waste statistics; 2011. www.gov.uk/defra Date of consultation: September 2012.

[4.50] Amutha Rani D, Boccaccini AR, Deegan D, Cheeseman CR. Air pollution control residues from waste incineration: current UK situation and assessment of alternative technologies. Waste Management 2008;28:2279–92.

[4.51] Huntzinger DN, Eatmon TD. A life-cycle assessment of Portland cement manufacturing: comparing the traditional process with alternative technologies. Journal Clean Production 2009;17:668–75.

[4.52] MPA. Performance 2008: a sector plan report from the UK cement industry; 2009. www.cementindustry.co.uk.

[4.53] van Oss HG, Padovani AC. Cement manufacture and the environment, part II: environmental challenges and opportunities. Journal of Industrial Ecology 2003;7(1):93–127.

[4.54] Merlin-Jones D. Rock solid? An investigation into the British cement industry, Civitas, Tufton Street, London, SW1P 3QL; 2010. http://civitas.org.uk/pdf/CementMerlinJones.pdf. Date of consultation: October 2011.

[4.55] Environment agency. Paper sludge ash. 2010; www.environment-agency.gov.uk/research/library/consultations/100377.aspx. Date of consultation: October 2011.

[4.56] Biomass Energy Centre. Co-firing; 2010. www.biomassenergycentre.org.uk/portal/page?_pageid=75,41175&_dad=portal&_schema=PORTAL. Date of consultation: October 2011.

[4.57] Mitchell C. Quarry fines and waste, Quarry &Mines; 2009. www.quariesandmines.co.uk/ebook/. Date of consultation: October 2011.

[4.58] Vogeli J, Reid DL, Becker M, Broadhurst J, Franzidis JP. Investigation of the potential for mineral carbonation of PGM tailings in South Africa. Mineral Engineering 2011;24:1348–56.

[4.59] Teir S, Eloneva S, Fogelholm CJ, Zevenhoven R. Dissolution of steelmaking slags in acetic acid for precipitated calcium carbonate production. Energy 2007;32:528–39.

[4.60] Wang L, Jin Y, Nie Y. Investigation of accelerated and natural carbonation of MSWI fly ash with a high content of Ca. J Hazard Mater 2010;174(1–3):334–43.

[4.61] Iron and Steel Statistics Bureau (ISSB); 2010. www.issb.co.uk. Date of consultation: October 2011.

[4.62] WRAP. AggRegain, Furnace Bottom Ash; 2010. http://aggregain.wrap.org.uk. Date of consultation: September 2011.

[4.63] IEAGHG, CO_2 Emissions Database, Maps of the CO_2 Emissions Database: UK map, 2010. www.ieaghg.org. Date of consultation: September 2011.

CHAPTER 5 – DISSOLUTION OF SELECTED WASTE MATERIALS IN NH_4HSO_4

Chapter 4 focused on assessing waste streams availability in the UK and their potential CO_2 storage capacity. It was clear that certain waste materials produced close to CO_2 emitters could be employed for mineral carbonation, although this would be a niche market using relatively small amounts of waste materials. In this chapter a closed-loop, multi-step mineralization process (Section 3.3) which allows precipitation of calcium carbonate ($CaCO_3$) from Ca-rich waste streams is presented. Investigations on this multi-step process in this chapter aim at providing a comprehensive analysis of the dissolution step, for several waste materials. Firstly, results from the characterization of the nine waste materials identified previously (Section 3.1) are reported. These samples were selected following the identification of potential waste materials suitable for mineral carbonation presented in the literature review (Section 2.2.3) and the opportunity to receive an appropriate amount of material from providers based in UK and the EU. Secondly, four samples with the highest calcium content and a low level of carbonates were considered for the dissolution experiments: steel slag (SS), recycled concrete aggregate (RCA), ground granulated blast furnace slag (GGBS) and phosphorus slag (PS). Finally, this chapter studies their mineral dissolution step in NH_4HSO_4.

5.1 Multi-step mineralization process

Waste materials identified for this work in Chapter 3 (Section 3.1) are rich in CaO, and therefore, a mineralization process which employs them must be able to convert CaO into calcium carbonate ($CaCO_3$). As described in the literature review (Section 2.3), multi-step processes seem more attractive than single-step because they allow the production of different streams of high quality products. Wang and Maroto-Valer developed a process to extract magnesium from mineral rocks and produce different streams of useful by-products at ambient pressure [5.1]. An analogue process employing waste streams (rich in CaO) to precipitate calcium carbonate instead of magnesium carbonate was introduced in Section 3.3 and it is presented in Table 5.1. In addition, thermodynamic data, performed using Chemical Reaction and Equilibrium Software HSC Chemistry 5.1, are also reported. HSC Chemistry 5.1 is a software able to perform thermodynamic calculation which has proved its reliability also for mineralization studies [5.1].

The multi-step mineralization process presented in Table 5.1 includes five main steps: i) mineral dissolution, ii) pH adjustment iii) precipitation of impurities, iv) carbonation reaction, and v) regeneration of additives. In this process, during mineral dissolution, metal ions are extracted from the feedstock material and solid calcium sulphate ($CaSO_4$(s)) precipitates. Ammonium carbonate, ($(NH_4)_2CO_3$), produced during the capture of CO_2 with ammonia (NH_3), is combined with $CaSO_4$ in the carbonation reaction and calcium carbonate ($CaCO_3$) precipitates. The pH is raised (adding NH_4OH) prior to the carbonation step and the impurities (containing Mg, Fe and Al) precipitate as hydroxides. Raising the pH is an important step because it allows the following precipitation of $CaCO_3$. The proposed carbonation process could also re-circulate and regenerate the chemicals involved, i.e. NH_4HSO_4 and NH_3. The proposed process differs from the one developed by Wang and Maroto-Valer because of different feedstock used (waste streams instead of mineral rocks) and a different chemical employed in the carbonation step, ammonium carbonate, $(NH_4)_2CO_3$, instead of ammonium bicarbonate, NH_4HCO_3. In the carbonation reaction, in fact, $(NH_4)_2CO_3$ will combine with $CaSO_4$(s) to produce calcium carbonate.

The energy balance reported in Table 5.1 is based on the thermodynamic calculations performed by the thermodynamic computer software (HSC Chemistry 5.1). In thermodynamics, ΔH (expressed in Joule) is the difference in enthalpy and represent the heat required (endothermic reaction, $\Delta H>0$) for a reaction to happen or released (exothermic reaction, $\Delta H<0$) when the reaction takes place. ΔH can be calculated by adding each heat of formation (obtained from scientific databases, e.g. NIST) of the reactants and products and then subtracting the latter from the former. ΔG is the Gibbs free energy, also expressed in Joules, and it expresses if a reaction happens spontaneously or not at a certain temperature and pressure. The Gibbs free energy basic expression is the following:

$$\Delta G = \Delta H - T\Delta S \qquad (5\text{-}1)$$

where ΔS is the internal entropy of the system and T is the temperature. A chemical reaction results spontaneous when $\Delta G<0$, while $\Delta G>0$ indicates that the reaction is non-spontaneous. Table 5.1 includes ΔH and ΔG and they were based on software HSC calculations and database.

Steps	Reactions	T[°C]	ΔH[kJ]	ΔG[kJ]
CO_2 capture	$\mathbf{2}NH_3 + CO_2 + H_2O \rightarrow (NH_4)_2CO_3$	10	-168.3	-29.6
Mineral dissolution	$CaO \cdot SiO_2 + 2NH_4HSO_4 \rightarrow CaSO_4 \downarrow + SiO_2 \downarrow + H_2O + (NH_4)_2SO_4$	50	-130.7	-206.1
	$MgO \cdot SiO_2 + 2NH_4HSO_4 \rightarrow MgSO_4 + SiO_2 \downarrow + H_2O + (NH_4)_2SO_4$		-68.7	-143.4
	$FeO \cdot SiO_2 + 2NH_4HSO_4 \rightarrow FeSO_4 + SiO_2 \downarrow + H_2O + (NH_4)_2SO_4$		-62.7	-138.0
	$Al_2O_3 \cdot SiO_2 + 6NH_4HSO_4 \rightarrow Al_2(SO_4)_3 + SiO_2 \downarrow + 3H_2O + 3(NH_4)_2SO_4$		84.1	-135.0
pH adjustment	$NH_4HSO_4 + NH_4OH \rightarrow (NH_4)_2SO_4 + H_2O$	25	-116	-134.4
Precipitation of impurities	$Al_2(SO_4)_3 + 6NH_4OH \rightarrow 2Al(OH)_3 \downarrow + 3(NH_4)_2SO_4$	25	-696.0	-567.7
	$(Fe, Mg)SO_4 + 2NH_4OH \rightarrow (Fe, Mg)(OH)_2 \downarrow + (NH_4)_2SO_4$		-673.4	-545.1
Carbonation reaction	$CaSO_4 + (NH_4)_2CO_3 \rightarrow CaCO_3 \downarrow + (NH_4)_2SO_4$	60	-1.4	-19.6
Regeneration of additives	$(NH_4)_2SO_4 \rightarrow NH_4HSO_4 + NH_3 \uparrow$	300	111.6	90.4

Table 5.1: Chemical reactions list and thermodynamic data of the different steps of the carbonation process studied

All the reactions result spontaneous apart from the regeneration of additives and compared to Wang and Maroto-Valer process (Table 2.4) the dissolution and carbonation reactions are less exothermic. In fact, for the dissolution step ΔH is -141.1kJ for Wang and Maroto-Valer and -130.7kJ for the process here described, while for the carbonation step ΔH is -6.6kJ for Wang and Maroto-Valer and -1.4kJ for the process here described. The pH adjustment and regeneration of additives steps have the same thermodynamic values, i.e. -116.0kJ and 111.6kJ, respectively. The capture and precipitation of impurities reactions, instead, release more heat in the process designed for waste streams (-168.3kJ and -696.0kJ).

5.2 Characterization and selection of wastes for mineralization experiments

In Chapter 3 (Section 3.1), nine suitable waste streams for mineral carbonation were identified. Six materials produced in the UK (Chapter 4, Section 4.2) were selected, namely RCA, CKD, GGBS, PFA, ISSA, SS.

	Chemical composition (wt%±0.1%)						
	CaO	MgO	Fe_2O_3	Al_2O_3	SiO_2	KCl	LOI
Recycled concrete aggregate (RCA)	39.9	0.4	1.1	2.0	27.9	n.d	27.2
Cement kiln dust (CKD)	28.5	0.4	1.2	1.8	4.9	55.2	0.1
Ground granulated blast furnace slag (GGBS)	39.0	8.7	0.5	12.5	34.6	n.d	0.4
Phosphorus slag (PS)	46.7	1.2	0.8	2.6	43.0	n.d	0.4
Pulverized fuel ash (PFA)	4.9	2.1	7.1	23.1	49.8	n.d	4.0
Water cooled copper smelt slag (WCSS)	2.8	0.9	54.3	3.1	31.0	n.d	6.0
Air cooled copper smelt slag (ACSS)	3.5	1.0	48.7	4.0	30.6	n.d	6.0
Incinerator sewage sludge ash (ISSA)	7.4	1.7	5.5	31.5	25.8	n.d	2.7
Steel slag (SS)	38.4	9.0	22.5	2.7	12.1	n.d	9.0

Table 5.2: Chemical composition by XRF of the samples analysed

Furthermore, samples of other three waste materials described in the literature review (Section 2.2.3) namely phosphorus slag (PS) and water and air cooled copper smelt slag (WCSS and ACSS) were obtained and added to the list of samples investigated. These last three materials are not produced in the UK but have a CaO content of 44wt% and 1-10wt% for PS and CSS respectively [5.2] [5.3]. Each sample was characterized employing XRF and results are reported in Table 5.2.

XRD patterns of the samples are included in Appendix A. The results obtained from XRD and XRF, together with QXRD results, are discussed below.

- Recycled concrete aggregate (RCA): The main compounds detected by XRF were silica and calcium oxide. The main crystalline phases present in RCA were calcite and quartz (Figure A1.1). Using BRUCKER AXS EVA software for the phase quantification, the phases wt% present were 59%wt and 41wt% for calcite ($CaCO_3$) and quartz (SiO_2), respectively. This was confirmed using MAUD software [5.4] for QXRD, where calcite and quartz were detected as 61wt% and 39wt%, respectively. Considering that the RCA analyzed was a fresh concrete (6 months), portlandite ($Ca(OH)_2$) formed during the hydration reaction of cement should have been detected [5.5]. In order to investigate this, additional XRD studies with higher resolution (scan speed of 1 degree 2-theta per minute, 0.02 step size) were performed in the range 0-65 2-theta degrees. These additional XRD studies detected the presence of portlandite (Figure A1.2). Using BRUCKER AXS EVA software for the quantification, the phases present were calcite (60%wt), quartz (36wt%) and portlandite (4wt%). Using MAUD, results from QXRD reported 65wt% and 35wt% of calcite and quartz, respectively.
- Cement kiln dust (CKD): XRF indicated a high KCl content (Table 5.1), and this was confirmed by XRD (Figure A1.3). BRUCKER AXS EVA software detected 81wt% sylvite (KCl), 7wt% portlandite ($Ca(OH)_2$), 6wt% calcite ($CaCO_3$) and 6wt% halite (NaCl). After further investigation with the supplier of this sample on the nature of the material, it was re-classified as kiln by-pass dust (BPD). Kiln BPD is produced by dry kilns during clinker manufacture where alkalis (mainly K and Cl) are volatilised and drawn back through the kiln, where they meet incoming, partly calcined, raw materials and condense. Afterwards, dust is extracted by the bypass system to remove the excess KCl. The amount of KCl depends on the bypass efficiency and it is quite variable depending on kiln operation and the level of recycled fuels in use. CKD historically is associated with wet kilns of which there

are very few (probably none) in the UK but could be an interesting resource in other parts of the world (like India), where this process is largely used in cement production.

- Ground granulated blast furnace slag (GGBS): XRF studies showed a high calcium oxide content (39wt%, Table 5.1). The XRD pattern showed that the material is mainly amorphous and therefore any trace of carbonates already present could not be detected (Figure A1.4).
- Phosphorus slag (PS): XRF studies showed a high calcium oxide content (46.7wt%, Table 5.1). XRD did not detect crystalline calcium carbonate (calcite) or magnesium carbonates (magnesite) (Figure A1.5).
- Pulverized fuel ash (PFA): The main compounds detected by XRF were silica and aluminum, while, calcium and magnesium oxides were present in small quantities (4.9wt% and 2.1wt%, respectively, Table 5.1). The main crystalline phases detected by XRD were silica and aluminium mixtures, while calcium carbonate (calcite) and magnesium carbonates (magnesite) were not detected (Figure A1.6).
- Copper smelt slag (CSS): XRF detected small quantities of calcium and magnesium oxide (2.8-3.5wt% and 0.9-1wt% respectively, Table 5.1). XRD from the two different CSS samples showed two different results. The water cooled CSS is mainly amorphous (Figure A1.8), while the air cooled CSS contains mainly phases with silica and iron and not calcium and magnesium carbonates (Figure A1.7).
- Incinerator sewage sludge ash (ISSA): Both calcium and magnesium oxide were determined by XRF in small amounts (7.4wt% and 1.7wt% respectively, Table 5.1). XRD did not detect crystalline calcium carbonate or magnesium carbonates in ISSA (Figure A1.9).
- Steel slag (SS): Results from XRF showed a content in calcium oxide of 38.4wt% and magnesium oxide of 9wt% (Table 5.1). From the XRD pattern only calcium carbonate was detected (Figure A1.10) while magnesium carbonate was not present. Because of the several phases present and no one predominant in the XRD pattern, QXRD using MAUD and BRUCKER AXS EVA could not be performed accurately (Section 3.2.2).

Following the characterization studies above, the samples with the highest calcium content and a low level of carbonates were considered for the next experiments. These included metal slags (GGBS, SS and PS) and, furthermore, RCA, due to its availability and high content of calcium oxide, despite also its high level of carbonates. As

discussed in Section 4.3, waste concrete is largely produced but also recycled in the construction sector in UK. However, if mineral carbonation from waste streams was able to produce carbonates which could be compatible to commercial ones and also competitive in terms of cost, then the use of these wastes as feedstock for mineralization would be preferred over low-end applications.

5.3 Dissolution of steel slag and recycled concrete aggregate

Employing the experimental set-up for the mineralization tests presented in Section 3.3 and the experimental conditions described in Section 3.4, the mineral dissolution phase of the mineralization process (Table 5.1) was firstly tested with SS and RCA. Trends of dissolution for metals allowed conducting a kinetic analyses based on models reported in literature. The solid residue, after the mineral dissolution experiments, were dried overnight in an oven at 105°C. The oxide composition of solid residue for each product was determined using XRF and XRD. SEM-EDS was instead employed to look at the morphology and nature of the particles.

5.3.1 Kinetic analyses

In order to determine the kinetic parameters of dissolution of SS and RCA, the experimental data was analysed according to the standard integral analysis method [5.6]. Firstly, experimental results were fitted into several heterogeneous reaction models represented by integral rate equations and secondly the multiple regression coefficients (R^2) were calculated. The shrinkage core model was selected, because previous studies conducted on dissolution of serpentine showed the formation of a silica layer on the surface of the particle [5.1] [5.7]. The experimental rig and conditions (particle size, temperature, S/L ratio) employed in this thesis were the same as the ones used with serpentine by Wang and Maroto-Valer [5.1] in order to be able to compare the kinetics of the experiments. Therefore, the only factors affecting the results obtained were the different physical and chemical characteristics of serpentine and industrial waste. Waste streams have higher Ca content compared to serpentine, as seen in Section 2.2, moreover, the content of impurities (elements wt%<1%) is also higher, because of their origin from industrial processes. Finally, serpentine consists of a limited number of physical phases (e.g antigorite, fosterite [5.1]) while industrial wastes have usually a much higher number of mineral phases (Figures A1.3, A1.5, A1.10)

In the shrinking core model the reaction occurs firstly at the outer layer of the particle. The zone of reaction then moves into the solid, leaving behind completely converted material and inert solid (called “ash”). Thus, at any time there exists an unreacted core of material which shrinks in size during the reaction. The main difference between the shrinking core model and real reactions is given by the assumption that the reaction converts completely the material of the particle leaving behind only inert solids and reaction products [5.6].

During chemical reactions in a shrinkage core model for spherical particles of unchanging size five steps occur [5.6]:

- Step 1. Diffusion of liquid/gaseous reactant through the film surrounding the particle to the surface of the solid.
- Step 2. Penetration and diffusion of the reactant through the blanket of ash to the surface of the unreacted core.
- Step 3. Reaction of the reactant with the solid at the reaction surface.
- Step 4. Diffusion of liquid/gaseous products through the ash back to the exterior surface of the solid.
- Step 5. Diffusion of liquid/gaseous products through the liquid/gas film back into the main body of fluid.

However, some of these steps may not exist in some situations (e.g. if no gaseous products are formed). In light of this, according to the shrinking-core model, dissolution reactions of waste materials take place at the outer surface of the un-reacted particle and heterogeneous reactions are controlled by one of the following mechanisms [5.6].

- Film diffusion control: this mechanism assumes that no reactant is present at the particle surface, while its concentration increases in the liquid film surrounding the particle. According to this mechanism, the reaction is controlled by the diffusion of the fluid reactant from the main body of the fluid film to the surface of the solid and this is represented by the equation:

$$kt = x \qquad (5\text{-}2)$$

- Reaction control: The reactant is fully available at the surface of the unreacted particle and the reaction is unaffected by the presence of any ash layer. According to this mechanism, the reaction is controlled by the reaction, on the surface of the particle, between the fluid reactant and the solid and this is represented by the equation:

$$kt = 1 - (1 - x)^{1/3} \quad (5\text{-}3)$$

- Product layer diffusion: Products of reaction do not form an ash layer and go back from the solid particle into solution. According to this mechanism, the reaction is controlled by the diffusion of the products of reaction from the surface of the solid through the fluid film back into the main body of the fluid (without ash layer) and this is represented by the equation:

$$kt = 1 - 3(1 - x)^{2/3} + 2(1 - x) \quad (5\text{-}4)$$

Where, in the equations just presented, k is the reaction rate constant and x the fraction transformed for the product phase at time t.

In addition to the three different shrinkage core model mechanisms, it can be assumed that also a combination of product layer diffusion and chemical reaction control could be a rate limiting step of the dissolution reaction and this can be represented by the following equation:

$$kt = (1 - 3(1 - x)^{2/3} + 2(1 - x)) + (1 - (1 - x)^{1/3}) \quad (5\text{-}5)$$

The activation energy can be estimated from the experimental data according to Arrhenius' law:

$$k = Ae^{-\frac{E_a}{RT}} \quad (5\text{-}6)$$

Where k is the kinetic rate constant, A is the pre-exponential or frequency factor, Ea is the apparent activation energy in J/mol, R is the universal gas constant (8.314J/(mol K)) and T is the temperature in Kelvin.

5.3.2 Steel slag

The main metals present in SS are Fe, Mg and Ca (Table 5.2). Following the dissolution experiments, the trends of the main metals into solution (as ions) obtained from Inductively Coupled Plasma Mass Spectrometry (ICP-MS) are presented in Figures 5.1, 5.2 and 5.3. The last sampling of the experiment (5h) was performed twice. After acidification with HNO_3, the two samples were analysed by ICP-MS to calculate the error on the values of metals dissolved and this error was calculated to be ±2% (error bars reported in Figures 5.1, 5.2 and 5.3).

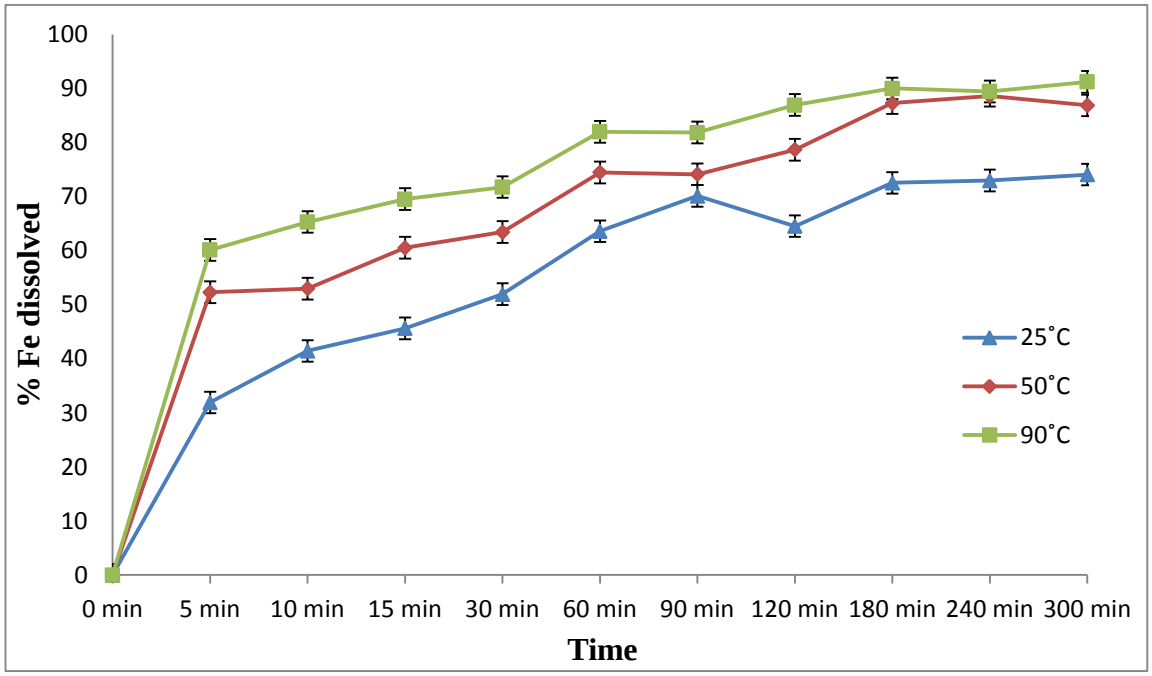

Figure 5.1: Fe dissolution trend for SS

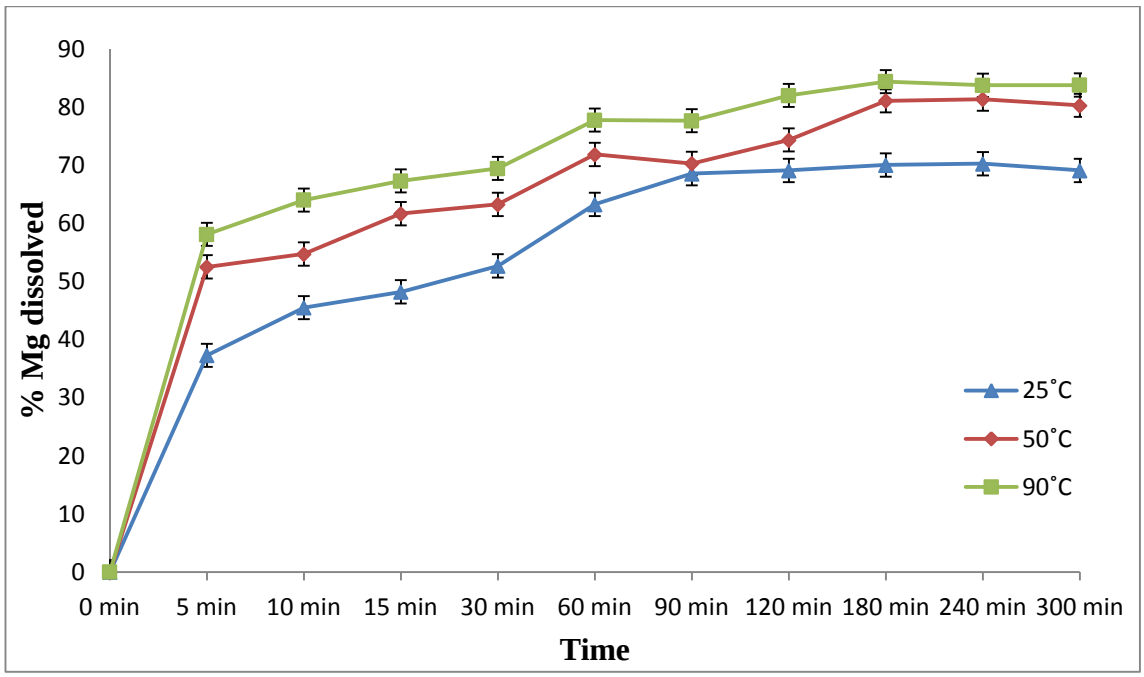

Figure 5.2: Mg dissolution trend for SS

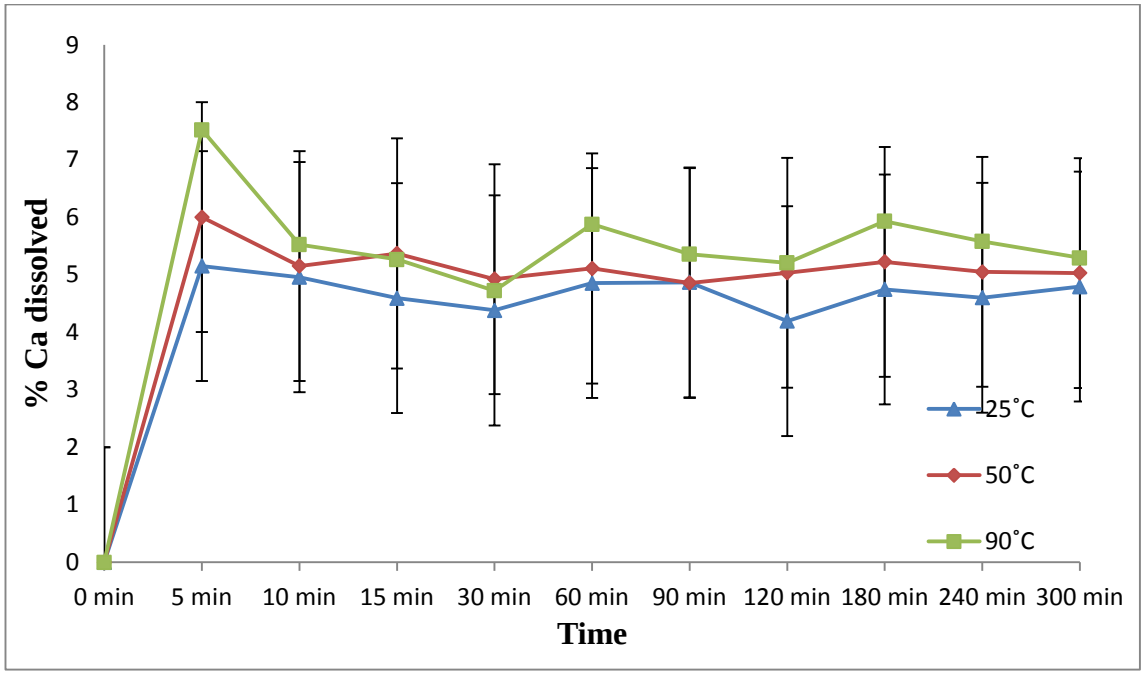

Figure 5.3: Ca dissolution trend for SS

As expected, temperature has an important effect on dissolution of Fe and Mg. Metal ion leaching is promoted when the temperature is increased [5.1] [5.7]. Furthermore, dissolution takes place quicker in the first five minutes of the experiment, slowing down as the experiment proceeds. Both Mg and Fe dissolved into solution and reached 85% and 90%, respectively, at 90°C. Trends of dissolution for SS can be compared with the ones from serpentine; 85% of Mg and 80% of Fe from serpentine were dissolved into

NH_4HSO_4 solution after 3h at 90°C [5.1]. Accordingly, dissolution rates of SS and serpentine are similar for magnesium. However, for SS, dissolution rates for iron are higher than the ones for serpentine. Therefore, it is likely to presume that iron present in the raw material is easier to extract from SS than from serpentine, supporting the fact that in general waste streams require a lower degree of pre-treatment and less energy-intensive carbonation conditions, in comparison to mineral rocks [5.8]. In fact, experimental conditions for testing mineral dissolution employed with serpentine by Wang and Maroto-Valer [5.1] and the ones used in this thesis were the same (i.e. particle size, temperature, stirring rate, S/L ratio). Therefore, differences in iron dissolution rates between serpentine and steel slag could be related to the diverse mineral phases forming the two materials, including differences in chemical and physical nature of iron present (e.g. type of iron, hydration and presence of contaminants). For instance, mineral phases where iron is contained in SS (i.e. Wustite, Figure A1.10) have weaker bonds (i.e. iron is easier to extract) compared to serpentine, which contains Magnetite (Fe_3O_4) [5.1]. In fact, since the shorter the bond is the greater its strength [5.9], the bond length for Wustite is 2.167Å [5.10] while for Magnetite it is 1.89Å [5.11].

The low Ca levels found in solution (~5%, Figure 5.3) mean that Ca mainly precipitated during the experiments. XRD, SEM and XRF results on the solid residue after dissolution at 50°C allowed identifying the nature of the precipitated Ca, and it emerges that it was in sulphate form ($CaSO_4$). Hydrated $CaSO_4$ in crystalline form was detected by XRD (Figure 5.4) with silica (SiO_2) present in the amorphous phase (not visible in the XRD pattern). Small crystals of $CaSO_4$ in the Secondary Electron (SE) SEM micrograph are clearly visible and they cover the surface of the particle analysed (Figure 5.5).

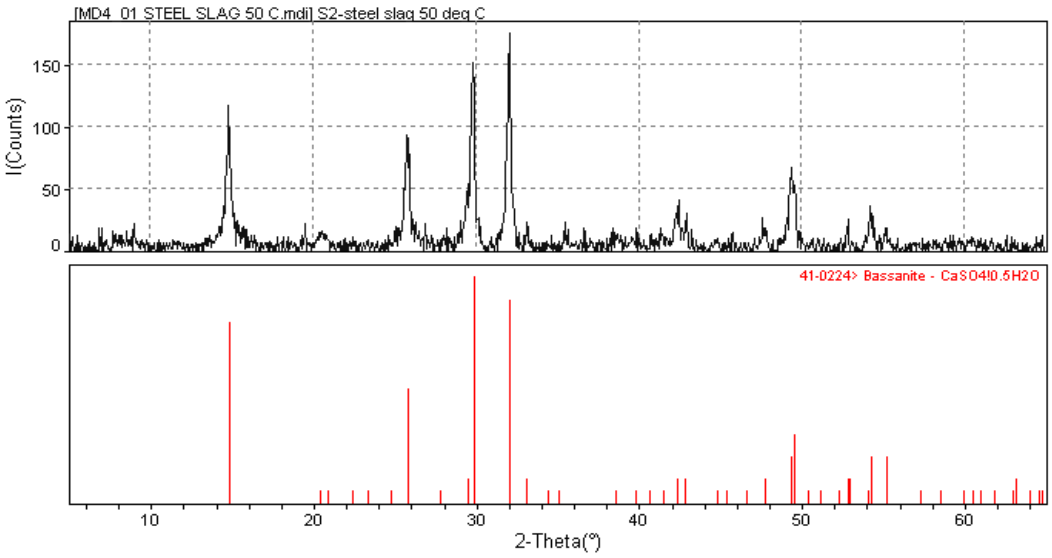

Figure 5.4: XRD diffractogram of solid residue after dissolution of SS at 50°C

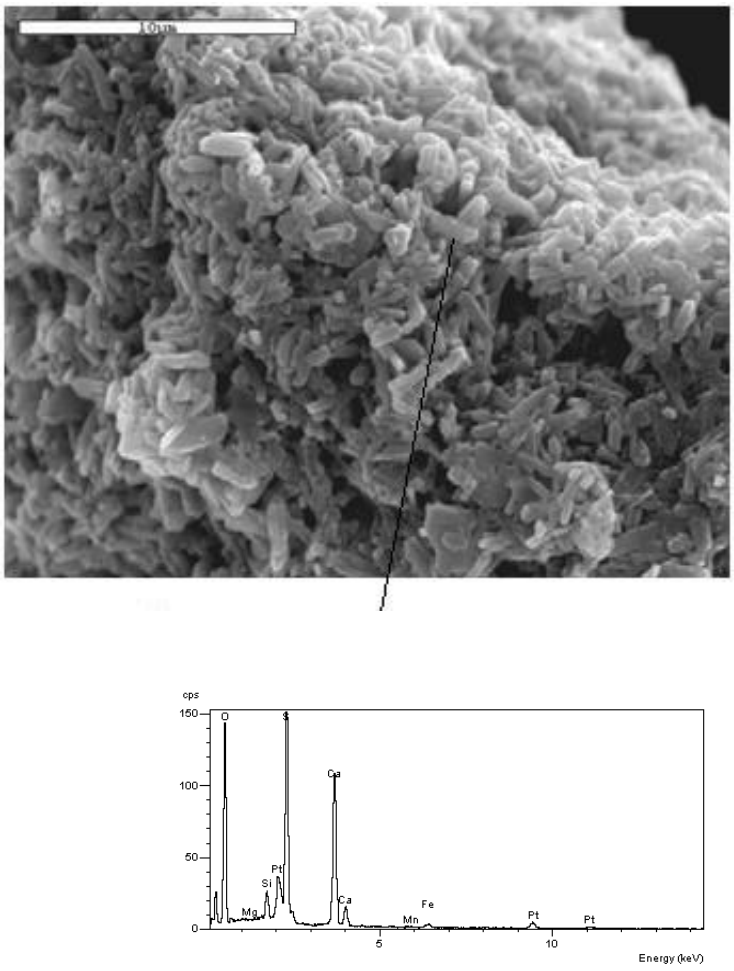

Figure 5.5: SEM-EDS of solid residue after dissolution of SS at 50°C

XRF analysis detected mainly CaO and SO_3 (29.4%wt and 42.0%wt, respectively), confirming the presence of calcium sulphate (%wt of $CaSO_4$ is 68.0%) together with 7.6%wt of silica (Table 5.3).

Component	Solid residue (wt%)
SiO_2	7.6
Al_2O_3	0.5
Fe_2O_3	5.0
MgO	0.7
CaO	29.4
SO_3	42.0
LOI	15.9

Table 5.3: XRF analyses of solid residue after dissolution of SS at 50°C

Precipitation of Ca as $CaSO_4$ is due to the low solubility of $CaSO_4$ into a solution of $(NH_4)_2SO_4$, which has previously been reported to be 0.045mol/kg in a 3.19mol/kg solution of $(NH_4)_2SO_4$ at 25°C [5.12]. The reported data on solubility of $CaSO_4$ in water shows that values range between 0.015mol/kg of water (at 25°C) to 0.013mol/kg of water (at 90°C), showing little dependence of solubility on temperature [5.13]. Therefore, it can be assumed that also the solubility of $CaSO_4$ into a solution of $(NH_4)_2SO_4$ is almost constant between 25°C and 90°C, confirming the low values of Ca dissolved (Figure 5.3) during the three experiments with SS and the precipitation of $CaSO_4$(s).

5.3.2.1 Kinetic analyses

Experimental data from dissolution experiments can be fitted into the kinetic models introduced in equations (5-2 – 5-5). For steel slag, *x* is represented by the rate of Mg dissolved into solution, because Mg trends correspond to the progress of the reaction and also because the rate of Mg dissolved were considered in kinetic analyses in previous studies for dissolution of serpentine [5.1] [5.7] [5.14]. When trying to fit data obtained from dissolution of SS into the shrinking-core models (equations 5-2 – 5-4), plotting calculated data against *t*, it was clear that none of these models were appropriate. In fact, the trends obtained were not a straight line and the multiple regression coefficients (R^2) were well below 1.00 (Table 5.4).

Model	R^2 (25°C)	R^2 (50°C)	R^2 (90°C)
film diffusion	-1.21	-1.71	-2.07
chemical reaction control	-0.64	-0.92	-1.26
product layer diffusion	0.46	0.15	-0.24
product layer diffusion and chemical reaction control	0.95	0.91	0.90

Table 5.4: R^2 coefficients for kinetic models applied to dissolution of SS

Negative R^2 values arise where linear regression is conducted without including an intercept. In fact, because of the need of calculating the activation energy in the following step, a model which passes through the axes origin is required. Instead, when experimental data, at different temperatures, were fitted into the combination of product layer diffusion and chemical reaction control (equation 5-5, Figure 5.6), R^2 values vary between 0.90 and 0.95 (Table 5.4) confirming the accurate approximation achieved with the model.

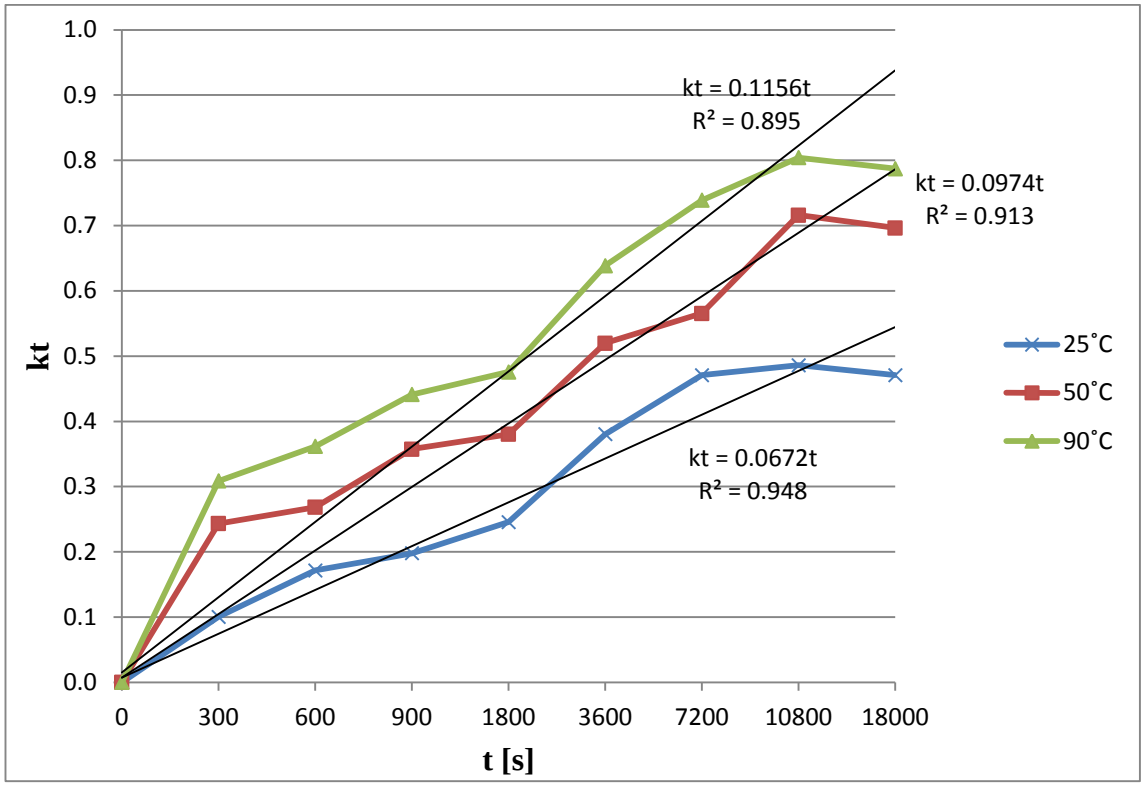

Figure 5.6: Combination of product layer diffusion and chemical reaction control for dissolution of SS

The good fit of the experimental results into the model combining product layer diffusion and chemical reaction control means that the dissolution reaction of SS is controlled at the same time by the reaction on the surface of the particle between the fluid reactant and the solid and by the diffusion of the products of reaction from the surface of the solid through the fluid film back into the main body of the fluid.

The activation energy can be calculated from the plot of lnk versus 1/T (Figure 5.7) employing Arrhenius' law (equation 5-6) and the calculated value is 2.3kJ/mol.

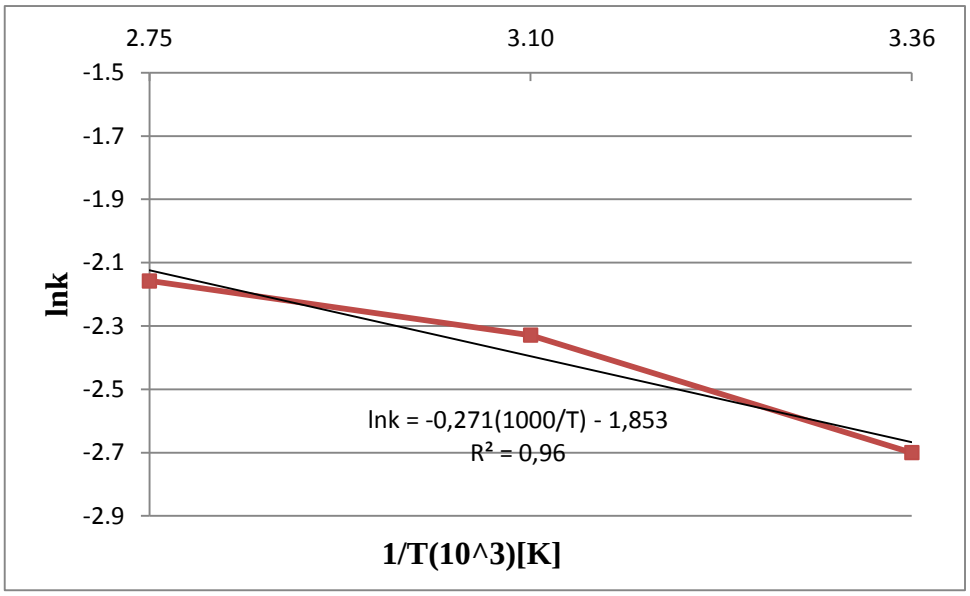

Figure 5.7: Plot for the calculation of activation energy for SS

Previous dissolution studies on serpentine found activation energy values of 40.9kJ/mol [5.1] where serpentine rock was dissolved into 1.4M NH_4HSO_4 solution, following the same procedure of this work. Fouda et al. calculated an activation energy of 68.1 kJ/mol [5.7], dissolving serpentine into 3M H_2SO_4 solution between 30°C and 75°C. Teir et al. determined the activation energy as 35.6 kJ/mol [5.14], using 2M H_2SO_4 solution between 30°C and 70°C (Table 5.5).

Authors	Solution	Activation energy [kJ/mol]
Wang et al. [5.1]	1.4M NH_4HSO_4, T=70-110°C	40.9
Fouda et al. [5.7]	3M H_2SO_4, T=30-75°C	68.1
Teir et al. [5.14]	2M H_2SO_4, T=30-70°C	35.6

Table 5.5: Examples of activation energy calculated for dissolution of serpentine

Therefore, values of activation energy from the present study on SS and previous on serpentine suggest that metals from SS are easier to dissolve compared to serpentine. In fact, as seen in Section 5.3.2, Fe dissolution rates for SS reach 90% compared to 80% obtained from previous experiments using serpentine [5.1].

5.3.3 Recycled concrete aggregate

The main metals present in RCA are Al and Ca (Table 5.2) and their trends of dissolution obtained during the experiments are reported in Figures 5.8 and 5.9, respectively. As described for SS, two samples were taken during the last sampling of each experiment and analysed by ICP-MS and the error calculated was ±2% (error bars reported in Figures 5.8-5.9).

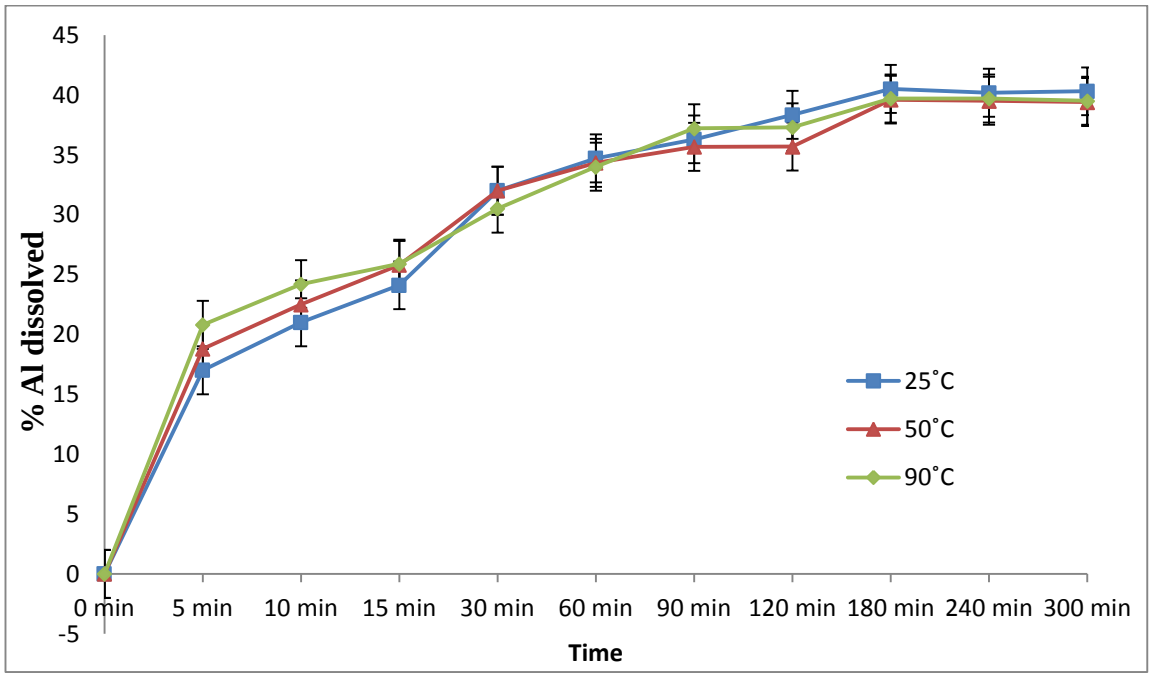

Figure 5.8: Al dissolution trend for RCA

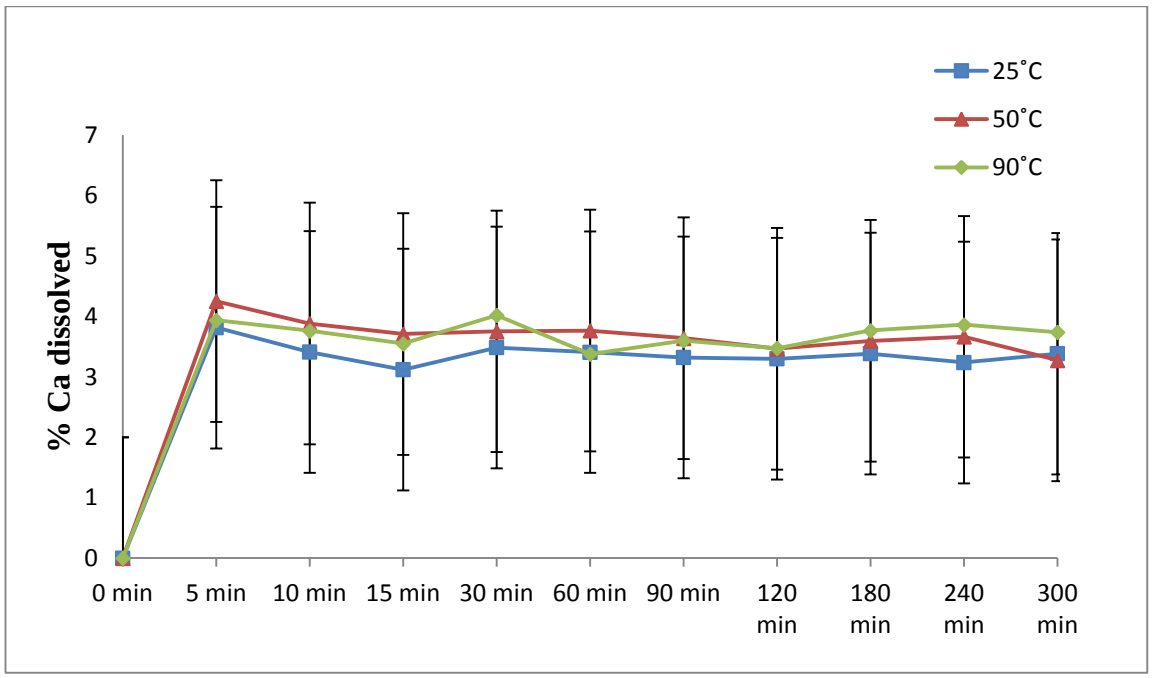

Figure 5.9: Ca dissolution trend for RCA

As for SS, Ca dissolution trend for RCA does not change substantially at different temperatures. In fact, as discussed for SS, $CaSO_4$ has low solubility in $(NH_4)_2SO_4$ (Section 5.2.3.1) and therefore Ca almost completely precipitated (only 3.5% into solution) producing $CaSO_4$(s) which can later be reacted with ammonium carbonate for the carbonation reaction. As for Ca, the dissolution trend of Al was not affected by temperature, reaching about 40% at 25-50-90°C (Figure 5.8).

The presence of $CaSO_4$(s) was confirmed by the results from XRD, SEM and XRF analyses of the solid residue after dissolution at 50°C. Hydrated $CaSO_4$ and SiO_2 in crystalline form were detected by XRD (Figure 5.10) and small crystals of $CaSO_4$ are deposited on the surface of the particle analysed with the Secondary Electron (SE) SEM (Figure 5.11).

Results from XRF analyses support these findings, as mainly CaO (24.0%), SO_3 (34.8%) and SiO_2 (25.1%) were observed (Table 5.6) and, therefore, wt% of $CaSO_4$ in the final residue is 59.1%. The fraction of Al precipitated is negligible because of its small concentration in absolute terms in the initial RCA (about 2% in oxidised form Al_2O_3).

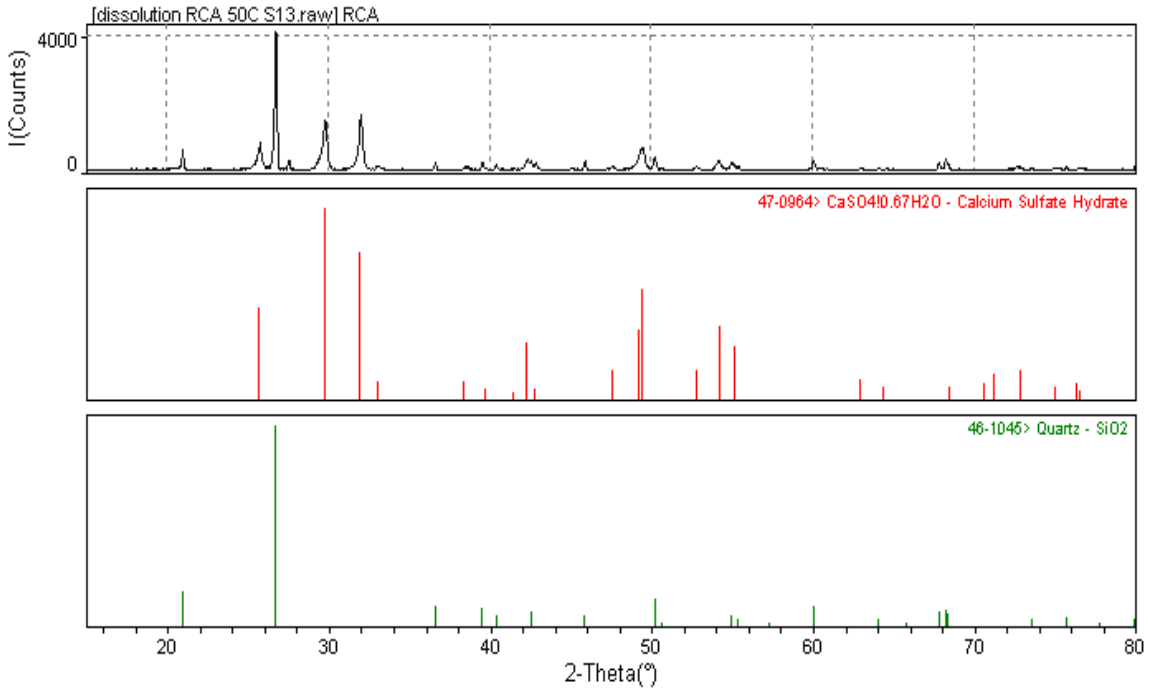

Figure 5.10: XRD diffractogram of solid residue after dissolution of RCA at 50°C

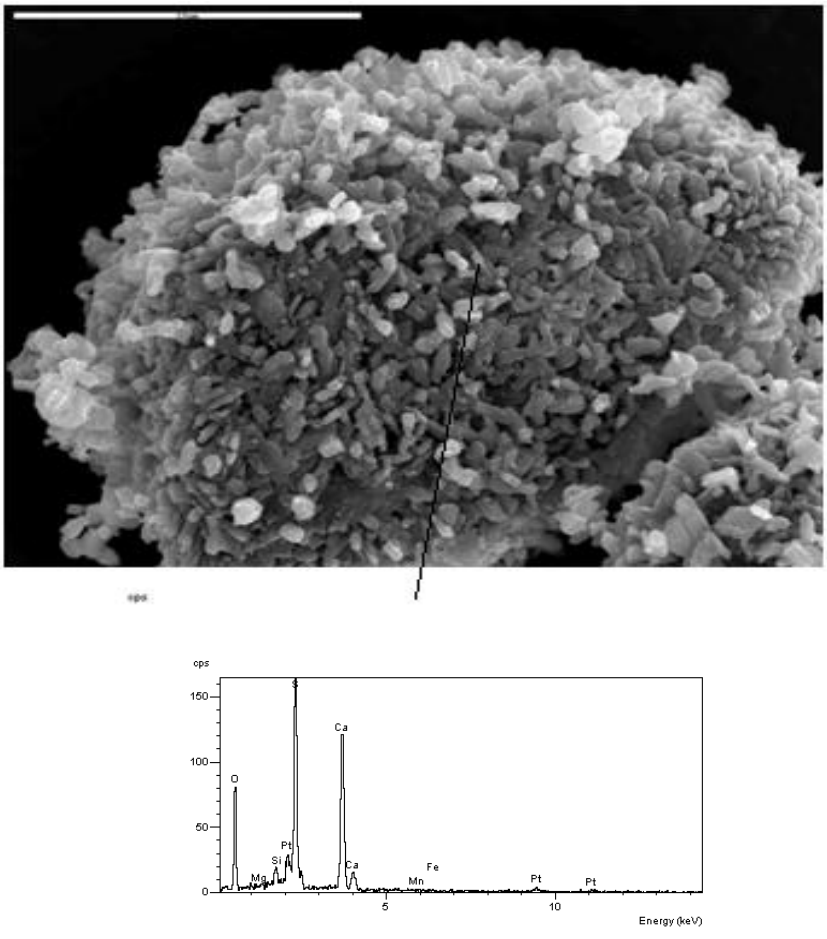

Figure 5.11: SEM-EDS of solid residue after dissolution of RCA at 50°C

Component	Solid residue (wt%)
SiO_2	25.1
Al_2O_3	0.9
Fe_2O_3	0.3
MgO	<0.1
CaO	24.0
SO_3	34.8
LOI	13.7

Table 5.6: XRF analyses of solid residue after dissolution of RCA at 50°C

5.3.3.1 Kinetic analyses

The concentration of Al into solution is indicative of the reaction progress, because Al is the most abundant element (Table 5.2) that is going to dissolve and produce the corresponding sulphate in aqueous form (Table 5.1).

In the kinetic models considered, *x* corresponds to the rate of Al dissolved. As for SS, data obtained from experiments was fitted into the shrinking-core models (equations 5-2 – 5-4). Values of the multiple regression coefficients R^2 are reported in Table 5.7.

Model	R^2 (25°C)	R^2 (50°C)	R^2 (90°C)
film diffusion	-2.09	-1.38	-2.66
chemical reaction control	-0.64	-1.16	-1.26
product layer diffusion	-0.83	0.05	-2.02
product layer diffusion and chemical reaction control	0.91	0.92	0.90

Table 5.7: R^2 coefficients for kinetic models applied to dissolution of RCA

Data from dissolution experiments at different temperatures were then fit into the combination of product layer diffusion and chemical reaction control (equation 5-5, Figure 5.12), R^2 values vary between 0.90 and 0.95 (Table 5.7) confirming the accurate approximation achieved with the model.

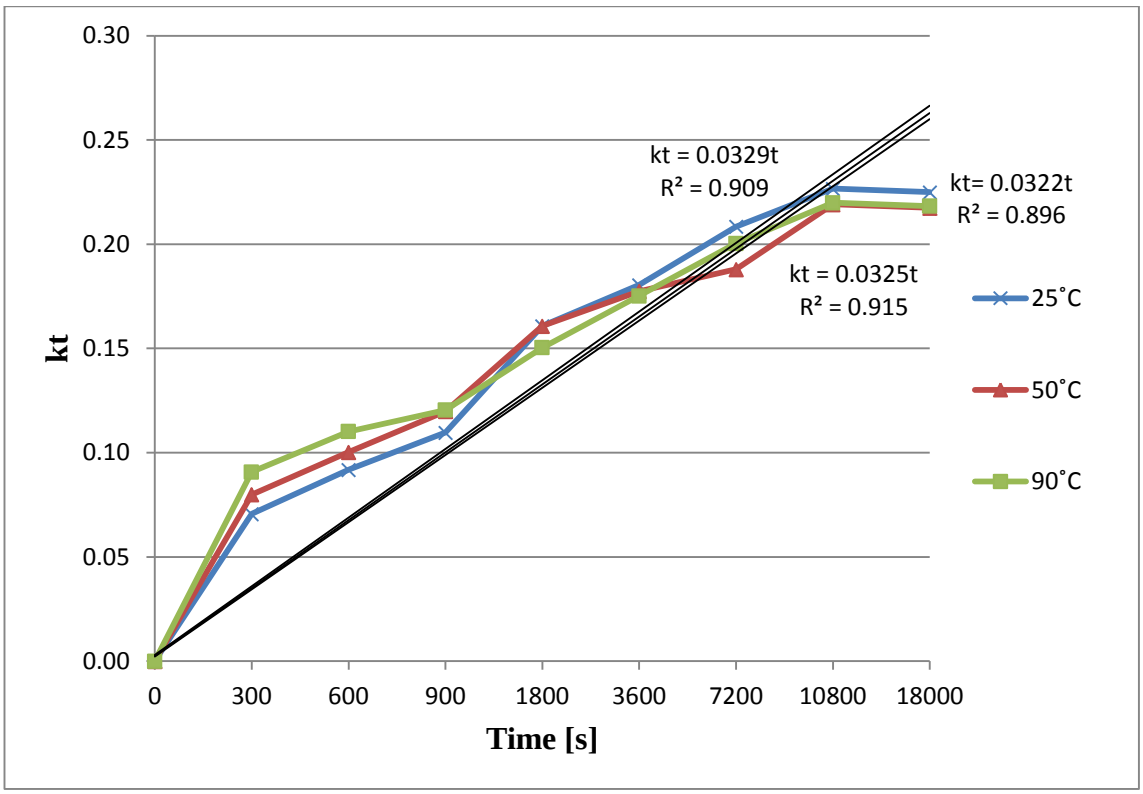

Figure 5.12: Combination of product layer diffusion and chemical reaction control for dissolution of RCA

As for SS, dissolution of RCA is well represented by the combination of product layer diffusion and chemical reaction control. The dissolution reaction of RCA is controlled at the same time by the reaction on the surface of the particle between the fluid reactant and the solid and by the diffusion of the products of reaction from the surface of the solid through the fluid film back into the main body of the fluid.

The activation energy can be calculated as for SS, plotting lnk versus 1/T (Figure 5.13) employing Arrhenius' law (equation 5-6) and the calculated value is 0.9kJ/mol.

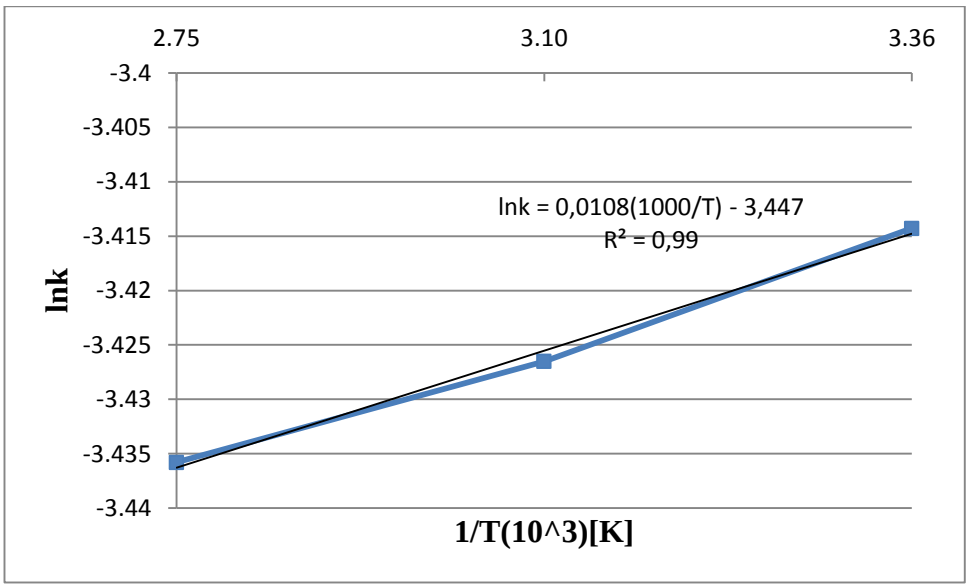

Figure 5.13: Plot for the calculation of activation energy for RCA

5.4 Dissolution of ground granulated blast furnace slag and phosphorus slag

Ground granulated blast furnace slag (GGBS) and phosphorus slag (PS) are well-known pozzolan materials available on the market [5.15]. In these materials, Ca is able to react with Si as soon as it goes into contact with water, to form calcium silicate hydrates. During dissolution experiments of GGBS and PS in NH_4HSO_4, Ca also reacts to form $CaSO_4$ and leaves the calcium silicate hydrate groups decalcified, forming silica gel, which makes the solution dense and viscous [5.16]. For this reason, dissolution experiments at 50g/l employing samples in particle size fraction 75-150µm at 50°C and 800rpm stirring rate produced a dense solution (worse for GGBS than for PS) causing problematic sampling and unreliable trends of dissolution for metals. Therefore, kinetic analyses based on standard models, as done for SS and RCA, could not be carried out. Consequently, precipitation of crystals of $CaSO_4$ during dissolution was based only on XRD and SEM studies from the final solid residues. Tests on GGBS and PS, were carried out at 50g/l for 3h and they were complemented by experiments lasting 5h and at 25g/l, to obtain more evidences on the dissolution mechanisms for these materials.

5.4.1 Phosphorus slag

PS was dissolved into a NH_4HSO_4 solution and the experiments were carried out at 50°C for 5h at 50g/l (1.3M NH_4HSO_4), 3h at 50g/l and 3h at 25g/l (0.65M NH_4HSO_4). After filtering the final solution, the solid residue was dried in an oven at 105°C overnight and analyzed by XRD and SEM. Overlay of PS XRD patterns are reported in

Figure 5.14 and it can be noticed that the peak at about 21 2-theta(°) is related to the presence of calcium sulphate hydrate. Decreasing time of dissolution and S/L ratio increases calcium sulphate hydrate presence and reduces other phases.

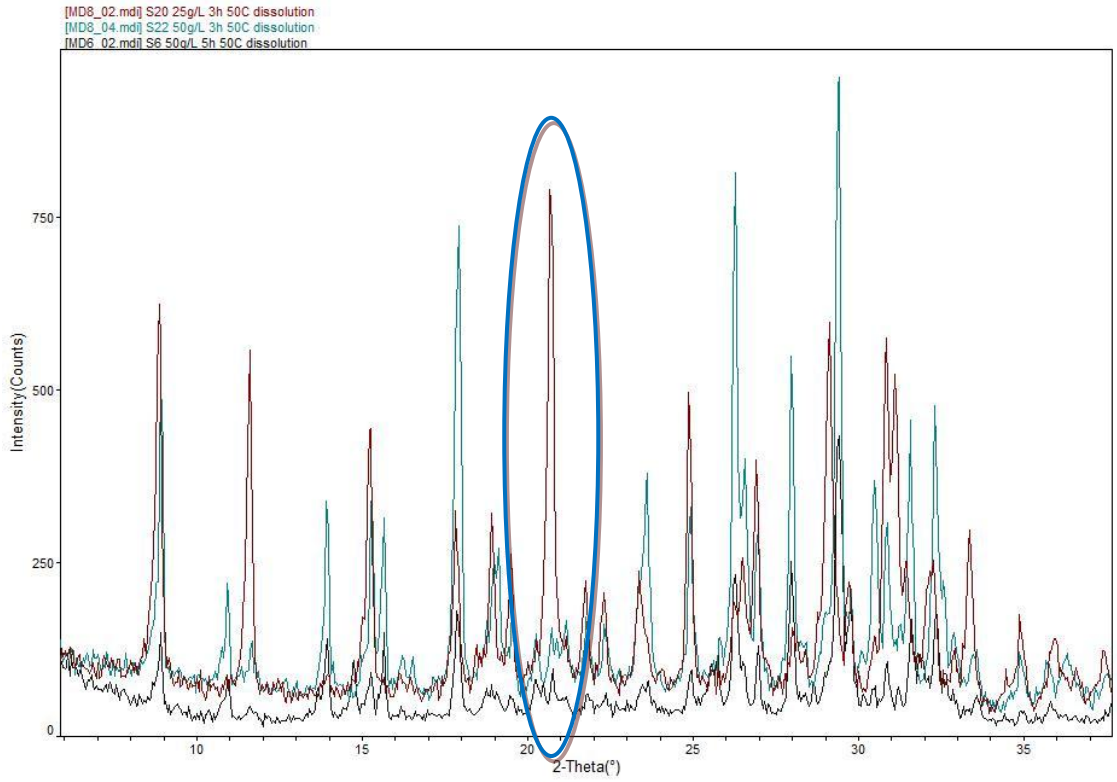

Figure 5.14: XRD patterns overlay for dissolution of PS

However, after 3h dissolution at 50°C and using 25g/l, the final solid residue still consisted of several phases (mainly aluminium and silicon phosphate, plus calcium sulphate), as it can be seen in Figure 5.15.

SEM pictures (Figure 5.16a, b, c) confirmed the observations derived from XRD, demonstrating that reducing the time of dissolution and the S/L ratio promotes the formation of $CaSO_4$ crystals (solid crystals, as seen for RCA and SS). Therefore, the subsequent carbonation reaction should take advantage of more calcium sulphate crystals present at lower S/L ratios.

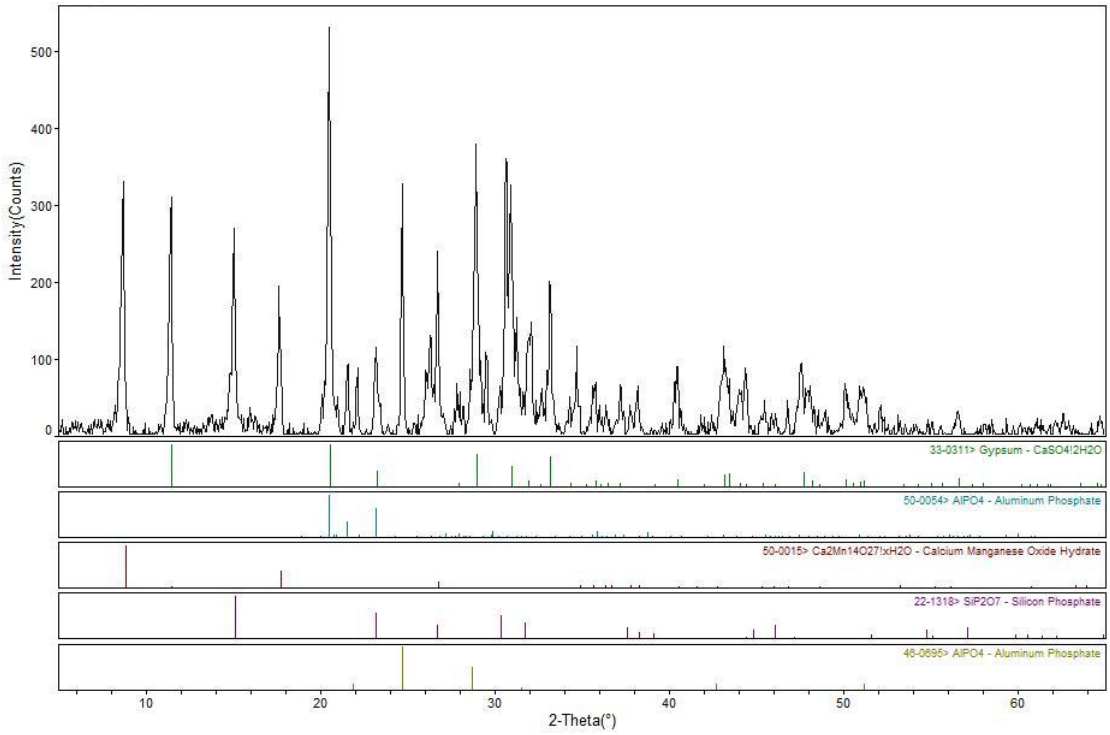

Figure 5.15: XRD patterns of dissolved PS at 25g/l, 3h, 50°C

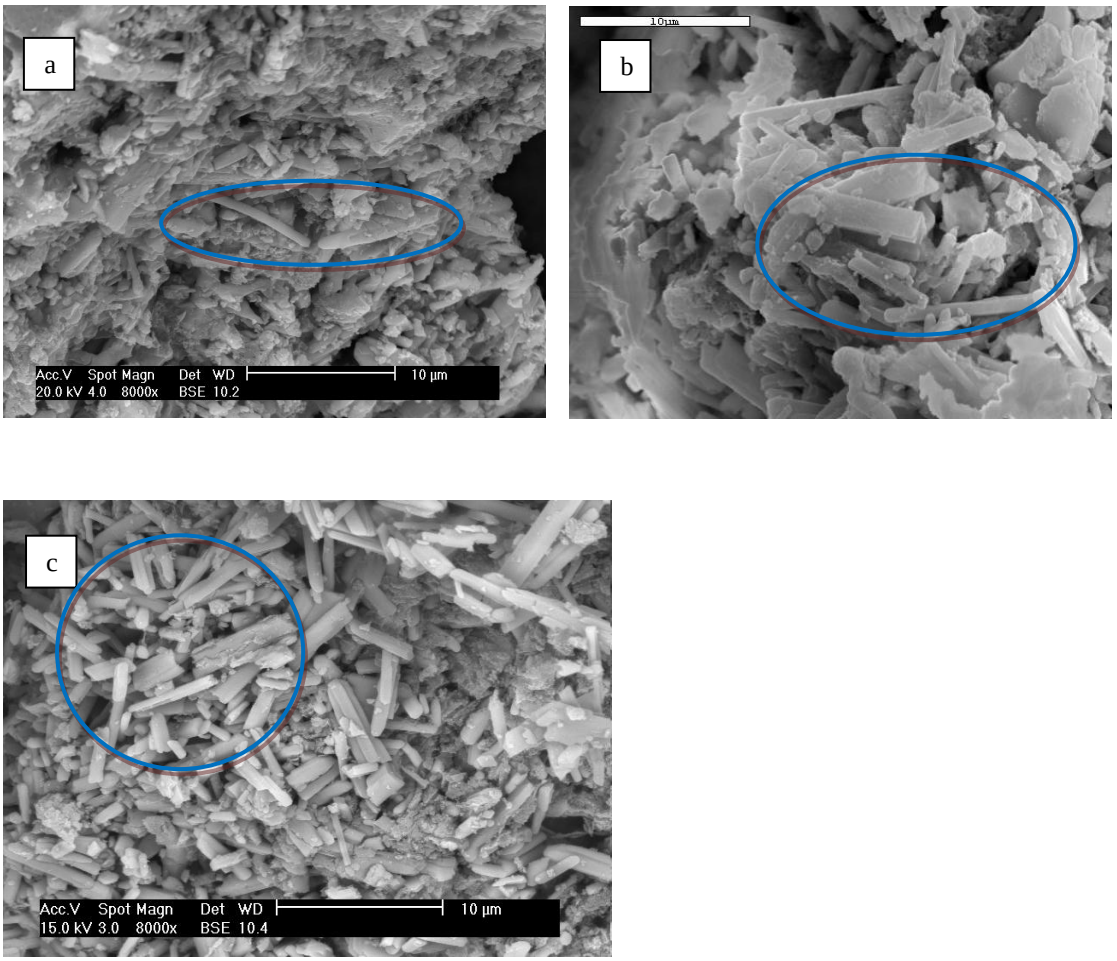

Figure 5.16: SEM of dissolved PS at a) 50g/l, 5h b) 50g/l, 3h c) 25g/l, 3h

5.4.2 Ground granulated blast furnace slag

GGBS was dissolved into a NH_4HSO_4 solution and the experiments were carried out at 50°C for 5h at 50g/l (1.1M NH_4HSO_4), 3h at 50g/l and 3h at 25g/l (0.55M NH_4HSO_4). As for PS, after filtering the final solution, the solid residue was dried in an oven at 105°C overnight and analyzed by XRD and SEM. Overlay of XRD patterns are presented in Figure 5.17 and it can be noticed that reducing dissolution time and S/L ratio, increases production of calcium sulphate (the peak at about 21 2-theta(°)), whilst decreases the presence of other phases.

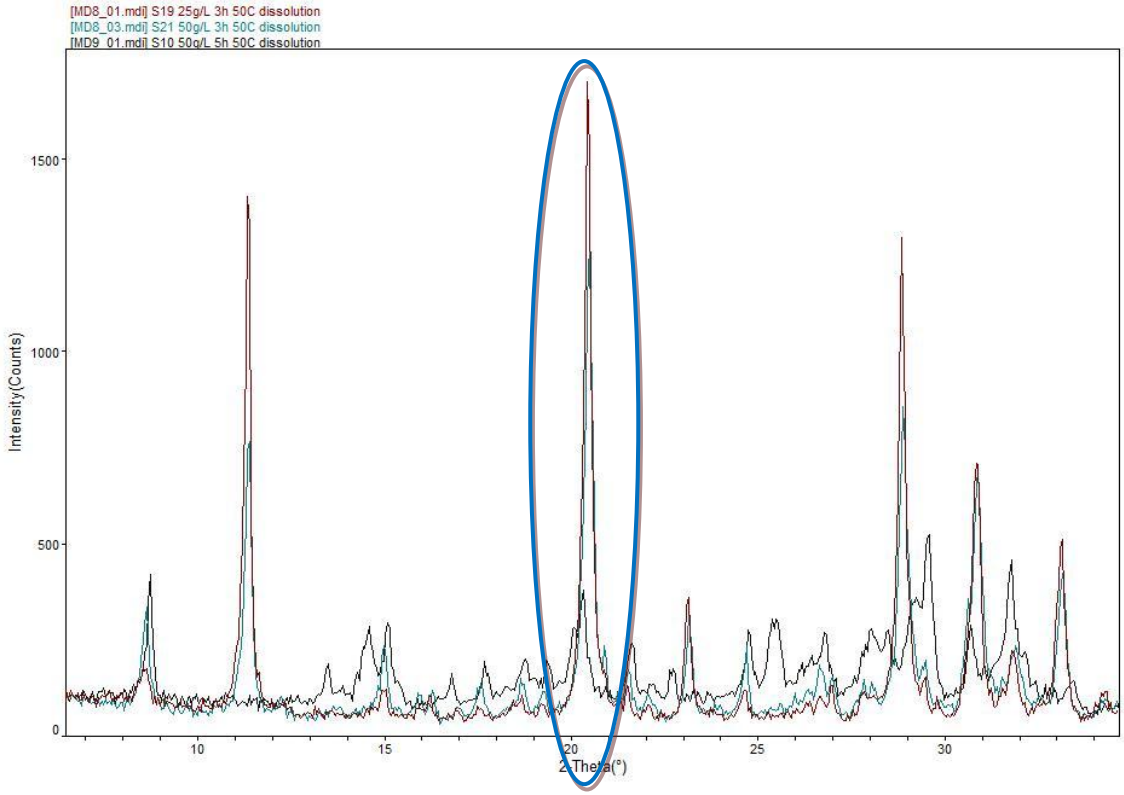

Figure 5.17: XRD patterns overlay for dissolution of GGBS

After 3h dissolution at 50°C and using 25g/l, the final solid residue was mainly crystalline calcium sulphate hydrated (Figure 5.18).

SEM pictures (Figure 5.19a, b, c) supported findings of the XRD studies. They demonstrate that when reducing the S/L ratio and the time of dissolution, the number of solid $CaSO_4$ crystals increased. Consequently, as for PS, the subsequent carbonation reaction will benefit of a higher number of calcium sulphate crystals when dissolution takes place at lower S/L ratios.

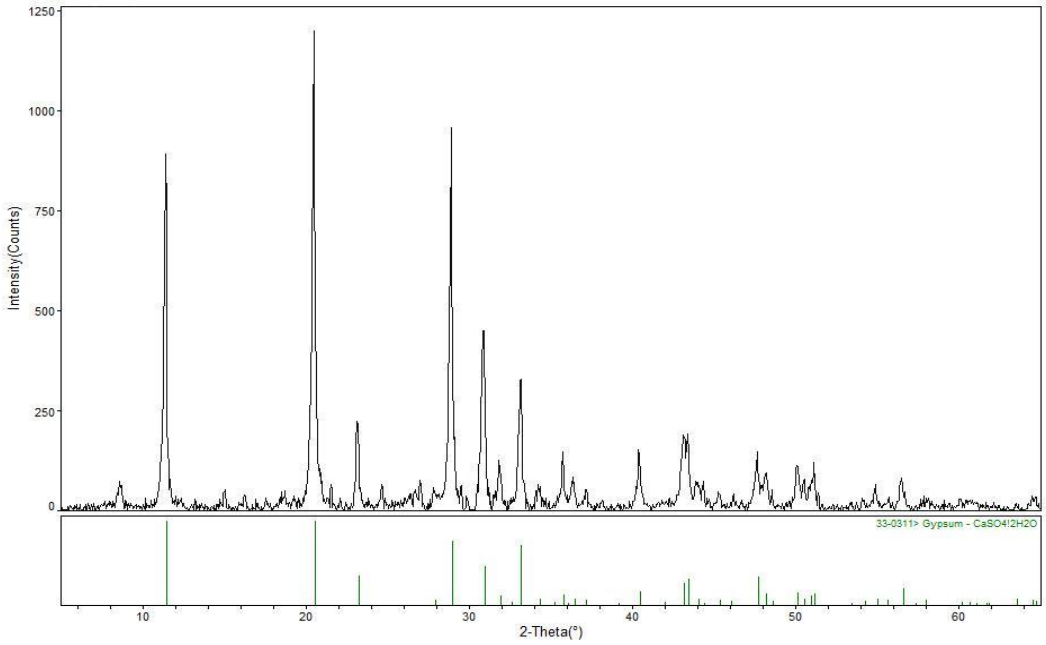

Figure 5.18: XRD pattern of dissolved GGBS at 25g/l for 3h at 50°C

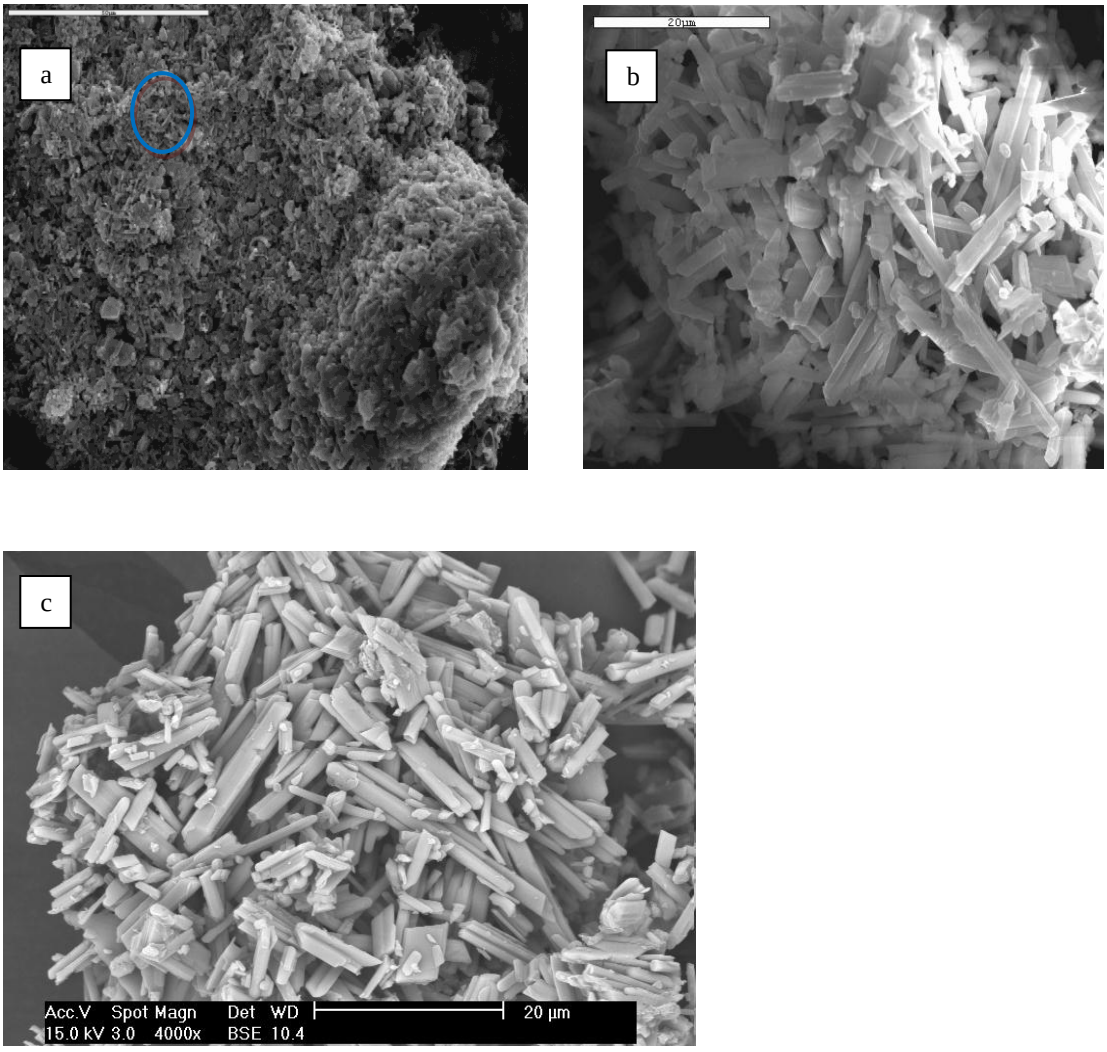

Figure 5.19: SEM of dissolved GGBS at a) 50g/l, 5h b) 50g/l, 3h c) 25g/l, 3h

5.5 Conclusions

This chapter, firstly, introduced an innovative mineralization multi-step process employing Ca-rich waste streams as feedstock. Chemical reactions and thermodynamics calculations are reported. The process described in this study can extract Ca from the feedstock and precipitate it as calcium sulphate, which afterwards is converted into calcium carbonate. NH_4HSO_4 is employed during the mineral dissolution phase, while NH_3 is used for capturing CO_2 and producing $(NH_4)CO_3$, which is then added during the carbonation reaction. All the reactions involved in the mineralization process are spontaneous ($\Delta G<0$) and exothermic ($\Delta H<0$) apart from the regeneration of additives step.

The characterization by XRD and XRF of nine potential feedstock materials for mineral carbonation was discussed. All the materials exhibited a higher content of Ca compared to Mg, and furthermore, for all of them, silica was the most abundant element. Based on their chemical composition (i.e. highest CaO content) and mineral phases present (i.e. low content of calcium carbonate), four samples (i.e. SS, GGBS, PS and RCA) were selected for carrying out mineral dissolution tests (Table 5.1). The waste materials selected can be divided into two groups on basis of their dissolution behaviour. For SS and RCA, it was possible to conduct kinetic analysis based on models reported in literature and using XRD and SEM studies. In contrast, GGBS and PS solutions became dense and viscous causing unreliable trends of dissolution due to the formation of silica gel during the dissolution experiments. In this case, precipitation of $CaSO_4$ crystals was investigated employing only XRD and SEM. To support findings on dissolution mechanisms of GGBS and PS at 50g/l for 3h, lower S/L ratio (25g/l) but also longer time of dissolution (5h) were also tested, allowing also assessing their effect on the precipitation of $CaSO_4$.

Investigation of the dissolution of SS and RCA confirmed the precipitation of $CaSO_4$. Results obtained from the dissolution of SS showed that Mg and Fe dissolved into a solution of NH_4HSO_4, while Ca precipitated as $CaSO_4$. Mg dissolution efficiency after 5h at 90°C (85%) for SS is similar to the one obtained from a previous study on serpentine (85%), employing the same dissolution procedure, while extraction of Fe occurs more easily, thus achieving higher levels of dissolution (90% for SS, 80% for serpentine). Kinetic analyses showed that the simultaneous effect of product layer diffusion and chemical reaction control fits the experimental results well. Activation

energy, calculated by the Arrhenius' law, was 2.3kJ/mol which is lower to the one calculated by previous papers on serpentine. This suggests that metals present in SS are easier to dissolve than the ones in serpentine. Since the experimental conditions employed in the previous study on serpentine and the ones used in this thesis were the same, the different iron dissolution rates could be related to the diverse mineral phases forming the two materials, including differences in chemical and physical nature of iron present (e.g. type of iron, hydration and presence of contaminants).

Similar to SS, RCA dissolved into NH_4HSO_4 solution extracting calcium and precipitating it as $CaSO_4$. The other main metal present, Al, dissolved partially (40% after experiment at 25°C) into solution. Also for RCA, the best fit of the experimental data was obtained with the combination of product layer diffusion and chemical reaction control mechanism. The activation energy for dissolution of RCA was 0.9kJ/mol. RCA, therefore, showed a dissolution process similar to SS and despite its large availability and high content of calcium oxide the high level of carbonates present limits its CO_2 storage capacity.

Investigation on dissolution of GGBS and PS confirmed that when dissolved into NH_4HSO_4 solution, they produced solid crystals of precipitated $CaSO_4$ (as during dissolution of RCA and SS). Furthermore, according to XRD patterns and SEM pictures, when reducing the S/L ratio from 50 to 25g/l and the time of dissolution from 5 to 3h the quantity of crystals increases.

5.6 References

[5.1] Wang X, Maroto-Valer MM. Dissolution of serpentine using recyclable ammonium salts for CO_2 mineral carbonation. Fuel. 2011;90:1229-37.

[5.2] TFHRC. Turner Fairbank Highway Research Centre (TFHRC). Manual on the use of waste and by-product materials in pavement construction. http://www.fhwa.dot.gov/publications/research/infrastructure/structures/97148/for.cfm2008. Date of consultation: November 2012.

[5.3] Shi C, Meyer C, Behnood A. Utilization of copper slag in cement and concrete. Resources, Conservation and Recycling. 2008;52:1115-20.

[5.4] Lutterotti L. MAUD - Materials Analysis Using Diffraction. http://www.ing.unitn.it/~maud/index.html, Computer program. Date of consultation: November 2012.

[5.5] Hewlett PC. Lea's chemistry of cement and concrete. 4th edition ed. London: Arnold. pp 241-254; 1998.

[5.6] Levenspiel O. Chemical Reaction Engineering. 2nd edition ed. New York, USA: John Wiley and Sons; 1972.

[5.7] Teir S, Revitzer H, Eloneva S, Fogelholm C-J, Zevenhoven R. Dissolution of natural serpentinite in mineral and organic acids. International Journal of Mineral Processing. 2007;83:36-46.

[5.8] Costa G, Baciocchi R, Polettini A, Pomi R, Hills C, Carey P. Current status and perspectives of accelerated carbonation processes on municipal waste combustion residues. Environmental monitoring and assessment. 2007;135:55-75.

[5.9] Pauling L. The nature of chemical bond. New York: Cornell Univ. Press; 1940.

[5.10] Boiocchi M, Caucia F, Merli M, Prella D, Ungaretti L. Crystal-chemical reasons for the immiscibility of periclase and wustite under lithospheric P,T conditions. 2001; 13: 881.

[5.11] Levy D, Giustetto R, Hoser A. - Structure of magnetite (Fe_3O_4) above the Curie temperature: a cation ordering study. 2012;39.

[5.12] Kusik CL, Meissner HP. Calculating activity coefficients in hydrometallurgy. A review. International Journal of Mineral Processing. 1975;2:105-15.

[5.13] Azimi G, Papangelakis VG, Dutrizac JE. Modelling of calcium sulphate solubility in concentrated multi-component sulphate solutions. Fluid Phase Equilibria. 2007;260:300-15.

[5.14] Fouda MFR, Amin RE, Mohamed M. Extraction of magnesia from Egyptian serpentine ore via reaction with different acids .2. Reaction with nitric and acetic acids. Bulletin of the Chemical Society of Japan. 1996;69:1913-6.

[5.15] Hai Qi G, Qin Peng X. Analysis on the Pozzolanic Effects of Phosphorus Slag Powder in Concrete. Key Engineering Materials. 2011;477:112-7.

[5.16] Chen JJ, Thomas JJ, Jennings HM. Decalcification shrinkage of cement paste. Cement and Concrete Research. 2006;36:801-9.

CHAPTER 6 – EFFECT OF S/L RATIO, PARTICLE SIZE AND TEMPERATURE ON THE EFFICIENCY OF CARBONATION

Chapter 5 discussed the dissolution of different waste streams in NH_4HSO_4 and the precipitation of $CaSO_4$. This chapter focuses on studying the effect of several operating variables on the main steps of the whole mineralization process (Figure 6.1) namely i) mineral dissolution in NH_4HSO_4, ii) pH adjustment and precipitation of impurities, iii) carbonation reaction, and iv) regeneration of additives. These steps can be integrated with the CO_2 capture from flue gases into ammonia producing $(NH_4)_2CO_3$ for the carbonation reaction and the ammonia absorption into water for obtaining NH_4OH for the pH adjustment step. Mineral dissolution, pH adjustment and carbonation reaction steps were tested at different S/L ratio, temperature and particle size for three metal slags: steel slag (SS), phosphorus slag (PS) and ground granulated blast furnace slag (GGBS). The dissolution step for these materials, as well as recycled concrete aggregate (RCA), was presented in Chapter 5. The dissolution of RCA was similar to that of the metal slags and, despite its large availability and high content of calcium oxide, the inherent high level of carbonates present in the parent sample limits its CO_2 storage capacity. Therefore, RCA was not included in the mineralization tests investigated in this chapter. Finally, scaled-up experiments (scaling-up factor 6) were carried out to asses any potential effect of increasing the size of the experimental rig on the efficiency of carbonation.

6.1 Effect of S/L ratio on efficiency of carbonation

Solid to liquid (S/L) ratio is an important parameter which has been shown to affect the efficiency of mineralization [6.1] [6.2]. Therefore, this section discusses the effect of three different S/L ratios, starting from 50g/l, (same value as that employed by Wang and Maroto-Valer [6.3]), and then reducing them to 25 and 15g/l in an attempt to improve the efficiency of mineralization, as previously reported for coal fly ash and wollastonite [6.1] [6.2] [6.4].

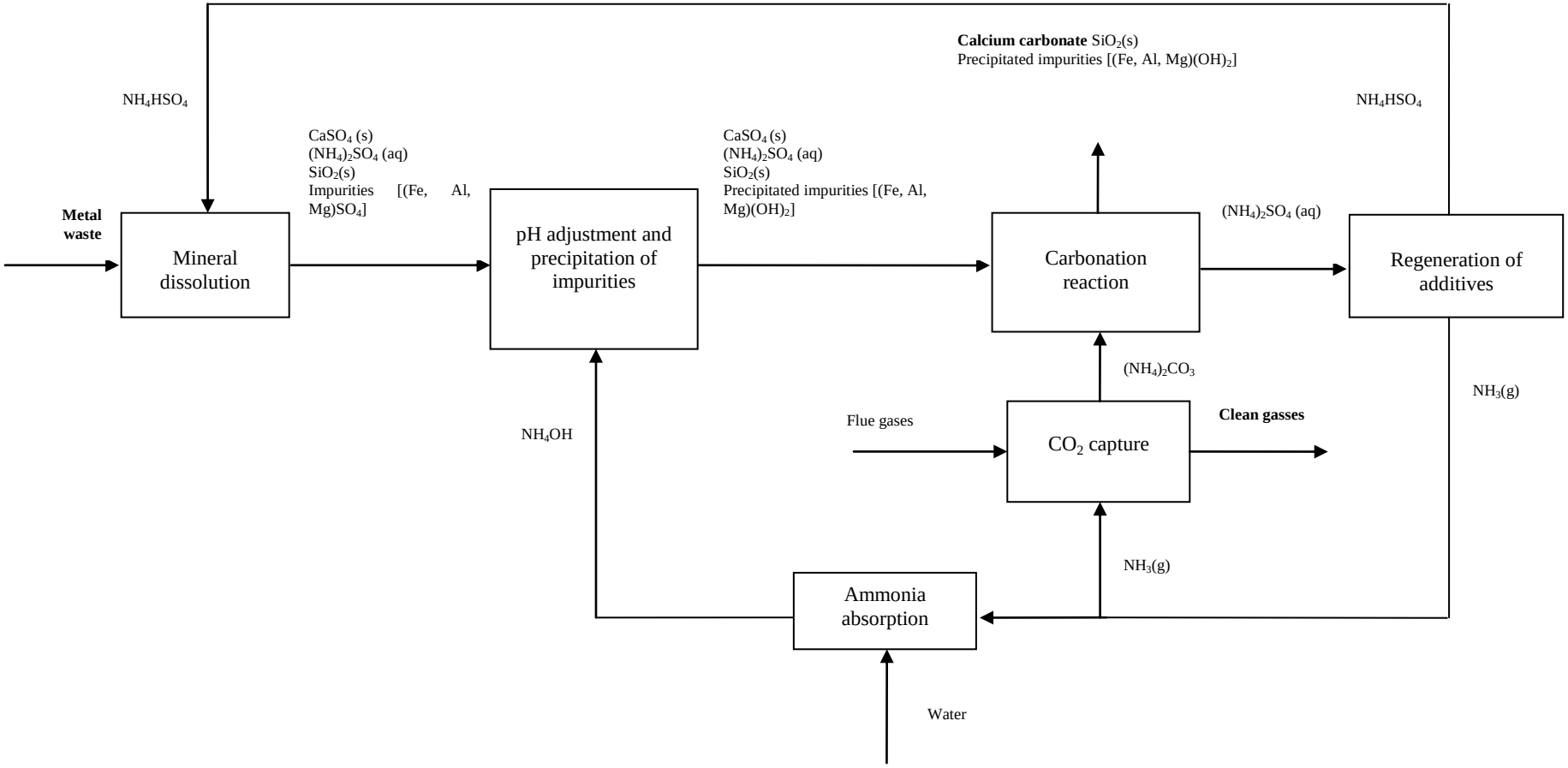

Figure 6.1: Block diagram for the multi-step closed loop mineralization process studied

Employing the experimental set-up presented in the methodology chapter (Section 3.3), experiments were carried out in a 500ml 3 necks glass flask which was heated by a temperature–controlled silicone oil bath and a thermocouple. The solution was continuously mixed by a stirrer and, to avoid evaporation losses, the rig was connected to a water cooling system via one of the necks. Samples were ground and sieved to a particle size fraction of 75-150μm as in previous studies [6.3] [6.5]. The starting solutions employed for the experiments testing mineral dissolution, pH adjustment and carbonation reaction steps were prepared with slightly above stochiometric NH_4HSO_4, as presented in Section 3.5. The addition of NH_4OH and $(NH_4)_2CO_3$ during the pH adjustment and mineral carbonation steps was also based on the methodology described in Section 3.5.

6.1.1 TGA of carbonated residues

TGA tests were carried out on the solid residues obtained after the mineralization experiments of SS, PS and GGBS samples using three different S/L ratios (15-25-50g/l). Consequently, also the amount of CaO introduced with the sample in the flask varied with the S/L ratio. Data presented in Table 6.1 report the amount of CaO introduced in the flask in g/L for each experiment with different waste streams and S/L ratio.

		S/L ratio [g/L]		
	CaO wt% in sample	15	25	50
PS	46.7%	7	12	24
GGBS	39.0%	6	10	20
SS	38.4%	6	10	19

Table 6.1: CaO content in each carbonation experiment with different waste streams and S/L ratio

The carbonation efficiencies obtained after the experiments, normalised with the CaO content, are presented in Figure 6.2. Carbonation efficiency, as seen in Section 3.5.1.1, represents the wt% of Ca initially contained as CaO in the raw material which is converted into $CaCO_3$ during the mineralization process. The Ca mass in the feeding material can be calculated from XRF analyses (which provides the CaO wt%) on the parent sample, while $CaCO_3$ before and after experiments can be calculated from TGA. The experimental error was estimated to be ±2% and it was obtained repeating 30% of

the tests. The maximum efficiencies achieved were for 15g/L as S/L ratio with values of 74%, 67% and 59% for SS, GGBS and PS, respectively.

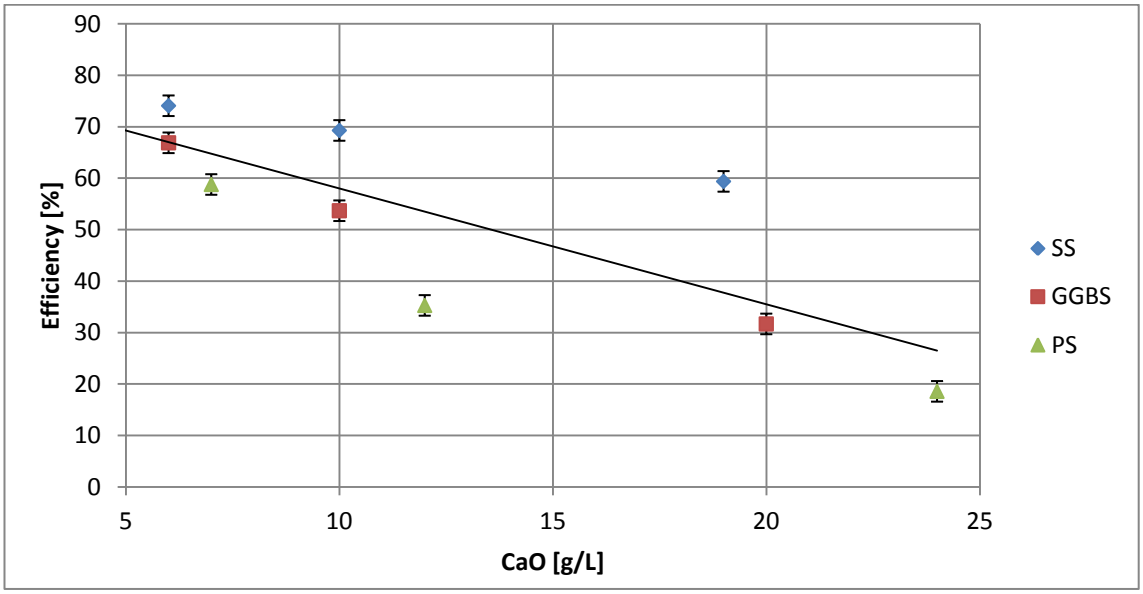

Figure 6.2: Efficiencies of carbonation for different CaO content in the sample

Figure 6.2 shows that the carbonation efficiency increases as the CaO content in the sample decreases, for all three materials. For multi-step mineralization processes, trends of efficiency of carbonation are primarily affected by the Ca extraction conditions during the first phase of the experiments [6.2]. When reducing the CaO content, Ca extraction efficiency improves meaning that the NH_4HSO_4 solution can better extract the Ca from the waste samples. Since the experimental conditions were the same (temperature, stirring rate, particle size, excess of stoichiometric NH_4HSO_4) in all the experiments, from the trend of efficiency it can be seen that there is a need of a higher excess of NH_4HSO_4 for higher levels of CaO in order to improve the extraction of Ca and consequently the efficiency of carbonation.

It should be noted that the carbonation efficiencies of SS are consistently higher than those reported for PS, despite SS presenting lower initial CaO content than PS (38.4wt% vs. 46.7wt%, Table 6.1). This could be related to the different mineral phases present in the parent samples, where extraction of calcium from the mineral phases present in SS (Figure A1.10) seems to be easier than from the mineral phases of PS (Figure A1.5). Relation between mineral phases present in the raw material and efficiency of carbonation could not be investigated for GGBS because of its amorphous structure, as described in Section 5.2.

As seen in Section 2.3.4, mineralization of waste materials, in general, requires milder reaction conditions in comparison to mineral rocks [6.7] [6.8]. As seen in Section 5.3.2, this could be due to the mineral structures forming wastes, which allow easier extraction of metals (Ca, etc.) and combination with CO_2 than in mineral rocks (e.g. serpentine). Consequently, in general, if the same mineralization conditions are applied for carbonating mineral rocks and waste materials, the latter would reach a higher carbonation efficiency. In fact, the carbonation efficiency achieved by the process developed by Wang et al. (similar to the one employed here) using serpentine at 50g/l was 25% [6.5] and, considering also the experimental error, it is similar to the one of PS (about 20%) and lower than that of GGBS and SS (about 30% and 60%, respectively) (Figure 6.2).

6.1.2 XRF of carbonated residues

XRF studies on the carbonated residues were carried out according to the methodology described in Chapter 3. Results from XRF analyses obtained from the carbonated residues are presented in Table 6.2 (instrumental error ±0.1%).

		Chemical composition (wt%)						
		CaO	MgO	Fe_2O_3	Al_2O_3	SiO_2	SO_3	LOI
SS	Residue from 15g/l	26.9	3.6	19.1	1.5	8.8	11.1	24.8
	Residue from 25g/l	25.9	3.5	18.2	1.4	8.1	14.9	23.8
	Residue from 50g/l	25.4	4.4	18.3	1.3	8.4	14.9	23.2
PS	Residue from 15g/l	29.1	0.5	0.2	1.7	27.1	12.8	26.8
	Residue from 25g/l	28.7	0.5	0.3	1.7	28.4	12.9	25.4
	Residue from 50g/l	24.9	0.6	0.2	1.4	23.7	15.9	31.6
GGBS	Residue from 15g/l	22.8	3.8	0.3	7.2	21.7	15.3	27.7
	Residue from 25g/l	22.6	3.8	0.4	7.8	22.1	15.7	26.5
	Residue from 50g/l	15.0	2.7	0.2	5.1	14.2	21.7	40.2

Table 6.2: XRF composition of final solid residues after the carbonation step

As expected, these samples present much higher LOI values than their parent samples (Table 5.2), as they have been carbonated (see Section 6.1.3 for further discussion of the

carbonated products). It can be seen that for the three materials investigated, as soon as the S/L ratio decreases, the SO_3 content diminishes. This is due to the production of calcium carbonate being higher when the S/L ratio is lower (higher carbonation efficiency, Figure 6.2) causing lower amounts of residual calcium sulphate left from the dissolution step. Values of Ca, Mg, Fe, Al and Si oxides in the carbonated samples are lower than those reported for the parent samples because of the precipitation of different phases during the carbonation reaction of the process (Figure 6.1).

6.1.3 XRD of carbonated residues

The solid residues from the carbonation step were analyzed by XRD and Figures 6.3, 6.4 and 6.5 show the XRD diffractograms obtained from the carbonated residues of SS, PS, GGBS, respectively, for experiments conducted at 15g/l. For all the samples, the main phases identified were calcium carbonate and residual hydrated calcium sulphate (gypsum). Moreover, the carbonated SS sample showed also the presence of iron oxide and magnetite (Figure 6.3), as expected from the iron content of the parent samples. Silica peaks (20.5 and 26.5 2-theta degrees) were detected as smaller peaks in carbonated SS and PS (Figures 6.3 and 6.4) compared to the raw materials. This is consistent with the values of silica from XRF in the carbonated samples (Table 6.2), which are smaller than the silica content in the parent samples (Table 5.2). SEM studies confirmed the presence of precipitated calcium carbonate and calcium sulphate (Section 6.1.4). Calcium carbonate and residual calcium sulphate were the main phases indentified in the residues for experiments using GGBS at 15g/l (Figure 6.5) and 25g/l (not shown here, but almost identical to Figure 6.5). However, the solid residue after the experiment at 50g/l, showed the presence of calcium carbonate and sulphate together with hydrated magnesium sulphate and calcium phosphate (Figure 6.6). The difference between the solid residue after experiment at 50g/l and the ones obtained at 15 and 25g/l is due to the dense solution generated during the experiment at 50g/l. The solution mixing resulted reduced and therefore the dissolution of Ca was limited. In fact, as seen in Section 5.4, GGBS is a pozzolan material, producing silica gel during the dissolution experiments [6.9] [6.10]. The more silica gel is produced the more the solution becomes dense and viscous.

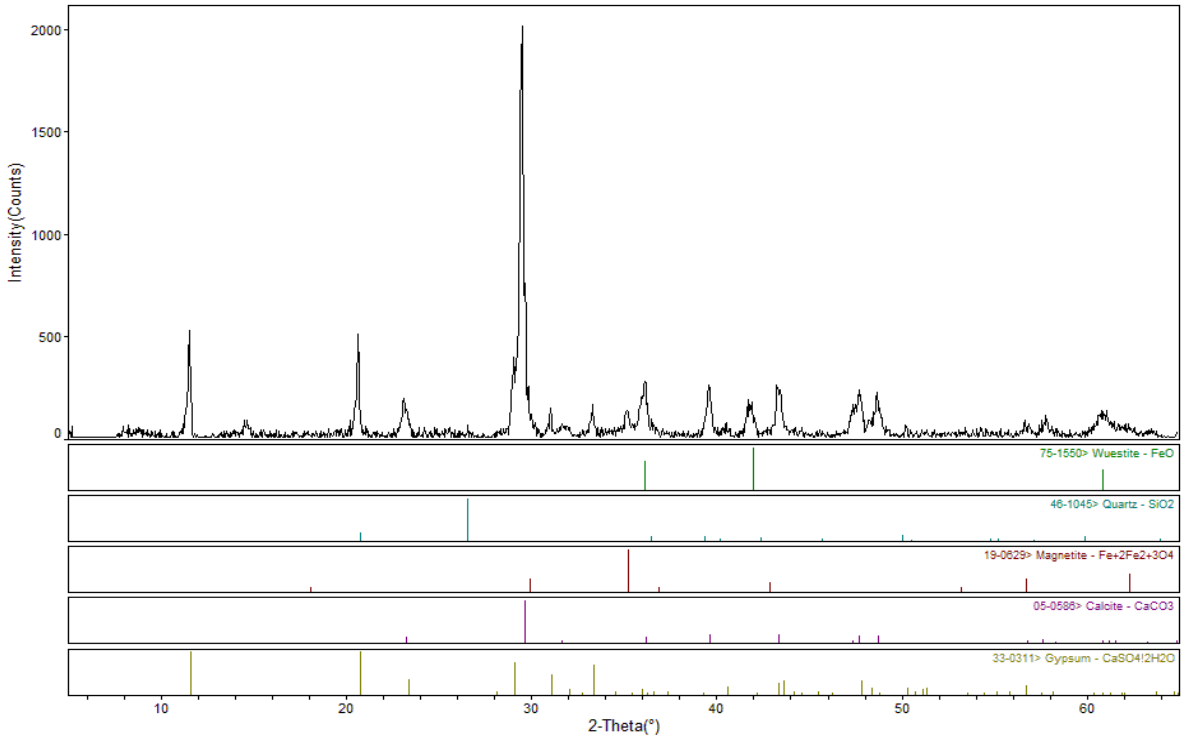

Figure 6.3: XRD diffractogram presenting crystalline phases detected in carbonated SS at 15g/l

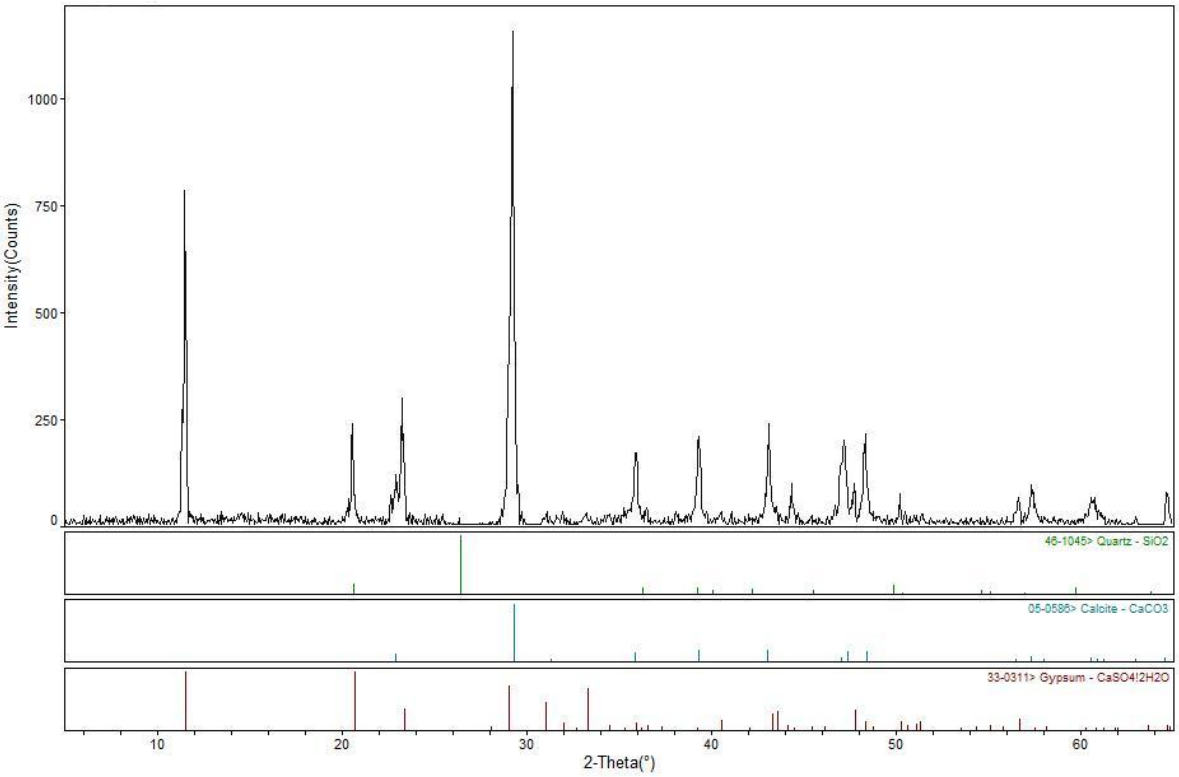

Figure 6.4: XRD diffractogram presenting crystalline phases detected in carbonated PS at 15g/l

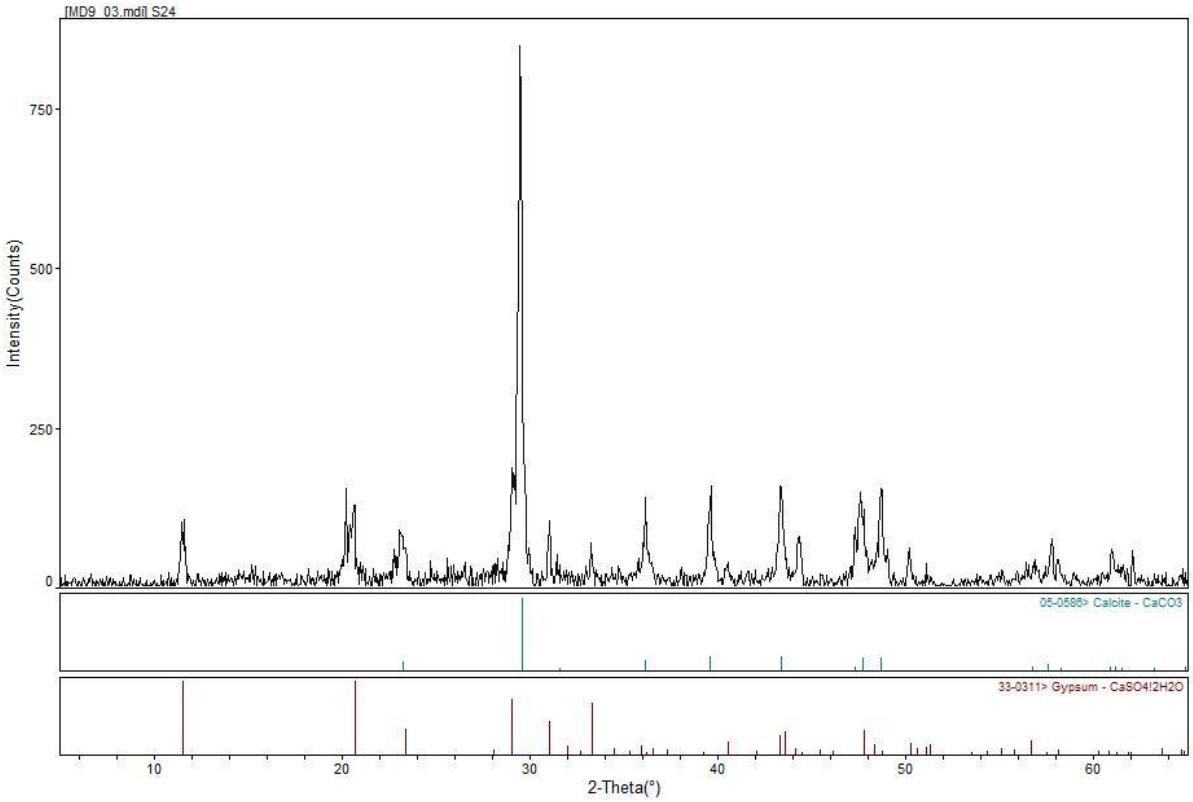

Figure 6.5: XRD diffractogram presenting crystalline phases detected in carbonated GGBS at 15g/l

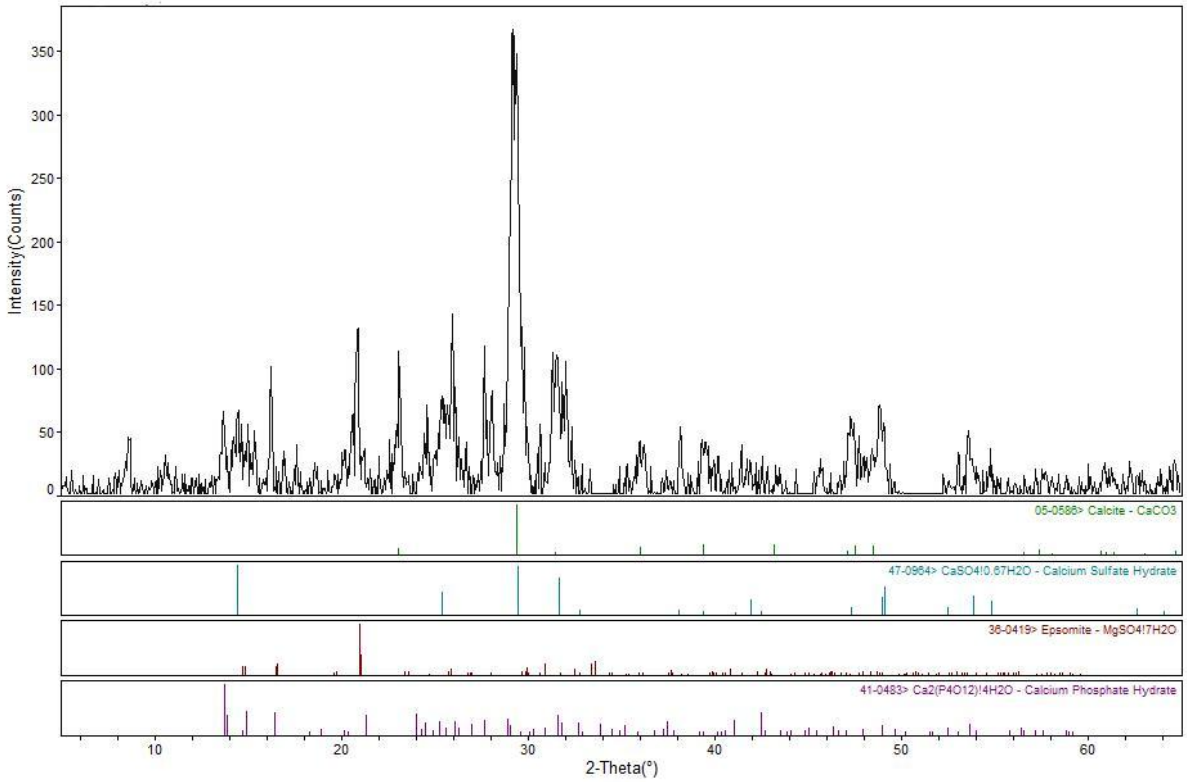

Figure 6.6: XRD diffractogram presenting crystalline phases detected in carbonated GGBS at 50g/l

6.1.4 SEM-EDS of carbonated residues

SEM-EDS studies of the final solid residues obtained after experiments on SS, PS and GGBS at 15g/l were also carried out to characterize the structure and morphology of the carbonated particles.

Representative images obtained from the PS carbonated residue at 15g/l are presented in Figures 6.7, 6.8 and 6.9. The dispersed small particles seen in Figure 6.7 and identified by the letter A, are precipitated calcium carbonate, magnified in Figure 6.8. The big particles in Figure 6.7 (identified by letter B), are mainly residual calcium sulphate from the dissolution step and silica from the starting material. This is confirmed by the EDS studies, as shown in Figure 6.9, where it can be seen that large calcium sulphate particles are plastered with small particles of calcium carbonate.

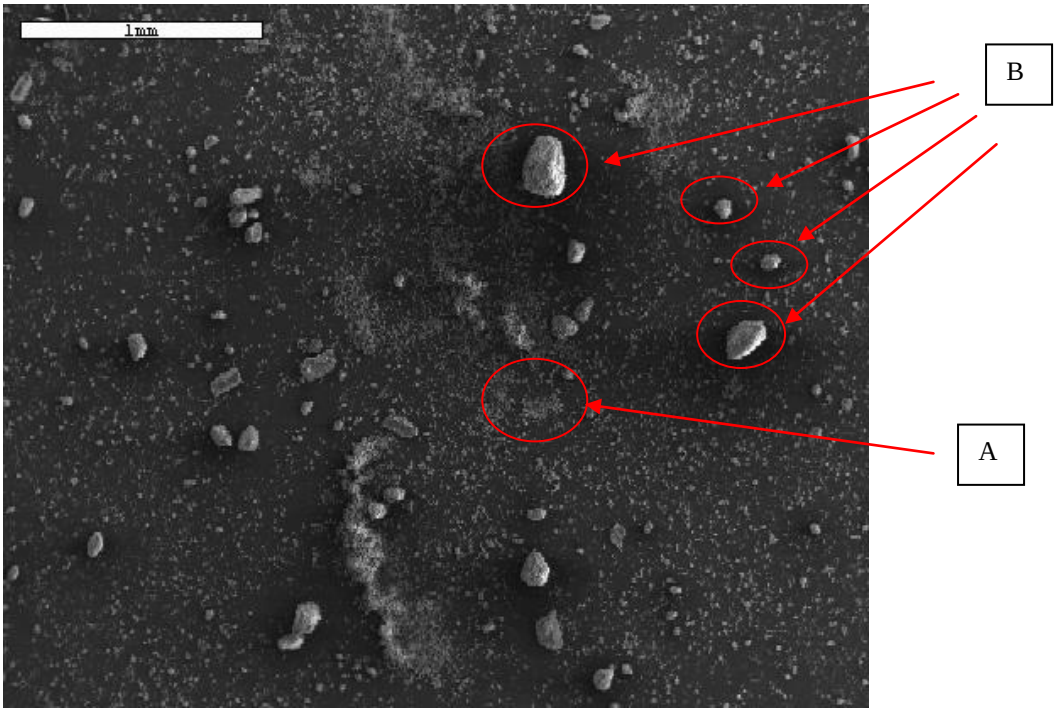

Figure 6.7: SEM image of PS carbonated residue at 15g/l. A) dispersed precipitated calcium carbonate B) residual calcium sulphate and silica

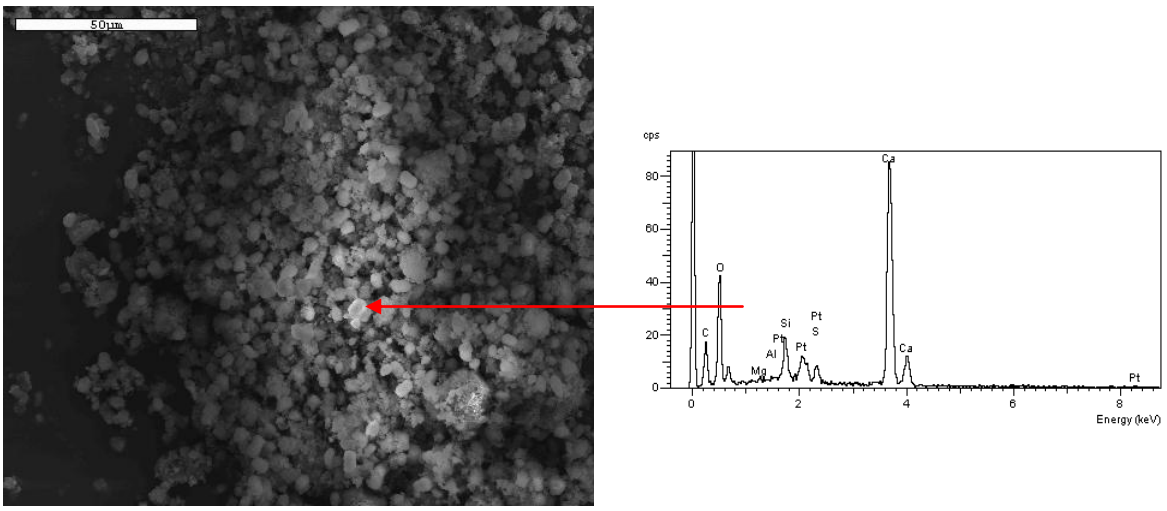

Figure 6.8: SEM-EDS spectrograph of small particles A of PS carbonated residue at 15g/l

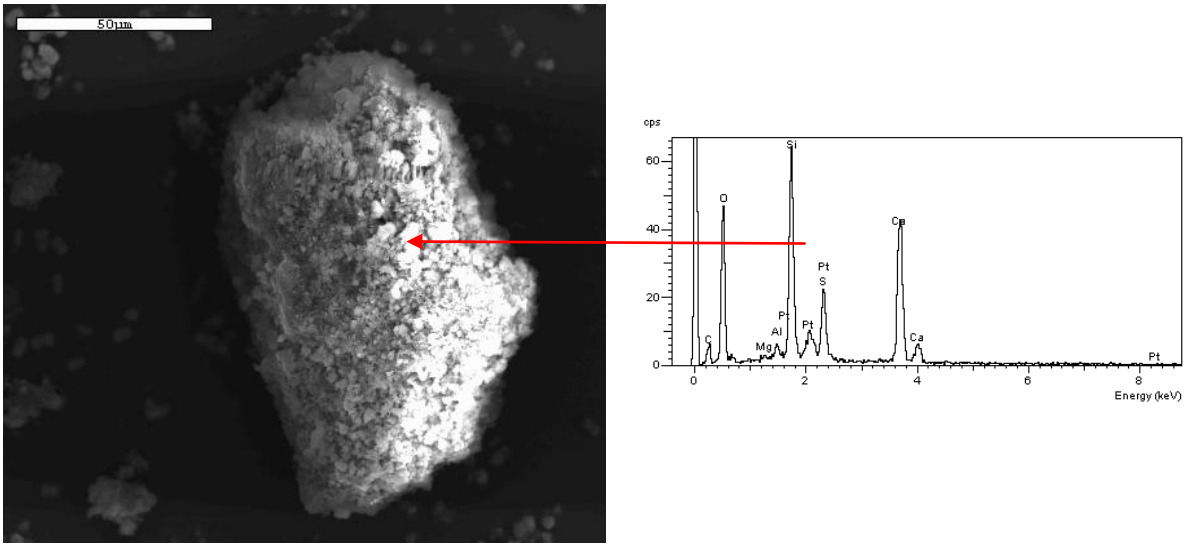

Figure 6.9: SEM-EDS of particles B of PS carbonated residue at 15g/l

6.2 Effect of temperature on efficiency of carbonation

Temperature is an important parameter affecting efficiency of carbonation of waste materials (Section 2.3.4.6). Accordingly, mineralization tests were carried out at various temperatures and employing the same conditions as the previous sections, namely particle size 75-150µm, stirring rate 800rpm, S/L ratio 15g/l. Temperatures between dissolution (3h) and carbonation (1h) phases were maintained constant, testing at 40, 50 and 65°C.

The efficiency of carbonation for the SS sample increases with temperature from 64 to 72% (Figure 6.11). This could be explained as the dissolution of alkali metals (Ca, Mg,

Fe) in NH_4HSO_4, during the first phase of the process, is more efficient at higher temperature [6.3] and consequently more calcium sulphate is formed after the carbonation step. Previous studies on steel slag have also confirmed the increase in efficiency when rising the temperature up to 150-200°C [6.1] [6.12].

For the PS sample, the temperature affects the efficiency of carbonation below 50°C, and then the efficiency seems to remain constant when the temperature is raised up to 65°C (Figure 6.10).

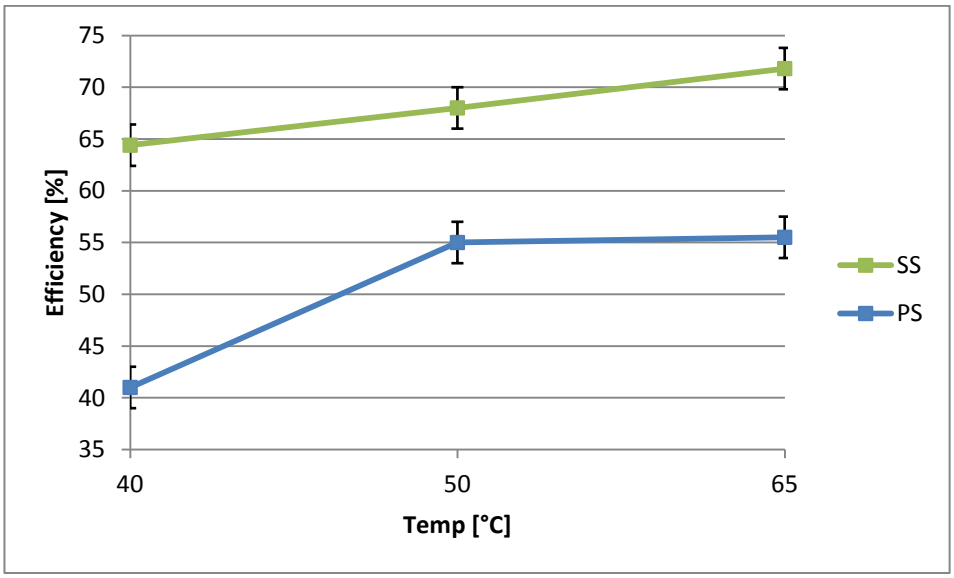

Figure 6.10: Effect of temperature on efficiency of carbonation for steel slag and phosphorus slag

Efficiency of carbonation in multi-step mineralization processes are primarily affected by the Ca extraction conditions during the first phase of the experiments [6.2]. Therefore, higher temperature during the experiments could increase the removal of Ca from the mineral structure of the raw material raising the efficiency of carbonation. However, Ca extraction reaches a plateau at a certain temperature, preventing further improvements for the efficiency of carbonation. Previous studies on different materials (wollastonite, SS and serpentine) also demonstrated this trend of reduced influence of the temperature on the dissolution/carbonation efficiency as the temperature increases [6.1] [6.11] [6.12].

For the GGBS sample, when rising the temperature from 40-65°C, the efficiency of carbonation (about 65%) does not seem to increase significantly (Figure 6.12), when

considering the experimental error of ±2 (represented with the error bars in Figure 6.11). An extra experiment at 30°C was then carried out to assess the influence of temperature also at this lower value and it was then noticed an efficiency reduction. Therefore, the effect of the temperature on efficiency of carbonation for GGBS is similar to PS, higher temperature during the experiments could increase the removal of Ca from the mineral structure of the raw material raising the efficiency of carbonation. The only difference between efficiency of carbonation for GGBS and PS is that it reaches its maximum at 40°C instead of 50°C and then it levels for temperatures up to 65°C.

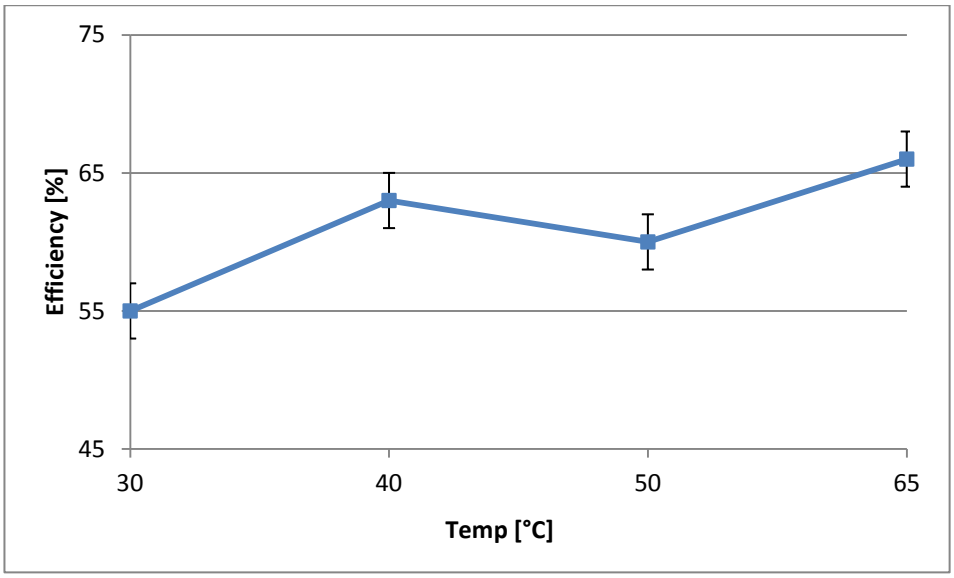

Figure 6.11: Effect of temperature on efficiency of carbonation for GGBS

6.3 Effect of particle size on efficiency of carbonation

As for temperature, particle size is another important factor affecting efficiency of carbonation (Section 2.3.4.6). Therefore, the effect of particle size on the efficiency of carbonation was also investigated. The particle size 150-300µm was employed maintaining the same experimental conditions used in the tests described in the previous sections (15g/l, 800rpm, 50°C dissolution for 3h, 65°C carbonation for 1h).

Results for steel slag are reported in Table 6.3 and show that when increasing particle size the efficiency of carbonation decreases (from 68% to 61%). This is consistent with previous studies on carbonation of steel slag and it is due to the higher specific surface area available for reaction in smaller particles [6.12]. For instance, specific surface areas

values for steel slag have been reported as 5.4m^2/g and 1.6m^2/g for particle size <80µm and 80-500µm, respectively [6.13].

Experiments on phosphorus slag showed a similar trend, where efficiency decreases from 59% to 45% (Table 6.3), confirming the higher availability of specific surface area for the reaction in smaller particles. It was not possible to study GGBS because the sample is finely grinded during the production process and the amount of sample received did not contain particles in the size range 150-300µm.

	Efficiency of carbonation (%)	
Material	Particle size 75-150µm	Particle size 150-300µm
SS	68	61
PS	59	45

Table 6.3: Effect of the particle size on the efficiency of carbonation for steel slag and phosphorus slag

6.4 Scaling-up tests

The purpose of the scaling-up tests was to investigate the potential presence of other factors affecting the efficiency of carbonation at bigger scale. Lab-scale experiments are normally carried-out in batch reactors which use less than 1000ml [6.14]. When investigating experimental scaling-up, it is reasonable to proceed by steps, starting from testing a pilot-scale experimental rig employing between 1 and 100l of solution [6.14]. Such wide range is due to the specificity of each technology tested, when moving from lab-scale to pilot-scale experiments.

In the case of the multi-step mineralization process tested in this thesis, considering budget and technical constrains for the rig set-up and the commercial availability, a scaling-up factor of 6 was chosen. A 3l glass flask (Figure 6.12), instead of 500ml where 2400ml of NH_4HSO_4 solution was employed for the experiments.

Figure 6.12: Set-up for scaling-up mineralization experiments

The three materials, SS, PS, GGBS, in the particle size range 75-150μm were tested at S/L ratio of 15g/l. The other experimental conditions were maintained identical as for the small scale experiments (3h dissolution at 50°C, 1h dissolution at 65°C). The results obtained (Table 6.4) show that increasing the reactor size, the efficiency values remain similar (within the experimental error), and therefore, there are not scaling-up factors able to affect the process, at least when the scaling-up factor is up to 6. This suggests that the reaction mechanisms governing the different steps of the mineralization process are the same at small and pilot scale (up to a scaling-up factor of 6). It is likely that the scaling-up tests did not lead to any change in the efficiency of carbonation because the equipment used for the reaction to take place (glass flask, stirrer) reproduced at bigger scale the conditions used at small scale. This avoided any alteration of the chemistry of the process which would have caused for instance incomplete reactions.

	Efficiency of carbonation (%)	
	Small scale	Pilot scale
SS	74	76
GGBS	67	68
PS	59	58

Table 6.4: Efficiency of carbonation results from scaling-up experiments

6.5 Conclusions

Firstly, the multi-step mineral carbonation process was investigated using three different S/l ratio (15-25-50g/l) for SS, PS and GGBS. It was observed that the carbonation efficiencies increased with decreasing CaO content introduced with each sample during the experiments. Experiments achieved 74%, 67% and 59% efficiency for SS, GGBS and PS, respectively. Wang and Maroto-Valer, using a similar process employing serpentine at 50g/l, reached 25% efficiency which is lower than that of GGBS and SS at the same S/L ratio, and similar to PS. This confirms that, in general, carbonation efficiency for waste materials is higher than the one from mineral rocks. As seen in the previous chapter, this could be due to the different mineral phases forming the samples, which allow during the first step of the process, easier extraction of metals from the waste streams than from rocks (i.e. serpentine). The solid residues from the carbonation step were analysed using several techniques (XRF, XRD, SEM-EDS). XRF studies showed that reducing the S/L ratio resulted in a decrease of SO_3 content. This is due to the production of $CaCO_3$ being higher, when the S/L ratio is lower because of higher carbonation efficiency. XRD analyses found that the main phases identified in the carbonated samples were $CaCO_3$ and residual hydrated calcium sulphate ($CaSO_4 \cdot 2H_2O$).

Moreover, the effect of temperature on the efficiency of carbonation was investigated. It was observed that when the experimental temperature for dissolution and carbonation was increased between 40 to 65°C, the efficiency of carbonation also raised for SS (up to 72%), while for PS the efficiency only increased between 40 and 50°C (up to about 55%) and then it remained constant till 65°C. GGBS behaved like PS with the only difference that efficiency of carbonation rose from 30 to 40°C (up to about 65%) and then it levelled for temperatures up to 65°C. In multi-step mineralization processes, efficiency of carbonation is mainly affected by the Ca extraction conditions during the mineral dissolution step and, therefore, the behaviour and values of efficiency of carbonation of SS, PS and GGBS are probably related to the effect of the temperature during the first step of the process. The removal of Ca from the mineral structure of the raw material could be increased when raising the temperature, leading to better efficiency of carbonation. However, Ca extraction reaches a plateau at a certain temperature, preventing further improvements for the efficiency of carbonation. Previous studies on different materials (wollastonite, SS, serpentine) also demonstrated this trend of reduced influence of the temperature on the dissolution/carbonation

efficiency as soon as the temperature is raised. In addition, the effect of particle size on the efficiency of carbonation was also analysed in this chapter. It was noticed that increasing the particle size from 75-150µm to 150-300µm the efficiency lowers for both SS and PS from 68% to 61% and from 59% to 45% respectively as found in previous studies. This is because, as reported in literature (e.g. for steel slag 5.4m^2/g and 1.6m^2/g for particle size <80µm and 80-500µm, respectively) [6.1] [6.13], larger specific surface area for reactions is available in smaller particles compared to the ones with bigger size. Finally, results from scaling-up test are reported. The scaling-up factor employed was 6, carrying out experiments in a 3l glass flask instead of 500ml. The results showed that the efficiency of carbonation remains the same (within the experimental error). This suggests that the reaction mechanisms governing the different steps of the mineralization process are the same at small and pilot scale and, therefore, there are not scaling-up factors able to affect the process, at least when the scaling-up factor is up to 6.

6.6 References

[6.1] Zevenhoven R, Wiklund A, Fagerlund J, Eloneva S, In't Veen B, Geerlings H et al. Carbonation of calcium-containing mineral and industrial by-products. Frontiers of Chemical Engineering in China. 2010;4:110-9.

[6.2] Jo HY, Kim JH, Lee YJ, Lee M, Choh S-J. Evaluation of factors affecting mineral carbonation of CO_2 using coal fly ash in aqueous solutions under ambient conditions. Chemical Engineering Journal. 2012;183:77-87.

[6.3] Wang X, Maroto-Valer MM. Dissolution of serpentine using recyclable ammonium salts for CO_2 mineral carbonation. Fuel. 2011;90:1229-37.

[6.4] Huijgen WJJ, Witkamp G-J, Comans RNJ. Mechanisms of aqueous wollastonite carbonation as a possible CO_2 sequestration process. Chemical Engineering Science. 2006;61:4242-51.

[6.5] Wang X, Maroto-Valer MM. Integration of CO_2 Capture and Mineral Carbonation by Using Recyclable Ammonium Salts. ChemSusChem. 2011;4:1291-300.

[6.6] Back M, Kuehn M, Stanjek H, Peiffer S. Reactivity of alkaline lignite fly ashes towards CO_2 in water. Environmental Science Technology. 2008;42:4520-6.

[6.7] Huijgen WJJ, Ruijg GJ, Comans RNJ, Witkamp G-J. Energy Consumption and Net CO_2 Sequestration of Aqueous Mineral Carbonation. Industrial & Engineering Chemistry Research. 2006;45:9184-94.

[6.8] Costa G, Baciocchi R, Polettini A, Pomi R, Hills C, Carey P. Current status and perspectives of accelerated carbonation processes on municipal waste combustion residues. Environmental monitoring and assessment. 2007;135:55-75.

[6.9] Hai Qi G, Qin Peng X. Analysis on the Pozzolanic Effects of Phosphorus Slag Powder in Concrete. Key Engineering Materials. 2011;477:112-7.

[6.10] Chen JJ, Thomas JJ, Jennings HM. Decalcification shrinkage of cement paste. Cement and Concrete Research. 2006;36:801-9.

[6.11] Teir S, Revitzer H, Eloneva S, Fogelholm C-J, Zevenhoven R. Dissolution of natural serpentinite in mineral and organic acids. International Journal of Mineral Processing. 2007;83:36-46.

[6.12] Huijgen W, Witkamp G, Comans R. Mineral CO_2 sequestration by steel slag carbonation. Environmental Science & Technology. 2005;39:9676-82.

[6.13] Santos RM, Ling D, Sarvaramini A, Guo M, Elsen J, Larachi F, et al. Stabilization of basic oxygen furnace slag by hot-stage carbonation treatment. Chemical Engineering Journal. 2012;203:239-50.

[6.14] Zeton B.V. scaling up step by step. Available on-line at: http://www.zeton.com/site/pdf_articles/Zeton_Scaling_Up.pdf. Zeton BV - The Netherlands 2012.

CHAPTER 7 – MASS, ENERGY, CO_2 BALANCES AND COST EVALUATION

The studies described in the previous chapters focused on understanding the main steps of the mineralization process proposed for waste materials. In this chapter the entire system including CO_2 capture, ammonia absorption and regeneration of additives, is investigated to evaluate its feasibility at industrial scale. Considering the theoretical chemical reactions of the multi-step process and data from a steel plant, energy and mass balances are obtained. Moreover, based on the heat required and electric consumption of the process, CO_2 emissions balance was then calculated to assess when the mineralization process becomes carbon negative. Furthermore, cost evaluations were performed considering the theoretical maximum efficiency as well as the process efficiency obtained from the previous chapter (Section 6.1).

7.1 Steel plant data

An industrial process emitting CO_2 which could be retrofitted on-site with a mineralization facility is a steel plant, where CO_2 is emitted and an appropriate waste material is produced. Steel making, together with cement production, is one of the industries responsible for large CO_2 emissions to the atmosphere, where emissions from the industrial sector are 20% of the total and, within industry, steel accounts for about a quarter of the emissions, which means about 4-5% of global CO_2 emissions [7.1].

Steel slag samples employed for carbonation experiments were obtained from one of the main steel plants in UK and, as mentioned in Section 3.1, because of confidentiality, full details on the location and company owning the plant cannot be disclosed. The steel plant considered emitted 7.4Mt of CO_2 in 2010 which means 965t/h (assuming 320 working days per year) and steel slag production was 43t/h.

7.2 Mass balance

The mass balance calculations carried out are presented in Figure 7.1. Starting from the chemical reactions listed in Table 5.1 and the steel slag production of the plant considered (43t/h), a mineralization process with S/L ratio at 15g/l able to sequester 13t/h of CO_2, employing all the steel slag produced, was developed. As an example, the calculations for the CO_2 capture are presented in Table 7.1 where the stoichiometric

amount of each reactant and the mass balance of the reaction are reported. The reaction is the following:

$$2NH_3 + CO_2 + H_2O \rightarrow (NH_4)_2CO_3 \quad (7\text{-}1)$$

	Molecular weight [g/mol]	**Amount** [mol]	**Amount** [g]
NH_3	17.03	2	34.06
CO_2	44.01	1	44.01
H_2O	18.02	1	18.02
$(NH_4)_2CO_3$	96.09	1	96.09

Table 7.1: Mass balance for the CO_2 capture reaction

The CO_2 planned to be sequestered by the process is 13t/h, therefore, the amount of $(NH_4)_2CO_3$ produced is 28.6t/h (96.09 divided by 44.01 and multiplied by 13), the H_2O and NH_3 required are 5.3t/h and 10.1t/h, respectively. The same calculations were performed for all the other steps of the process, starting from the stoichiometric reactions reported in Table 5.1 and the known amount of inputs. Details of the mass balance calculations are reported in Appendix B.

The dissolution and carbonation steps of the mineralization process applied to the steel plant are designed to have a duration of 1 hour each. The process takes place in a series of reactors of suitable size at S/L ratio of 15g/l (the same as the one used during lab experiments which allowed to achieve the best efficiency) and, because of the volumes of solution involved, most of the process equipment will consist of multiple units operating in parallel. The different phases of the process detailed in Figure 7.1 are:

- CO_2 capture by ammonia absorption. The capture unit is able to sequester CO_2 from flue gases using ammonia and water. $(NH_4)_2CO_3$ is produced at 28.6t/h rate and then employed in the carbonation reactor. The ammonia absorption unit uses the recycled ammonia and water to produce ammonium hydroxide, NH_4OH, (5.1t/h) to be used in the pH adjustment and precipitation of impurities phase.
- Mineral dissolution. Steel slag produced in the plant at a rate of 43t/h is conveyed to the mineralization reactor and then mixed for 1h together with NH_4HSO_4 (about 85.7t/h, stoichiometric value) and water. This phase allows extraction of Ca and

precipitation of $CaSO_4$ for 40.6t/h. Moreover, other sulphate phases are produced at a lower rate (i.e. magnesium, iron, aluminum sulphate) and are listed in detail as Stream 1 in Figure 7.1.

- pH adjustment and removal of impurities. Following the mineral dissolution, NH_4OH is added in the slurry to raise the pH. Mg, Fe, Al hydroxides are precipitated at 1.1, 4.0, 0.5t/h rate respectively (Stream 2), while calcium sulphate is not affected by the operation.
- Carbonation reaction. It takes place in 1h and $CaSO_4$ is converted into calcium carbonate at a rate of about 30t/h, while other mineral phases present are not affected by the reaction (Stream 3). Residual $(NH_4)_2SO_4$ solution, 98t/h, is then passed to the water evaporation unit (Stream 4).
- Water evaporation and regeneration of additives. Water consumed in the process (Streams 1, 2 and 4) is about 2850m^3/h which needs to be evaporated to allow the recovery of 98t/h $(NH_4)_2SO_4$ for the following regeneration step. Once water is evaporated, it must be condensed to be reutilized within the process. When regeneration of the additives takes place in a melting vessel, from $(NH_4)_2SO_4$ about 85.4t/h of NH_4HSO_4 and 12.6t/h of NH_3 are regenerated and recirculated within the process.
- Water and NH_4HSO_4 management units. These two units do not carry-out any chemical reaction, but they allow to regulate the amount of water and NH_4HSO_4 used in the process. The units receive the recovered streams from the end of the process (2857t/h water and 85.4t/h NH_4HSO_4) and they integrate them with the limited amount required (1t/h water and 0.3t/h NH_4HSO_4) to allow the mineral dissolution and CO_2 capture steps to work properly.

Overall, it can be noticed that despite the large amount of water required (about 2850t/h, Streams 1,2 and 4) the process can reuse it, limiting the requirement of fresh water to 1t/h. This is also the case for the chemicals employed for dissolution, NH_4HSO_4, where about 85t/h are needed, but the process can regenerate and recirculate it, requiring only 0.3t/h to be supplied every hourly cycle. These results allow understanding that the impact on the process of input materials is limited, because of their small amount required (only 1t/h water and 0.3t/h NH_4HSO_4).

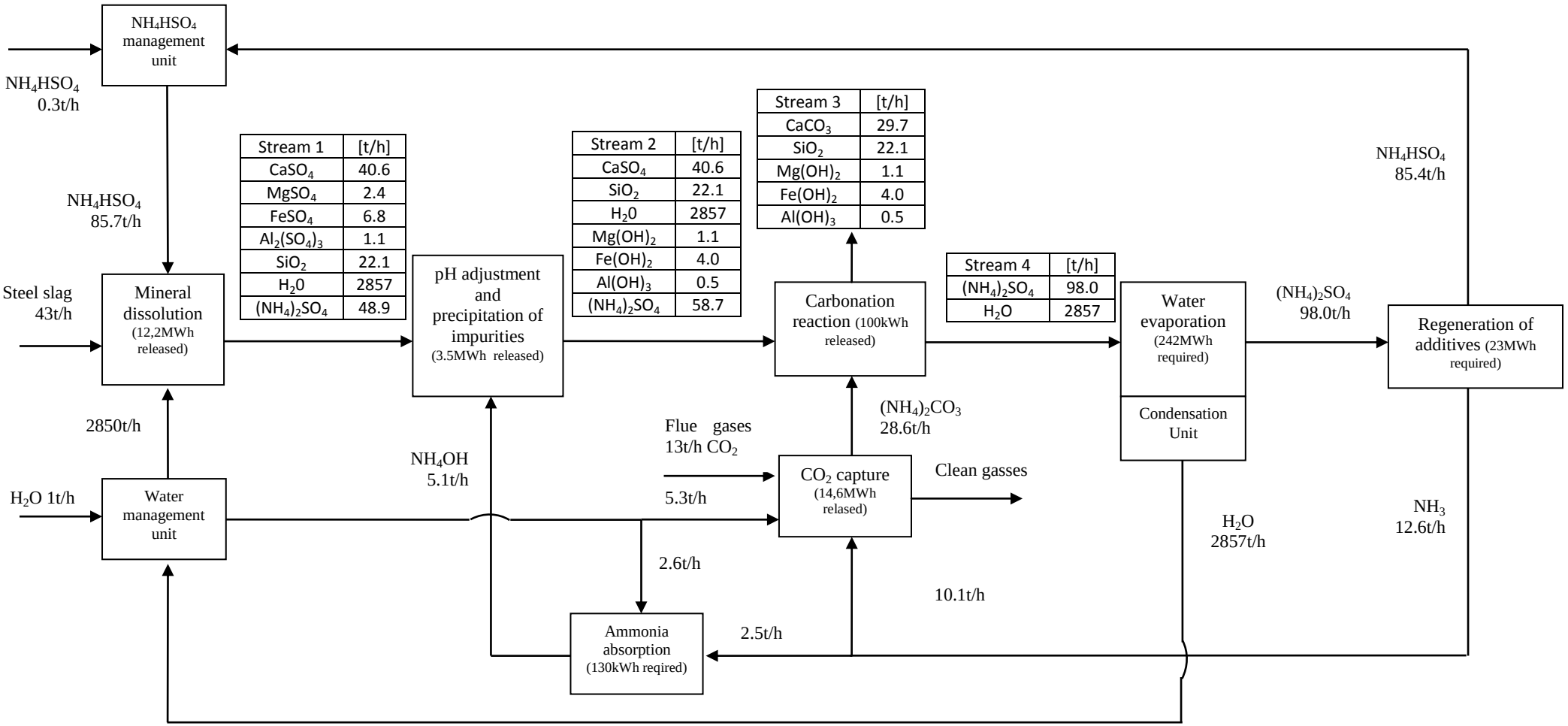

Figure 7.1: Mass balance for a mineralization process in a steel plant

The final product of the mineralization process is a mixture of different phases among which the predominant is calcium carbonate. However, to separate the final phases to obtain a valuable product further treatment is required. In fact, as seen in the literature review (Section 2.4), high level of purity are needed for silica and calcium carbonate to reach an interesting market value (£189-350/t).

7.3 Energy and CO_2 balance

Results from the energy balance for each step of the process, obtained using the software HSC Chemistry 5.1 and the mass balance reported in the previous section, are included in Figure 7.1. As an example, the calculations carried out for the CO_2 capture step were based on the following table (Table 7.2), reporting the amount of reactants and products and giving the total heat released by the reaction (difference between the sum of the total enthalpy (H) of the reactants and the products). Calculations show that the reaction releases 12577Mcal (negative values characterize exothermic reactions, Section 5.1), which corresponds to 14628kWh (1Mcal=1.16kWh).

Input	TEMP [°C]	AMOUNT [kmol]	AMOUNT [kg]	Latent H [Mcal]	Total H [Mcal]
NH_3	20	593.057	10100	-25.37	-6537
CO_2	20	295.389	13000	-13.06	-27794
H_2O	20	294.196	5300	-26.44	-20124
Output					
$(NH_4)_2CO_3$	20	297.651	28600	0	-67034
				Balance	-12577

Table 7.2: Energy balance for the CO_2 capture step

Tables reporting the energy balance calculations for the other chemical reactions of the mineralization process are presented in Appendix B. Water evaporation after the mineralization reaction needs specific heat (4186J/Kg K) to increase the temperature from 65 to 100°C and then latent heat (2260kJ/Kg) to evaporate all the water. These two contributions give the total amount of heat required by the water evaporation phase which is carried out in a MVR (mechanical vapor recompression) evaporator. MVR evaporators allow a more efficient water evaporation, usually between 0.05 and 0.15kWh/Kg [7.2], therefore the total heat required for this phase of the process is about 242000kWh since the total water evaporated is 2857t/h.

Table 7.3 summarizes the energy balance, where negative values indicate heat released, while positive values represent heat required for each step. The process investigated, i.e. mineralization system retrofitted into a steel plant, can sequester a theoretical maximum of 13t/h CO_2 (1.4% of the total emission) using 43t/h steel slag. The total heat released corresponds to 2.3MWh/tCO_2, while the total heat required is 20MWh/tCO_2. The highest contribution to the total heat required is due to the water evaporation step (18.6MWh/tCO_2). The regeneration step, instead, requires 1.8MWh/tCO_2 which is however much lower than the value reported in a previous study for mineral carbonation process with chemical regeneration using NaCl and HCl (3277 and 4361kWh/tCO_2, respectively) [7.3].

Capture of 13t/h CO_2 43t/h steel slag	
Heat released	**kWh**
CO_2 capture	-14628
mineral dissolution	-12201
precipitation of impurities	-3549
carbonation	-100
TOTAL HEAT RELEASED	**-30478**
Heat required	**kWh**
water evaporation (MVR)	242000
regeneration	22945
ammonia adsorption	131
TOTAL HEAT REQUIRED	**265076**

Table 7.3: Energy balance for the mineralization process applied to a steel plant

Similarly, direct mineral carbonation processes, such as that developed at the U.S. Department of Energy's National Energy Technology Laboratory (NETL), consume large amounts of energy in the mineral activation stage (977kWh/tCO_2). Also, the recovery of the employed chemicals (0.64M $NaHCO_3$ and 1M NaCl), which was not addressed in their work, would require additional energy [7.4].

7.3.1 Heat released and required

The heat release during CO_2 capture, mineral dissolution, precipitation of impurities and carbonation can be recovered using heat exchangers and reused within the mineralization process to heat-up the incoming streams of steel slag, ammonium sulphate and water. This would allow minimizing the energy requirement necessary for the dissolution, carbonation and ammonia adsorption at 50°C, 65°C and 20°C, respectively.

The heat required for evaporating the water and regenerating the additives (Table 5.1) at 300°C is high temperature heat. Flue gases from the steel plant are already cooled down to 250-300°C (not lower to avoid condensation of acid compounds) before being released in the atmosphere from the stack. The cooling of the flue gases allows recovering heat for pre-heating the combustion gas and air for the blast furnace. Therefore, heat from flue gases cannot be further recovered for the mineralization process.

The ammonium sulphate is separated from the water solution by a MVR evaporator, requiring lower energy than the theoretical evaporation energy calculated from heat of vaporization and specific heat. This is possible in a MVR evaporator thanks to a compressor which increases the pressure of the vapor produced and consequently its condensation temperature [7.2]. The compressed vapor, therefore, increases the heat provided to the water for producing more vapor.

The condensed water is then recovered and reutilized within the process. The heat required from the MVR evaporator and the regeneration of chemicals (in a melting vessel) would be provided by a hot oil system heated by a stand-alone natural gas fired heater. HHV (high heating value) for natural gas is 54GJ/t and heat to be provided for evaporation and regeneration is 265MWh (Table 7.3), which corresponds to 954GJ. Therefore 17.6t of natural gas are required every hour. Natural gas emission is $2.8kgCO_2/Kg_{fuel}$, therefore, the emissions associated with the water evaporation and regeneration of additives are $49.3tCO_2/h$.

7.3.2 Electric consumption

Further to heat requirement, which releases CO_2, electric consumption for pumps, conveyors, agitators and compressor for the MVR evaporator should also be considered, as they contribute to the CO_2 emissions from the process. Table 7.4 reports the electric consumption for each of them and details of the calculations are reported immediately after.

Equipment unit	Electric consumption
MVR compressor	39MW
Water pumps	3MW
Conveyors	100kW
Agitators	2MW
TOTAL	43MW

Table 7.4: Electric consumption for an industrial mineralization plant operating at 15g/l

- MVR compressor: a unit evaporating 50t/h requires about 700kW [7.2], therefore, considering 2850t/h of water to be evaporated, the electric consumption for the compressor will be around 39MW.
- Water pumps: a pump moving 60m^3/min (3600m^3/h) consumes 650kW [7.5], therefore moving 2400t/h requires about 450kW. The mineralization process requires 4 pumps (between dissolution, pH adjustment, carbonation, water evaporation and then one for the recirculation of water). Therefore the total electrical consumption for pumps would be around 2MW. Adding then other service pumps (lubricant circuit, liquid for heat exchangers, water compensation, circulation of ammonia), the total electric consumption can be raised to 3MW. A summary of the pumps required and their characteristics are reported in Table 7.5. Axial pumps are suitable for streams with high flow rate (about 2800t/h), while for the service pumps, centrifugal ones are more appropriate.
- Conveyors for solid materials: A conveyor requires about 100kW to move 400t/h of material [7.6]. The mineralization process requires to handle 43t/h of steel slag, 98t/h ammonium sulphate, 57.5t/h final solid residue and 85t/h ammonium bisulphate. Therefore the 4 conveyors consume about 100kW in total.
- Agitators: an agitator with a capacity of 22m^3 consumes 5.5kW [7.7], therefore for 2850t/h of solution, 700kW are required for each step needing an agitator (dissolution, pH raise and carbonation reactors), consequently about 2MW are totally required.

Pump unit	Location (stream reported in Figure 7.1)	Type	Electric consumption [kW]
Pump 1	Stream 1	Axial pump	450
Pump 2	Stream 2	Axial pump	450
Pump 3	Stream 4	Axial pump	450
Pump 4	Water recirculation from condensation unit	Axial pump	450
Pump 5	Circulation of ammonia after regeneration	Centrifugal pump	200
Pump 6	Water compensation input	Centrifugal pump	200
Other service pumps	Heat exchangers in exothermic steps and oil and lubricant circuits	Centrifugal pump	600

Table 7.5: List and characteristics of pumps employed in the designed process

The total electric consumption for the mineralization process studied would be around 43MW. As seen in Section 2.3.1, emission of CO_2 from electricity produced in UK is about 380g/kWh, therefore, CO_2 emissions from electric consumption would be 16.0tCO_2/h.

7.3.3 CO_2 balance

7.3.3.1 Theoretical maximum CO_2 balance

Adding the contributions of CO_2 released from the heat required and electric consumption, the total CO_2 emissions are 65.3t/h. The process is designed to capture 13t/h of CO_2, therefore the CO_2 balance is positive and the process emits more CO_2 than sequesters (carbon positive process).

Increasing the S/L ratio does not affect the chemical reactions of the process reported in Table 5.1 (same amount of CO_2 stored), but only the amount of water required to be evaporated. As an example, instead of 15g/l, with 30g/l, the water amount would be 1432t/h (about half of 2857t/h), which means CO_2 emission for its evaporation to be reduced to 25t/h (heat required for evaporation 132MWh which correspond to 8.8t/h natural gas).

When considering S/L ratio of 80g/l, CO_2 emissions from water evaporation would be 9.8t/h (51MWh required for evaporation which correspond to 3.5t/h of natural gas). In this case, the electrical consumption (Table 7.6) for MVR compressor, pumps,

conveyors and agitators is 7.3MW, 1.5MW, 100kW and 400kW, respectively. Total electrical consumption would be about 9.4MW which means 3.5t/h CO_2 emissions. Total emissions are, therefore, 13.3t/h and the designed process begins to be carbon negative (i.e. able to sequester more CO_2 than the one emitted to carry out the process) with S/L ratio of 80g/l or higher.

For a S/L ratio of 120g/l, CO_2 emission from water evaporation would be 6.5t/h (heat required for evaporation is 35MWh which corresponds to 2.2t/h of natural gas). Also in this case the electrical consumption is reported in detail in Table 7.6 and the total would be about 6.8MW, which means 2.4t/h CO_2 emissions. Total emissions from operating the process would be therefore 8.9t/h while CO_2 sequestered would be 13t/h.

Equipment unit	Electric consumption 80g/l	Electric consumption 120g/l
MVR compressor	7.3MW	4.9MW
Water pumps	1.6MW	1.4MW
Conveyors	100kW	100kW
Agitators	400kW	350kW
TOTAL	9.4MW	6.8MW

Table 7.6: Electric consumption for an industrial mineralization plant operating at 80g/l and 120g/l

7.3.3.2 Experimental CO_2 balance

The energy and CO_2 balance (Section 7.3) used in this chapter are based on the theoretical 100% maximum conversion efficiency. However, dissolution and carbonation efficiencies are not 100% and vary also with S/L ratio (Section 6.1), achieving about 75% after experiments employing steel slag at 15g/l S/L ratio. Therefore, in the case of mineralization at 15g/l, the efficiency penalty between experimental results and the maximum theoretical value is 25%. The industrial application of a mineral carbonation system in a steel plant presented in this chapter is designed to sequester 13t/h of CO_2, meaning that, due to the 75% experimental efficiency achieved, the value is reduced to 9.75t/h. Based on the experimental data presented in Section 6.1 for steel slag, trends of efficiency of carbonation at higher S/L ratio (120 and 240g/l) could be extrapolated (Figure 7.2). Extrapolation was based on the assumption that the trend of efficiency obtained from experiments (15, 25, 50g/l) continues at higher S/L ratios as seen previously [7.8] [7.9] [7.10].

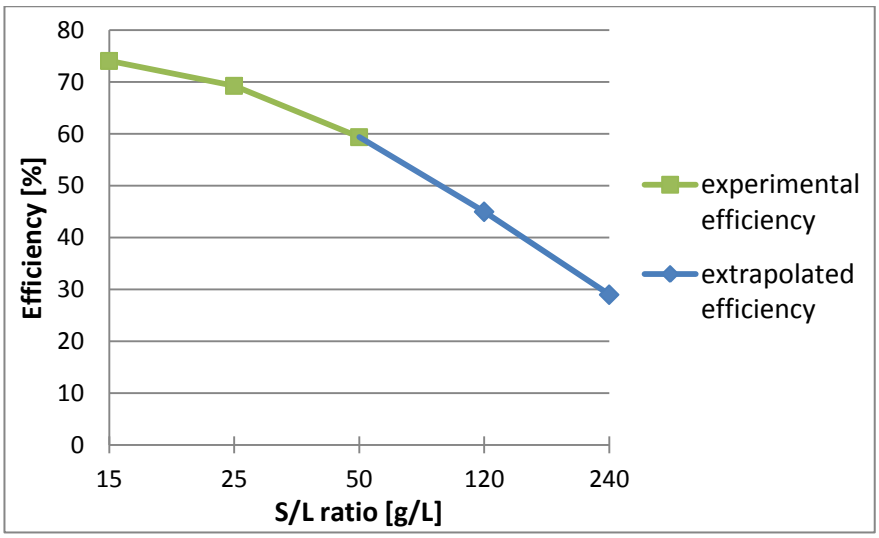

Figure 7.2: Experimental and extrapolated efficiency of carbonation for steel slag

S/L ratio range [g/l]	Values of carbonation efficiencies at different S/L ratio	Drop of carbonation efficiencies between different S/L ratio
	Experimental	
15-30	75-67%	8%
25-50	70-60%	10%
	Extrapolated	
30-60	67-57%	10%
60-120	57-45%	12%
120-240	45-30%	15%
240-480	30-11%	19%

Table 7.7: Details of the experimental and extrapolated efficiencies of carbonation for steel slag

Extrapolation of efficiencies of carbonation at 120 and 240g/L were carried out based on the following calculations, which are summarized in Table 7.7. Experimental efficiency reported in Figure 7.2 shows that carbonation efficiency for steel slag drops 8% when doubling the S/L ratio between 15 and 30g/l and the drop is 25% higher than 8% (therefore 10%) when doubling the S/L ration between 25 and 50g/l. Extrapolated data were based on the experimental evidences just presented, therefore, the drop of carbonation efficiency between 30 and 60g/l could be assumed still 10% and the drop between 60 and 120g/l should be 25% more than 10%, i.e. about 12% (carbonation efficiency drops from 57% at 60g/l to 45% at 120g/l). Finally, the drop of carbonation efficiency between 120 and 240g/l should be 25% more than 12%, i.e. 15%

(carbonation efficiency drops from 45% at 120g/l to 30% at 240g/l). The same reasoning applies for the case of doubled S/L ratio between 240 and 480g/l.

The theoretically maximum CO_2 sequestered (13t/h) at 120g/l, considering the experimental efficiency, would be reduced to 5.9t/h (45% of 13t/h) in the case of employing the mineralization process investigated, while the CO_2 emissions due to water evaporation and electrical consumption would still be 8.9t/h (as seen in Section 7.3.3.1). Therefore, the mineralization process would not be carbon negative at 120g/l, considering the experimental efficiency, as it is, instead, in the case of considering the process with 100% efficiency. At 240g/l carbonation efficiency would be 30% (Table 7.7), therefore 3.8t/h (30% of 13t/h) of CO_2 would be sequestered, while CO_2 emitted would be 4.4t/h (about 50% of the CO_2 emissions due to water evaporation and electrical consumption compared to the case at 120g/l) and the process would still be carbon positive (i.e. emitting more CO_2 than the amount sequestered during the process).

Considering the experimental results and extrapolations of carbonation efficiency presented in Figure 7.2 and Table 7.7, increasing the S/L ratio above 240g/l (30% efficiency) further reduces the efficiency of carbonation and the process cannot become carbon negative. Therefore, a carbon negative process would be achieved only if efficiency of carbonation was 34% (or above) at 240g/l. In fact, CO_2 captured would be 4.4t/h (34% of 13t/h), while the CO_2 emitted would be 4.4t/h. This value of efficiency could be obtained by raising the temperature of dissolution and carbonation, as presented in Section 6.2, where it was shown that increasing the temperature from 50 to 65°C resulted in an increased efficiency by 4%. According to these results, if the temperature of dissolution and carbonation for the mineralization system retrofitted to the steel plant is raised by 15°C, from 50 to 65°C for dissolution and from 65°C to 80°C for carbonation, efficiency of carbonation at 240g/l would achieve 34% (4% more than 30%). Therefore, when considering the efficiency of carbonation, the mineralization system applied to the steel plant would be carbon negative for S/L ratio of 240g/l or higher, with dissolution and carbonation temperature of 65°C and 80°C, respectively.

Considering dissolution and carbonation temperature of 65°C and 80°C, respectively, the efficiency of carbonation at 480g/l would be 15% (4% more than 11%, Table 7.6), while at 300g/l the efficiency would be 29%, as presented in Table 7.8. In fact, it can

assumed that one quarter of the 19% drop (i.e. 5%) between 34% at 240g/l and 15% at 480g/l happens between 240g/l and 300g/l.

S/L ratio [g/l]	Values of carbonation efficiencies
240	34%
300	29%
480	15%

Table 7.8: Details of the extrapolated efficiencies of carbonation with dissolution and carbonation temperature of 65°C and 80°C, respectively

In the case of mineralization process carried out at 300g/l and dissolution and carbonation temperature of 65°C and 80°C, respectively, CO_2 captured would be 3.7t/h (29% of 13t/h), while CO_2 emissions due to water evaporation and electric consumption would be 3.2t/h (one twentieth of the emissions calculated for the case of 15g/l, Section 7.3.3.1).

7.4 Cost estimation

7.4.1 Capital cost

The process reported in Figure 7.1 involves many operational units of equipment and the main ones are summarized below.

- Agitators/reactors: They are the units where the reactions of the process are held (mineral dissolution, pH adjustment and precipitation of the impurities, carbonation reaction, regeneration of additives, ammonia absorption, CO_2 capture) and because of the volumes of solution involved, parallel operations are foreseen in each step. The reactors are to be supplied with electricity to allow stirring the solution when required and they have a system of heat exchangers which enable the heat recovery from the exothermic reactions and to supply heat for the endothermic reactions.
- Water evaporator and condensation unit: They consist of a MVR evaporator supplied with natural gas and electricity for the compressor. The condensation unit, thanks to the heat exchangers, allows to cool down the steam and condense the water.

- Pumps: As seen in Section 7.3.2, they move the solutions from one step of the process to another and recirculate also the recovered streams of water and ammonia. Moreover, other pumps are needed for the lubricant and oil circuits and to move the liquids employed in the heat exchangers.
- Conveyors: Fresh steel slag and ammonium sulphate (recirculated and fresh) are moved thanks to electric conveyors for solid materials.

The capital cost of the designed process was calculated by considering the fixed-capital investment required for each separate functional unit. The functional unit may be identified as a unit operation, unit process, or separation method, which involves energy transfer or moving parts. For the mineralization process investigated there are 7 functional units, namely CO_2 capture, mineral dissolution, pH adjustment and precipitation of impurities, carbonation reaction, water evaporation, regeneration of additives, ammonia absorption.

Bridgwater developed a relatively simple correlation for plants that are predominantly liquid and/or solid phase handing processes [7.11]. The correlation equation for the year 2012 is [7.12]:

$$C = A \times N(\frac{Q}{s})^{0.675} \quad (7\text{-}2)$$

Where, C is the capital cost [£] in the year 2012, A is 1320, a coefficient which varies according to the year, N is the number of functional units, Q is the plant capacity [t/year] and s is the reactor conversion.

For the process with theoretical maximum efficiency the plant capacity would be 4Mt/year for 120g/l, N is 7 and s is 1 (100% conversion efficiency). Therefore, the estimated capital cost is £170M.

When taking into account the experimental efficiency, at 300g/l the capital cost can also be calculated using the Formula 7-2. The same parameters as in the theoretical maximum efficiency case, can be used, changing only Q, the plant capacity, to about 2Mt year and s to 0.84 (efficiency of the process at 300g/l is 0.29, therefore 7 single

units having 84% efficiency have a global efficiency of 29%). The estimated capital cost is then £190M.

7.4.2 Variable costs

7.4.2.1 Raw materials and energy costs

Estimations of the raw materials and energy costs calculated for the process with theoretical maximum efficiency for the case 120g/l S/L ratio are reported in Table 7.9. Unit costs reported refer to the current market situation in UK, while the quantities needed were presented previously (Section 7.3.3.1). The total raw materials and energy cost annualized are therefore (assuming 320 working days) £7.3M/year.

Material	Quantity	Unit cost [£]	Total [£/h]
Natural gas	33MWh	19.11 / MWh	630
Electricity	6MWh	50 / MWh	300
Water and ammonium sulphate integration	0.1t/h 1t/h	20 / t	20
TOTAL			**950**

Table 7.9: Raw materials and energy cost estimation for the designed carbonation process

When introducing the effect of the experimental efficiency on the mineralization process, considering S/L ratio of 300g/l the cost of the raw material and energy would be £3M/year.

7.4.2.2 Other costs

According to Coulson et al. other costs must be considered when evaluating the economic feasibility of a process [7.12]. In the case of process with theoretical maximum efficiency (120g/l) and for the process considering also the effect of the experimental efficiency (300g/l) these costs are reported in Table 7.10. These costs include mainly labor cost related to operation and maintenance cost, as well as capital charges and insurance and taxes. These values are usually calculated based on a fixed percentage value of the capital cost.

Item	Unit cost	Other costs for the process with theoretical maximum efficiency [£M/year]	Other costs for the mineralization process considering the experimental efficiency [£M/year]
Maintenance	5% capital cost	9.0	10.0
Operating labour	15% operating cost	1.5	1.5
Supervision	20% of operating labour	0.3	0.3
Laboratory costs	20% of operating labour	0.3	0.3
Plant overheads	50% of operating labour	0.7	0.8
Capital charges	10% of fixed capital	17.0	19.0
Insurance, local taxes and royalties	4% of fixed capital	6.8	7.6
TOTAL		**35.6**	**39.5**

Table 7.10: Other costs estimation for the designed carbonation process

The total amount of other costs is £35.6M/year for the process with theoretical maximum efficiency, while they are £39.5M/year when considering the experimental efficiency obtained for the process.

7.4.2.3 Total variable costs

The total variable cost for the process with theoretical maximum efficiency investigated, in the case of 120g/l, is £42.9M (£7.3M for raw material and energy and £35.6M of other costs). Consequently, each ton of CO_2 sequestered costs £430 (13t/h is equivalent to 0.1Mt/year, considering 320 working days). When considering the experimental efficiency of the process, the total variable costs are estimated to be £42.5M. Consequently, each ton of CO_2 sequestered would cost £1500 (CO_2 sequestered would be 3.7t/h which means 28.4kt/year). Therefore, the variable costs increased significantly from the case with theoretical maximum efficiency to the case when the efficiency of the process is considered.

A previous cost evaluation for mineralization of steel slag was carried out by Huijgen et al. in 2007 [7.13]. According to their study, variable costs for sequestering CO_2 in their single-step process were 77€/tCO_2 (£65/tCO_2). The substantial difference in costs

between the process studied in this work and the one studied by Huijgen et al. is due to the type of the processes employed (multi-step vs single-step) and the cost evaluation approach (HSC and Coulson's cost analyses vs ASPEN). However, another substantial difference is the S/L ratio considered for the cost analyses, 2kg/l for Huijgen et al. [7.13] compared to 120g/l and 300g/l in the process studied in this thesis. This last parameter has a huge impact on the cost evaluation, as seen in this chapter, because it influences the amount of water employed, and therefore, the heat required for its evaporation. If 2kg/l is reasonable for a single-step process, pumping such dense solutions from one reactor to the other in a multi-step process is not feasible (i.e. damage/corrosion of the facilities/equipment used in the process).

7.5 Conclusions

This chapter presented the mass and energy balance for the overall mineralization process in the case of sequestering 13t/h of CO_2 from a steel plant producing 43t/h of steel slag and employing a S/L ratio of 15g/l. Because of the close loop, the impact of the quantity of NH_4HSO_4 and H_2O needed to be fed continuously into the system is small (1t/h for H_2O, and 0.3t/h for NH_4HSO_4).

Heat released from mineral dissolution, pH adjustment and precipitation of impurities, carbonation reaction and CO_2 capture is 2.3MWh/tCO_2 and could be recovered using heat exchangers and reused within the mineralization process to heat-up the incoming streams of steel slag, ammonium sulphate and water. Heat required, mainly from water evaporation and regeneration of additives, is instead 20MWh/tCO_2 and it causes, together with electric consumption of compressors, pumps, conveyors and agitators, CO_2 release of about 65t/h. Therefore, the process is carbon positive, i.e. emits more CO_2 than the amount sequestered.

Increasing the S/L ratio decreases the heat and electricity required from the mineralization system. The process with theoretical maximum efficiency results carbon negative when S/L ratio is 80g/l or higher. For the case of 120g/l, capital cost of the process would be around £170M while annual variable costs £43M (£430/t$CO_{2\ sequestered}$). However, if experimental data are introduced in the cost evaluations, efficiency of the process decreases significantly. It was found that the process would be carbon negative when the S/L ratio is 240g/l or higher. Consequently, costs raise to £190M for capital cost and £1500/t$CO_{2\ sequestered}$ for variable costs. A cost

evaluation of a mineralization process employing steel slag was carried out by Huijgen et al. in 2007 [7.13]. In their work the mineralization of steel slag employing a single-step process costs £65/tCO_2. However, such difference in costs compared to the ones obtained from the process analyzed in this chapter is mainly due to the different processes employed (single-step and multi-step), the value of the S/L ratio and the different method for cost evaluation.

As reported in the literature review (Section 2.2.4), there are only a few cost evaluations for mineral carbonation employing mineral rocks. The current cost ranges between £75-110/tCO_2, therefore much cheaper compared to the costs of the process investigated in this work. The mineralization route analysed in this chapter is still uneconomic and needs further research, especially in reducing the energy required for the evaporation of water. Moreover, as seen in Section 2.1.2, cost of CCS geological storage is about £50-75/tCO_2, and thus, the mineral carbonation process investigated is much more expensive compared to CCS geological storage. However, it should be noted that, as already mentioned in Section 4.10, certain waste materials produced close to large CO_2 emitters could be employed for mineral carbonation although this would be a niche market using relatively small amounts of waste materials. Mineral carbonation in fact, does not aim to be in competition with CCS geological storage.

7.6 References

[7.1] IEA. CO_2 emissions from fuel consumption: 2011 Highlights. Paris - France: IEA-International Energy Agency; 2011.

[7.2] GEA process engineering. http://www.niroinc.com/html/evaporator/evpdfs/evap_mech_vapor_recomp.pdf. Date of consultation: February 2013.

[7.3] Teir S, Eloneva S, Fogelholm C-J, Zevenhoven R. Fixation of carbon dioxide by producing hydromagnesite from serpentinite. Applied Energy. 2009;86:214-8.

[7.4] Gerdemann SJ, O'Connor WK, Dahlin DC, Penner LR, Rush H. Ex Situ Aqueous Mineral Carbonation. Environmental Science & Technology. 2007;41:2587-93.

[7.5] Torishima pumps. http://www.torishima.co.jp/en/pdf/products/cdm600.pdf. Date of consultation: February 2013.

[7.6] Zenith mining and construction machinery. http://www.crusherdealers.com/applications/canada/conveyor-belt-manufacturer-canada.html. Date of consultation: February 2013.

[7.7] Zhenghou Xinguang mining machinery manufacturing. http://www.alibaba.com/product-gs/547751301/Low_consumption_cheap_mine_Machine_Agitator.html. Date of consultation: February 2013.

[7.8] Zevenhoven R, Wiklund A, Fagerlund J, Eloneva S, In't Veen B, Geerlings H et al. Carbonation of calcium-containing mineral and industrial by-products. Frontiers of Chemical Engineering in China. 2010;4:110-9.

[7.9] Huijgen WJJ, Witkamp G-J, Comans RNJ. Mechanisms of aqueous wollastonite carbonation as a possible CO_2 sequestration process. Chemical Engineering Science. 2006;61:4242-51.

[7.10] Jo HY, Kim JH, Lee YJ, Lee M, Choh S-J. Evaluation of factors affecting mineral carbonation of CO_2 using coal fly ash in aqueous solutions under ambient conditions. Chemical Engineering Journal. 2012;183:77-87.

[7.11] Bridgwater A. A new guide to capital cost estimation. London: Institution of Chemical Engineers, IChemE; 1988.

[7.12] Coulson JM, Richardson JF, Sinnot RK. Coulson and Richardson's Chemical Engineering: Chemical Engineering Design. Oxford - UK: Elsevier; 1999.

[7.13] Huijgen WJJ, Comans RNJ, Witkamp G-J. Cost evaluation of CO_2 sequestration by aqueous mineral carbonation. Energy Conversion and Management. 2007;48:1923-35.

CHAPTER 8 – CONCLUSIONS AND FUTURE WORK

8.1 Conclusions

The aim of this thesis was to to determine the potential use of waste materials as feedstock for permanent sequestration of CO_2. The technical feasibility and costs of a novel mineralization process, for several suitable feeding materials, was investigated. This chapter summarizes the main findings of the thesis, following the order they were presented.

Carbon dioxide capture and storage by mineralization has been increasingly popular among researchers due to the slow deployment of underground storage and the technical/economical barriers in some areas for this option. Mineral carbonation, however, suffers from several drawbacks, mainly pre-treatment energy requirement and slow reaction rates. This thesis has proposed a novel multi-step pH swing mineralization process suitable for waste materials rich in calcium to precipitate calcium carbonate. The process employs ammonium carbonate, $(NH_4)_2CO_3$, obtained from the capture of CO_2 in NH_3 instead of direct CO_2 carbonation. This work, firstly, investigated the availability and potential CO_2 storage capacity of suitable waste materials for mineral carbonation in UK (Chapter 4). Afterwards, analyses were focused on understanding the mechanisms of dissolution of the first step of the novel mineralization process, employing four different wastes as feedstocks (Chapter 5). The effect on the efficiency of carbonation of several parameters was investigated and mechanisms of carbonation were also discussed (Chapter 6). Finally, the costs of implementing the multi-step process in a steel production plant were investigated (Chapter 7).

8.1.1 Waste materials for mineral carbonation in UK

The availability of suitable materials which could be employed as feedstock was investigated. It was reported that a variety of inorganic waste streams are potential feedstock for mineralisation in the UK. The waste streams identified in this thesis include recycled concrete aggregate, steel slag, ground granulated blast furnace slag, pulverised fuel ash including oil shale pulverised ash, incinerator bottom ash, air pollution control residue, cement kiln dust, incinerator sewage sludge ash, paper sludge ash and biomass ash.

It was found that mineral waste resources, suitable for mineralization in the UK, are mainly re-used for low-end applications to avoid landfill disposal costs and the aggregate levy in the case of primary aggregate production for the construction industry. Therefore, only a small fraction of these wastes are nowadays available with a capture potential of 1Mt/year of the annual UK emissions, which are estimated being about 490Mt. The location of the mineral waste is widely distributed across the UK, and in many of the cases, the waste resource is located very close to the CO_2 emitters. For instance, steel and cement works and incinerators represent the ideal locations for the application of this technology considering that CCS by geological storage mainly targets large power emitters. Consequently, the use of waste resources for mineral carbonation should be considered as a niche market that could utilise relatively small amounts of feed materials for mineralization.

8.1.2 Suitable waste materials and dissolution mechanisms

A novel closed-loop, multi-step process which allows precipitation of calcium carbonate from Ca-rich waste streams was investigated in this thesis, as this route was not studied before using such feedstocks. This multi-step mineralization process includes five main steps: i) mineral dissolution, ii) pH adjustment iii) precipitation of impurities, iv) carbonation reaction, and v) regeneration of additives. Samples of nine suitable waste materials were collected and their chemical and mineral phases composition were analyzed. The materials investigated included recycled concrete aggregate, cement kiln dust, ground granulated blast furnace slag, pulverized fuel ashes, incinerator sewage sludge ashes, steel slag, phosphorus slag, water and air cooled copper smelt slag. Based on the mineral phases present (i.e. low content of calcium carbonate) and chemical composition (i.e. highest CaO content), four samples (i.e. steel slag, ground granulated blast furnace slag, phosphorus slag and recycled concrete aggregate) were selected as the most suitable for mineral carbonation experiments. The first step (mineral dissolution) of the examined mineralization process was studied, including understanding the mechanisms of dissolution.

For the steel slag and recycled concrete aggregate samples, dissolution kinetic analyses were conducted based on standard models available in literature, XRD and SEM. Results obtained from the dissolution of steel slag indicated that calcium precipitated as solid crystals of calcium sulphate while Mg and Fe dissolved into a solution of NH_4HSO_4. Kinetic analyses for steel slag showed that the combination of product layer

diffusion and chemical reaction control fits well the experimental results. Employing the Arrhenius' law, the calculated activation energy was 2.3kJ/mol. Comparison between dissolution of serpentine (from a previous paper) and steel slag, under the same experimental conditions, showed that it is easier to extract metals (e.g. iron) from steel slag rather than from serpentine, since SS activation energy is lower than serpentine and iron dissolved into solution achieved 90 and 80% for steel slag and serpentine, respectively. This could be linked to the diverse mineral phases forming the two materials, including differences in chemical and physical nature of iron present.

Recycled concrete aggregate also dissolved into NH_4HSO_4 extracting calcium and precipitating it as calcium sulphate while the other main metals present, aluminium, dissolved partially (40% after experiment at 25°C) into solution. Recycled concrete aggregate showed a dissolution process similar to steel slag, with calcium precipitating as solid crystals of calcium sulphate and the combination of product layer diffusion and chemical reaction control mechanism fitting well the experimental results. Activation energy for RCA calculated thanks to the experimental results was 0.9kJ/mol.

For ground granulated blast furnace slag and phosphorus slag, instead, solutions became dense and viscous causing unreliable trends of dissolution, due to the formation of silica gel during the dissolution experiments. In this case, precipitation of calcium sulphate crystals was investigated employing only XRD and SEM. It was observed that dissolution of ground granulated blast furnace slag and phosphorus slag in NH_4HSO_4 produced solid crystals of precipitated calcium sulphate (as during dissolution of recycled concrete aggregate and steel slag). Evidences from XRD and SEM studies for ground granulated blast furnace slag and phosphorus slag showed that the quantity of calcium sulphate crystals increased when reducing the S/L ratio from 50 to 25g/l and the time of dissolution from 5 to 3h.

8.1.3 Mineral carbonation from metal waste

The effect of several parameters on the efficiency of carbonation was investigated, including assessing the best operational conditions in terms of S/L ratio, temperature, particle size. The main steps of the complete mineralization process (mineral dissolution, adjustment of pH with precipitation of impurities and carbonation reaction) were tested at different S/L ratio, temperature and particle size for three metal slags, namely steel slag, phosphorus slag and ground granulated blast furnace slag.

The carbonation efficiencies increased with decreasing CaO content in the samples. Experiments achieved 74%, 67% and 59% efficiency of carbonation for steel slag, ground granulated blast furnace slag and phosphorus slag, respectively. Carbonation efficiency of phosphorus slag resulted about the same as that obtained from a similar process employing serpentine (25% at 50g/l) while steel slag and ground granulated furnace slag achieved higher values, 60 and 30%, respectively. This confirmed the fact that wastes employed for mineral carbonation achieve higher efficiencies of carbonation, compared to natural rocks. In fact, in multi-step processes, efficiency of carbonation is mainly affected by the metals extraction during the first phase of the experiments. Therefore, as seen when investigating the dissolution step, it is easier to extract metals from the mineral structure of waste streams (e.g. steel slag) than from natural rocks (e.g. serpentine). Further XRD analyses on the carbonated products showed that the main phases identified in the carbonated samples were $CaCO_3$ and residual hydrated calcium sulphate ($CaSO_4 \cdot 2H_2O$). XRF studies showed reduced SO_3 content in samples after experiments at lower S/L ratio, because of higher production of $CaCO_3$, supporting the observations on the trends of carbonation efficiencies (i.e. higher efficiency at lower S/L ratio).

It was found that temperature affects differently efficiencies of carbonation for the three metal wastes. When the experimental temperature for dissolution and carbonation was increased between 40 to 65°C, the efficiency of carbonation raised for steel slag (up to 72%). For PS the efficiency, instead, only increased between 40 and 50°C (up to about 55%) and then it remained constant till 65°C. Ground granulated blast furnace slag behaved like phosphorus slag with the only difference that efficiency of carbonation rose from 30 to 40°C (up to about 65%) and then it levelled for temperatures up to 65°C. Because efficiency of carbonation in multi-step mineralization processes is primarily affected by the calcium extraction conditions during the first phase of the experiments, the behaviour and different values of efficiency of carbonation for steel slag, phosphorus slag and ground granulated blast furnace slag are probably related to the effect of the temperature during the first step of the process. The extraction of calcium from the mineral structure of the raw material could increase with the temperature, raising the efficiency of carbonation. However, calcium extraction reaches a plateau at a certain temperature, and the efficiency of carbonation does not raise more. Previous studies on different materials (wollastonite, steel slag, serpentine) also demonstrated this trend of reduced influence of the temperature on the

dissolution/carbonation efficiency as soon as the temperature is raised [8.1] [8.2] [8.3]. The three waste materials investigated in this thesis have different mineral structures (Appendix A), and therefore, also their behavior during the experiments is different. In fact, as seen when comparing the dissolution step of steel slag and serpentine, depending on the mineral phases forming the different wastes, the extraction of metals (i.e. the efficiency of carbonation) could vary.

Efficiencies of carbonation for two of the metal wastes decreased when the particle size increased. In fact, it was noticed that increasing the particle size from 75-150μm to 150-300μm lowers the efficiency for both steel slag and phosphorus slag from 68% to 61% and from 50% to 45%, respectively. This is because larger specific surface area for reactions is available in smaller particles compared to the ones with bigger size.

Tests investigating a pilot scale experimental rig with a scaling-up factor of 6 were also reported and it was demonstrated that the efficiency of carbonation remains the same (within the experimental error) during the small and pilot scale experiments. This means that there are not scaling-up factors able to affect the process, at least when the scaling-up factor is up to 6, suggesting that the reaction mechanisms governing the different steps of the mineralization process are the same.

8.1.4 Mass, energy and CO_2 balances and cost evaluation in a real case scenario

The laboratory studies conducted allowed investigating and understanding the mechanisms of dissolution and carbonation of the process and to analyze the effect on the efficiency of carbonation of several parameters. The cost evaluation of the technology applied to a steel plant was then studied considering mass, energy and CO_2 balances of all the steps of the process. The steel plant considered for the calculations produces 43t/h of steel slag and the mineralization plant considered would sequester 13t/h of CO_2.

The thermal and electrical energy required for the process, mainly coming from water evaporation and regeneration of additives, compressors, pumps, conveyors and agitators, cause CO_2 emissions. Therefore, it was found that the process with theoretical maximum efficiency results carbon negative (i.e. storing more CO_2 than the amount emitted during the process) when S/L ratio is 80g/l or higher. Introducing the

experimental data (i.e. efficiency of carbonation obtained from the experiments) the mineralization process applied to a steel plant results carbon negative when S/L ratio is 240g/l or higher.

In the case of process with theoretical maximum efficiency, with S/L ratio of 120g/l, capital cost of the mineralization plant would be around £170M with annual variable costs of £43M, resulting in a cost of £430/$tCO_{2\ sequestered}$. However, if experimental data are introduced in the cost evaluations, efficiency of the process decreases significantly and consequently costs raise to £190M for capital cost and £1500/$tCO_{2\ sequestered}$ for variable costs.

The economic evaluation of the mineralization process applied to an existing steel plant resulted more expensive compare to a previous study carried out by Huijgen et al. on the cost of a mineralization process employing steel slag (£65/tCO_2 [8.4]). The substantial difference in costs between the process studied in this work and the one studied by Huijgen et al. is due to the type of the processes employed (multi-step vs single-step) the different S/L ratio and the approach for the cost evaluation (HSC and Coulson's cost analyses vs ASPEN).

8.2 Future work

Based on the results and conclusion of this thesis, to continue developing the mineralization process described, there are several areas worth to be further investigated, as described below.

- The studies on the mineral dissolution step of the process showed that crystals of calcium sulphate are formed from the dissolved calcium into solution and then they react with the ammonium carbonate during the carbonation reaction. It was clear that producing more crystals of calcium sulphate increases the carbonation efficiency. Therefore, it could be interesting to investigate how to improve the precipitation of calcium sulphate.
- Since the experiments were carried out in a reactor consisting in a 500ml, 3 necks glass flask, research into different reactor set-up (e.g. fluidized bed), to assess any improvement in the achieved efficiency of carbonation, could be a path for improving the process. It would also be usefull for the future development of the

process to investigate the potential of using a continuous process instead of batch reactor to reduce the reaction time.

- This thesis did not investigate the post-processing of the carbonated products obtained. Therefore, to further assess the economy of the process (i.e. the market potential of the final products and the potential income which they could generate), it is required to research on the separation techniques which could split the different phases present in the final carbonated products. Moreover, the potential presence of hazardous substances (e.g. heavy metals) should be considered and appropriate removal techniques investigated.

8.3 References

[8.1] Zevenhoven R, Wiklund A, Fagerlund J, Eloneva S, In't Veen B, Geerlings H et al. Carbonation of calcium-containing mineral and industrial by-products. Frontiers of Chemical Engineering in China. 2010;4:110-9.

[8.2] Huijgen W, Witkamp G, Comans R. Mineral CO_2 sequestration by steel slag carbonation. Environmental Science & Technology. 2005;39:9676-82.

[8.3] Teir S, Revitzer H, Eloneva S, Fogelholm C-J, Zevenhoven R. Dissolution of natural serpentinite in mineral and organic acids. International Journal of Mineral Processing. 2007;83:36-46.

[8.4] Huijgen WJJ, Comans RNJ, Witkamp G-J. Cost evaluation of CO_2 sequestration by aqueous mineral carbonation. Energy Conversion and Management. 2007;48:1923-35.

APPENDIX A - XRD PATTERNS FROM SAMPLE CHARACTERIZATION

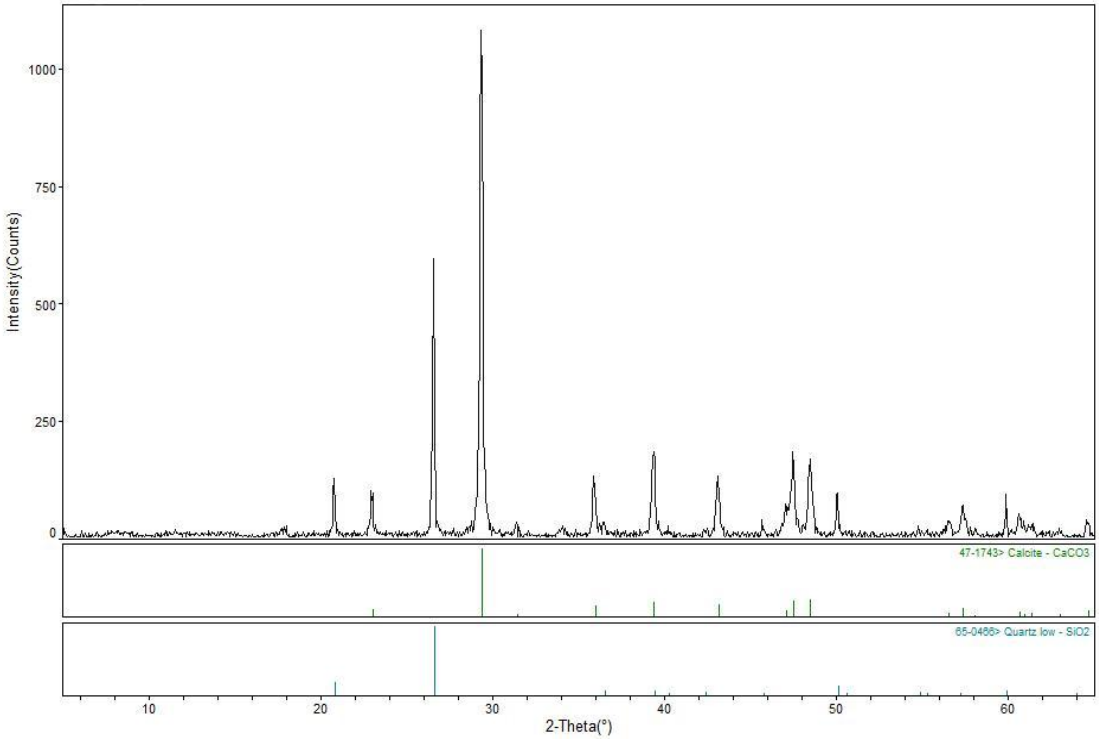

Figure A1.1: XRD pattern for RCA

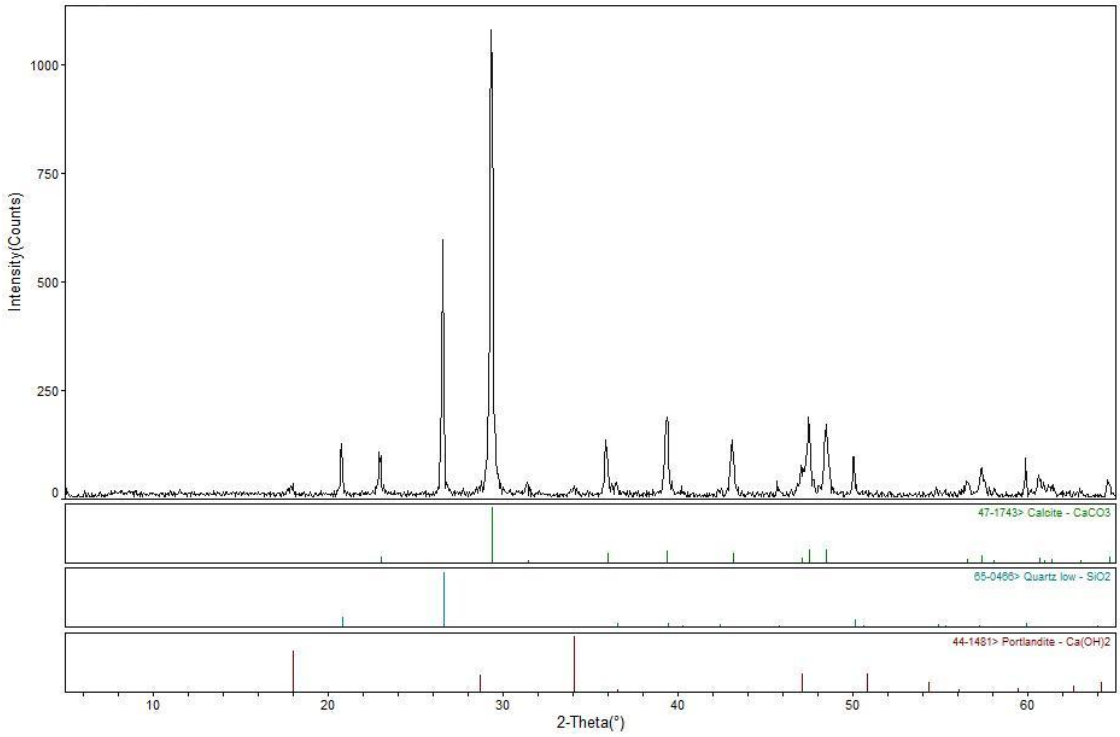

Figure A1.2: Higher resolution XRD for RCA (scan speed of 1 degree 2-theta per minute, 0.02 step size)

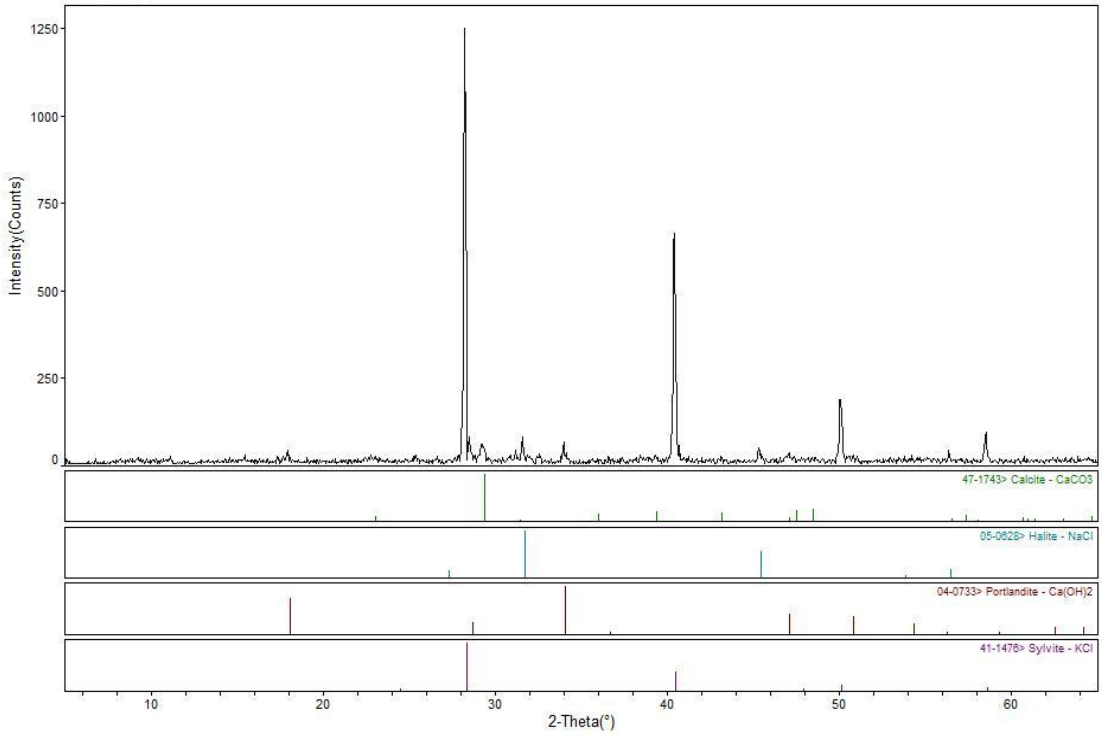

Figure A1.3: XRD pattern for CKD

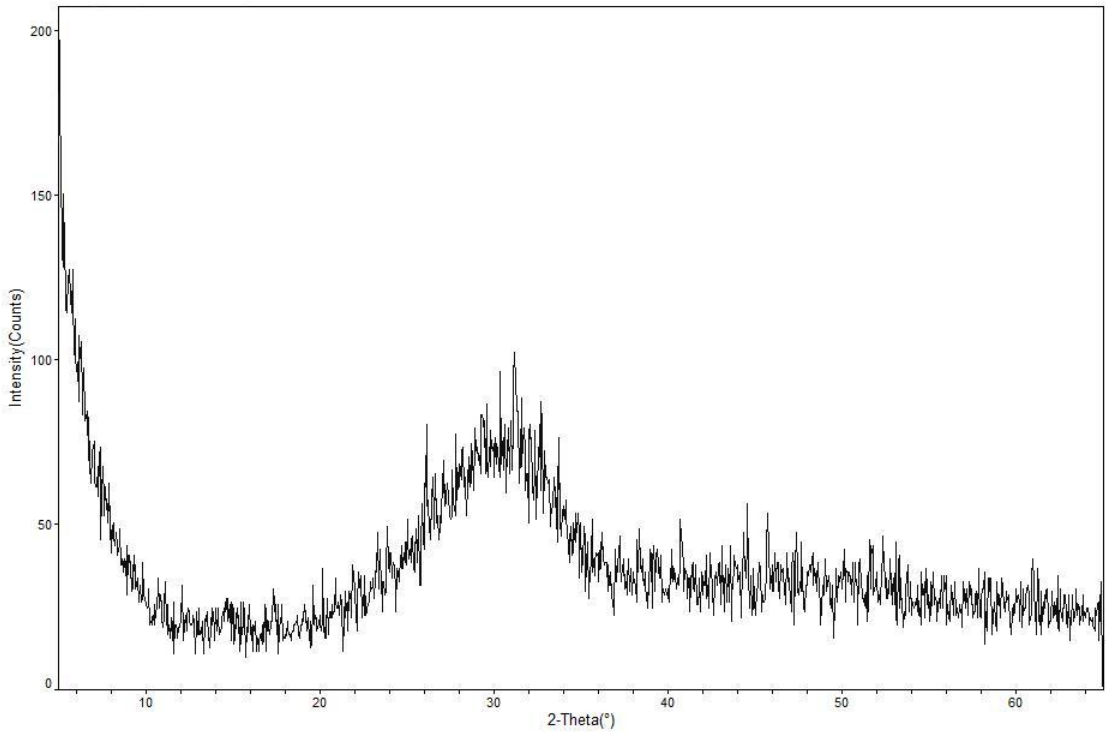

Figure A1.4: XRD pattern for GGBS

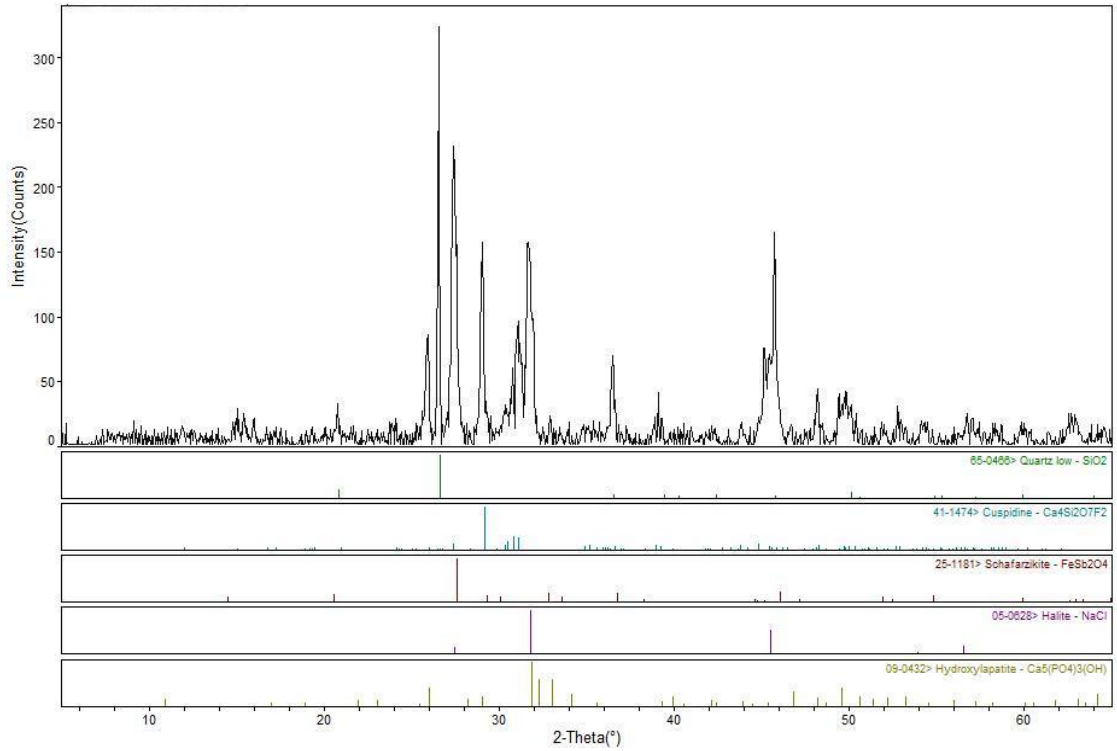

Figure A1.5: XRD pattern for PS

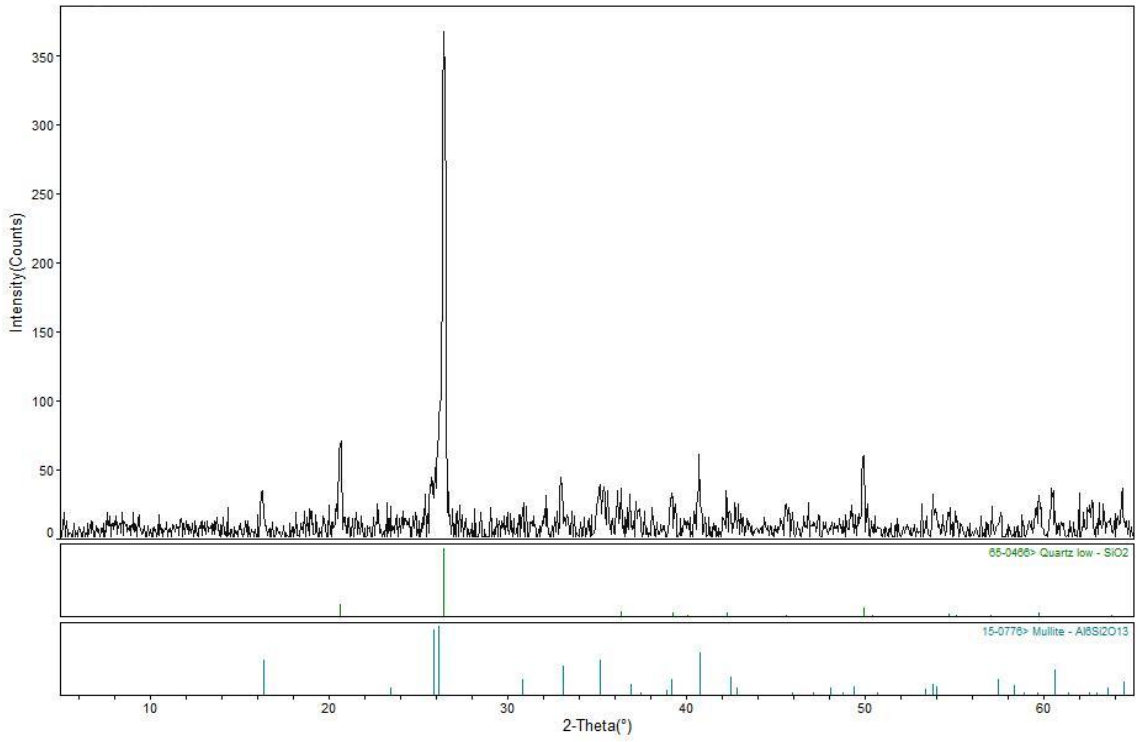

Figure A1.6: XRD pattern from PFA

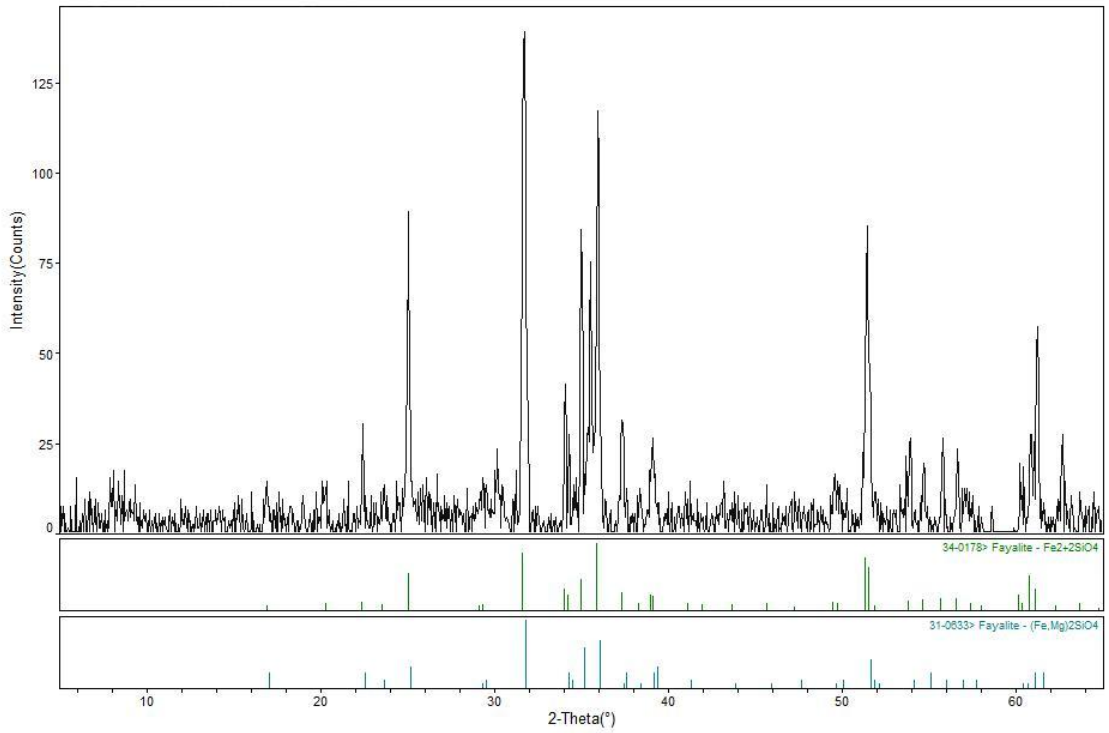

Figure A1.7: XRD pattern for air-cooled CSS

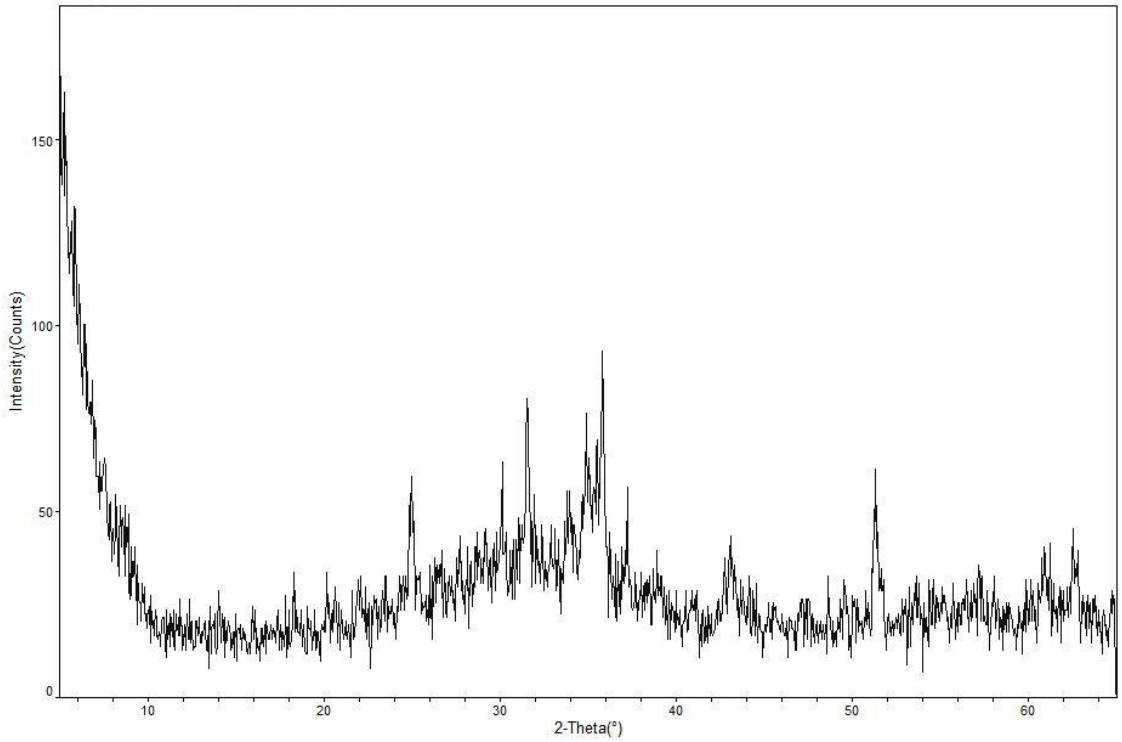

Figure A1.8: XRD pattern for water-cooled CSS

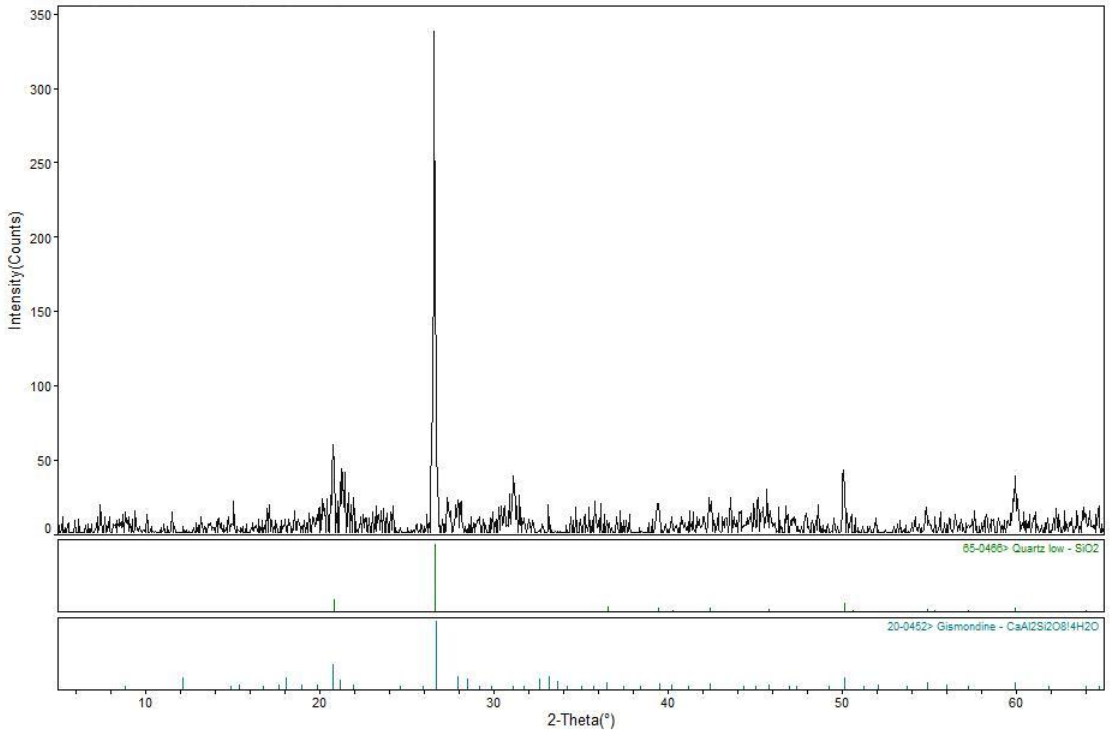

Figure A1.91: XRD pattern for ISSA

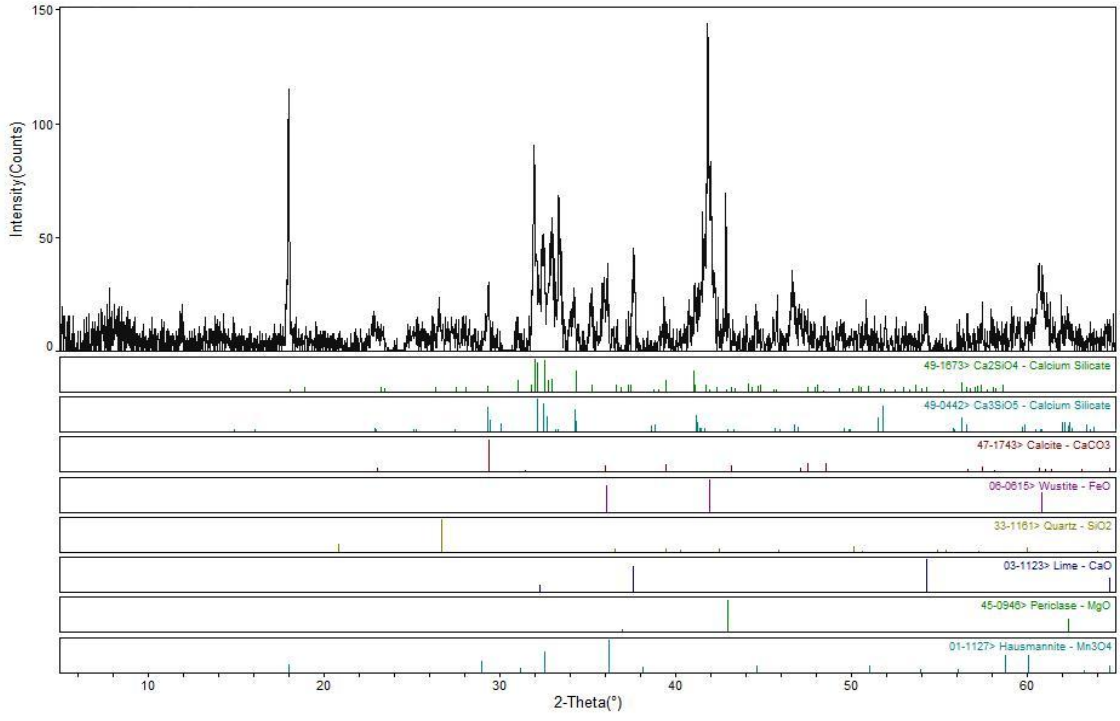

Figure A1.10: XRD pattern for SS

APPENDIX B – MASS AND ENERGY BALANCE FOR THE MINERALIZATION PROCESS APPLIED TO A STEEL PLANT

Mass balance for the mineralization process applied to a steel plant

Carbonation reaction

$CaSO_4 + (NH_4)_2CO_3 = CaCO_3 + (NH_4)_2SO_4$

Formula	Molecular weight	Amount	Amount
	g/mol	mol	g
$CaSO_4$	136.138	1	136.138
$(NH4)_2CO_3$	96.086	1	96.086
	g/mol	mol	g
$CaCO_3$	100.089	1	100.089
$(NH4)_2SO_4$	132.134	1	132.134

1t $(NH_4)_2CO_3$ produces 100.089/96.086=1.04t $CaCO_3$ and requires 136.138/96.086=1.42t $CaSO_4$

28.6t/h $(NH_4)_2CO_3$ require 40.6t/h of $CaSO_4$

28.6t/h $(NH_4)_2CO_3$ produce 29.7t/h $CaCO_3$ and 39.3t/h $(NH_4)_2SO_4$

Mineral dissolution

$CaSiO_3 + 2NH_4HSO_4 = CaSO_4 + SiO_2 + H_2O + (NH_4)_2SO_4$

Formula	Molecular weight	Amount	Amount
	g/mol	mol	g
$CaSiO_3$	116.164	1	116.164
NH_4HSO_4	115.104	2	230.208
	g/mol	mol	g
$CaSO_4$	136.138	1	136.138
SiO_2	60.084	1	60.084
H_2O	18.015	1	18.015
$(NH_4)_2SO_4$	132.134	1	132.134

1t $CaSO_4$ requires 116.164/136.138=0.85t $CaSiO_3$

40.6t/h of $CaSO_4$ require 34.5t/h $CaSiO_3$

40.6t/h of $CaSO_4$ require 2*(115.104/136.138)*40.6=68.7t/h NH_4HSO_4

Calculation of the amount of $(NH_4)_2SO_4$ produced from dissolution of Ca: 34.5t/h $CaSiO_3$ are fed therefore 34.5*132.1/116.2=39.2t/h

Calculation of the amount of SiO_2 produced from dissolution of Ca: 36.0t/h $CaSiO_3$ are fed therefore 34.5*60.08/116.164=17.8t/h

Calculation of the amount of H_2O produced from dissolution of Ca: 34.5t/h $CaSiO_3$ are fed therefore 34.5*18.015/116.164=5.35t/h

From the analyses on the steel slag saple (Chapter 5, Table 5.2) it contains 38.44% CaO=>Ca=38.4(40/(40+16))=27.43%.

$CaSiO_3$ employed in the dissolution step is 34.5t/h this means that Ca content= 34.5*(40/(40+28+16*3))=11.9t/h

Steel slag required is threfore 11.9/0.274=42.9t/h

MgO content in steel slag is 8.96% (Chapter 5, Table 5.2)
Mg content=8.96(24/(24+16)=5.37%

Fe_2O_3 content in steel slag is 22.53% (Chapter 5, Table 5.2)
Fe content=22.53(56*2/(16*3+56*2))=15.8%

Al_2O_3 content in steel slag is 2.74% (Chapter 5, Table 5.2)
Al content=2.74(27*2/(16*3+27*2))=1.45%.

Apart from $CaSiO_3$, assuming that all the remaining 42.9-34.5=8.4t/h in the steel slag are formed by $MgSiO_3$, $FeSiO_3$, Al_2SiO_5

The amoun of $MgSiO_3$ in steel slag is (5.37/(5.37+15.8+1.45))*8.4=2.0t/h

The amount of $FeSiO_3$ in steel slag is (15.8/(5.37+15.8+1.45))*8.4=5.9t/h

The amount of Al_2SiO_5 in steel slag is (1.45/(5.37+15.8+1.45))*8.4=0.5t/h

The dissolution reaction for $MgSiO_3$ is:

$MgSiO_3 + 2NH_4HSO_4 = MgSO_4 + SiO_2 + H_2O + (NH_4)_2SO_4$

Formula	Molecular weight	Amount	Amount
	g/mol	mol	g
$MgSiO_3$	100.389	1	100.389
NH_4HSO_4	115.104	2	230.208
	g/mol	mol	g
$MgSO_4$	120.363	1	120.363
SiO_2	60.084	1	60.084
H_2O	18.015	1	18.015
$(NH_4)_2SO_4$	132.134	1	132.134

1t $MgSiO_3$ produces 120.363/100.389=1.2t $MgSO_4$

Therefore from 2.0t/h $MgSiO_3$, 2.4t/h $MgSO_4$ are produced

2.0t/h $MgSiO_3$ require 2*(115.104/100.389)*2.0=4.6t/h NH_4HSO_4

Amount of SiO_2 produced from dissolution of Mg: 2.0t/h $MgSiO_3$ are fed therefore 2.0*60.08/100.389=1.2t/h

Amount of H_2O produced from dissolution of Mg: 2.0t/h $MgSiO_3$ are fed therefore 2.0*18.015/100.389=0.36t/h

Amount of $(NH_4)_2SO_4$ produced from dissolution of Mg: 2.0t/h $MgSiO_3$ are fed therefore 2.0*132.134/100.389=2.6t/h $(NH_4)_2SO_4$

The dissolution reaction for $FeSiO_3$ is:

$FeSiO_3 + 2NH_4HSO_4 = FeSO_4 + SiO_2 + H_2O + (NH_4)_2SO_4$

Formula	Molecular weight	Amount	Amount
	g/mol	mol	g
$FeSiO_3$	131.931	1	131.931
NH_4HSO_4	115.104	2	230.208
	g/mol	mol	g
$FeSO_4$	151.905	1	151.905
SiO_2	60.084	1	60.084
H_2O	18.015	1	18.015
$(NH_4)_2SO_4$	132.134	1	132.134

1t $FeSiO_3$ produces 151.905/131.931=1.15t $FeSO_4$

Therefore from 5.9t/h $FeSiO_3$, 6.8t/h $FeSO_4$ are produced.

5.9t/h $MgSiO_3$ require 2*(115.104/131.931)*5.9=10.3t/h NH_4HSO_4

Amount of SiO_2 produced from dissolution of Fe: 5.9t/h $FeSiO_3$ are fed therefore 5.9*60.08/131.931=2.7t/h

Amount of H_2O produced from dissolution of Fe: 5.9t/h $FeSiO_3$ are fed therefore 5.9*18.015/131.931=0.81t/h

Amount of $(NH_4)_2SO_4$ produced from dissolution of Fe: 5.9t/h $FeSiO_3$ are fed therefore 5.9*132.134/131.931=5.9t/h $(NH_4)_2SO_4$

The dissolution reaction for Al_2SiO_5 is:

$Al_2SiO_5 + 6NH_4HSO_4 = Al_2(SO_4)_3 + SiO_2 + 3H_2O + 3(NH_4)_2SO_4$

Formula	Molecular weight	Amount	Amount
	g/mol	mol	g
Al_2SiO_5	162.046	1	162.046
NH_4HSO_4	115.104	6	690.623
	g/mol	mol	g
$Al_2(SO_4)_3$	342.136	1	342.136
SiO_2	60.084	1	60.084
H_2O	18.015	3	54.046
$(NH_4)_2SO_4$	132.134	3	396.403

1t Al_2SiO_5 produces 342.136/162.136=2.11t $Al_2(SO_4)_3$

Therefore from 0.5t/h Al_2SiO_5, 1.1t/h $Al_2(SO_4)_3$ are produced

0.5t/h Al_2SiO_5 require 6*(115.104/162.046)*0.5=2.1t/h NH_4HSO_4

Amount of SiO_2 produced from dissolution of Al: 0.5t/h Al_2SiO_5 are fed therefore 0.5*60.08/162.046=0.37t/h

Amount of H_2O produced from dissolution of Al: 5.9t/h Al_2SiO_5 are fed therefore 0.5*(18.015/162.046)*3=0.17t/h

Amount of $(NH_4)_2SO_4$ produced from dissolution of Al: 0.5t/h Al_2SiO_5 are fed therefore 0.5*(132.134/162.046)*3=1.22t/h $(NH_4)_2SO_4$

The total amount of NH_4HSO_4 required for the disslution step is therefore 2.1+10.3+4.6+68.7=85.7t/h

The total amount of $(NH_4)_2SO_4$ produced during the dissolution step is 1.22+5.9+2.6+39.2=48.9t/h

pH adjustment and precipitation of impurities

$MgSO_4 + 2NH_4OH = Mg(OH)_2 + (NH_4)_2SO_4$

Formula	Molecular weight	Amount	Amount
	g/mol	mol	g
$MgSO_4$	120.363	1	120.363
NH_4OH	35.046	2	70.091
	g/mol	mol	g
$Mg(OH)_2$	58.32	1	58.32
$(NH_4)_2SO_4$	132.134	1	132.134

2.4t/h $MgSO_4$ require 2*(35.046/120.363)*2.4=1.4t/h NH_4OH

2.4t/h $MgSO_4$ produce 58.32/120.363*2.4=1.16t/h $Mg(OH)_2$ and 2.6t/h $(NH_4)_2SO_4$

$FeSO_4 + 2NH_4OH = Fe(OH)_2 + (NH_4)_2SO_4$

Formula	Molecular weight	Amount	Amount
	g/mol	mol	g
$FeSO_4$	151.905	1	151.905
NH_4OH	35.046	2	70.091
	g/mol	mol	g
$Fe(OH)_2$	89.862	1	89.862
$(NH_4)_2SO_4$	132.134	1	132.134

6.8t/h $FeSO_4$ require 2*(35.046/151.905)*6.8=3.14t/h NH_4OH

6.8t/h $FeSO_4$ produce 89.86/151.905*6.8=4.02t/h $Fe(OH)_2$ and 5.9t/h $(NH_4)_2SO_4$

$Al_2(SO_4)_3 + 6NH_4OH = 2Al(OH)_3 + 3(NH_4)_2SO_4$

Formula	Molecular weight	Amount	Amount
	g/mol	mol	g
$Al_2(SO_4)_3$	342.136	1	342.136
NH_4OH	35.046	6	210.274
	g/mol	mol	g
$Al(OH)_3$	78.003	2	156.007
$(NH_4)_2SO_4$	132.134	3	396.403

1.1t/h $Al_2(SO_4)_3$ requires 6*(35.046/342.136)*1.1=0.68t/h NH_4OH

1.1t/h $Al_2(SO_4)_3$ produces 2*(78/342.136)*1.1=0.50t/h $Al(OH)_3$ and 1.27t/h $(NH_4)_2SO_4$

The total amount of $(NH_4)_2SO_4$ produced during precipitation of impurities is 1.27+5.9+2.6=9.8t/h

The stoichiometric amount of NH_4OH required for precipitation of impurities is 0.68+3.14+0.7=4.5t/h

The total amount of $(NH_4)_2SO_4$ genrated during dissolution, pH adjustment and carbonation is 48.9+9.8+39.3=98t/h

Regeneration of additives

$(NH_4)_2SO_4 = NH_4HSO_4 + NH_3$

Formula	Molecular weight	Amount	Amount
	g/mol	mol	g
$(NH_4)_2SO_4$	132.134	1	132.134
	g/mol	mol	g
NH_4HSO_4	115.104	1	115.104
NH_3	17.03	1	17.03

The total amout of $(NH_4)_2SO_4$ produced during mineral dissolution, precipitation of impurities and the carbonation reaction is 39.3+48.9+9.8=98t/h

From 98t/h $(NH_4)_2SO_4$: 17.03/132.134*98=12.6t/h NH_3 are produced

From 98t/h $(NH_4)_2SO_4$: 115.104/132.134*98=85.4t/h NH_4HSO_4 are produced

Ammonia absorption

$NH_3+H_2O = NH_4OH$

Formula	Molecular weight	Amount	Amount
	g/mol	mol	g
NH_3	17.03	1	17.03
H_2O	18.015	1	18.015
	g/mol	mol	g
NH_4OH	35.046	1	35.046

The capture of CO_2 requires 10.1t/h NH_3, therefore the remaining NH_3 part (2.5t/h) can be used to produce ammonia water

From 2.5t/h NH_3: 18.015/17.03*2.5=2.6t/h H_2O are required for the reaction

From 2.5t/h NH_3: 35.046/17.03*2.5=5.1t/h NH_4OH which is slightly above the stoichiometric amount required for precipitating the impurities (4.5t/h)

Energy balance for the mineralization process applied to a steel plant

Mineral dissolution

$CaSiO_3 + 2NH_4HSO_4 = CaSO_4 + SiO_2 + H_2O + (NH_4)_2SO_4$

BALANCE	TEMP [C]	AMOUNT [kmol]	AMOUNT [kg]	Latent H [Mcal]	Total H [Mcal]
IN1	50	893.847	103200	680.53	-261500
OUT1	50	1188.118	102950	735.12	-270245
BALANCE	50	294.27	-250	54.59	-8745

-10170 kWh

$MgSiO_3 + 2NH_4HSO_4 = MgSO_4 + SiO_2 + H_2O + (NH_4)_2SO_4$

BALANCE	TEMP [C]	AMOUNT [kmol]	AMOUNT [kg]	Latent H [Mcal]	Total H [Mcal]
IN1	50	59.886	6600	47.29	-17110.4
OUT1	50	79.572	6560	48.63	-17359.9
BALANCE	50	19.685	-40	1.34	-249.47

-290 kWh

$FeSiO_3 + 2NH_4HSO_4 = FeSO_4 + SiO_2 + H_2O + (NH_4)_2SO_4$

BALANCE	TEMP [C]	AMOUNT [kmol]	AMOUNT [kg]	Latent H [Mcal]	Total H [Mcal]
IN1	50	134.205	16200	103.6	-34569.9
OUT1	50	179.315	16210	111.09	-35283.1
BALANCE	50	45.111	10	7.49	-713.15

-829 kWh

$Al_2SiO_5 + 6NH_4HSO_4 = Al_2(SO_4)_3 + SiO_2 + 3H_2O + 3(NH_4)_2SO_4$

BALANCE	TEMP [C]	AMOUNT [kmol]	AMOUNT [kg]	Latent H [Mcal]	Total H [Mcal]
IN1	50	21.33	2600	18.38	-6429.93
OUT1	50	28.043	2860	21.65	-7213.41
BALANCE	50	6.713	260	3.27	-783.48

-911 kWh

Precipitation of impurities

$FeSO_4 + 2NH_4OH = Fe(OH)_2 + (NH_4)_2SO_4$

BALANCE	TEMP [C]	AMOUNT [kmol]	AMOUNT [kg]	Latent H [Mcal]	Total H [Mcal]
IN1	50	134.362	9940	110.53	-16815.9
OUT1	50	89.387	9920	77.06	-18640.8
BALANCE	50	-44.975	-20	-33.48	-1824.91
					-2122.37 kWh

$Al_2(SO_4)_3 + 6NH_4OH = 2Al(OH)_3 + 3(NH_4)2SO_4$

BALANCE	TEMP [C]	AMOUNT [kmol]	AMOUNT [kg]	Latent H [Mcal]	Total H [Mcal]
IN1	50	22.618	1780	23.14	-4134.28
OUT1	50	16.021	1770	14.62	-4653.06
BALANCE	50	-6.597	-10	-8.52	-518.77
					-603.32951 kWh

$MgSO_4 + 2NH_4OH = Mg(OH)_2 + (NH_4)_2SO_4$

BALANCE	TEMP [C]	AMOUNT [kmol]	AMOUNT [kg]	Latent H [Mcal]	Total H [Mcal]
IN1	50	59.888	3800	48.69	-9209.3
OUT1	50	39.567	3760	31.88	-9917.33
BALANCE	50	-20.32	-40	-16.81	-708.03
					-823.439 kWh

Carbonation reation

$CaSO_4 + (NH_4)_2CO_3 = CaCO_3 + (NH_4)_2SO_4$

BALANCE	TEMP [C]	AMOUNT [kmol]	AMOUNT [kg]	Latent H [Mcal]	Total H [Mcal]
IN1	65	595.878	69200	295.12	-169209.81
OUT1	65	596.158	69200	796.53	-169295.76
BALANCE	65	0.28	0	501.41	-85.95
					-99.96 kWh

Regeneration of additives

$(NH_4)_2SO_4 = NH_4HSO_4 + NH_3$

BALANCE	TEMP [C]	AMOUNT [kmol]	AMOUNT [kg]	Latent H [Mcal]	Total H [Mcal]
IN1	300	741.67	98000	11010.15	-198311
OUT1	300	1481.792	98000	11190.57	-178582
BALANCE	300	740.122	0	180.42	19729.48
					22945.39 kWh

Ammonia absorption

$NH_3+H_2O = NH_4OH$

BALANCE	TEMP [C]	AMOUNT [kmol]	AMOUNT [kg]	Latent H [Mcal]	Total H [Mcal]
IN1	20	291.119	5100	-19.25	-11490.5
OUT1	20	145.525	5100	-26.94	-11377.9
BALANCE	20	-145.594	0	-7.69	112.61
					130.9654 kWh